

GC  
7.1  
W84  
1976

DISSOLVED INORGANIC AND  
PARTICULATE IODINE IN THE OCEANS

by

GEORGE TIN FUK WONG

B.S., California State University. Los Angeles  
(1971)

S.M., Massachusetts Institute of Technology  
(1973)

SUBMITTED IN PARTIAL FULFILLMENT OF THE

REQUIREMENTS FOR THE DEGREE OF

DOCTOR OF PHILOSOPHY

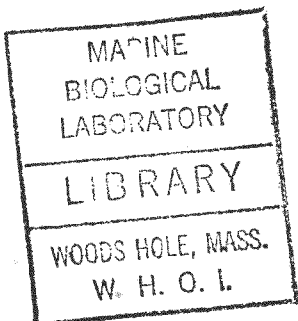
at the

MASSACHUSETTS INSTITUTE OF TECHNOLOGY

and the

WOODS HOLE OCEANOGRAPHIC INSTITUTION

February, 1976



Signature of Author..

.....  
Joint/Program in Oceanography, Massachusetts Institute of Technology - Woods Hole Oceanographic Institution, and Department of Earth and Planetary Sciences, and Department of Meteorology, Massachusetts Institute of Technology, February 1976

Certified by.....

.....  
Thesis Supervisor

Accepted by.....

.....  
Chairman, Joint Oceanography Committee in the Earth Sciences, Massachusetts Institute of Technology - Woods Hole Oceanographic Institution

## ACKNOWLEDGMENTS

I am much indebted to Dr. Peter Brewer, who has not only been a thesis advisor but also a precious friend to me, for his timely and invaluable advice, patience, guidance and encouragement which have made this work enjoyable and possible.

Instructive discussions with Drs. Derek Spencer, John Edmond, Oliver Zafiriou, Vaughan Bowen and Carrell Morris at various stages of this work have helped to shape the course of this study.

Drs. Peter Brewer, Oliver Zafiriou, Derek Spencer, John Edmond, Vaughan Bowen and Carrell Morris have critically reviewed the preliminary versions of this manuscript.

Roy Smith, Alan Fleer, Susan Kadar and Janet Fredericks have provided valuable technical assistance and advice during cruises and sample analyses.

Dr. Michael Bender and the reactor staff at the Rhode Island Nuclear Science Center provided facilities, laboratory space and technical assistance for neutron activation analysis.

This work was supported at various phases by NSF Grant GA-13574, NSF-IDOE Grant GX 33295, NSF Grant DES 74-22292 and by a research fellowship from the Woods Hole Oceanographic Institution.

Finally, I wish to thank my parents for their sacrifices in their effort to provide opportunities for a

1977-WHOI

higher education to their children, and, my wife for her love, understanding and devotion which have made my life as a graduate student enjoyable.

## BIOGRAPHY

The author came to the United States in 1967 upon the completion of his high school education in Hong Kong. After spending a year at the Santa Ana College, he transferred to the California State University, Los Angeles where he subsequently received his B.S. degree in chemistry in 1971 with honors from the University and from the chemistry department. He transferred to the Massachusetts Institute of Technology in the same year and received a S.M. degree in oceanography in 1973. Since then, he has been a doctoral candidate in chemical oceanography in the joint program of the Massachusetts Institute of Technology and the Woods Hole Oceanographic Institution. He has been nominated for membership in Alpha Gamma Sigma, Phi Theta Kappa, Phi Kappa Phi and Sigma Xi. He is an active member of the American Association for the Advancement of Science, the American Geophysical Union and the American Society of Limnology and Oceanography. He is married to the former Virginia Wai-Shu Chin. His contributions to the literature are as follows:

- Onak, T. P. and G. T. F. Wong (1970). Preparation of the pentagonal pyramidal carborane, 2,3,4,5-tetra carbano-nido-hexaborane (6). J. Amer. Chem. Soc., 92, 5226.
- Wong, G. T. F. (1970). The preparation and structural determination of 2,3,4,5-tetra carbano-nido-hexaborane (6). Honors Thesis, B.S., California State University, Los



Angeles.

- Groszek, E., J. B. Leach, G. T. F. Wong, C. Ungermann and T. Onak (1971). Carboranes from alkylboron hydrides. *Inorg. Chem.*, 10, 2770-2775.
- Wong, G. T. F. (1973). The marine chemistry of iodate. Thesis, M.S., Massachusetts Institute of Technology.
- Wong, G. T. F. and P. G. Brewer (1974). The determination and distribution of iodate in South Atlantic waters. *J. Mar. Res.*, 32, 25-36.
- Brewer, P. G., G. T. F. Wong, M. P. Bacon and D. W. Spencer (1975). An oceanic calcium problem? *Earth Plan. Sci. Lett.*, 26, 81-87.
- Wong, G. T. F. and P. G. Brewer (1976). The determination of iodide in seawater by neutron activation analysis. *Anal. Chim. Acta*, 81, 81-90.
- Wong, G. T. F. (1976). The distribution of iodine in the upper layers of the Equatorial Atlantic. Submitted to *Deep-Sea Res.*
- Wong, G. T. F. and P. G. Brewer (1976). The marine chemistry of iodine in anoxic basins. *Trans. Amer. Geophys. Union (Abstract)*, 56, 1002. Submitted to *Geochim. Cosmochim. Acta*.

## TABLE OF CONTENTS

	Page
Approval Page.....	1
Acknowledgments.....	2
Biography.....	4
Table of Contents.....	6
List of Figures.....	9
List of Tables.....	16
Abstract.....	18
 Chapter	
I. Introduction.....	20
1. Introduction.....	21
2. A brief review of some aspects of the geochemistry of iodine.....	25
3. The scope and organization of the research.....	42
II. The analytical chemistry of iodine in sea- water.....	43
1. Introduction.....	44
2. Historical review.....	45
3. The determination of iodate in seawater	50
4. The determination of iodide in seawater by instrumental neutron activation analysis.....	61
5. The determination of iodine in marine suspended matter.....	84

III.	Field observations.....	99
	1. The distribution of iodine in the upper layers of the Equatorial Atlantic.....	100
	2. The marine chemistry of iodine in anoxic basins.....	123
	3. The distribution of iodine in a coastal basin, the Gulf of Maine.....	154
	4. The distribution of iodine in marine suspended matter.....	167
IV.	The interconversion of the dissolved iodine species in the ocean.....	182
	1. Introduction.....	183
	2. The thermodynamic properties of the aqueous iodine system.....	184
	3. The complexation of iodide in sea water	195
	4. Chemical kinetics in the interconver- sion of aqueous iodine species.....	199
	5. Biologically mediated interconversion of the iodine species.....	205
	6. Previous laboratory studies.....	209
	7. Laboratory studies.....	211
	8. A possible oceanic iodine cycle.....	228
V.	Concluding remarks.....	231
	References.....	235

Appendix A. Dissolved iodine measurements in the Equatorial Atlantic during cruise AII-83 (June, July, 1974).....	251
Appendix B. Dissolved iodine measurements and hydrographic data from the Venezuela Basin and the Cariaco Trench during cruise AII- 79.....	258
Appendix C. Dissolved iodine measurements and hydrographic data from the Black Sea during cruise CHAIN-120.....	263
Appendix D. Dissolved iodine measurements and hydrographic data from the Gulf of Maine during cruise AII-86.....	266
Appendix E. Iodine content of suspended particulate matter collected during the GEOSECS Atlantic Expedition.....	269

## LIST OF FIGURES

Figure		Page
I-2-1	The vertical distribution of iodine at 12° 01'N, 158°02'E in the North Pacific.....	33
I-2-2	The cycle of iodine in the ocean.....	40
II-3-1	A calibration curve for the colorimetric determination of iodate.....	55
II-3-2	A comparison of data by the colorimetric and the titrimetric methods.....	56
II-3-3	A profile of iodate determined on board ship.....	58
II-4-1	An analytical scheme for the determination of iodide in seawater.....	67
II-4-2	The loading and elution behavior of halides as determined by an iodide electrode.....	69
II-4-3	Changes in the concentration of total halide in the eluate during loading and elution of 250 ml of seawater.....	71
II-4-4	The elution behavior of iodide from 250 ml of seawater.....	72
II-4-5	Test of the ion-exchange capacity of the column during loading and elution of 1 liter of seawater.....	74
II-4-6	The $\gamma$ -ray spectra of a standard iodate- iodine sample, a Woods Hole surface water sample and a filter blank.....	77

II-4-7	The region around 442.7 KeV of the $\gamma$ -ray spectra of a standard iodate-iodine sample, a Woods Hole surface water sample and a blank filter.....	78
II-4-8	Iodide and iodate profiles at 00°01'N, 09°58'W.....	82
II-5-1	The $\gamma$ -ray spectrum of a standard.....	89
II-5-2	The $\gamma$ -ray spectrum of a sample of marine suspended matter.....	90
II-5-3	A profile of particulate iodine in the North Atlantic.....	97
III-1-1	The cruise track and station locations of cruise AII-83.....	102
III-1-2	The distribution of iodate in the upper layers along the Equator of the Atlantic...	104
III-1-3	Salinity along the Equator of the Atlantic.	104
III-1-4	The profiles of iodate in two nearby stations occupied during cruise AII-83 and the GEOSECS expedition.....	106
III-1-5	The concentrations of iodate in the Equatorial Atlantic along 33°W.....	107
III-1-6	A section of salinity in the Equatorial Atlantic along 33°W.....	107
III-1-7	A section of oxygen in the Equatorial Atlantic along 33°W.....	107
III-1-8	A section of the E-W current velocity in	

	the Equatorial Atlantic along 33°W.....	107
III-1-9	The concentrations of iodate in the Equatorial Atlantic along 28°W.....	109
III-1-10	A section of salinity in the Equatorial Atlantic along 28°W.....	109
III-1-11	A section of oxygen in the Equatorial Atlantic along 28°W.....	109
III-1-12	A section of the E-W current velocity in the Equatorial Atlantic along 28°W.....	109
III-1-13	The concentrations of iodate in the Equatorial Atlantic along 22°W.....	111
III-1-14	A section of salinity in the Equatorial Atlantic along 22°W.....	111
III-1-15	A section of oxygen in the Equatorial Atlantic along 22°W.....	111
III-1-16	A section of the E-W current velocity in the Equatorial Atlantic along 22°W.....	111
III-1-17	The concentrations of iodate in the Equatorial Atlantic along 16°W.....	112
III-1-18	A section of salinity in the Equatorial Atlantic along 16°W.....	112
III-1-19	A section of oxygen in the Equatorial Atlantic along 16°W.....	112
III-1-20	A section of the E-W current velocity in the Equatorial Atlantic along 16°W.....	112
III-1-21	The concentrations of iodate in the Equatorial Atlantic along 16°W.....	112

	torial Atlantic along 10°W.....	113
III-1-22	A section of salinity in the Equatorial Atlantic along 10°W.....	113
III-1-23	A section of oxygen in the Equatorial Atlantic along 10°W.....	113
III-1-24	A section of the E-W current velocity in the Equatorial Atlantic along 10°W.....	113
III-1-25	Profiles of iodate, iodide, phosphate and $\sigma_{\theta}$ at station AII-83-2086.....	116
III-1-26	Profiles of iodate, iodide, phosphate and $\sigma_{\theta}$ at station AII-83-2078.....	117
III-1-27	Profiles of iodate, iodide, phosphate and $\sigma_{\theta}$ at station AII-83-2068.....	118
III-1-28	Profiles of iodate, iodide, phosphate and $\sigma_{\theta}$ at station AII-83-2048.....	119
III-2-1	Profiles of salinity and $\theta$ in the Black Sea at station CHAIN-120-1355.....	128
III-2-2	Profiles of salinity and $\theta$ in the Cariaco Trench.....	130
III-2-3	Positions of the stations in the Black Sea, the Cariaco Trench and the Venezuela Basin.	133
III-2-4	Profiles of iodate and iodide in the Venezuela Basin at station AII-29-2033.....	135
III-2-5	Profiles of iodate and iodide in the Cariaco Trench at station AII-79-2038.....	136
III-2-6	Profile of iodate in the Cariaco Trench at	



	station AII-79-2037.....	137
III-2-7	Profiles of iodate and iodide in the Black Sea at station CHAIN-120-1355.....	138
III-2-8	A concentration diagram of the iodine system in an aqueous solution at pH 8.1 and a total iodine concentration of 0.5 uM.....	141
III-2-9	Profiles of specific total iodine in the Venezuela Basin, the Cariaco Trench and the Black Sea.....	144
III-2-10	The distribution of iodide, iodate and total iodine in the mixing zone of the Black Sea.....	147
III-2-11	The distribution of iodide, iodate and total iodine in the mixing zone of the Cariaco Trench.....	148
III-3-1	The cruise track and station locations of cruise AII-86.....	156
III-3-2	Profiles of iodate, iodide and specific total iodine at station AII-86-2122.....	159
III-3-3	Profiles of $\sigma_{\theta}$ , salinity and $\theta$ at station AII-86-2122.....	160
III-3-4	Profiles of phosphate, silicate and oxygen at station AII-86-2122.....	160
III-3-5	Profiles of $\sigma_{\theta}$ , salinity and $\theta$ at station AII-86-2138.....	161
III-3-6	Profiles of iodate, phosphate, silicate and	

	oxygen at station AII-86-2138.....	161
III-3-7	Profiles of $\sigma_{\theta}$ , salinity and $\theta$ at station AII-86-2151.....	162
III-3-8	Profiles of iodate, phosphate, silicate and oxygen at station AII-86-2151.....	162
III-4-1	The cruise track and station locations of the GEOSECS Atlantic expedition.....	169
III-4-2	Typical profiles of particulate iodine and total particulate matter.....	173
III-4-3	A profile of the ratio of particulate iodine to particulate scandium.....	176
III-4-4	A section of particulate iodine in the Western Atlantic from 75°N to 55°S.....	177
III-4-5	The distribution of primary productivity in the Atlantic Ocean.....	180
IV-2-1	A concentration diagram of the aqueous iodine system at a pH of 8.1 and a total iodine concentration of 0.5 $\mu\text{M}$ .....	187
IV-2-2	The oxidation state diagram of the aqueous iodine system.....	189
IV-2-3	The electron free energy level diagram of the iodine system and some other redox couples.....	192
IV-3-1	Potentiometric titrations of sea water and a 0.5 M sodium chloride solution with standard iodide solutions.....	197

IV-5-1	A possible mechanism for the absorption of iodide by brown algae.....	207
IV-7-1	An apparatus for studying the interconversion of iodine species.....	212
IV-7-2	Dark auto-oxidation of iodide, experiments 1 to 3.....	213
IV-7-3	Dark auto-oxidation of iodide, experiments 4 and 5.....	214
IV-7-4	Rate of production of iodate in sea water at 25°C.....	218
IV-7-5	The stability of elemental iodine in various media.....	223
IV-8-1	A possible oceanic iodine cycle.....	229

LIST OF TABLES

Table		Page
I-1-1	The calculated and observed ratios of the concentrations of the reduced species to the concentrations of the oxidized species in the nitrogen, arsenic and iodine systems in the sea at a pH of 8 and a pE of 12.5...	23
I-2-1	Iodine content of rocks and minerals.....	26
I-2-2	Iodine containing minerals.....	27
I-2-3	The concentration of total iodine in various geochemical reservoirs and agents..	29
I-2-4	Ion pairing of the iodide ion with the major ions in the ocean.....	31
I-2-5	The concentration of iodine in marine organisms.....	35
I-2-6	Concentration factor of iodine in marine organisms.....	36
II-2-1	Analytical methods for the determination of dissolved iodine in sea water.....	46
II-3-1	Data for the calibration curves for the colorimetric determination of iodate during cruise AII-83.....	54
II-4-1	Check of recovery of added radiotracer from sea water.....	75
II-4-2	Reagent blank of the instrumental neutron activation analysis of iodide in sea water.	80

II-4-3	Precision of repeated analyses of Woods Hole surface water.....	81
II-5-1	Blanks in the neutron activation analysis of particulate iodine.....	91
II-5-2	Check on flux and geometry variations.....	94
II-5-3	Reproducibility of sample counts.....	96
III-1-1	Properties at the iodate concentration maxima.....	115
III-2-1	The redox buffer capacity of oxygen and sulfide in the mixing zone and the oxic and anoxic layers.....	142
III-4-1	Iodine content of particulate matter collected closest to the surface and the bottom of the Atlantic.....	171
III-4-2	Standing crops of particulate iodine in the top 200 m of the Atlantic.....	179
IV-2-1	The thermodynamic properties of some iodine species.....	185
IV-2-2	Thermodynamic properties for the intercon- version of iodine species.....	186
IV-2-3	Data for the construction of the oxidation state diagram of the aqueous iodine system.	190
IV-2-4	The thermodynamic properties of some common redox couples in natural waters.....	193
IV-4-1	The dark auto-oxidation of iodide.....	200
IV-4-2	The disproportionation of hypiodite.....	204

## ABSTRACT

### DISSOLVED INORGANIC AND PARTICULATE IODINE IN THE OCEANS

GEORGE TIN FUK WONG

Submitted to the Department of Earth and Planetary Sciences on February 20, 1976 in partial fulfillment of the requirements for the degree of Doctor of Philosophy

Analytical methods have been developed for the determination of iodate, iodide and particulate iodine in sea water. Iodate is converted to tri-iodide and the absorbance of tri-iodide at 353 nm is measured. The precision of this method is ca.  $\pm 3\%$ . Iodide is first separated from most other anions by an AG 1-x8 anion exchange column and then precipitated as palladous iodide with elemental palladium as the carrier. The precipitate is analyzed by neutron activation analysis. The precision of the method is  $\pm 5\%$  and the reagent blank is 0.005  $\mu\text{M}$ . Marine suspended matter is collected by passing sea water under pressure through a 0.6  $\mu$  (37 mm diameter) Nuclepore filter. The iodine content of the particles is determined by neutron activation analysis. The method has excellent reproducibility and the filter blank is ca. 3 ng.

Iodate is depleted in the surface waters of the Equatorial Atlantic. The depletion is more pronounced than in the Argentine Basin and possibly reflects the higher productivity in the equatorial area. Superimposed on this feature, a thin lens of water, of a few tens of meters thick and with high iodate concentrations, can be traced across the Atlantic. Along the equator, this lens occurs at 80 m at  $33^{\circ}\text{W}$  and rises upwards to 55 m at  $10^{\circ}\text{W}$  and it coincides with a core of highly saline water which is characteristic of the Equatorial Undercurrent. Longitudinal sections reflect the complexity of the equatorial current system. At least three cores of water with high iodate concentrations may be identified. These waters may be transported to the equatorial region from the highly productive areas along the north-western and western African coasts and the Amazon plume.

In anoxic basins, the concentration of iodide increases rapidly in the mixing zone from 0.02  $\mu\text{M}$  to 0.44  $\mu\text{M}$  in the Cariaco Trench and from 0.01  $\mu\text{M}$  to 0.23  $\mu\text{M}$  in the Black Sea. The iodate concentration, meanwhile, decreases to zero. A maximum in the total iodine to salinity ratio is observed just above the oxygen-sulfide interface (15 to 17

nmoles/g); it is suggestive of particle dissolution in a strong pycnocline. Below the interface, the total iodine to salinity ratio is constant at 12.3 nmoles/g in the anoxic zone of the Cariaco Trench, whereas, in the Black Sea, it increases with depth from 10.0 to 19.4 nmoles/g and suggests a possible flux of iodide from the sediments. By considering the distribution of iodate and iodide in oxic and anoxic basins and our present analytical capability, the lower limit of the pE of the oceans is estimated to be 10.7. Thermodynamic considerations further suggest that the iodide-iodate couple is a poor indicator for the pE of the oceans with a limited usable range of 10.0 to 10.7.

In the Gulf of Maine during the winter of 1974 to 1975, the effect of winter mixing was conspicuous. Uniform concentrations of iodide and iodate were observed in the mixed layer above the sill. The absence of a depletion of iodate and the low iodide concentration (0.04  $\mu\text{M}$ ) in the surface waters reflect the low biological activity in this region during winters.

Profiles of particulate iodine are characterized by high concentrations in the euphotic zone ( $>5$  ng/kg), and lower concentrations ( $<2$  ng/kg) at greater depths. Occasionally, high concentrations have also been observed in the nepheloid layer. The iodine-containing particles are probably biogenic. A section in the Western Atlantic from  $75^{\circ}\text{N}$  to  $55^{\circ}\text{S}$  shows evidence of the transport of particles along isopycnals and the re-suspension of surface sediments to considerable distance from the bottom. The standing crops in the top 200 m may be qualitatively correlated with the primary productivity.

Thermodynamic considerations show that iodide is a metastable form at the pH of sea water. Laboratory studies fail to show the oxidation of iodide at measurable rates. Elemental iodine is unstable in sea water and undergoes hydrolysis to form hypoiodous acid in seconds. Hypoiodous acid is also unstable and has a life time of minutes to hours. It may react with organic compounds to form iodinated derivatives or it may be reduced to iodide by a reducing agent. The disproportionation of hypoiodite to form iodate seems to be a slower process. A possible chemical cycle for iodine in the marine environment is proposed.

Thesis Supervisor: Peter G. Brewer  
Title: Associate Scientist  
Department of Chemistry  
Woods Hole Oceanographic Institution  
Woods Hole, Massachusetts.

CHAPTER I. INTRODUCTION



## I.1 Introduction

This thesis presents an investigation on the marine chemistry of the element iodine, a multi-oxidation-state element known to be in redox dis-equilibrium, in an attempt to gain a better understanding concerning biological-chemical interactions in the ocean.

Ever since Sillen's classic paper on 'the physical chemistry of sea water' (1961), many attempts have been made to examine the controls on the chemical composition of the oceans by computing the composition of an equilibrium mixture from the existing thermodynamic information (Garrels and Thompson, 1962; Sillen, 1963; Holland, 1965; Kramer, 1965; Zirino and Yamamoto, 1972). There are two basic assumptions in this model. First, that the ocean is a closed system and secondly, that sufficient time is available for the attainment of a chemical equilibrium. However, the ocean in reality is not a closed system as there are frequent exchanges of both energy and matter among the atmosphere, hydrosphere and the lithosphere. Moreover, since different elements have different residence times in the ocean varying from 100 years for aluminum to  $10^8$  years for chloride (Brewer, 1975 and references cited therein), it is unclear that there is sufficient time for all elements to reach a chemical equilibrium. Thus, it is not surprising that 'exceptions' are often observed and, even in his classic paper, Sillen (1961) has noted that gross dis-equilibrium does

occur in some elements.

Dis-equilibria are especially noticeable in the bio-active and multi-oxidation-state elements. Some of the better known examples are: iodide-iodate, ammonia-nitrogen-nitrite-nitrate and arsenite-arsenate (Goldberg, 1963; Riley and Chester, 1971; Johnson and Pilson, 1972). Under the oceanic conditions of a pH of 8 and a pE of 12.5 (Sillen, 1961), the reduced species in all these systems should be undetectable within the limits of our present analytical capabilities. However, significant quantities of these reduced species are often found. The predicted and observed concentrations of the different species in these systems are summarized in table I-1-1.

At least two processes are involved in maintaining an observed redox dis-equilibrium. The first one is the perturbation of a stable system to produce the unstable species. This reaction will be thermodynamically unfavorable. The production of these unstable species such as iodide, arsenite and nitrite has often been attributed to biological activity (Tsunogai and Sase, 1969; Johnson, 1972; Fiadeiro and Strickland, 1968) for a number of reasons. First, organisms can utilize solar energy through photosynthetic processes and they may subsequently use this energy, directly or indirectly, to drive these thermodynamically unfavorable reactions. Secondly, organisms possess complicated enzyme systems which can be used as catalysts to lower the activation energies

Table I-1-1 The calculated and observed ratios of the concentrations of the reduced species to the concentrations of the oxidized species in the nitrogen, arsenic and iodine systems in the sea at a pH of 8 and a pE of 12.5

Reaction	log K	log of Calculated Ratio	log of Observed Ratio	Concentration Observed
$\text{NO}_3^- + 2\text{H}^+ + 2\text{e}^- = \text{NO}_2^- + \text{H}_2\text{O}$	28.3	$\frac{(\text{NO}_2^-)}{(\text{NO}_3^-)} = -12.9$	-3.5	$(\text{NO}_3^-) = 3 \times 10^{-5}\text{M}$
$\text{NO}_3^- + 10\text{H}^+ + 8\text{e}^- = \text{NH}_4^+ + 3\text{H}_2\text{O}$	119.2	$\frac{(\text{NH}_4^+)}{(\text{NO}_3^-)} = -61.8$	-3.5	$(\text{NO}_2^-) = 10^{-8}\text{M}^*$ $(\text{NH}_4^+) = 10^{-8}\text{M}^{**}$
$\frac{1}{2}\text{NO}_3^- + 6\text{H}^+ + 5\text{e}^- = \frac{1}{2}\text{N}_2(\text{g}) + 3\text{H}_2\text{O}$	105.25	$\frac{(\text{PN}_2)^{\frac{1}{2}}}{(\text{NO}_3^-)} = -5.85$	4.5	$(\text{PN}_2) = 0.78 \text{ atm.}$
-----				
$\text{HASO}_4^= + 4\text{H}^+ + 2\text{e}^- = \text{HASO}_2 + 2\text{H}_2\text{O}$	30.9	$\frac{(\text{HASO}_2)}{(\text{HASO}_4^=)} = -26.5$	-0.2	$(\text{HASO}_4^=) = 0.05 \text{ } \mu\text{M}^\#$
-----				
$\text{IO}_3^- + 6\text{H}^+ + 6\text{e}^- = \text{I}^- + 3\text{H}_2\text{O}$	110.1	$\frac{(\text{I}^-)}{(\text{IO}_3^-)} = -13.5$	-0.4	$(\text{IO}_3^-) = 0.5 \text{ } \mu\text{M}^\#\#$ $(\text{I}^-) = 0.2 \text{ } \mu\text{M}^\#\#$
-----				

\* Wada and Hattori (1972)

\*\* Sagi (1969)

# Johnson and Pilson (1972)

## Tsunogai and Henmi (1971)

of these reactions. Thirdly, organisms need an electron acceptor during their metabolic processes. The primary electron acceptor for aerobic organisms is oxygen. In the absence of oxygen, some organisms may use in succession nitrate, sulfate and carbon dioxide as the terminal electron acceptor. During such processes, other species may be directly or indirectly reduced.

The second process is the tendency to re-establish the stable system. The rate of this thermodynamically favorable process will determine the persistence of the disequilibrium. For example, although molecular nitrogen is unstable relative to nitrate (table I-1-1), it amounts to 78% of our atmosphere and its presence is ubiquitous in our oceans. Sillen (1961) suggested that its presence is due to the high internal energy barrier of the N-N bond which greatly reduces its rate of oxidation. However, although this step is thermodynamically favorable, the possibility of biological mediations such as nitrification is not ruled out, and, in such cases, the rate of the reaction may either be enhanced or retarded.

In this study, I have chosen to use the iodine system to illustrate some of the implications of these concepts on the chemistry of the oceans.

## I.2 A brief review of some aspects of the geochemistry of iodine

### I.2.1 Occurrence

Iodine, as an element, was not recognized until the early nineteenth century when Courtois isolated elemental iodine from seaweed (Courtois, 1813). Elemental iodine has not been detected in the lithosphere, except as small traces in certain mineral springs. However, as iodide and iodate, it occurs widely as a trace constituent (Anonymous, 1951; Sneed et al., 1954; Hills, 1956; Fuge, 1974). Table I-2-1 summarizes the iodine contents of various rocks and minerals. Minerals having iodine as an essential constituent are rare although dietzeite and lautarite have been found in the Chilean saltpetre deposits. A list of the known iodine-containing minerals is presented in table I-2-2.

The history of investigations on the chemistry of iodine in marine environments has been briefly reviewed by Riley (1965a). He traced the first study to 1825 when Pfaff detected iodine in Baltic Sea water. This report was later confirmed by Laurens (1835) who found iodine in French coastal water. Early investigators reported a wide range of concentrations from 0.017 ug/l (Macadam, 1852) to 8000 ug/l (Marchand, 1855). Since then, a series of measurements have been made (Reith, 1930; Skopintsev and Michailovskaya, 1933; Dubravcic, 1955; Sugawara et al., 1955; Sugawara and Terada,

Table I-2-1 Iodine content of rocks and minerals\*

Rock Type	Iodine Content (ppm)	Mineral Type	Iodine Content (ppm)
Amphibolite	0.25-0.38	Apatite	0.23-0.44
Basalt	0.31-0.80	Biotite	0.50
Diabase	0.49-1.04	Calcite	0.23
Gneiss	0.38	Cinnabar	0.50
Granite	0.20-1.25	Cuprite	3.8-4000
Limestone	0.44	Dolomite	0.32
Marble	0.07-1.98	Fluorite	0.55
Mica Schist	0.54	Gypsum	0.25-0.27
Porphyry	0.38-0.54	Limonite	0.75
Pumice	0.25	Pitchblende	0.94
Quartzite	1.10-3.70	Pyrite	0.20
		Serpentine	0.38
		Wulfenite	8.56

\* Data from Hills (1956).

Table I-2-2 Iodine containing minerals\*

Mineral Name	Formula
Coccinite	$\text{Hg}_2\text{I}_2$
Cuproiodargyrite	$(\text{Ag}, \text{Cu})\text{I}$
Iodembolite	$\text{Ag}(\text{Br}, \text{I}, \text{Cl})$
Iodobromite	$2\text{AgCl}, 2\text{AgBr}, \text{AgI}$
Iodargyrite	$\text{AgI}$
Marshite	$\text{Cu}_2\text{I}_2$
Miersite	$4\text{AgI}, \text{CuI}$
Salesite	$\text{CuIO}_3\text{OH}$
Schwarzenbergite	$\text{Pb}(\text{I}, \text{Cl})_2, 2\text{PbO}$
Tocornalite	$(\text{Ag}, \text{Hg})\text{I}$
Dietzeite	$7\text{Ca}(\text{IO}_3)_2, 8\text{CaCrO}_4$
Lautarite	$\text{Ca}(\text{IO}_3)_2$

\* Data from Hills (1956).

1957; Barkley and Thompson, 1960a, 1960b; Voipio, 1961; Kappanna et al., 1962; Tsunogai, 1971a, 1971b; Tsunogai and Henmi, 1971; Liss et al., 1973; Wong and Brewer, 1974), and, presently, most investigators agree that the concentration of total dissolved iodine in sea water is about 60 to 70 ug/l (0.5 uM) (Goldberg et al., 1971).

Relative to sea salt, iodine is more concentrated in the atmosphere, in rain, in river waters and in interstitial waters. Surface sediments also have high iodine concentrations. The concentrations of iodine in natural waters, sediments and the atmosphere are summarized in table I-2-3.



Table I-2-3 The concentration of total iodine in various geochemical reservoirs and agents

Material	Concentration Range	Average Concentration	I/Cl	Reference
Sea water		60 ug/kg	$3 \times 10^{-6}$	Goldberg et al. (1971)
Atmosphere				
Aerosol	0.5-25 ng/SCM	2 ng/SCM	$1 \times 10^{-3}$	Duce et al. (1965)
Gaseous phase	2.4-18.3 ng/SCM	6 ng/SCM	$3 \times 10^{-3}$	Duce et al. (1965)
Rain water	1-15 ug/kg	4 ug/kg	$5 \times 10^{-3}$	Miyake and Tsunogai (1963)
River water		7 ug/kg	$9 \times 10^{-4}$	Turekian (1971)
Interstitial water	0.35-1.9 mg/kg	1 mg/kg	$10^{-4}$	Bojanowski and Paslawska (1970)
Surface sediment	121-900 ppm	300 ppm		Price and Calvert (1973)

SCM -  $m^3$  of air at standard temperature and pressure.

### I.2.2 The speciation of dissolved iodine in sea water

Thermodynamic calculations show that iodate should be the only detectable iodine species in the sea (Sillen, 1961). However, it has been long recognized that at least two species of iodine are present. Winkler (1916) suggested that they are iodate and iodide. The identity of the oxidized species later developed into a controversial subject. Sugawara (1957) supported Winkler's view of iodate as the oxidized species while Shaw and Cooper (1957) thought that hypiodous acid might be the dominant oxidized species instead. Later investigations by Sugawara and Terada (1958) and Johanneson (1958) confirmed the presence of iodate and Shaw and Cooper (1958) subsequently retracted their hypothesis. The fraction of the inorganic iodide that may be present as ion pairs with the major ions can be estimated from partial molal volumes (Millero, 1969). It is negligible (table I-2-4). Recently, the possibility of the presence of 'organic iodine' has been proposed by Truesdale (1975). He claimed concentrations of up to 5% of the total dissolved iodine in the surface waters of the Irish Sea. Lovelock et al. (1973) detected the presence of methyl iodide. However, its kinetic stability in sea water is low and it is susceptible to exchange reactions with chloride ions to form iodide ions instead (Zafirion, 1975). The present discussion will deal only with the inorganic species.

Table I-2-4 Ion pairing of the iodide ion with the major ions in the ocean\*

r (A)	$Z^2/r$ (A <sup>-1</sup> )	$\bar{V}_{(calc)}^0$ (ml/mole)	$\bar{V}_{(meas)}^0$ SW (ml/mole)
2.16	0.46	41.8	41.4

$$\bar{V}_{(elect)}^0 \text{ SW} = -7.5 \times Z^2/r = -3.45 \text{ ml/mole}$$

% contact ion-pair:

$$\frac{\bar{V}_{(meas)}^0 \text{ SW} - \bar{V}_{(calc)}^0 \text{ SW}}{\bar{V}_{(elect)}^0 \text{ SW}} = \frac{41.4 - 41.8}{-3.45} = 1.2\%$$

r - Pauling crystal radius

Z - Charge of ion

$\bar{V}_{(calc)}^0$  SW - Partial molal volume calculated

$\bar{V}_{(meas)}^0$  SW - Partial molal volume measured

$\bar{V}_{(elect)}^0$  SW - Electrostriction partial molal volume

\* Data from Millero (1969).

### I.2.3 The distribution of iodine in the oceans

The average concentration of total dissolved iodine in the oceans is about 0.5  $\mu\text{M}$  (64  $\mu\text{g/l}$ ) (Goldberg et al., 1971). The ratio of iodide to iodate varies with depth and with geographical locality. The concentration ranges of iodide and iodate in the open oceans are <0.01  $\mu\text{M}$  to 0.2  $\mu\text{M}$  and 0.2  $\mu\text{M}$  to 0.5  $\mu\text{M}$  respectively (Tsunogai and Henmi, 1971). Iodide maxima and corresponding iodate minima are often found in surface waters. Below the euphotic zone, iodide decreases to below the detection limit of about 0.01  $\mu\text{M}$  while iodate increases to an approximately constant level. Low but significant iodide concentrations have been observed in bottom waters (Tsunogai, 1971b; Tsunogai and Henmi, 1971). Typical profiles of iodide and iodate are shown in figure I-2-1. The distribution of organic iodine in the water column is unknown. The concentration of iodine in marine suspended matter has not previously been measured.

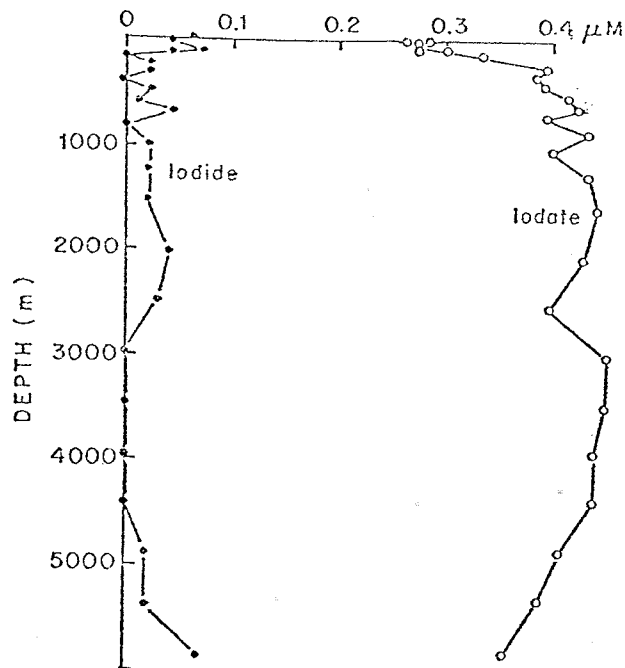


Fig. I-2-1 The vertical distribution of iodine at  $12^{\circ}01'N$ ,  $158^{\circ}02'E$  in the North Pacific where the depth is 5855 m. (Tsunogai, 1971b)

#### I.2.4 The biogeochemistry of iodine

The presence of measurable amounts of iodide in the oceans implies that the iodine system in the sea is not at chemical equilibrium with the  $O_2$ - $H_2O$  system. Sugawara and Terada (1967) found that the alga *Navicula* can interconvert iodate and iodide. Tsunogai and Sase (1969) demonstrated that bacteria that are capable of reducing nitrate to nitrite, or their enzyme extracts, can also reduce iodate to iodide. Thus, they proposed the enzymatic reduction of iodate to iodide using nitrate-reductase as the catalyst.

Tsunogai and Henmi (1971) later observed that the concentrations of iodide in the surface waters of various parts of the Pacific can be qualitatively correlated to their primary productivity. Wong and Brewer (1974) reported that in the Argentine Basin, iodate is linearly related to the micronutrients phosphate and nitrate, and consequently to apparent oxygen utilization (AOU) as well. They obtained the molar ratios of  $AOU:NO_3^-:PO_4^{3-}:IO_3^-$  of 2440:357:23:1. These relationships and the recent detection of methyl iodide (Lovelock et al., 1973), which is a possible metabolite, in sea water, suggest that iodine may be intimately involved in the marine biochemical cycles.

Indeed, iodine can be found in the body tissue of all marine species (Hansen, 1963). (The concentrations of iodine in various organisms are shown in tables I-2-5 and I-2-6.) It is an essential nutrient for red and brown

Table I-2-5 The concentration of iodine in marine organisms

	Iodine Content (ppm dry weight)	Reference
I. Plant		
Plankton	300	Vinogradov (1953)
Brown algae	1500	Vinogradov (1953) Young and Langille (1958)
Marine algae	4-500	Young and Langille (1958)
Indian sea weed	10 <sup>4</sup>	Pillai (1956)
II. Animals		
Coelenterata	15	Vinogradov (1953)
Mollusca	4	Vinogradov (1953)
Echinodermata	6	Vinogradov (1953)
Crustacea	1	Vinogradov (1953)
III. Hard tissues		
Red algae (CaCO <sub>3</sub> )	55	Vinogradov (1953)
Porifera (CaCO <sub>3</sub> )	4800	Low (1949)
Porifera (SiO <sub>2</sub> )	2100	Low (1949)
Corals (CaCO <sub>3</sub> )	5000	Vinogradov (1953)

Table I-2-6 Concentration factor of iodine in marine organisms

	Concentration Factor	Reference
I. Plant		
Plankton	1200	Bowen (1966)
Brown algae	6200	Bowen (1966)
Brown algae	3000-10000	Mauchline and Templeton (1964)
Algae	184	Hiyama and Khan (1964)
Marine algae	500-60000	Young and Langille (1958)
Gracilaria foliifera	150	US Dept. of Interior (1966)
II. Animal		
Fish	4	Hiyama and Khan (1964)
Shrimp	30	Hiyama and Khan (1964)
Sea urchin	39	Hiyama and Khan (1964)
Shell fish	1	Hiyama and Khan (1964)
III. Hard tissue		
Shell fish shell	2	Hiyama and Khan (1964)



algae (Bowen, 1966) and Shaw (1959, 1962) reported that only iodide can be absorbed. Marine plankton also take in and excrete iodine, mostly in the form of iodide (Kolemainen, 1969; Kuenzler, 1969). For land plants, a suitable amount of iodine is actually necessary for optimal growth (Hanson, 1963) and it is also essential for mammals (Bowen, 1966). However, although iodine has long been classified as a biophile (Goldschmidt, 1954) and its metabolic pathways in the higher mammals have already been intensively studied (Gross, 1962), its physiological functions in marine organisms in general are not well documented. Thus, the link between iodine and biological activity in the sea is still based on indirect observations.

### I.2.5 Iodine in the sediments and interstitial waters

Price and co-workers (Price et al., 1970; Price and Calvert, 1973) have studied the distribution of iodine in sediments. They observed high iodine content in surface sediments which decreased rapidly with depth and also decreased from oxidizing to reducing sediments. A linear relationship between iodine and organic carbon content was shown. Shishkina and Pavlova (1965) have also reported enrichment of iodine in sediments and the iodine content was found to increase with increasing organic content and the degree of fineness of the sediments. Bojanowski and Paslawska (1970) measured iodine in interstitial waters and reported the range of iodine concentrations to be 0.35 to 1.9 mg/kg. Recently, Pavlova and Shishkina (1973) further reported that the concentration of iodine in interstitial waters increases with depth. These observations suggest intense diagenesis and post-depositional migration of iodine in recent sediments and indicate a possible flux of iodine from the sediments into the ocean. This was proposed by Tsunogai (1971b) who observed a low but significant excess of iodide in the bottom waters.

### I.2.7 The marine geochemical cycle of iodine

Since iodine is involved in many geochemical processes as described earlier, its geochemical cycle will no doubt be complex. Miyake and Tsunogai (1963) presented a scheme for the cycling of iodine in the oceans and it has subsequently been modified twice (Tsunogai and Sase, 1969; Tsunogai, 1971b). The latest version is shown in figure I-2-2. Many of the values of the fluxes involved are speculative and unconfirmed. However, the relative magnitudes of the processes in the cycle are worth noting.

The permanent loss of iodine to the sediments by burial is the smallest flux. It is at least three orders of magnitude smaller than other fluxes and suggests the cyclic nature of iodine in the water column. Three cycles can be readily identified. By far, the most important cycle quantitatively is the incorporation of iodine into the organisms in the surface layers and subsequent re-mineralization at depth. The regenerated iodine is transported back to the euphotic zone by advection and diffusion. A secondary, and possibly significant, cycle is the sedimentation of iodine containing particles which undergo diagenesis in the sediments. The dissolved iodine thus formed diffuses back into the water column. The quantitatively almost insignificant cycle is the input of iodine from river runoff and fallout and the removal by transferring iodine from the oceans to the atmosphere.

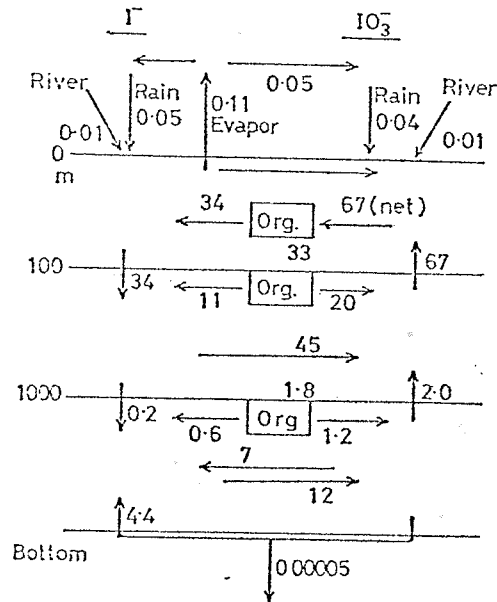
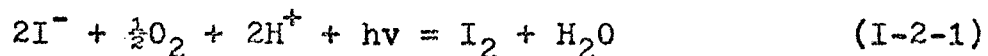


Fig. I-2-2 The cycle of iodine in the ocean. The figures indicated are the annual rates in a unit of  $10^{-4}$  g at/m<sup>2</sup>-yr or  $3.6 \times 10^{10}$  g at/yr in the whole ocean. (Tsunogai, 1971b)

### I.2.6 Iodine in the atmosphere

Since the report of an enrichment of iodine in the atmosphere and especially in the marine atmosphere (Rankama and Sahama, 1949; Goldschmidt, 1954; Duce et al., 1963), much effort has been devoted to study the atmospheric chemistry of iodine. It is generally accepted that the ocean is the most likely source of the excess iodine in the atmosphere. However, the mechanism for the transfer of iodine from the ocean into the atmosphere is still unclear. Miyake and Tsunogai (1963) suggested that the transfer is accomplished by the evaporation of the volatile elemental iodine which may be formed by the photo-oxidation of iodide according to the reaction



Others (Bolin, 1959; Dean, 1963) favored the transfer of organic iodine into the atmosphere by a bubble bursting mechanism. The volatile methyl iodide has been suggested as a possible candidate (Lovelock et al., 1973). Seto and Duce (1972) found in their laboratory experiments that both the organic and the gaseous iodine are important in determining the total iodine enrichment on marine atmospheric particles.

### I.3 The scope and organization of the research

My efforts in studying the marine chemistry of iodine can be sub-divided into three sections. First, techniques were developed for the analysis of dissolved iodine in both oxidation states, namely, iodate and iodide, and also for particulate iodine with improvements in simplicity, sensitivity and precision over the existing methods. Then, samples were collected for analysis from specific geographical areas with distinct characteristics in their productivity or oxidation potential. Data for dissolved iodine have been obtained from the Equatorial Atlantic, the Black Sea, the Cariaco Trench, the Venezuela Basin and the Gulf of Maine. Samples of marine suspended matter were obtained from the Atlantic through the GEOSECS (Geochemical Ocean Sections Study) program. Laboratory experiments have also been designed to study the stability, and the mechanisms for the interconversion, of the iodine species in sea water.

CHAPTER II. THE ANALYTICAL CHEMISTRY OF IODINE IN SEA WATER

## II.1 Introduction

Since iodine is present in the oceans at the  $\mu\text{M}$  level, it is considered a trace element. The concentration ranges of iodate and iodide in the open oceans are usually 0.2 to 0.5  $\mu\text{M}$  and  $<0.01$  to 0.2  $\mu\text{M}$  respectively. With such low abundances and narrow ranges of concentrations, precise and sensitive analytical techniques are absolutely necessary for reliable quantitative studies. I have developed a suitable method for measuring iodate in the oceans with a precision of better than 1% in an earlier study (Wong, 1973; Wong and Brewer, 1974). In this chapter, I shall report on methods for measuring iodide and particulate iodine in sea water. Moreover, the method for the determination of iodate has been modified. This modified version is simpler and more suitable for rapid surveys although the precision may be slightly poorer.



## II.2 Historical review

Riley (1965) has reviewed the earlier literature through 1962. A few more methods have been reported since then. They are all summarized in table II-2-1.

Analytical schemes for the determination of iodate can be categorized into three groups according to their methodologies: titrimetry (Skopintsev and Mikhailovskaya, 1933; Barkley and Thompson, 1960a, 1960b; Matthews and Riley, 1970; Wong and Brewer, 1974; Truesdale and Spencer, 1974), photometry (Reith, 1930; Dubravcic, 1955; Sugawara et al., 1955; Voipio, 1961; Kappanna et al., 1962; Tsunogai, 1971a; Schnepfe, 1972; Truesdale and Spencer, 1974) and polarography (Petek and Branica, 1968, 1969; Herring and Liss, 1973). The titrimetric methods involve the titration of liberated iodine using the starch-iodine or the tri-iodide ion color as the end point indicator. Amperometric end point detection has also been used. The photometric procedures may depend on: (1) the catalytic action of iodide on the oxidation of arsenic (III) by cerium (IV); (2) the color intensity of the extracted iodine; or (3) the color intensity of the iodine-starch complex. Some of the procedures require tedious initial concentration and separation steps (for example, Reith, 1930; Skopintsev and Mikhailovskaya, 1933; Sugawara et al, 1955; Matthews and Riley, 1970; Tsunogai, 1971a). Others may require stringent control of experimental

Table II-2-1 Analytical methods for the determination of dissolved iodine in sea water

Approx. conc. found (ug/l)	Method of separation and detection	Methodology	Reference
43	Iodate reduced with $As_2O_3 + HCl$ , iodine liberated with nitrite and extracted with $CCl_4$ .	Photometry	Reith 1930.
26-56	Oxidized to $IO_3^-$ with $MnO_4^-$ , reduced the latter with $C_2O_4^{2-}$ , treated with $I^-$ and acid, liberated iodine titrated.	Titrimetry	Skopintsev and Mikhailovskaya 1933.
61	Direct method, depending on catalytic action of $I^-$ on reaction between $Ce^{4+}$ and $As^{3+}$ , remaining $Ce^{4+}$ determined.	Photometry	Dubravcic 1955.
Total I = 7-57 $IO_3^-$ -I = 0-50	$I^-$ co-precipitated with $AgCl$ , converted to $IO_3^-$ with $Br$ . Reacted with acidified $I^-$ , liberated iodine measured. Total I by reduction of $IO_3^-$ with $SO_3^{2-}$ , followed by determination of $I^-$ as described above.	Photometry	Sugawara et al. with starch 1955; Sugawara and iodine color Terada 1957.
Total I=45-70 $IO_3^-$ -I= 50-76	$IO_3^-$ reacted with $I^-$ , liberated iodine treated with excess $S_2O_3^{2-}$ , which was titrated with $IO_3^-$ . Total I by oxidation of $I^-$ with $Br$ to $IO_3^-$ , which was determined as described above. Total I also determined by its catalytic effect on the reaction of $Ce^{4+}$ with $As^{3+}$ .	Amperometric titration	Barkley and Thompson 1960a, 1960b.

Total I=60-118	Catalytic effect of $I^-$ on reaction of $Ce^{4+}$ with $As^{3+}$ .	Photometry $Ce^{4+}$ color	Voipio 1961; Kappanna et al. 1962.
$IO_3^-$ -I=36-172	Direct method. Acidify to pH 3. Remove $O_2$ . Record $IO_3^-$ peak at -0.3 v.	Pulse polarography	Petek and Branica 1968,1969.
-----	Modified Sugawara method, reduction of $IO_3^-$ with $(NH_2)_2 \cdot H_2SO_4$ . $I_3^-$ determined by photometry or photometric micro-titration.	Photometry $I_3^-$ color. Titrimetry	Matthews and Riley 1970.
$I^-$ -I=0-25	Improved Sugawara method.	Photometry	Tsunogai 1971a.
$IO_3^-$ -I=25-50		Starch- $I_2$ color.	
Total I=55-90	$IO_3^-$ reacted with iodide-starch mixture directly. Total I by oxidation of $I^-$ with alkaline $KMnO_4$ to $IO_3^-$ and reaction with $I^-$ -starch mixture.	Photometry starch- $I_2$ color	Schnepfe 1972.
$IO_3^-$ -I=37-64			
$IO_3^-$ -I=41-56	Direct method for $IO_3^-$ . Record $IO_3^-$ peak at -1.090 v. $I^-$ determined by difference by oxidizing $I^-$ to $IO_3^-$ by UV irradiation.	Differential pulse polarography	Herring and Liss 1973
$I^-$ -I=1-11	$IO_3^-$ react with $I^-$ and acid to form $I_3^-$ . $I_3^-$ color measured or titrated with $S_2O_3^{2-}$ . Total I by catalytic effect of $I^-$ on reaction of $Ce^{4+}$ with $As^{3+}$ . Measure brucine color.	Photometry Amperometric titration	Truesdale and Spencer 1974.
-----			
$IO_3^-$ -I=35-65	$IO_3^-$ reacted with $I^-$ . Liberated $I_2$ titrated with $S_2O_3^{2-}$ by spectrophotometric titration.	Titration	Wong and Brewer 1974.

conditions (Dubravcic, 1955; Barkley and Thompson, 1960a; Voipio, 1961; Kappanna et al., 1962; Truesdale and Spencer, 1974). Some of the earlier methods (Reith, 1930; Skopintsev and Mikhailovskaya, 1933; Dubravcic, 1955) do not distinguish between the oxidation states and may not have sufficient precision and sensitivity to detail the variations of iodate in the oceans.

Because of its low abundance, the measurement of iodide in sea water is even more difficult. In most cases, iodide is measured as the difference between iodate and total iodine. Consequently, the precision and sensitivity, and thus the usefulness, of such methods are much reduced. The only known direct method is Sugawara's method and its later modifications (Sugawara et al., 1955; Matthews and Riley, 1970; Tsunogai, 1971a). In these methods, iodide is first concentrated from sea water by precipitating mixed silver halides. The precipitate is treated with bromine water to oxidize iodide to iodate. The excess bromine and hypobromite are carefully removed and the iodate is determined by iodometric titration. This method is time consuming and considerable manipulative skill is required to remove the bromine compounds quantitatively. Moreover, the use of rather large amounts of the obnoxious bromine water can become a problem especially on board ship where fume hood facilities may not be available.

Most of the presently available data were mea-

sured by Sugawara's method and its modifications (Sugawara and Terada, 1957; Sugawara, 1957; Sugawara et al., 1962; Tsunogai, 1971b; Tsunogai and Henmi, 1971). Few of the remaining methods have been tested by measuring natural samples from the open oceans. Representative profiles of iodide and iodate are shown in figure I-2-1. Although the claimed precision of the analytical methods used is  $\pm 3\%$  for iodide and  $\pm 6\%$  for iodate, large haphazard variations are found in these profiles and they are almost certainly due to analytical uncertainties.

In light of the above, the precision and reliability of the existing analytical methods seemed inappropriate for this study. Consequently, I have developed new schemes for the analysis of iodide, iodate and particulate iodine in the oceans.

## II.3 The determination of iodate in sea water

### II.3.1 Introduction

In my earlier work, I have reported a method for the determination of iodate in sea water by spectrophotometric micro-titration (Wong, 1973; Wong and Brewer, 1974). The precision of this method is better than 1%. I also found that the iodate can be determined colorimetrically by measuring at 353 nm the absorbance of the tri-iodide ions generated by the addition of acid and excess potassium iodide to the sample using a scheme of standard additions. The precision is about  $\pm 3\%$  (Wong, 1973). Although its precision is poorer, this method is simpler and will be most appropriate for surveying the large variations (up to 50%) of the iodate concentrations in the surface layers. The addition method has been modified and the results will be reported in this section.

My previous data (Wong and Brewer, 1974) were obtained from frozen samples analyzed in my laboratory at Woods Hole. There was some concern about the possible interference by nitrite. I have tested the sea-worthiness of the titration method and designed schemes to remove nitrite from the samples and the results will also be included in this section.

## II.3.2 Experimental

### II.3.2.1 Reagents

All reagents used were of the analytical reagent grade.

Standard potassium iodate solution (8  $\mu\text{M}$ ). Dissolve 0.856 g (4  $\mu\text{moles}$ ) of potassium iodate in distilled water and dilute to 500 ml. The resulting solution is 8  $\mu\text{M}$ .

Prepare an 8  $\mu\text{M}$  solution from this stock solution by successive dilutions.

Potassium iodide solution (10% w/v). Dissolve 2.5 g of potassium iodide in distilled water and dilute to 25 ml. This solution should be prepared daily.

Sulfuric acid (0.1 M). Add 25 ml of concentrated sulfuric acid (18 M) to 400 ml of distilled water in small increments with intermittent swirling and cooling in an ice-water slush bath. Add 25 ml of distilled water. The resulting solution is approximately 1 M. Prepare a 0.1 M solution from this stock solution by a ten-fold dilution.

Sulfamic acid solution (0.1 % w/v). Dissolve 0.1 g of sulfamic acid in distilled water and dilute to 100 ml.

### II.3.2.2 Procedure

Filter about 250 ml of surface sea water through a Whatman 40 filter paper. Pipette 40 ml of the filtered sea water into each of a set of four 50 ml volumetric flasks and mark them 0, 1, 2 and 3. Add 1 ml of 0.1 M sulfuric acid and 1 ml of 0.1% sulfamic acid to each flask. Swirl each flask and allow the solutions to sit for 15 minutes with occasional shaking. Pipette 1, 2 and 3 ml of 8  $\mu\text{M}$  potassium iodate solution to the flasks marked 1, 2 and 3 respectively. Add 1 ml of the 10% potassium iodide solution and dilute to volume with distilled water. Again, allow the solutions to sit with occasional swirling for 15 minutes. Then, measure the absorbance of the solution in each flask at 353 nm in a 10 cm cell. Repeat the procedure twice for the same surface sea water. Plot absorbance against the amount of iodate-iodine added and compute the slope (S) of the graph.

Treat each sample in the same manner except omitting the addition of iodate. Note the absorbance (A) of each sample. The concentration of iodate in the samples can be calculated from the formula

$$(\text{IO}_3^-) = (A/S) \times 0.197 \mu\text{M} \quad (\text{II-3-1})$$



### II.3.3 Results and discussions

Sea water samples were collected in the Equatorial Atlantic during cruise AII-83 and were analyzed for iodate on board ship by the colorimetric method. Table II-3-1 shows the raw data for constructing the calibration curves through out the entire cruise. Figure II-3-1 shows one of the calibration curves. The slopes of the calibration curves were calculated by a linear least square fit. Within each day, the uncertainty of the slope varies from  $\pm 0.2\%$  to  $\pm 1.3\%$ . The average slope for the calibration curves in six weeks has  $1\sigma$  of  $\pm 2.3\%$ . The precision of the colorimetric method relies heavily on the consistency of the slope of the calibration curve as shown in equation II-3-1. Thus, it is comforting to observe such reproducible results and the uncertainty of the method can be estimated to be about  $\pm 3\%$ .

In order to further check the reliability of the colorimetric method, I have attempted to intercalibrate results from this method and the titration method. Figure II-3-2 shows the data from GEOSECS station 109 ( $2^{\circ}\text{S}$ ,  $4^{\circ}33'\text{W}$ ) and the nearby station AII-83-2052 ( $2^{\circ}\text{S}$ ,  $10^{\circ}\text{W}$ ). The GEOSECS samples were analyzed by the titrimetric method while station AII-83-2052 samples were analyzed by the colorimetric method. The profiles of  $\sigma_{\theta}$  of these stations are indistinguishable below 40 m while the profiles of salinity and potential temperature become identical below 500 m. The

Table II-3-1 Data for the calibration curves for the colorimetric determination of iodate during cruise AII-83

Date	Trial	Absorbances with various amount of IO <sub>3</sub> <sup>-</sup> -I added (in ug)	2.03	3.045	Slope for the day
June 17, 1974	1.	0.173	0.357	0.441	0.0887 ± 1.1%
	2.	0.166	0.352	0.439	
	3.	0.167	0.352	0.438	
June 25, 1974	1.	0.162	0.347	0.435	0.0887 ± 1.1%
	2.	0.172	0.352	0.442	
	3.	0.171	0.354	0.440	
July 8, 1974	1.	0.171	0.348	0.436	0.0873 ± 0.3%
	2.	0.170	0.347	0.436	
	3.	0.170	0.349	0.437	
	4.	0.173	0.349	-----	
July 11, 1974	1.	0.171	0.344	0.434	0.0865 ± 0.8%
July 20, 1974	1.	0.162	0.348	0.438	0.0888 ± 1.3%
	2.	0.170	0.351	0.438	
July 27, 1974	1.	0.190	0.361	0.445	0.0837 ± 0.2%
Average slope for the entire cruise					0.0873 ± 2.3%

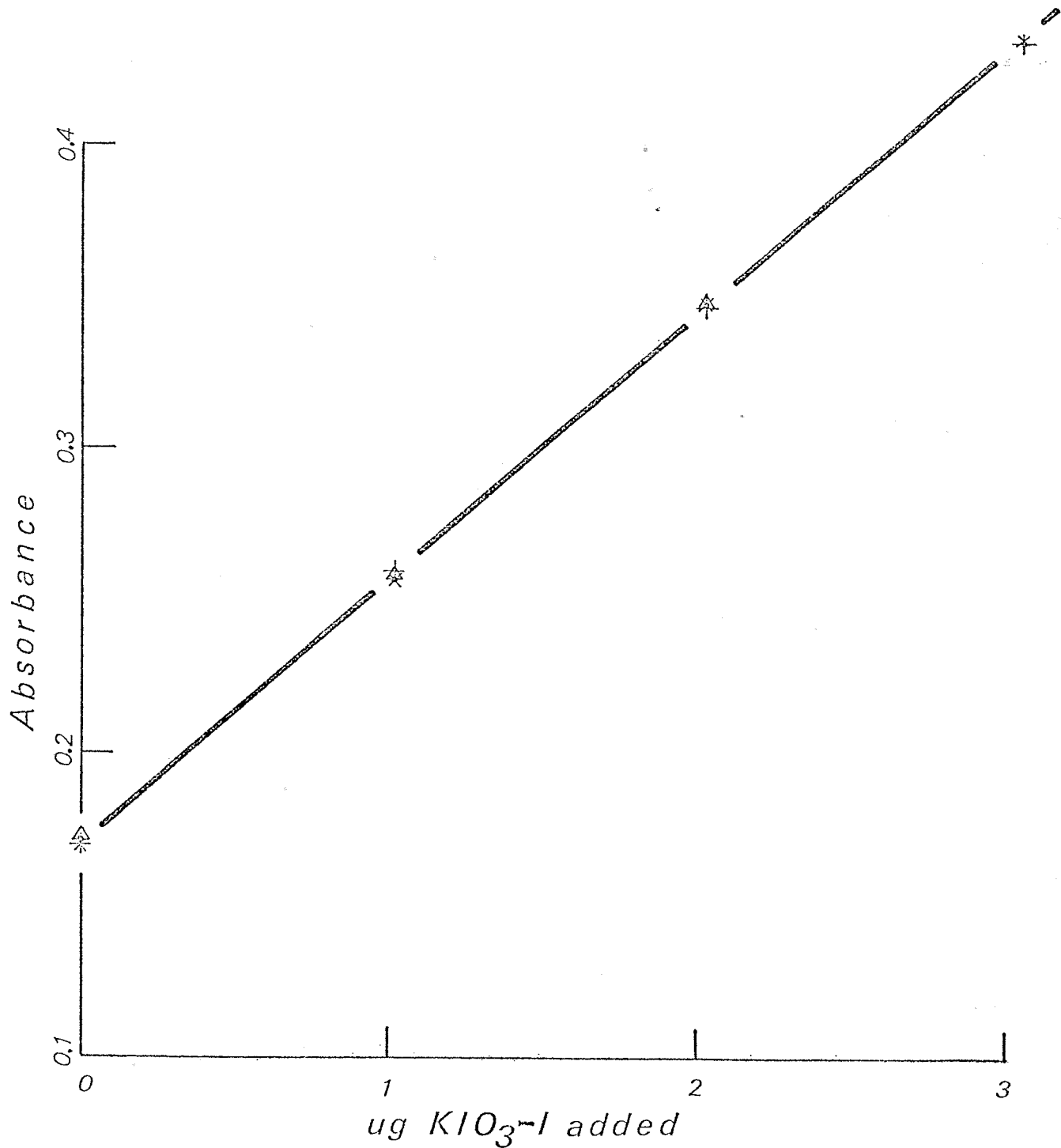


Fig. II-3-1 A calibration curve for the colorimetric determination of iodate. (July 8, 1974)

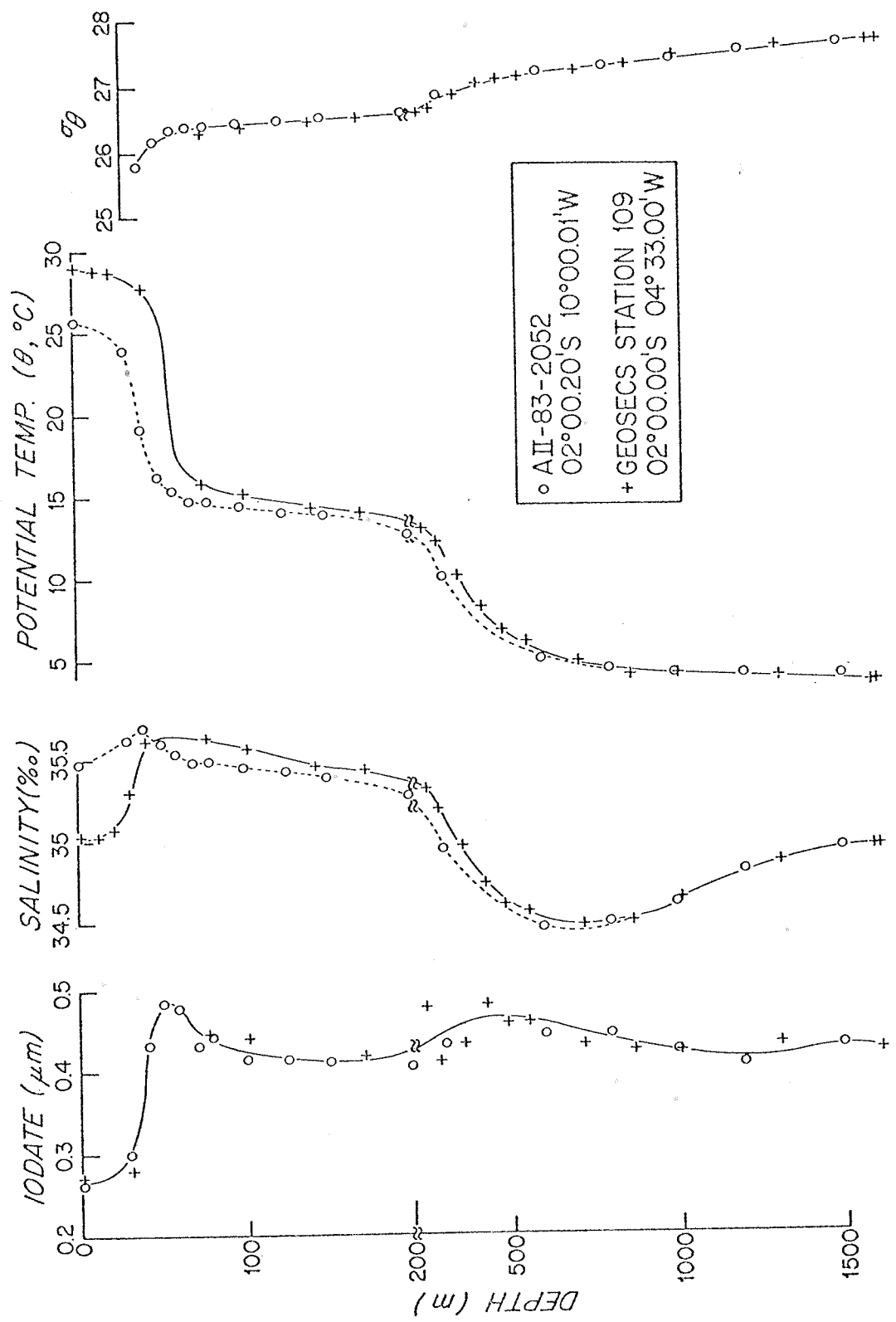
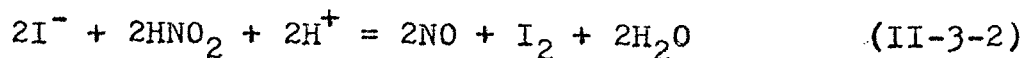


Fig. II-3-2 A comparison of data by the colorimetric and the titrimetric methods.

iodate profiles, within the precision of the analytical methods, are indistinguishable throughout the entire depth. This agreement indicates that there is no systematic difference between these two methods.

I have also measured iodate in the Venezuela Basin on board ship during cruise AII-79 by the spectrophotometric micro-titration method. No special difficulties were encountered and the method seems to be sea-worthy. This profile of iodate is shown in figure II-3-3. The profile is remarkably smooth and the variation in the deep water is only  $\pm 2\%$ . A few of the samples were frozen and analyzed in the laboratory four months later. The stored samples give absolute concentrations that are slightly lower than those nearby samples analyzed on board ship as shown in figure II-3-3. However, this difference is insignificant within the uncertainty of the analytical method and may be due to a slight error in calibrating the strength of the sodium thiosulfate titrant, as different titrant solutions have been used. Thus, it is apparently safe to freeze sea water for an extended period of time for the analysis of iodate on a later date. A more detailed study on the effect of storage on iodate analysis has been reported in Wong (1973).

The interference of nitrite on iodometric titrations is well known. The reaction involved is



Thus, in an acidic solution, nitrite may oxidize the

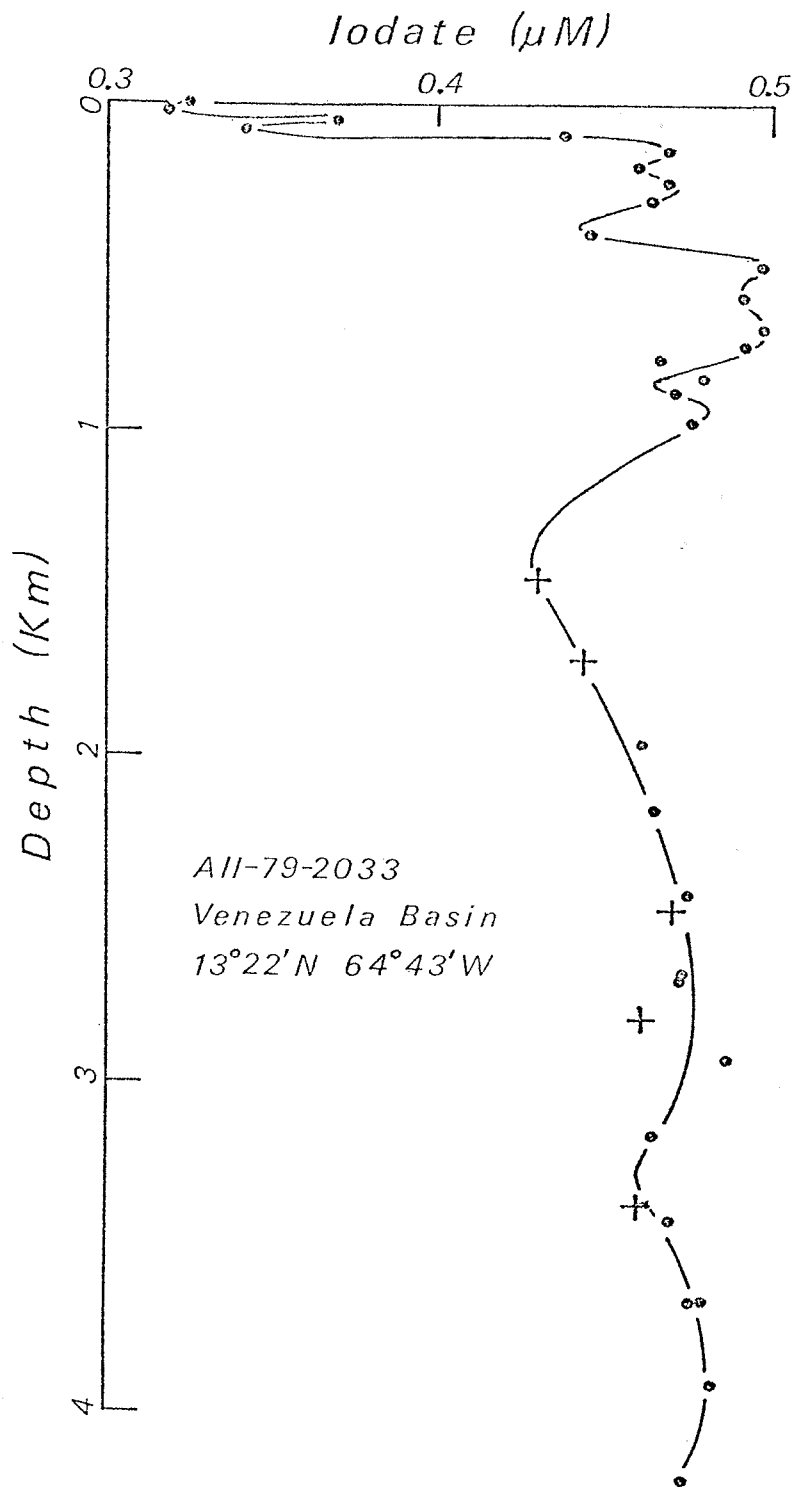
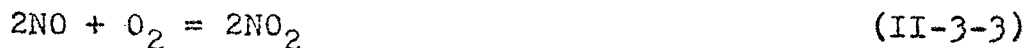
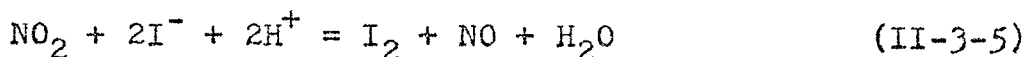


Fig. II-3-3 A profile of iodate determined on board ship.  
+ denote samples stored frozen and analyzed four  
months later.

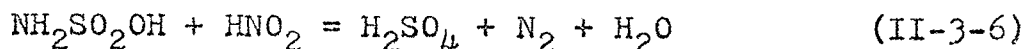
excess potassium iodide added to produce additional tri-iodide ions and yield high results. Furthermore, nitrite can be regenerated from nitric oxide by the reactions



Nitrogen dioxide can also oxidize iodide to iodine in an acidic solution according to the equation



Thus, theoretically, in the presence of acid and even a trace of nitrite, iodide may be continuously oxidized to iodine until it is exhausted. Methods for the removal of this interference have been well studied (Kolthoff and Belcher, 1957). Cohen and Ruchhocht (1941) proposed the use of sulfamic acid for removing nitrite in the Winkler titrations for dissolved oxygen by the reaction



This reaction is rapid and quantitative and the products do not react with any iodine species. Thus, I have adopted the use of sulfamic acid as a precaution against the interference by nitrite.

Nitrite occurs at very low concentrations in the open oceans. In deep waters, its concentration is less than 0.024  $\mu\text{M}$  (Wada and Hattori, 1972). In the surface layers, the concentration is quite variable. I have tested for possible interference in the oxic zone of the Cariaco Trench. I chose two close by samples that were about 100 m

above the oxic-anoxic interface at 158 m and 162 m. Sulfamic acid was added only to the sample at 158 m. The concentrations of iodate of these two samples were found to be 0.463  $\mu\text{M}$  and 0.462  $\mu\text{M}$  respectively and should be considered indistinguishable within the analytical uncertainties. The maximum nitrite concentration in the Cariaco Trench was reported to be 0.6  $\mu\text{M}$  and occurs at a slightly shallower depth (Okuda et al., 1969). It seems likely that the nitrite, because of its extremely low concentrations in the open oceans, will not significantly affect the analysis. However, in the surface layers, nitrite concentrations in excess of 5  $\mu\text{M}$  have been observed (Fiadeiro and Strickland, 1968). Thus, it would be advisable to take proper precautions against an interference from nitrite by destroying it with sulfamic acid.



## II.4 The determination of iodide in sea water by instrumental neutron activation analysis

### II.4.1 Introduction

I have previously reported on the distribution of iodate in sea water (Wong, 1973). In this section, I shall describe a simple and sensitive method for the determination of iodide.

The nuclear characteristics of iodine make it a particularly favorable candidate for instrumental neutron activation analysis. It occurs in nature as the mono-isotopic I-127 with a rather large  $(n,\gamma)$  cross section of 5.6 barns. Upon bombardment with thermal neutrons, I-128 is formed. It has a half life of 25 minutes and undergoes  $\beta$ -decay emitting  $\gamma$  rays with energies of 442.7 KeV, 526.3 KeV and 743.5 KeV and relative intensities of 100:9:1 (Adams and Dams, 1969), and  $\beta$ -particles with energies of 1.13 MeV, 1.67 MeV and 2.12 MeV and relative intensities of 2:16:76 (Wilson, 1966). Instrumental neutron activation analysis has been used extensively to determine the total iodine content of biological (Bowen, 1959; Ohno, 1971; Heurtebise, 1971; Malvano et al., 1972), industrial (Cosgrove et al., 1958; Ballaux et al., 1969) and some meteorological (Duce et al., 1965; Owens and Warburton, 1973; Moyers and Duce, 1974) materials. However, all of these methods involve a post-irradiation separation of iodine from the sample matrix, and because of the short half life

of I-128, the usefulness of the methods is much reduced. I have applied neutron activation analysis to the determination of iodide in sea water. Post-irradiational chemical manipulations of the samples have been eliminated in favor of a simple pre-irradiation separation step. The simplicity and higher sensitivity of this method yield distinct advantages over the existing methods.

The procedure involves a separation of iodide in the sample from iodate, other halides and most other anions by passing sea water through an ion exchange column containing the strongly basic AG 1-x8 resin in the nitrate form. Iodide, being retained in the column, is recovered by eluting the column with a 2 M sodium nitrate solution. The iodide is selectively precipitated from the eluate as palladous iodide in the presence of excess palladous ions using elemental palladium as a carrier. The elemental palladium is produced by reducing some of the excess palladous ions with sodium thiosulfate. The precipitate is filtered and analyzed by instrumental neutron activation analysis.

## II.4.2 Experimental

### II.4.2.1 Reagents

All reagents used were of the analytical reagent grade.

Sodium nitrate solution (2 M). The reagent should be recrystallized so as to be free from iodine. Dissolve 340 g of sodium nitrate in distilled water to form 2 l of solution.

Sodium thiosulfate solution (1.5 mM). Dissolve 0.37 g of sodium thiosulfate pentahydrate and 0.1 g of sodium carbonate in freshly boiled, distilled water to make 1 l of solution.

Standard palladium solution (1 mg Pd<sup>+2</sup>/ml). Dissolve 0.67 g of ammonium chloropalladite in about 150 ml of distilled water. Add 41.7 ml of concentrated hydrochloric acid and dilute to 250 ml.

Standard rubidium sulfate solution (1000 ppm Rb<sup>+</sup>). Dissolve 0.78 g of rubidium sulfate in distilled water and dilute to 500 ml.

Standard potassium iodate solution (10 ug I/100 ul). Dissolve 0.1687 g of potassium iodate in distilled water and dilute to 1 l.

Bio-rad AG 1-x8 resin, 100 - 200 mesh in chloride form.

#### II.4.2.2 Preparation of the ion-exchange column

Transfer about 100 g of the AG 1-x8 resin to an erlenmeyer flask. Add 150 ml of 1:4 (v/v) hydrochloric acid. Swirl the mixture vigorously. Allow the resin to settle and decant the supernatant liquid. Repeat this procedure with 150 ml of distilled water, then 150 ml of 0.5 M sodium hydroxide solution and then with 150 ml of distilled water again. Repeat this cycle three times. Wash the resin once with 150 ml 2 M sodium nitrate solution and store it in 2 M sodium nitrate solution overnight. Pack the resin into glass columns, with an internal diameter of 1 cm, to a length of 11 to 12 cm.

#### II.4.2.3 Flux monitor

Pipette 100  $\mu$ l of the standard rubidium sulfate solution onto a 0.45  $\mu$  47 mm diameter Nuclepore filter. Dry the filter under an infrared lamp. Press the filter into a pellet of size approximately 8 mm in diameter in a stainless steel pellet press as described by Spencer et al. (1972). One of these pellets will accompany each sample or standard throughout the irradiation and counting procedure.

#### II.4.2.4 Standard

Pipette 100 ul of the standard potassium iodate solution onto a 0.45 u 47 mm diameter Nuclepore filter. Dry it under an infrared lamp and then press it into a pellet. Treat the standard exactly the same as a sample pellet.

#### II.4.2.5 Procedure

Pass 250 ml of a sea water sample through the ion-exchange column at a rate of 2 ml/minute using a peristaltic pump to control the flow rate. Wash the column with approximately 5 ml of distilled water. Discard the eluate. Elute the column with a 2 M sodium nitrate solution at the same rate. Discard the first 30 ml of the eluate. Collect the next 80 ml in a 125 ml erlenmeyer flask. Add 1 ml of the standard palladium solution and 2.5 ml of the 1.5 mM sodium thiosulfate solution. Swirl the mixture vigorously and let it sit for 5 minutes. Place the flask in a hot water bath at 80°C for 30 minutes, then allow the mixture to cool. Collect the precipitate by filtering the mixture through a 0.45 u 47 mm diameter Nuclepore filter. Wash the filter with distilled water. Dry the filter in a dessicator for at least two hours. Press the filter into the form of a pellet to give it desirable physical characteristics for neutron irradiation and counting.

Irradiate the sample together with a rubidium flux monitor for 5 minutes in a thermal neutron flux of

about  $4 \times 10^{12}$  n cm<sup>-2</sup> sec<sup>-1</sup>. Let the pellets cool for 30 minutes. Count both pellets for 800 seconds on a Ge(Li) detector coupled with a pulse height analyzer.

A schematic presentation of the procedure is shown in figure II-4-1.

Separation

Co-precipitation

Sample Loading

Elution

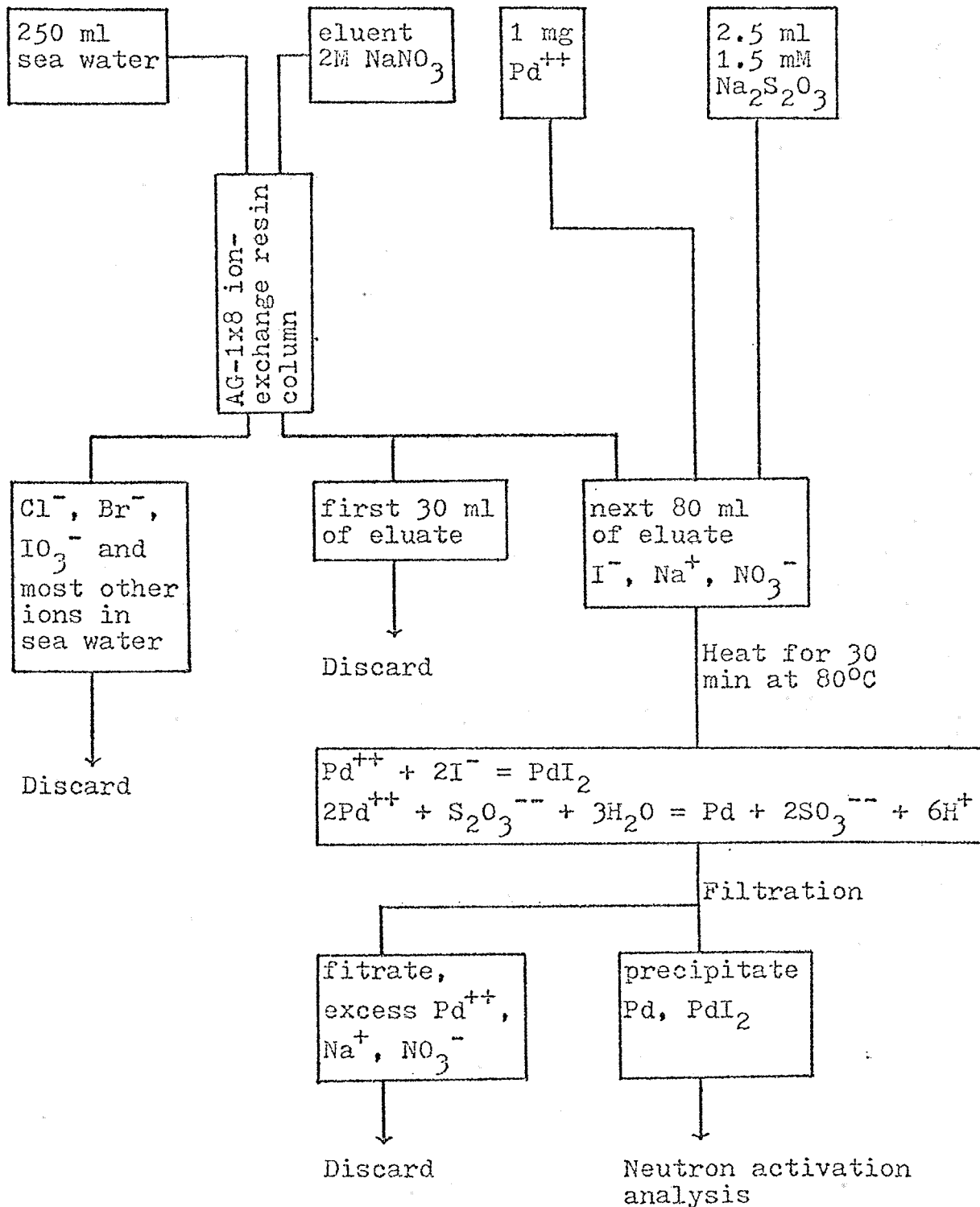
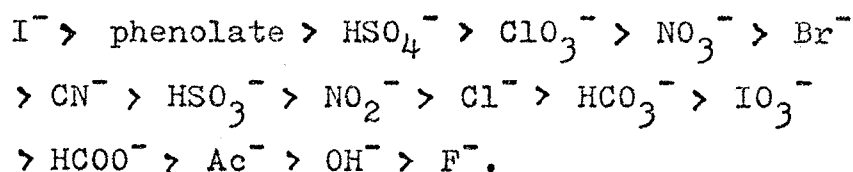


Fig. II-4-1 An analytical scheme for the determination of iodide in sea water.

### II.4.3 Results and discussion

Strongly basic anion exchange columns such as AG 1-x8 have been shown to be a very effective means to separate the halide elements, chloride, bromide and iodide, from each other (Atteberry and Boyd, 1950; Degeiso et al., 1954; Zalevskaya and Starobinets, 1969). Recently, this technique has been used to concentrate iodide from melted snow (Owens and Warburton, 1973). The affinities of the various anions for the resin are in the order (Wheaton and Bauman, 1951):



Thus, when sea water is passed through the column with the resin in the nitrate form, few anions other than iodide will be retained.

I have followed the behavior of iodide during column loading and elution by using both an iodide specific electrode and the radioactive isotope I-125. Figure II-4-2 summarizes the behavior of the halides during the loading and elution of the column. The electrode potential produced by each halide at the concentration used in the experiment differs. Bromide and chloride give a positive electrode potential, whereas iodide at a concentration of  $10^{-6}$  M or



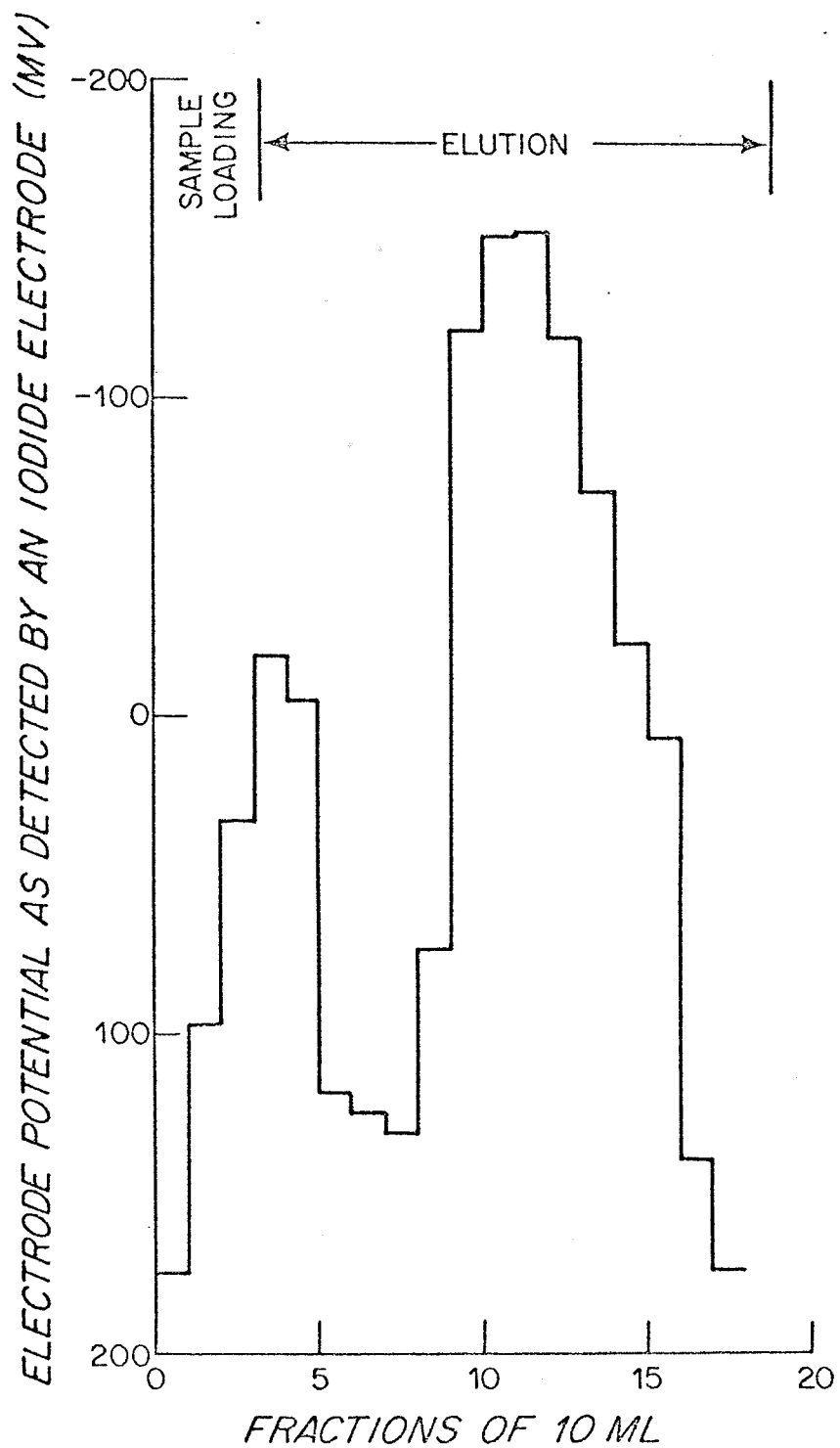


Fig. II-4-2 The loading and elution behavior of halides as determined by an iodide electrode. The sample is a mixture of 25 ml of sea water and 5.3 ml of 1 mM KI. The flow rate is 0.5 ml/min.

above gives a negative electrode potential. By making use of this property, one can readily identify the peaks in the elution diagram. The iodide peak was later further confirmed by radioisotopic studies. As reported in previous work (Atteberry and Boyd, 1950; DeGeiso et al., 1954; Zalevskaya and Starobinets, 1969), chloride and bromide are eluted earlier than iodide. In fact, since the resin is in the nitrate form, a large portion of the chloride and bromide is not retained in the loading process. I have followed the changes in total halide concentration during the loading of 250 ml of sea water onto the column, and the subsequent elution, by potentiometric titration of fractions of the eluate with silver nitrate using the iodide electrode to detect the end-point. The results are summarized in figure II-4-3. Again, they show that most of the chloride and bromide escapes from the column prior to elution. The residual amount is eluted after passing 20 ml of 2 M sodium nitrate solution through the column. I have also used I-125 to study the elution behavior of iodide. I-125 has a half life of 60 days and is a pure  $\gamma$  emitter, emitting  $\gamma$  rays of 35 and 27 KeV. The half life is convenient for tracer use, however, the low  $\gamma$  ray energies cause some counting problems. Figure II-4-4 summarizes the results of such a study. The major portion of the activity is confined to the 10 ml fractions of 6 to 10. Quantitative recovery is ensured by collecting fractions 4 to 11.

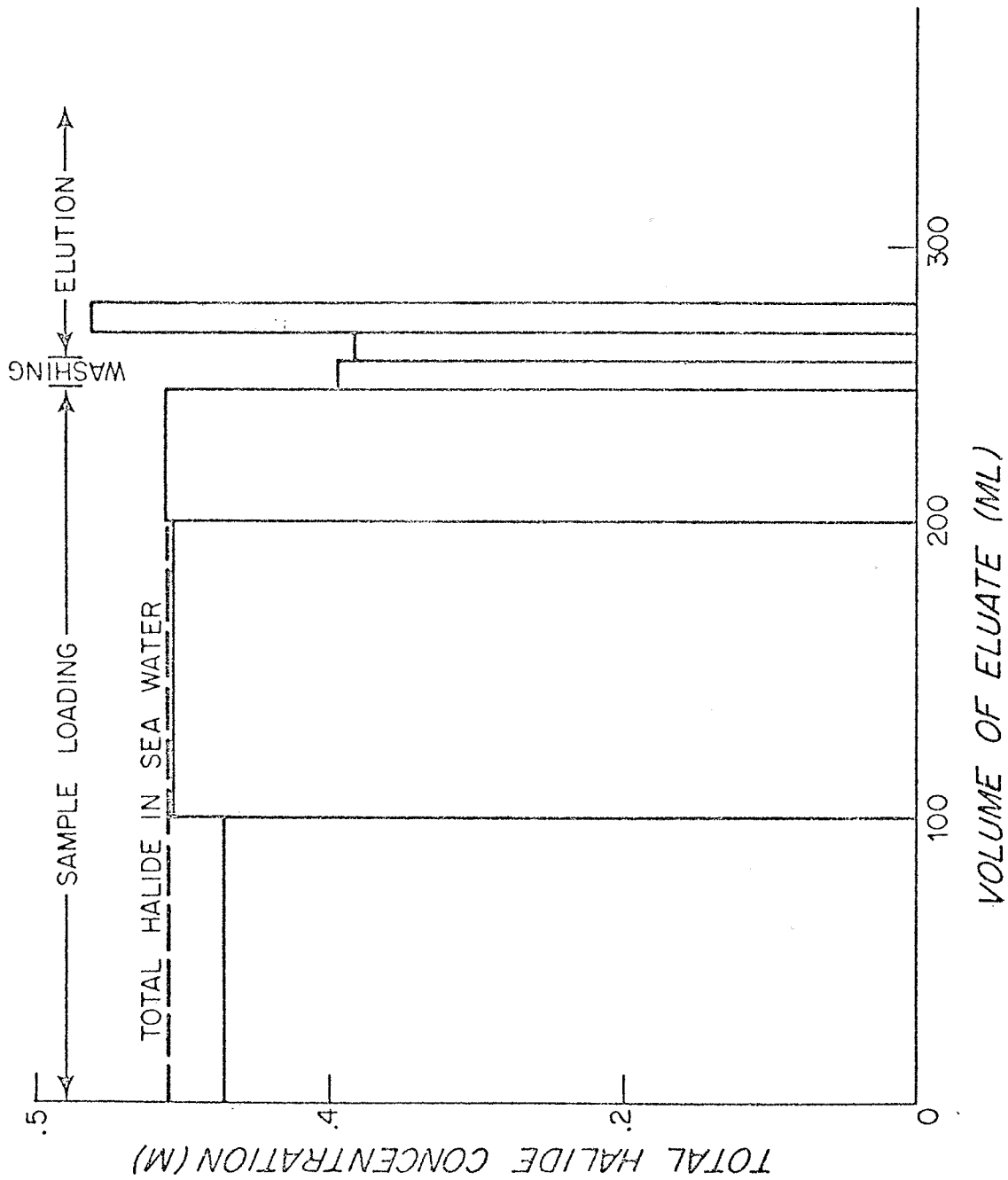


Fig. II-4-3 Changes in the concentration of total halide in the eluate during loading and elution of 250 ml of sea water.

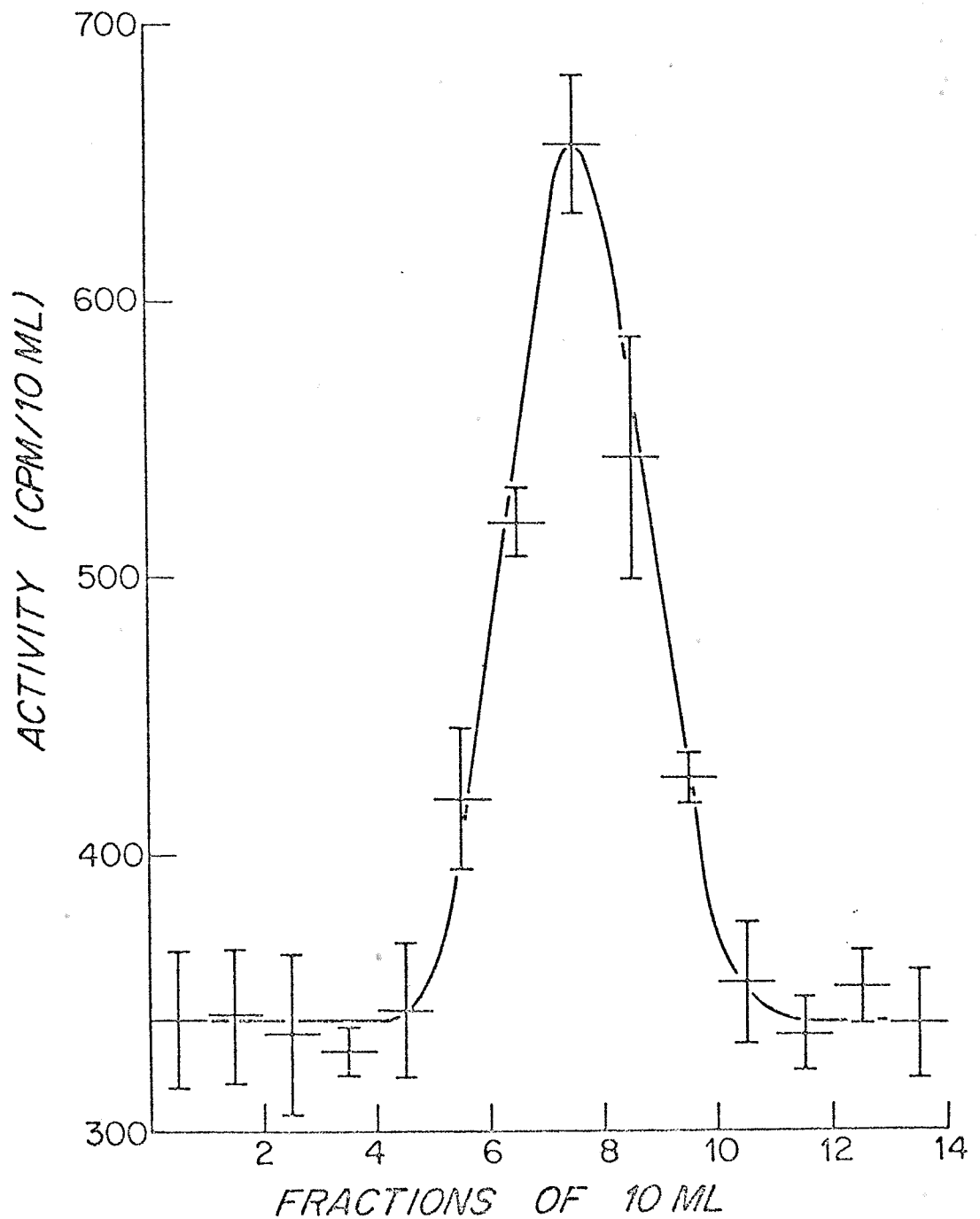


Fig. II-4-4 The elution behavior of iodide from 250 ml of sea water. Error bars show 1 S.D. calculated from three 1 minute counts. Background is  $332 \pm 15$  cpm.

I have also studied the ion exchange capacity of the column for iodide. The results are shown in figure II-4-5. After passing 1 l of sea water (four times the sample size) through the column, the capacity has not yet been reached and break through does not occur.

Palladous ion is a well known selective precipitant for iodide (Winkler, 1918; Vogel, 1953) in the presence of bromide and chloride. However, in producing elemental palladium as the co-precipitant, care must be taken to control the amount of reducing agent used. Excess thio-sulfate will slowly reduce palladous iodide causing poor and variable yield. Thus, an excess of palladous ions should always be maintained and this is evident from the persistence of the slight straw yellow color in the supernatant liquid. The elemental palladium thus produced forms large spongy clumps and is ideal for separation by filtration.

I have tested the yield of this procedure using the radioactive isotope by comparing the activities in sample pellets and in standards. The standard is prepared by adding carrier iodide to the same amount of tracer and then precipitating the iodide as palladous iodide with excess palladous ions. Table II-4-1 shows the results of the study. The three samples gave activities that, within the counting and handling uncertainties, were indistinguishable from the standards.

Since palladium is used as the precipitant and

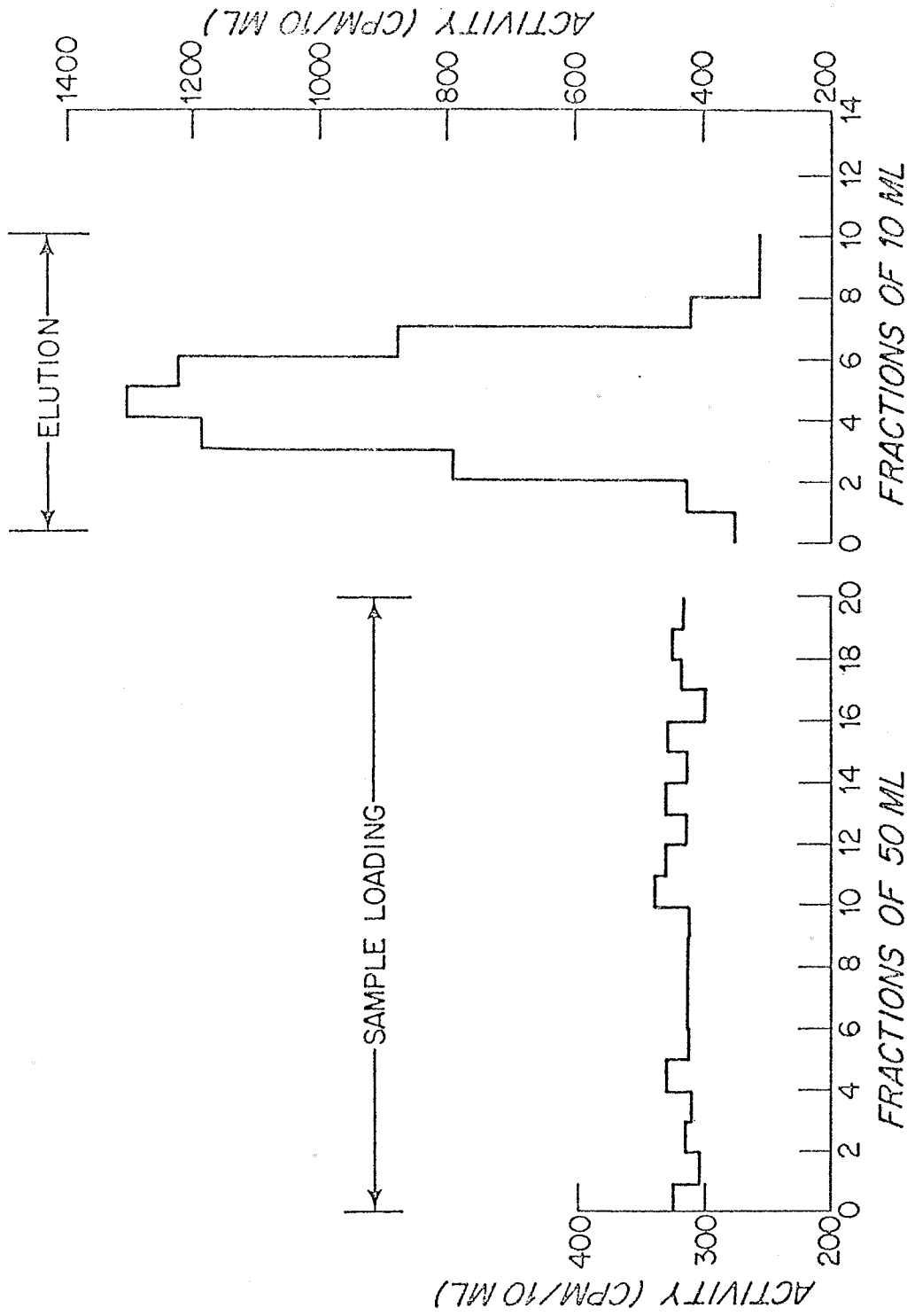


Fig. II-4-5 Test of the ion-exchange capacity of the column during loading and elution of 1 liter of sea water. Background is  $304 \pm 14$  cpm.

Table II-4-1 Check of recovery of added radiotracer from  
sea water

	*Activity (cpm)	Mean	A.D.
Woods Hole Surface Water	1. 2010, 2059, 2012	2027	21
	2. 1979, 1951, 2072	2001	48
	3. 2001, 1990, 2008	2000	6
Mean of 3 samples		2009	26
Standards	1. 2045, 1980, 1968	1998	32
	2. 1929, 1942, 1918	1930	8
	3. 1918, 1932, 1970	1940	20
Mean of 3 standards		1956	31
% Recovery		103%	

\* The figures for each sample represent three consecutive one-minute counts.

A.D. - Average deviation.

one of its stable isotope (Pd-108) has a large thermal neutron cross section of 12 barns, dead time can present a serious counting problem. Natural palladium contains 26.7% of Pd-108. During neutron activation, Pd-108 is transformed to Pd-109m or Pd-109. Pd-109m decays to Pd-109 with a half life of 4.75 minutes by emitting  $\gamma$ -rays of 188.9 KeV (Adams and Dams, 1969). Pd-109 in turn decays to Ag-109 with a half life of 13.5 hours via  $\beta$ -decay and emits  $\gamma$ -rays of 88 KeV and 311.5 KeV in the process. I have minimized the amount of palladium in the precipitate to the least amount that can be easily handled. A relatively long cooling period of 30 minutes is used. In addition, I have used pellets containing a rubidium standard for each sample or iodide standard as a dead time and neutron flux monitor.

Figure II-4-6 shows the  $\gamma$ -ray spectra of a blank filter, a standard iodate-iodine sample and a Woods Hole surface water sample. The major  $\gamma$  peaks are identified on the spectra. The region around the iodine  $\gamma$  peak of 442.7 KeV is expanded in figure II-4-7. The blank is insignificant and for all practical purposes can be ignored. In the sample, the peak shows no shoulder, suggesting no spectral interferences within the resolution of the detector (2.5 KeV FWHM for Co-60 1.33 MeV gammas). The ratio of the photo-peaks at 442.7 KeV, 526.3 KeV and 743.5 KeV in the standard and the sea water sample are 100:7.4:0.7 and 100:7.6:0.5 respectively. They agree with each other well. This further



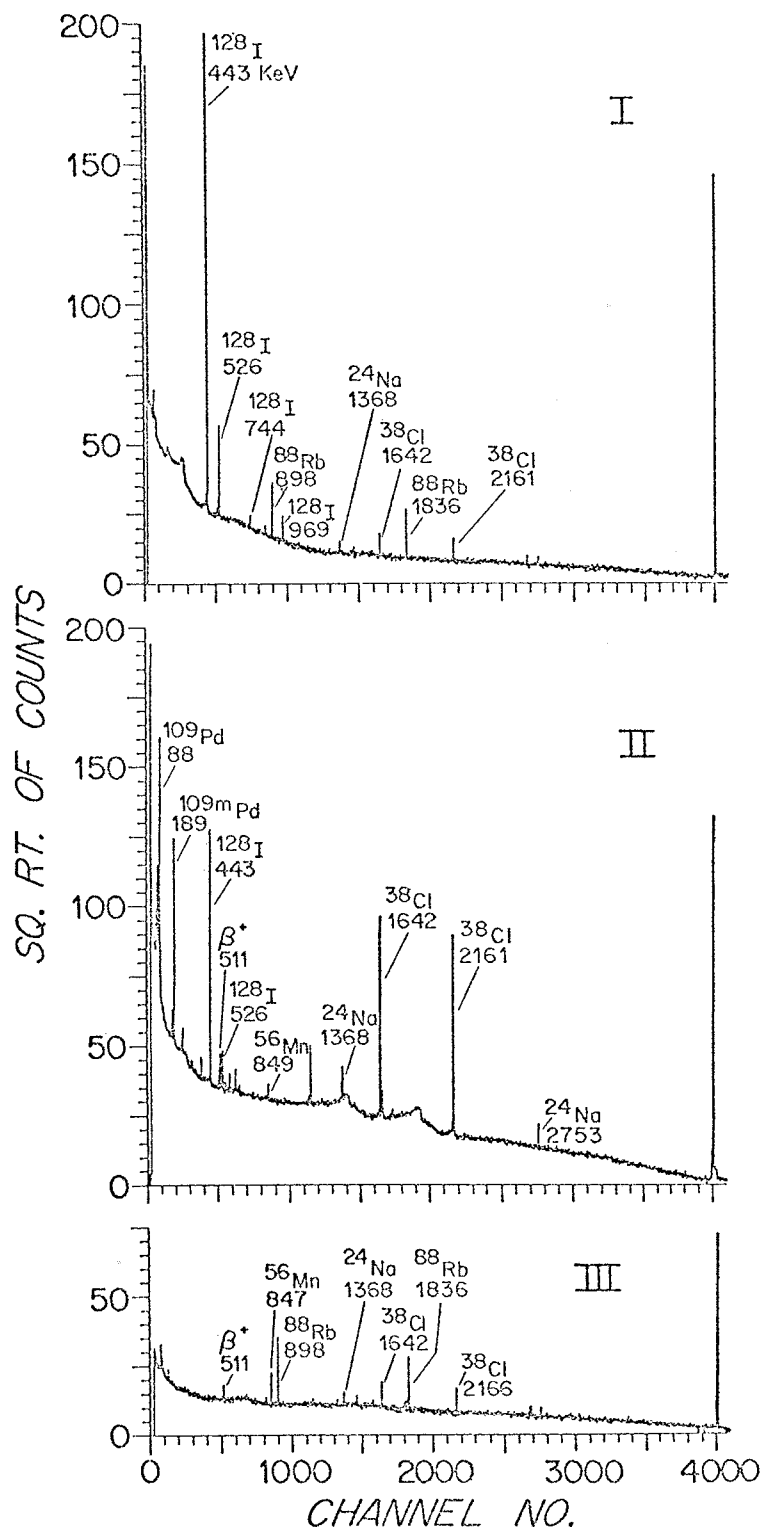


Fig. II-4-6 The  $\gamma$ -ray spectra of a standard iodate-iodine sample (I), a Woods Hole surface water sample (II) and a blank filter (III). Energies of major  $\gamma$  peaks are given in KeV.

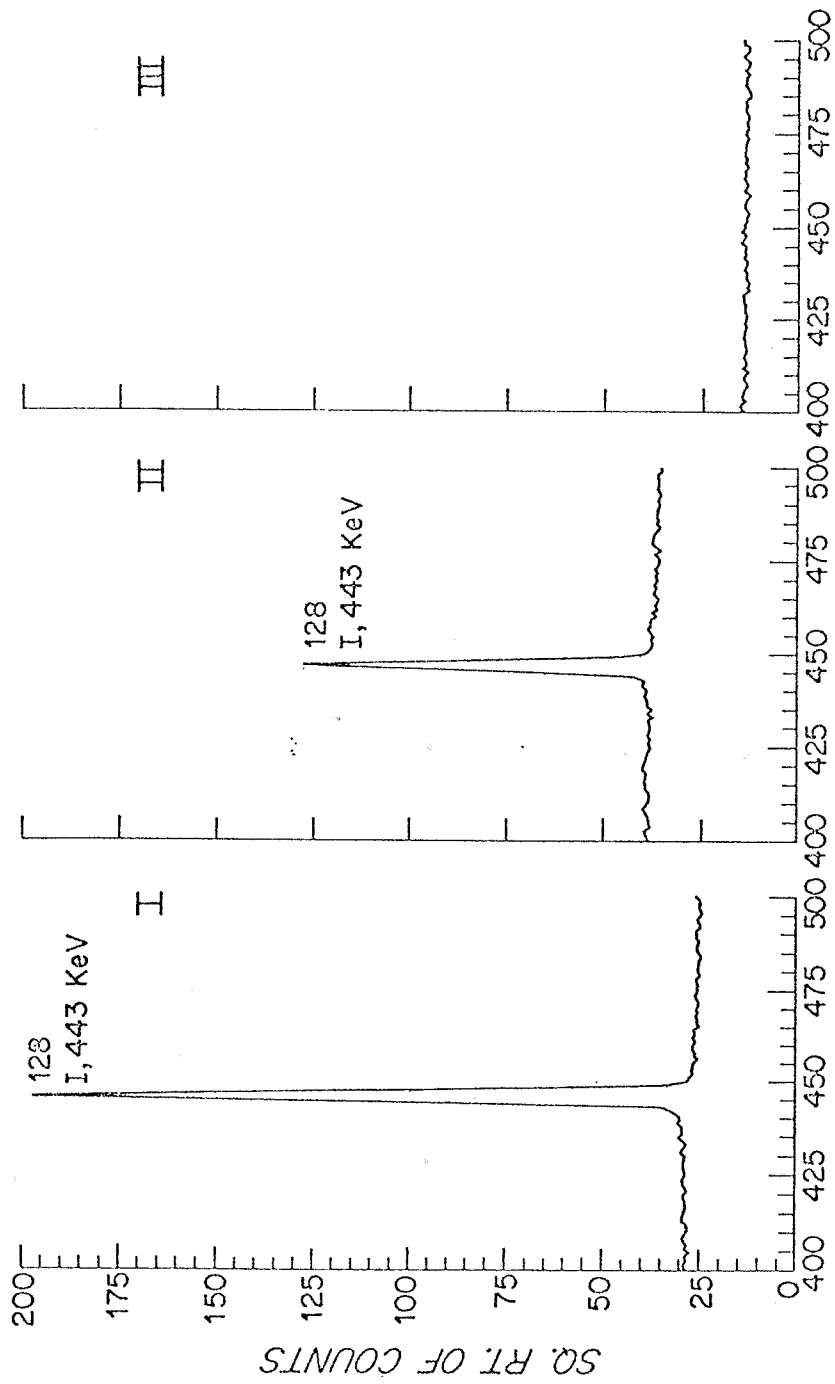


Fig. II-4-7 The region around 442.7 KeV of the  $\gamma$ -ray spectra of a standard iodate-iodine sample (I), a Woods Hole surface water sample (II) and a blank filter (III).

suggests that there are no spectral interferences.

The reagent blank from the sodium nitrate solution has been determined five times. The results are shown in table II-4-2. The average reagent blank is 0.0046  $\mu\text{M}$  with a standard deviation of 0.00145  $\mu\text{M}$ .

The iodide concentrations in three sub-samples from one sample of surface water collected near Woods Hole were determined by this method. The results are shown in table II-4-3. The average concentration including the reagent blank is 0.123  $\mu\text{M}$  and the standard deviation is 0.006  $\mu\text{M}$ . This precision is better than or comparable to the precision of the presently available methods (for example, Tsunogai, 1971b).

Figure II-4-8 shows a profile of dissolved iodide from near surface waters in the Equatorial Atlantic. As in other parts of the oceans (Tsunogai, 1971b; Tsunogai and Henmi, 1971), the iodide concentration is highest at the surface and decreases rapidly with depth to an almost constant level of less than 0.01  $\mu\text{M}$ . The absolute concentrations agree well with others reported in the literature (Tsunogai, 1971b; Tsunogai and Henmi, 1971). The smoothness of the profile is as expected and gives confidence in the reliability of the method. The data presented here have not been corrected for the reagent blank. The three data points from 400 m to 750 m have an average concentration of 0.007  $\mu\text{M}$  which is indistinguishable from the blank of 0.005  $\mu\text{M}$ . This shows

Table II-4-2 Reagent blank of the instrumental neutron  
activation analysis of iodide in sea water

Trial	Blank Concentration (uM)
1	0.0037
2	0.0068
3	0.0052
4	0.0042
5	0.0031
Average blank	0.0046 S.D. ( $1\sigma$ ): 0.00145 uM

Table II-4-3 Precision of repeated analysis of Woods Hole  
Surface Water

Trial	Concentration* ( $\mu\text{M}$ )	
1	0.116	
2	0.125	
3	0.127	
Average concentration	0.123	S.D. ( $1\sigma$ ): 0.006 $\mu\text{M}$

\* The concentration includes the reagent blank.

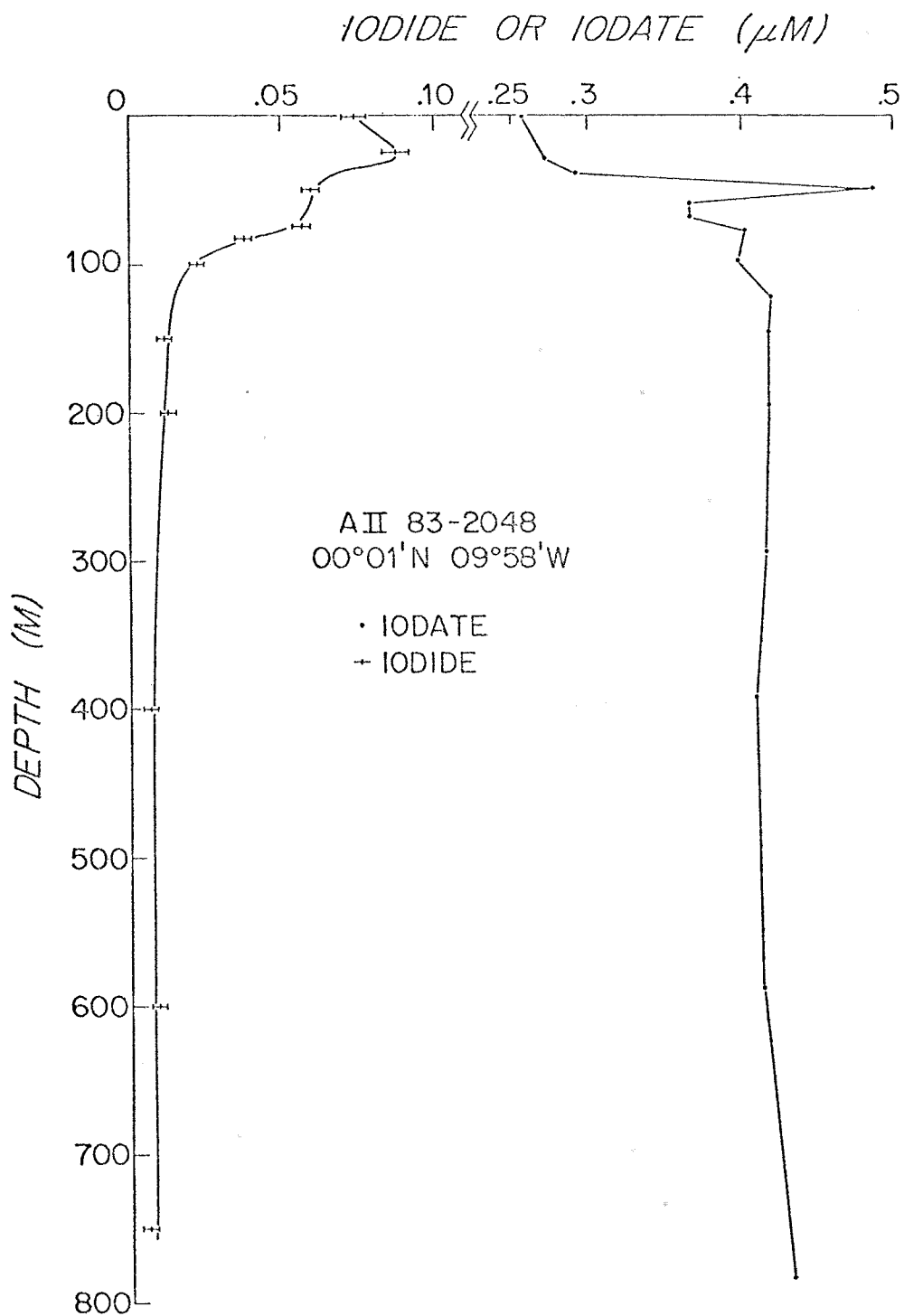


Fig. II-4-8 Iodide (+) and iodate (.) profiles at 00° 01' N and 09° 58' W. Error bars in iodide profile represent 5% uncertainty.

that there is no serious contamination problem during the pre-irradiation manipulations.

## II.5 The determination of iodine in marine suspended matter

### II.5.1 Introduction

Previous studies have demonstrated the bio-active nature of iodine (Bowen, 1966; Sugawara and Terada, 1967; Tsunogai and Sase, 1969) and I have briefly discussed its biogeochemistry in section I.2.4. My own study also indicates a slight depletion of total dissolved iodine in surface waters of the oceans. This evidence suggests that a significant portion of iodine may be present in the particulate form like the other micro-nutrients such as nitrogen and phosphorus (Menzel and Ryther, 1964; Holm-Hansen et al., 1966; Hobson and Menzel, 1969; Holm-Hansen, 1972). Thus, a knowledge of the heretofore unknown distribution of particulate iodine may be essential for a better understanding of the geochemical cycling of iodine in the oceans.

Neutron activation analysis has frequently been used for the determination of the bulk chemical composition of suspended matter because it is non-destructive; it has high sensitivity for many elements; and it gives a multi-element analysis (Spencer et al., 1972). I have extended this method to the determination of iodine in marine suspended matter as iodine also has many favorable nuclear characteristics for neutron activation analysis as described in section II-4-1.



## II.5.2 Experimental

### II.5.2.1 Reagents

All reagents used were analytical reagent grade.

Standard potassium iodate solution (1 ug I/100 ul). Dissolve 0.1687 g of potassium iodate in distilled water and dilute to one liter. Further dilute this stock solution ten fold to form the standard solution.

Standard rubidium sulfate solution (100 ppm  $Rb^+$ ). Dissolve 0.78 g of rubidium sulfate in distilled water and dilute to 500 ml. Dilute 25 ml of this stock solution to 250 ml.

### II.5.2.2 Sampling

For each sample, about 10 l of sea water was filtered by air pressure through a pre-weighed Nuclepore filter (0.6 u pore size, 37 mm in diameter) immediately after sample collection. Incoming air was filtered and passed through non-metallic lines to avoid contamination. The filter was carefully rinsed with distilled water to remove sea salt and then stored in a clean plastic box.

### II.5.2.3 Sample preparation for irradiation

The filter is equilibrated in a room at constant humidity. Then, it is pressed into a pellet by using a hand press in order to minimize geometry problems and to increase its resistance to irradiation damage and fragmentation during analysis. The resulting pellet is approximately 4 mm x 1 mm. Filter blanks are prepared identically.

### II.5.2.4 Standard

Pipette 100 ul of the standard potassium iodate solution onto a 0.6 u 37 mm diameter Nuclepore filter. Dry it under an infrared lamp and then press it into a pellet. Treat the standard exactly the same as a sample pellet.

### II.5.2.5 Flux monitor

Pipette 100 ul of the standard rubidium sulfate solution onto a 0.6 u 37 mm diameter Nuclepore filter. Dry the filter under an infrared lamp. Press the filter into a pellet. One of these pellets will accompany each sample or standard throughout the irradiation and counting procedure.

#### II.5.2.6 Irradiation and data processing

Irradiate the sample together with a rubidium flux monitor for 10 minutes in a thermal neutron flux of about  $4 \times 10^{12}$  n cm<sup>-2</sup> sec<sup>-1</sup>. Let the pellets cool for 5 minutes. Count both pellets simultaneously for 800 seconds on a Ge(Li) detector coupled with a pulse height analyzer. Analyses of the spectra are carried out via magnetic tape and the computer program GAMANL. Upon irradiation, the radioactive I-128 is formed from the monoisotopic stable natural I-127. It decays with a half life of 25 minutes and its gamma ray with an energy of 443 KeV is used for analyses.

### II.5.3 Results and discussion

The spectra of a standard pellet and a sample are shown in figures II-5-1 and II-5-2. The major photopeaks are identified on the spectra. The ratios of the major photopeaks of I-128 at 443 KeV, 526 KeV and 744 KeV in the standard and the sample are 100:7:1 and 100:6:1 respectively. The peak at 443 KeV which is used for calculating the iodine concentrations shows no shoulder. This evidence suggests that there are no detectable spectral interferences within the resolution of the detector (2.5 KeV FWHM for Co-60 1.33 MeV gammas).

Since neutron activation analysis is such a sensitive method, blanks may constitute a serious problem. For analyses of suspended matter, the filter blank is the major source of uncertainty. Since no chemical treatment is involved, there is no reagent blank. In the method reported here, iodine impurities in the rubidium sulfate which acts as the flux monitor will be included as a blank too. The results of a series of tests are shown in table II-5-2. The blank for iodine is quite variable even within one batch of filters. The average blank for batch #2718 is about 3 ng with a standard deviation of 51%. Since about 10 l of sea water was processed for each sample, this blank is equivalent to about 0.3 ng-I/kg. In an earlier batch I observed no detectable blank from the filters. The magnitude of the blank is small relative to the sample concentrations in surface waters where concentrations above 10 ng/kg are frequently encount-

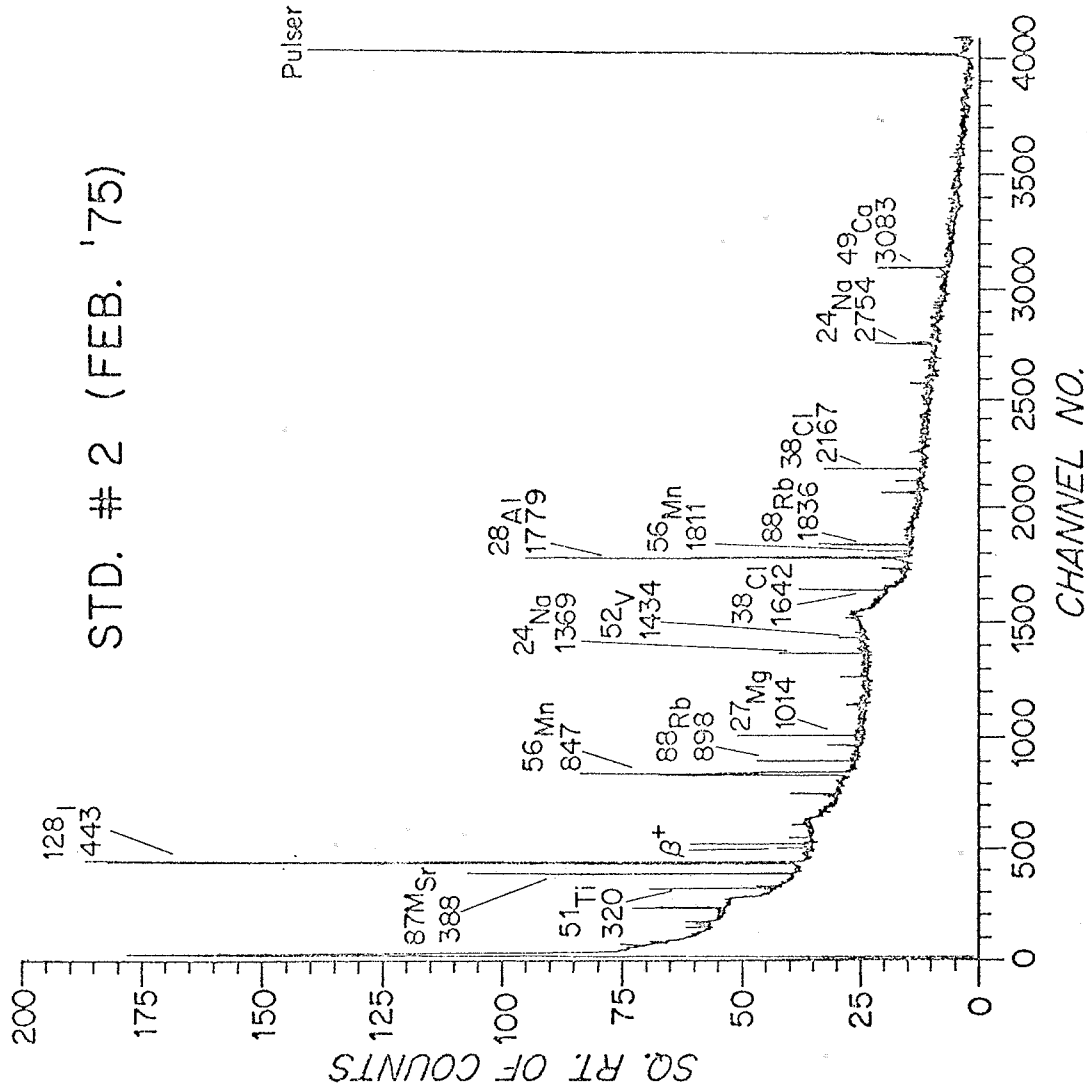


Fig. II-5-1 The  $\gamma$ -ray spectrum of a standard. Energies of the major  $\gamma$  peaks are given in KeV.

STA. 60 2270 M

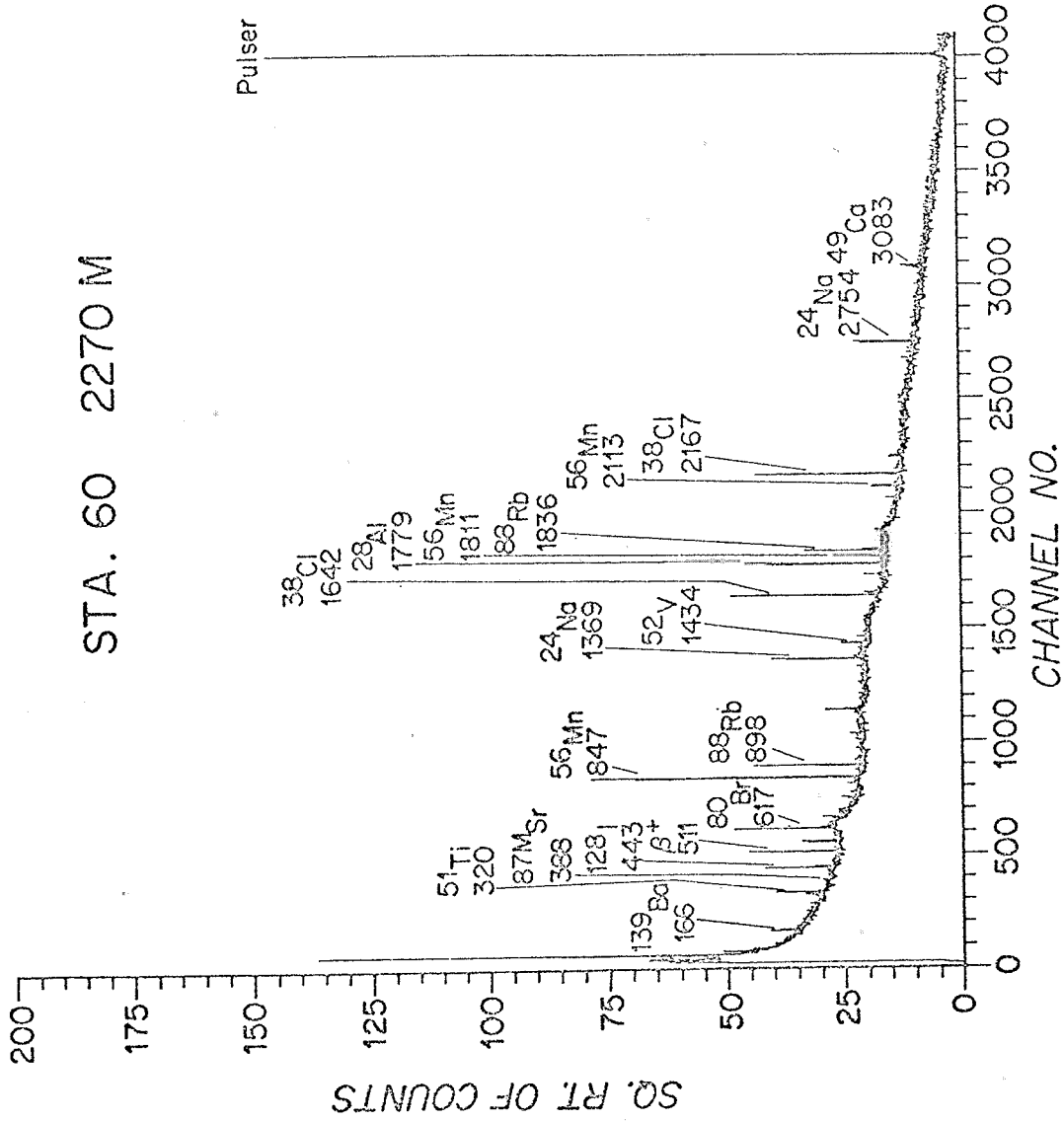


Fig. II-5-2 The  $\gamma$ -ray spectrum of a sample of marine particulate matter. Energies of the major  $\gamma$  peaks are given in KeV.

Table II-5-1 Blanks in the neutron activation analysis of particulate iodine<sup>+</sup>

Sample description	Counts per 800 sec.	Average	$\sigma$ %	Equivalent I content (ng)
I. GESECS sample blanks				
A. Without Rb pellet	402, 365	388	--	2.8
B. With Rb pellet	382, 496	439	--	3.2
II. Standard and Rb blanks				
Filter batch #2718	299, 782, 419 368, 284, 730 223, 281	423	51	3.0

+ Counts per 800 seconds for blanks from both standard and sample filters. All counts pulser corrected for dead time.

ered. However, in deep waters, the blank may be significant since the concentrations in the samples drop to about 1 ng/kg. Thus, proper cautions must be taken in interpreting small changes in concentration in the deep waters.

As a short cooling time is used, dead time is another possible problem. Residual sea salt on the filter can cause high dead time and consequently high counting uncertainties. Countings were made based on clock time. At first, dead time corrections were calculated from the mean value by the dead time meter. Later on, the pulser counts accumulated in channel 4000 which also served as an energy calibration was used. The pulser gives a signal fed into the analyzer at the rate of 60 cps. The difference between the observed and preset counts will be the sum of the dead time losses. A further improvement was made by using the area of the major peak of the rubidium sulfate flux monitor. Since the same amount of rubidium is used each time, the difference in counts between samples and standards can be used to correct for dead time losses as well as geometry differences and flux variations.

Since the half life of I-128 (25 minutes) is short, the irradiation technique used permits the irradiation of only one sample at a time. Standards were irradiated periodically each day and the iodine contents in the samples are calculated by comparing their activities to those of the standards. This procedure assumes a constant neutron flux and negligible geometry differences between



standards and samples. The consistency of the neutron flux is checked by the Rb flux monitor which accompanies each sample during irradiation and the results are shown in table II-5-2. Over a six months period, the fluctuations were of the order of  $\pm 4\%$ . Most of this variation can probably be attributed to counting errors.

The reproducibility of the method has also been checked by repeated analyses of one set of samples over a one year time span. The results are presented in raw counts in table II-5-3. The agreement is excellent with a correlation coefficient of 0.97 and a slope of 1.00.

The contribution of residual sea salt to the measured concentrations of particulate iodine can be easily estimated. The iodine to salinity ratio in sea water is  $1.7 \times 10^{-6}$  (w/w) (Brewer, 1975). Total suspended matter in the oceans measured by the present collection method is usually less than 0.03 mg/kg. Even if it is 100% sea salt, the iodine content will only correspond to 0.05 ng/kg which is much lower than the observed concentrations of  $> 1$  ng/kg. Since the residual sea salt should only be a minor portion of the total suspended matter, the contribution from sea salt should be minimal and the iodine content of the material retained on the filter should represent the true concentration of iodine in marine suspended matter.

Figure II-5-3 shows a profile of particulate

Table II-5-2 Check on flux and geometry variations<sup>+</sup>

Date irradiated	Identity	899 KeV		Rb Counts 1836 KeV		Counting ± error	Pulsar	Pulsar Corrected Rb Counts 1836 KeV	
		KeV	± error	KeV	± error			KeV	± error
Feb 26, 1975	STD#1 (2'75)	3378	5.5%	2460	3.3%	39343	4121	3001	
	STD#2 (2'75)	3404	2.9%	2747	3.1%	41788	3910	3155	
	STD#1 (2'75)	3388	4.9%	2489	3.6%	38887	4182	3072	
	STD#2 (2'75)	3752	3.4%	2637	3.2%	42687	4219	2965	
Apr 16, 1975	STD#1 (2'75)	3438	4.1%	2324	3.7%	39944	4131	2793	
	STD#1 (2'75)	3454	3.1%	2669	3.2%	42346	3915	3025	
	STA.60-65m	3449	3.3%	2445	4.4%	40549	4083	2894	
Apr 17, 1975	STD#1 (2'75)	3872	4.5%	2642	3.2%	39990	4647	3171	
	STD#2 (2'75)	3716	3.3%	2754	3.3%	41968	4250	3150	
	STA.60-928m	3513	3.7%	2920	4.6%	40003	4215	3504	
June 3, 1975	STA.60-4324m	3698	4.5%	2431	4.1%	39238	4524	2974	
	STD#1 (2'75)	3476	5.5%	2534	3.9%	39689	4204	3065	
	STD#2 (5'75)	3993	2.8%	2739	2.9%	41293	4642	3184	
	STA.54-4883m	3535	3.6%	2516	3.5%	41484	4090	2911	

+ 10 ugRb2SO<sub>4</sub> standard.

Table II-5-2 Check on flux and geometry variations (continued)

Date Irradiated	Energy (KeV)	Mean (Counts per 800 sec.)	Standard Deviation (%)	Average Counting Error (%)
Feb 26, 1975	899	4108	3.4	4.2
	1836	3048	2.8	3.3
Apr 16, 1975	899	4043	2.8	3.5
	1836	2904	4.0	3.8
Apr 17, 1975	899	4409	4.8	4.0
	1836	3200	6.9	3.8
June 3, 1975	899	4312	6.7	4.0
	1836	3053	4.5	3.4
Meas Feb-June (using daily mean)	899	4218	4.1	
	1836	3051	4.0	

Table II-5-3 - Reproducibility of sample counts<sup>+</sup>

Depth (m) <sup>#</sup>	1974 <sup>*</sup>	1975 <sup>*</sup>
40	2707	2508
101	2831	3144
152	2771	2606
202	3472	4292
303	5867	5518
395	5699	6206
549	3066	3525
622	3463	4061
787	1944	1999
1100	1890	2182
1404	1219	1671
2712	1751	1754
2906	1492	1753
3102	1549	1552
3295	1610	1916
Correlation coefficient	0.97	
Slope	1.00	
Intercept	232	

+ Counts are raw counts per 800 seconds.

# Samples from GEOSECS station 17.

\* First irradiation was performed in April/May 1974 (x) and re-irradiation was performed in Jan./Feb. 1975 (y).

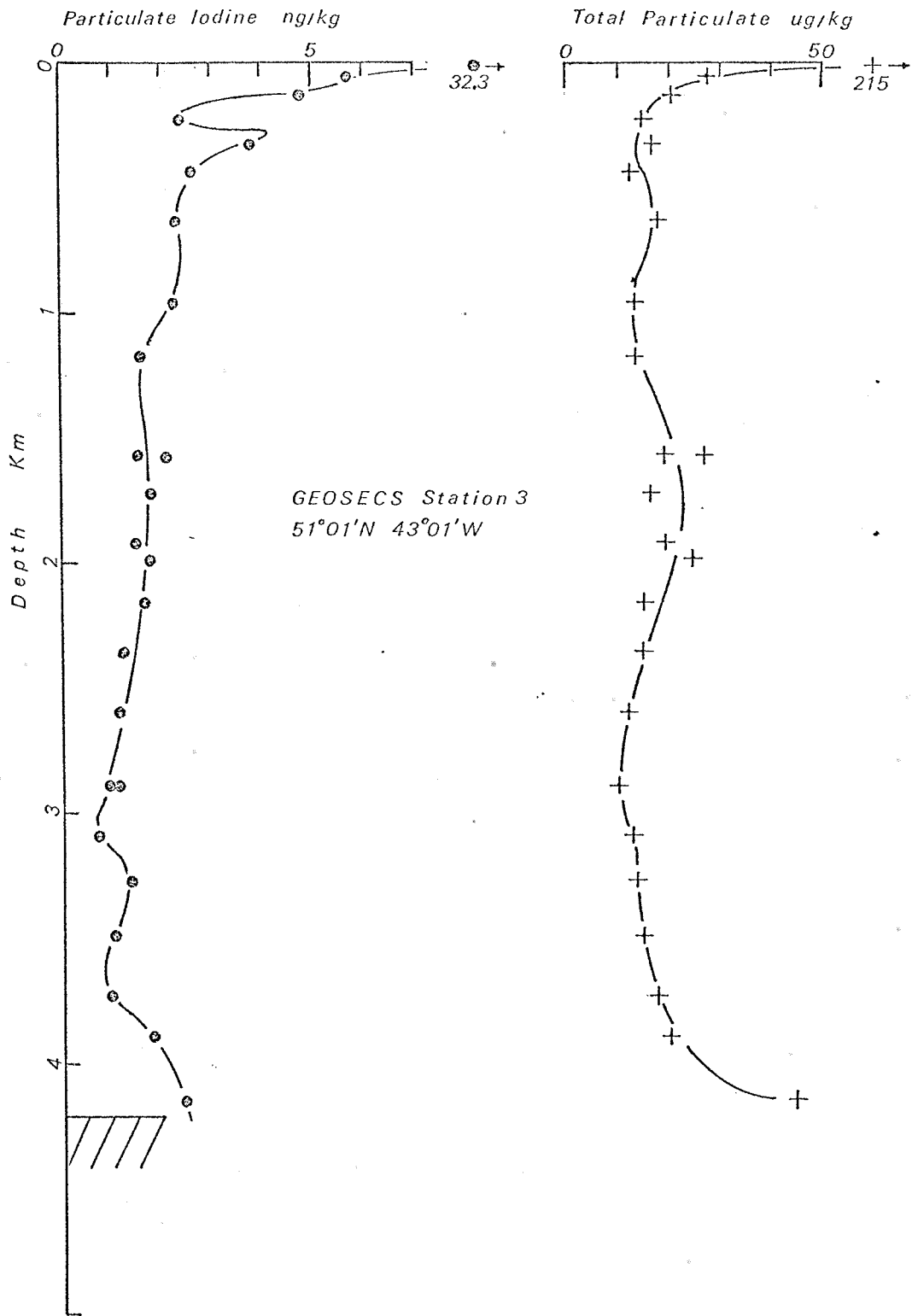


Fig. II-5-3 A profile of particulate iodine in the North Atlantic.

iodine in the North Atlantic. A concentration maximum is observed in the surface waters. Below this maximum, the concentration decreases rapidly with depth to a background level in the deep water of about 1 to 2 ng/kg. A slight increase in concentration is also observed in the bottom water. Duplicate samples obtained at 2890 m give concentrations of 1.1 and 0.9 ng/kg. The average deviation of these two samples ( $\pm 0.1$  ng/kg) is small and is well within the variability of the blank. The profile is remarkably smooth and all the features can be explained with our present oceanographic knowledge as discussed in section III.4.

CHAPTER III. FIELD OBSERVATIONS

### III.1 The distribution of iodine in the upper layers of the Equatorial Atlantic

#### III.1.1 Introduction

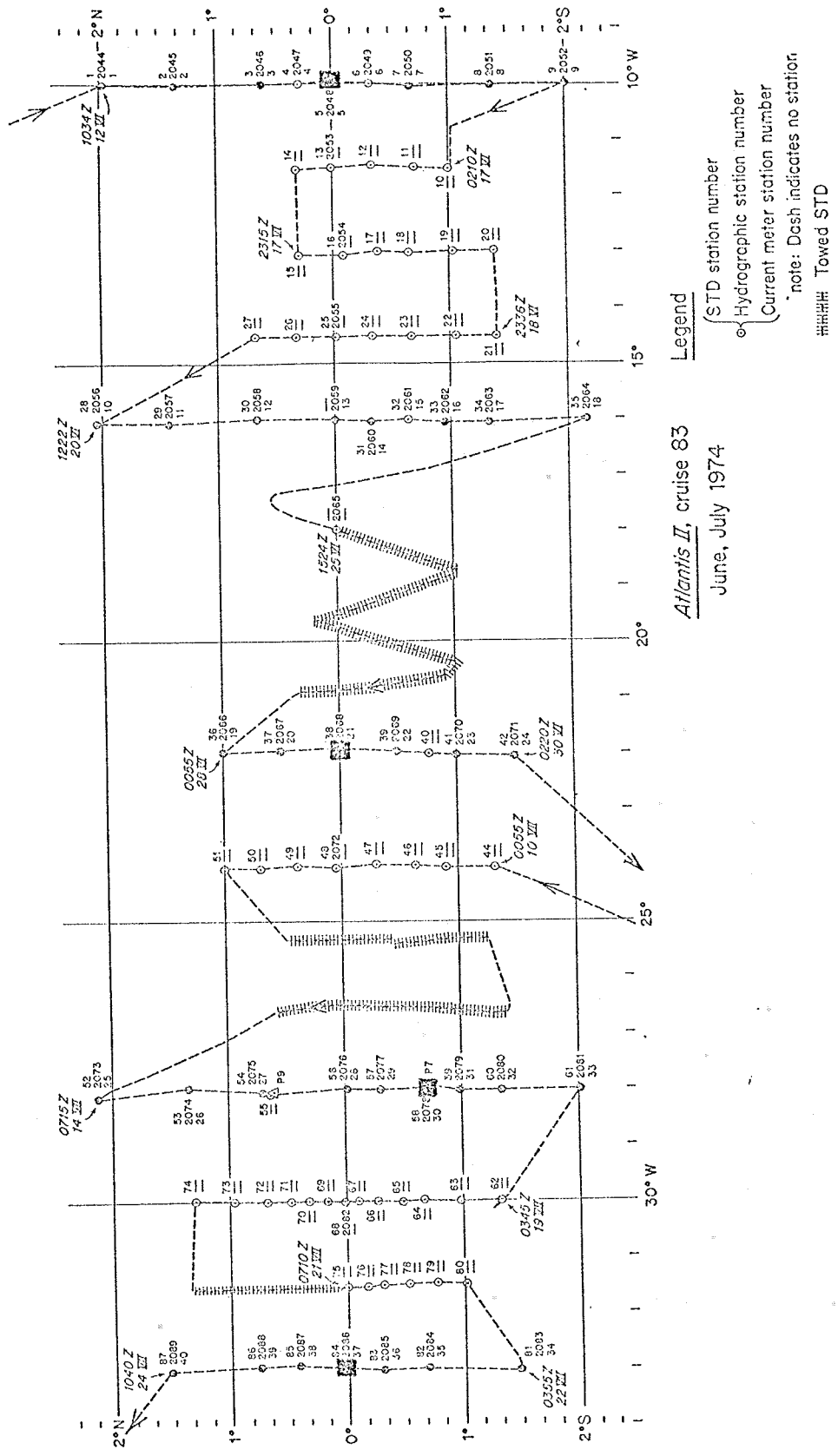
The marine biogeochemistry of iodine has been briefly discussed in section of I.2. In this section, I shall report the distribution of iodate and iodide in the Equatorial Atlantic. The Equatorial Atlantic is one of the more productive regions in the open oceans (Ryther, 1963; Koblentz-Mishke et al., 1970). The primary productivity is generally in the range of 150 to 500 mg C/m<sup>2</sup>/day. In the upwelling areas along the African coast, values above 1000 mg C/m<sup>2</sup>/day have been reported (Corcoran and Mahnken, 1969). This region is also characterized by large salinity and temperature gradients in the upper layers and is thus strongly stratified (Metcalf et al., 1962; Metcalf and Stalcup, 1967). Consequently, vertical mixing is much restricted and the characteristics resulting from biological-chemical interactions may be amplified and preserved. With closely spaced samples and closely spaced stations, I have attempted to study the finer structure in the distribution of iodine in the upper layers of the oceans.



### III.1.2 Sampling and analytical method

Sea water samples were collected from the Equatorial Atlantic during cruise AII-83 of the R/V Atlantis II during the GARP (Global Atmospheric Research Program) Atlantic Tropical Experiment (gate). Five transects were made between 2°N and 2°S along the longitudes 33°W, 28°W, 22°W, 16°W and 10°W. The cruise track and the locations of the stations are shown in figure III-1-1. Samples from stations 2044-2046, 2048, 2050-2052, 2056-2060, 2062-2064, 2066-2071, 2073-2081 and 1083-2089 were analyzed for iodate. Samples from stations 2048, 2068, 2078 and 2086 were analyzed for iodide as well.

The samples were analyzed for iodate on board ship by a colorimetric method modified from the titration method (Wong and Brewer, 1974) as described in section II.3. The precision of the method is about  $\pm 3\%$ . Samples for iodide analysis were frozen immediately after sampling and were shipped to Woods Hole for later analysis by neutron activation analysis as described in Wong and Brewer (1976) and in section II.4. The precision of the method is  $\pm 5\%$  and the reagent blank is about 0.005  $\mu\text{M}$ . The iodide data reported here have not been blank corrected. The complete listing of iodate and iodide measurements is compiled in Appendix A. Detailed hydrographic data may be obtained from Bruce and Katz (1976).



Atlantis II, cruise 83  
June, July 1974

Fig. III-1-1 The cruise track and station locations of cruise AII-83. Solid circles denote stations with iodate data. Solid squares denote stations with both iodate and iodide data.

### III.1.3 Results and discussion

Figure III-1-2 shows the distribution of iodate from the surface to 200 m depth in a zonal section along the equator. The most prominent feature is the low iodate concentration in the upper 30 to 40 m. The iodate concentration in this region is less than 0.30  $\mu\text{M}$ . A concentration less than 0.10  $\mu\text{M}$  was observed at station 2079 ( $1^{\circ}\text{S}$ ,  $28^{\circ}\text{W}$ ). Below 140 m, the iodate concentration is uniformly higher at about 0.40 to 0.45  $\mu\text{M}$ . At  $33^{\circ}\text{W}$  the concentration below 120 m approaches 0.50  $\mu\text{M}$ , similar to deep water concentrations in the South Atlantic (Wong and Brewer, 1974). The lower iodate concentrations in the surface waters of the Equatorial Atlantic, relative to that in the Argentine Basin (0.39 to 0.40  $\mu\text{M}$ , Wong and Brewer, 1974), probably reflect the higher productivity in this region.

Superimposed on these features, figure III-1-2 shows a lens of water with high iodate concentration extending across the Atlantic. It occurs at 80 m at  $33^{\circ}\text{W}$  and rises upwards to 55 m at  $10^{\circ}\text{W}$ . The concentration in the core of this lens ranges from 0.45 to 0.60  $\mu\text{M}$ , generally higher than the concentrations at greater depths. Thus, this feature appears as a maximum between the iodate-poor surface water and the less iodate-rich deeper waters. This core of high iodate water correlates with the Equatorial Undercurrent as defined by its salinity (Metcalf et al., 1962; Metcalf and Stalcup, 1967; Neuman, 1969). Figure

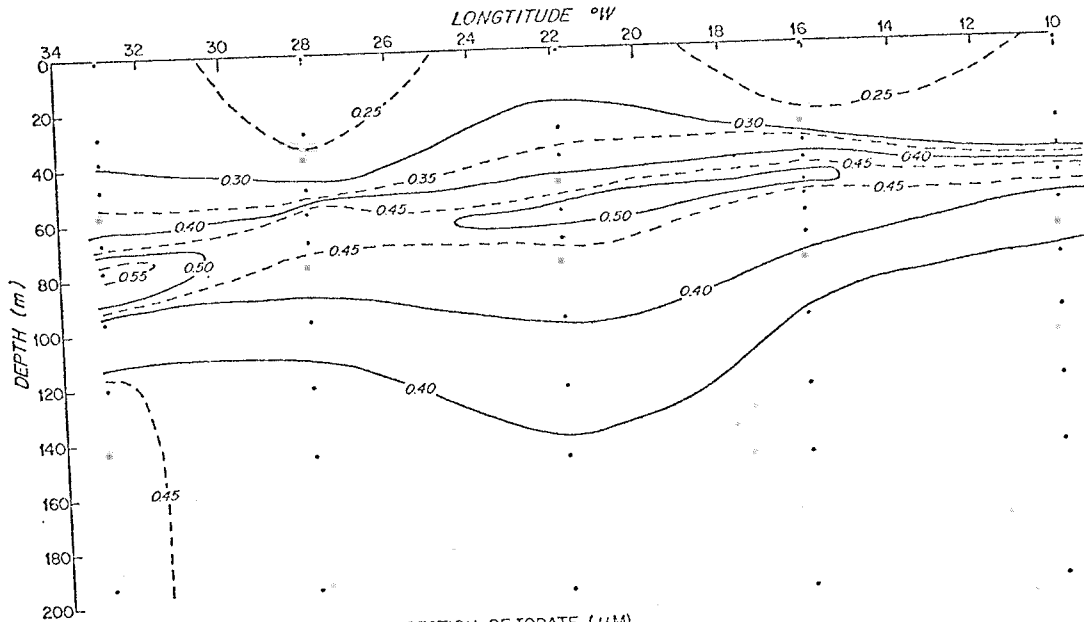


Fig. III-1-2 The distribution of iodate in the upper layers along the Equator of the Atlantic.

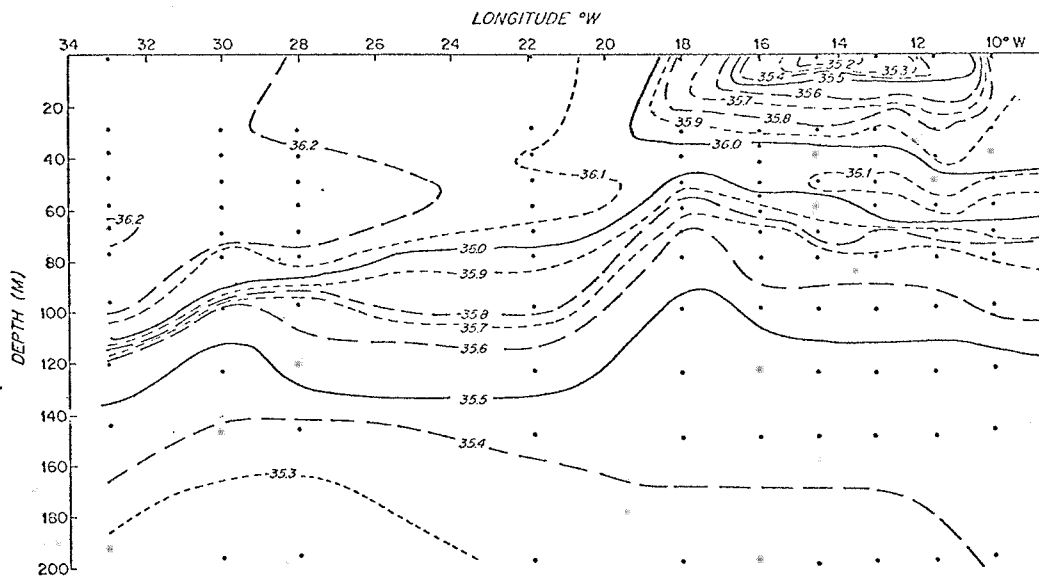


Fig. III-1-3 Salinity along the Equator of the Atlantic.

III-1-3 shows the corresponding distribution of salinity along the equator. A core of high salinity water can be readily identified. It is located at about 75 to 95 m at  $33^{\circ}\text{W}$  and again rises upwards to 50 m at  $10^{\circ}\text{W}$ . The striking similarity tends to suggest that high iodate concentration is a significant property of this advective core

Sharp maxima in iodate concentrations have not been previously reported. One reason may be inadequate sampling coverage. The lens of high iodate water reported here has a thickness of only ten to twenty meters and can easily be missed. During the GEOSECS (Geochemical Ocean Sections Studies), a station (station 109,  $2^{\circ} 00'\text{S}$ ,  $4^{\circ} 33'\text{W}$ ) was occupied in this region and a profile of iodate was obtained (Wong and Brewer, 1974). Figure III-1-4 shows that profile and a profile from a closeby station occupied during the present cruise (station AII-83-2052,  $2^{\circ} 00'\text{S}$ ,  $10^{\circ} 00'\text{W}$ ). In GEOSECS station 109, the iodate maximum was not observed because of poor sample coverage in that depth interval. Even in this study, with samples 10 m apart, one may still miss the depth with even higher iodate concentration.

The longitudinal sections of iodate along  $33^{\circ}\text{W}$ ,  $28^{\circ}\text{W}$ ,  $22^{\circ}\text{W}$ ,  $16^{\circ}\text{W}$  and  $10^{\circ}\text{W}$  show the complexity of the circulation in the Equatorial Atlantic. Along  $33^{\circ}\text{W}$  (figure III-1-5), there is a high iodate core at 80 m centered around the equator. This feature coincides with a high

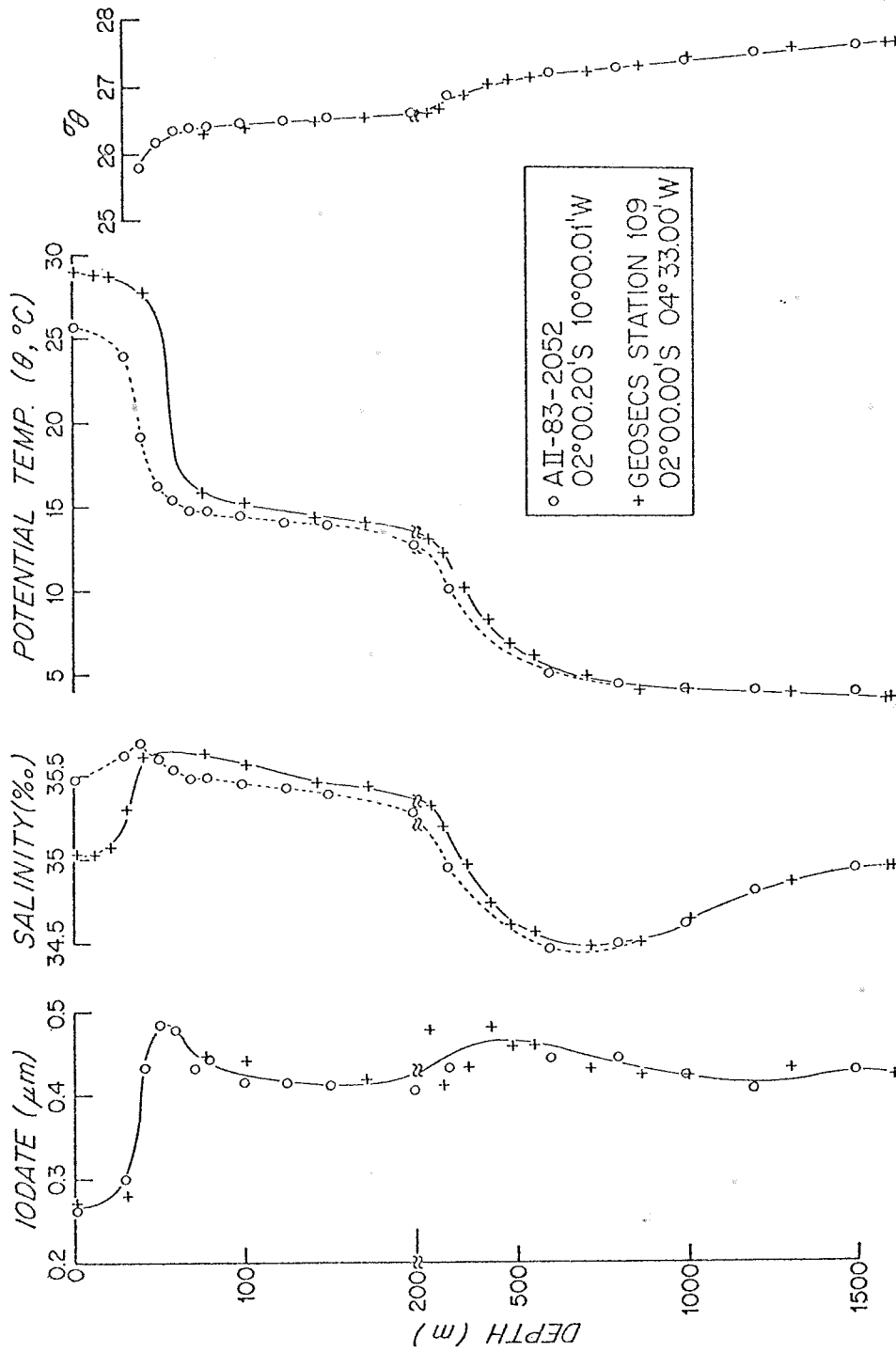


Fig. III-1-4 The profiles of iodate in two nearby stations occupied during cruise AII-83 and the GEOSECS expedition.

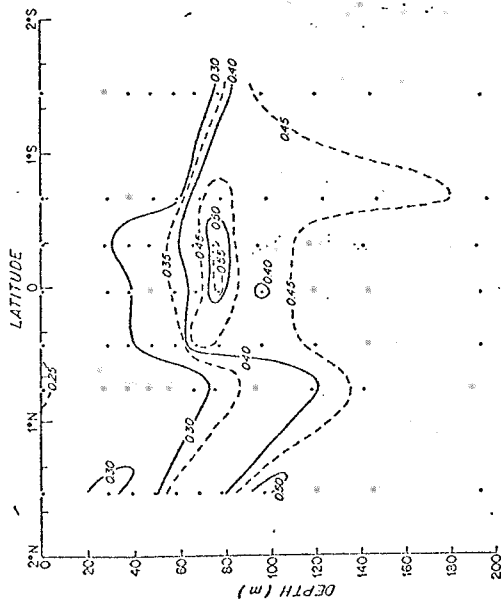


Fig. III-1-5 The concentrations of iodate in the Equatorial Atlantic along 33°W.  
 33°W SECTION OF IODATE (μM)  
 AT 85 STATIONS 2083-2089

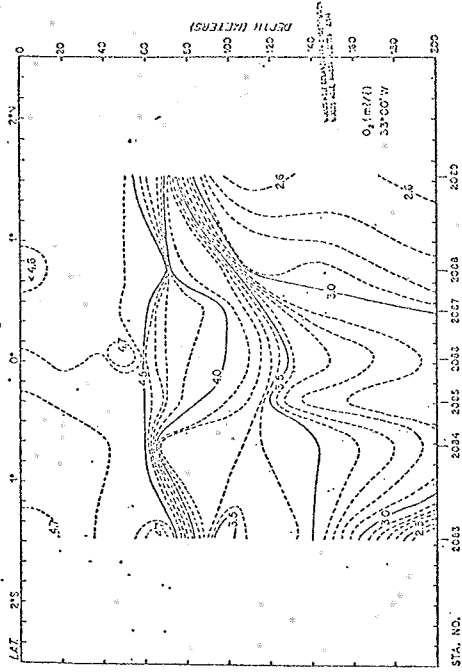


Fig. III-1-7 A section of oxygen in the Equatorial Atlantic along 33°W.  
 STA. NO. 2083 2084 2085 2086 2087 2088 2089

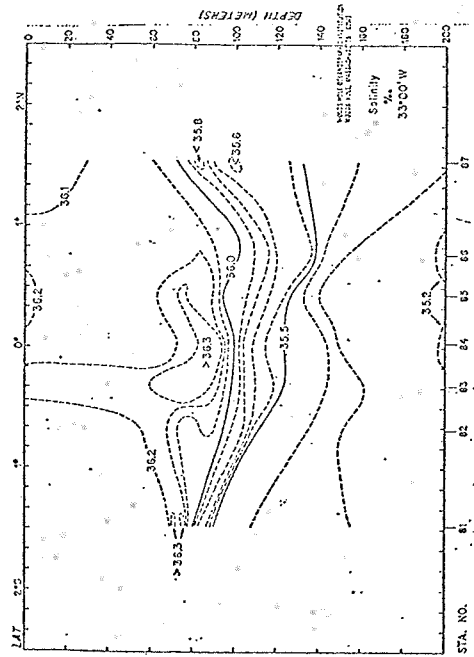


Fig. III-1-6 A section of salinity in the Equatorial Atlantic along 33°W.  
 STA. NO. 81 82 83 84 85 86 87

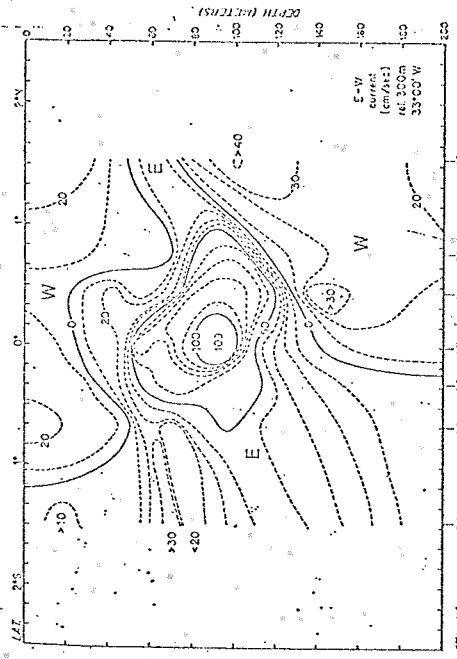


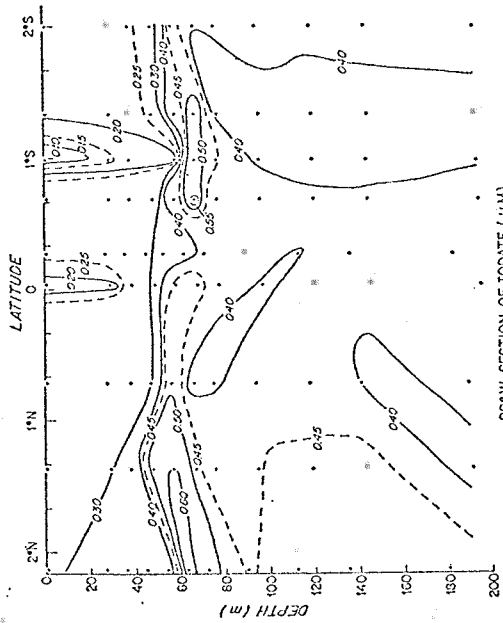
Fig. III-1-8 A section of the E-W current velocity in the Equatorial Atlantic along 33°W.  
 STA. NO. 2083 2084 2085 2086 2087 2088 2089

salinity ( $>36.2$  ‰), high oxygen ( $>4$  ml/l) and eastward flowing core, and represents the Equatorial Undercurrent. There is a second region of high iodate concentration at 100 m at  $1^{\circ} 32'N$ . This northern core is associated with lower salinity and oxygen content and is flowing westwards. Sections of salinity, oxygen and current speed along  $33^{\circ}W$  are shown in figures III-1-6 to III-1-8.

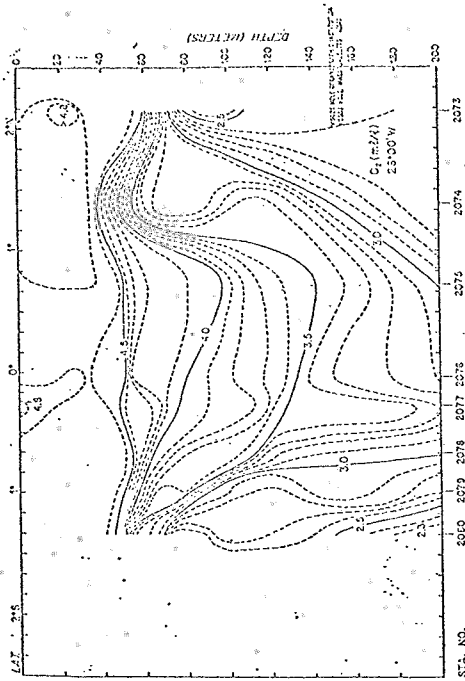
Along  $28^{\circ}W$ , the picture is more complex. Three cores with high iodate concentrations can now be identified (figure III-1-9). Between 0 and  $40'N$ , a core at 60 m is associated with high oxygen, high salinity and an eastward flow. At  $2^{\circ}N$ , a core is associated with lower oxygen, lower salinity and a westward flow. These two cores correspond to those two described previously. However, the northern core has apparently intruded into the equatorial core and some mixing may have occurred. Moreover, there is evidence of a parcel of water with low iodate concentration at  $18'S$  mixing with the equatorial core and it is associated with a corresponding oxygen maximum and a westward flow. The third core is around  $1^{\circ}S$ . Relative to the equatorial core, this southern core has lower salinity, lower oxygen content and a slower eastward flow. Sections of salinity, oxygen and current velocity along  $28^{\circ}W$  are shown in figures III-1-10 to III-1-12.

Along  $22^{\circ}W$ , one can identify the equatorial and the southern cores by their association with higher salinity,

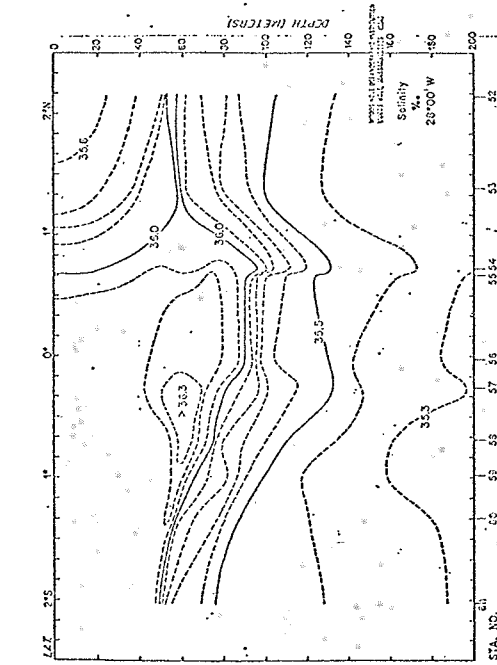




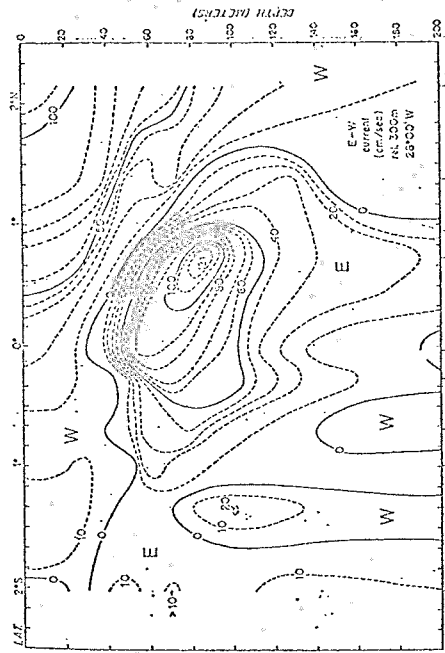
28°W SECTION OF IODATE ( $\mu\text{M}$ )  
 A.I.-83 STATIONS 2073-2081  
 Fig. III-1-9 The concentrations of iodate in the Equatorial Atlantic along 28°W.



STA. NO. 2070 2071 2072 2073 2074 2075  
 Fig. III-1-11 A section of oxygen in the Equatorial Atlantic along 28°W.



STA. NO. 2070 2071 2072 2073 2074 2075  
 Fig. III-1-10 A section of salinity in the Equatorial Atlantic along 28°W.



STA. NO. 35 36 37 38 39 40 41 42 43 44 45  
 Fig. III-1-12 A section of the E-W current velocity in the Equatorial Atlantic along 28°W.

higher oxygen, fast eastward flow and lower salinity, lower oxygen and slower eastward flow, respectively. The Equatorial Undercurrent is centered at 70 m and 22'S. Apparently, there is mixing between the Undercurrent and the southern core. The data are summarized in figures III-1-13 to III-1-16.

Along 16°W (figures III-1-17 to III-1-20), these three cores of water are discretely separated from one another. Their relative magnitudes in salinity, oxygen and direction of flow are the same as previously described. In between the cores are regions of lower iodate concentration which are associated with oxygen maxima. Here the Equatorial Undercurrent is at 0° and at a depth of 50 m.

At 10°W (figures III-1-21 to III-1-24), these three cores of water with high iodate concentrations can again be identified although their properties have become much more uniform than before. Among these three cores, the equatorial core, which supposedly represents the Undercurrent, still has the highest salinity and oxygen content, and an eastward flow and it is centered at 40°N and at 70 m depth. However, it does not coincide with the region with the highest salinity and highest eastward flow in this section anymore. Instead, this region corresponds to a region of higher oxygen content and lower iodate at about 20°S and 50 m depth where the iodate maximum is absent. The northern core still maintains its characteristically low salinity and oxygen content. However, instead of moving

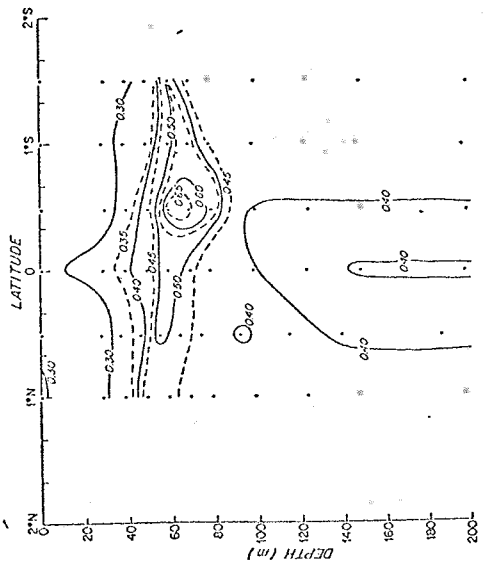


Fig. III-1-13 The concentrations of iodate in the Equatorial Atlantic along 22°W.  
 22°W SECTION OF IODATE ( $\mu\text{M}$ )  
 AM-63 STATIONS 2666-2071

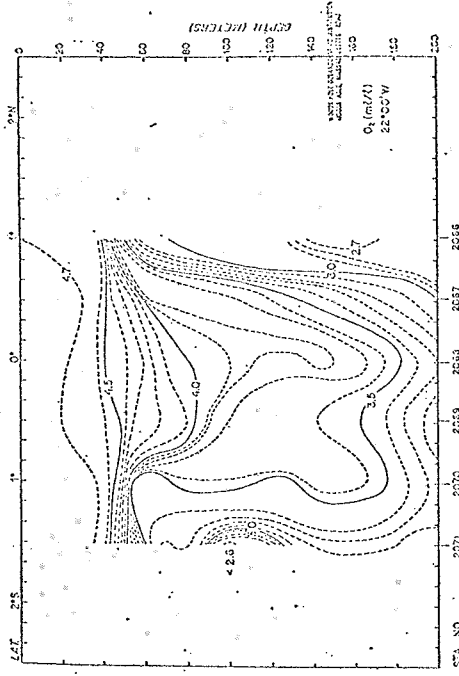


Fig. III-1-15 A section of oxygen in the Equatorial Atlantic along 22°W.  
 STA. NO. 2571 2570 2559 2543 2537 2526  
 O<sub>2</sub> (ml/l)  
 22°00'W

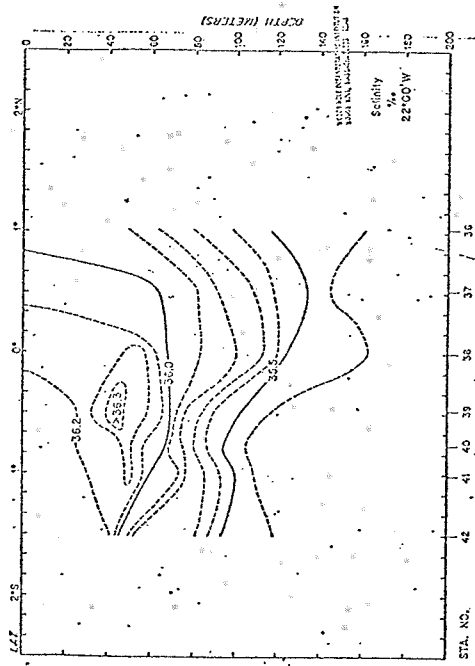


Fig. III-1-14 A section of salinity in the Equatorial Atlantic along 22°W.  
 STA. NO. 42 41 40 39 38 37 36  
 SALINITY (‰)  
 22°00'W

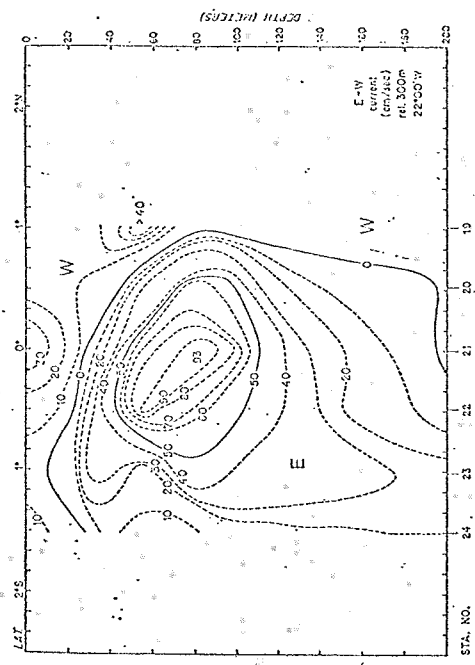


Fig. III-1-16 A section of the E-W current velocity in the Equatorial Atlantic along 22°W.  
 STA. NO. 24 23 22 21 20 19  
 E-W current (cm/sec) rel. 300m  
 22°00'W

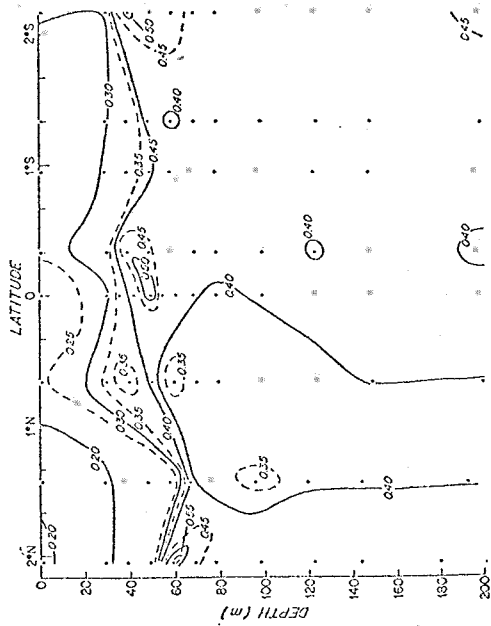


Fig. III-1-17 The concentrations of iodate in the Equatorial Atlantic along 16°W.  
 16°W SECTION OF IODATE (µM)  
 AIR-83 STATIONS 2059-2060, 2062-2064

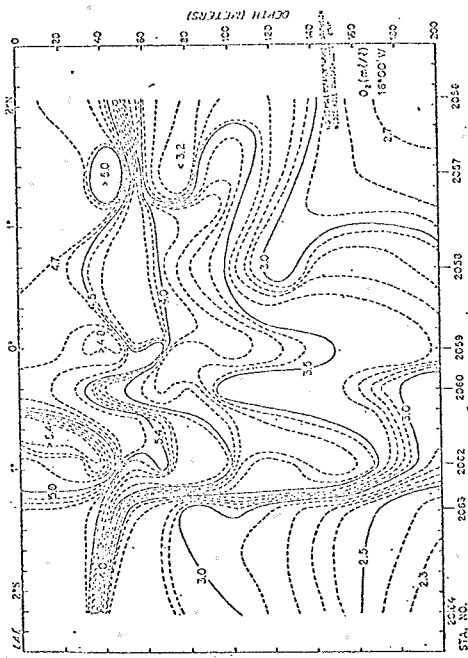


Fig. III-1-19 A section of oxygen in the Equatorial Atlantic along 16°W.

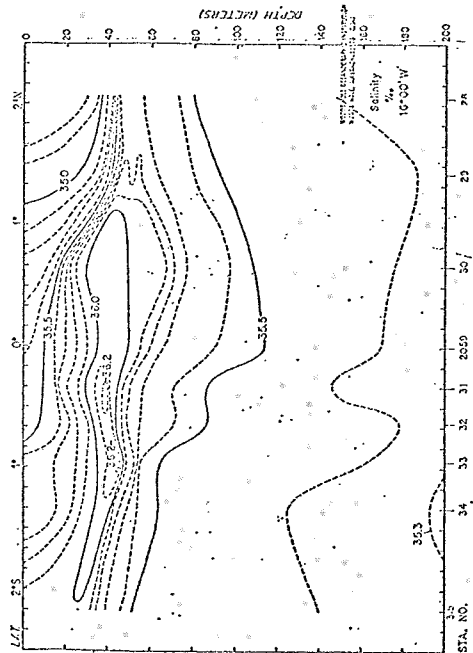


Fig. III-1-18 A section of salinity in the Equatorial Atlantic along 16°W.

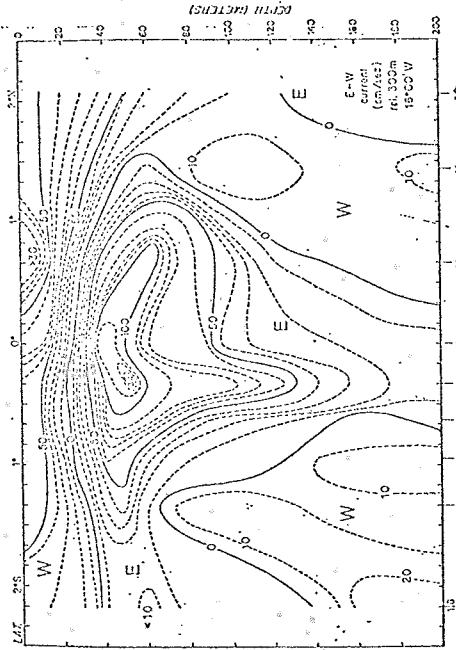
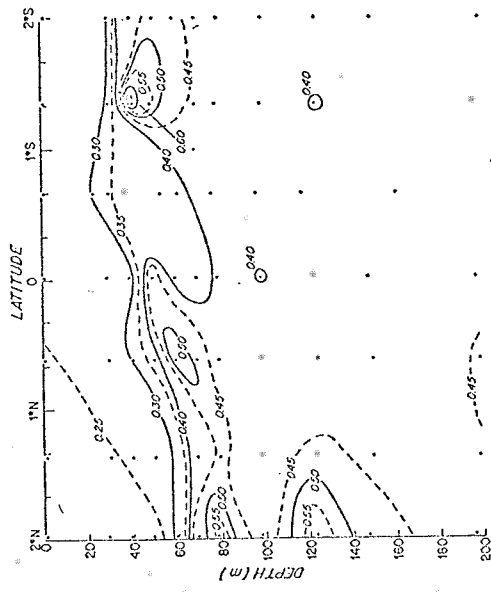


Fig. III-1-20 A section of the E-W current velocity in the Equatorial Atlantic along 16°W.



10°W SECTION OF IODATE ( $\mu\text{M}$ )  
 AI-SS STATIONS 2044-2046, 2048, 2050-2052  
 Fig. III-1-21 The concentrations of iodate in the Equatorial Atlantic along 10°W.

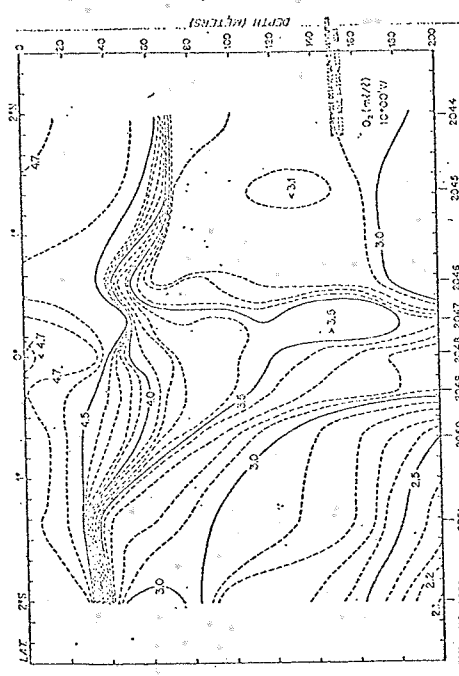


Fig. III-1-23 A section of oxygen in the Equatorial Atlantic along 10°W.

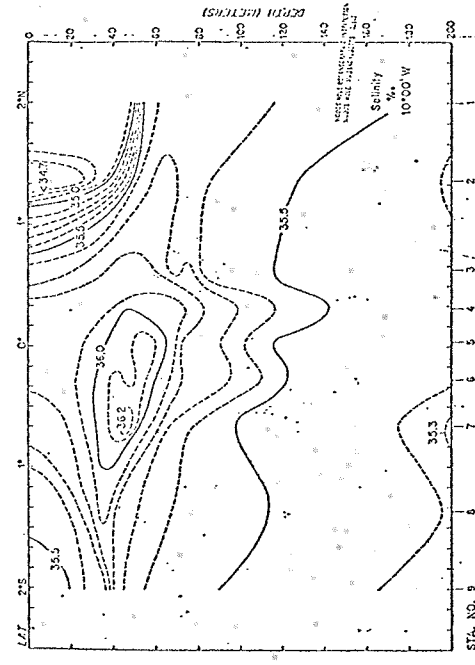


Fig. III-1-22 A section of salinity in the Equatorial Atlantic along 10°W.

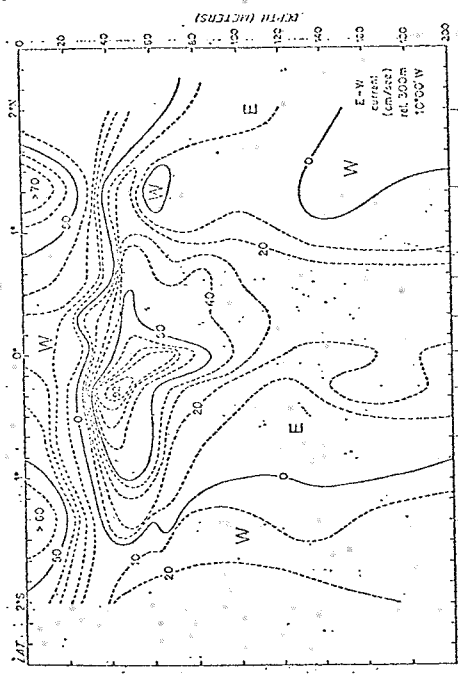


Fig. III-1-24 A section of the E-W current velocity in the Equatorial Atlantic along 10°W.

westward, it is flowing towards the east at a slow speed of 0 to 10 cm/sec. There is a fourth region of high iodate at  $2^{\circ}\text{N}$  and 120 m depth. There is a suggestion of such a core at  $28^{\circ}\text{W}$  and  $2^{\circ}\text{N}$ . However, with the limited data, its relationship to the other cores is unclear at this point. The properties of the northern, equatorial and southern cores of water with high iodate concentrations at various longitudes are summarized in table III-1-1.

The sources of these high iodate cores are unclear at this point. The iodate maxima observed in this region are situated in the pycnocline as shown in typical profiles in figures III-1-25 to III-1-28. If iodate is being depleted in the surface water by organisms then, upon death, a major portion of these organisms may sink and re-mineralize at this pycnocline since the high density stratification tends to decrease the sinking speed of the particles. This is also evident from the corresponding phosphate profiles (figures III-1-25 to III-1-28) where a sharp increase in phosphate is observed in the same depth interval. However, the phosphate profile does not show a maximum. This may be due to the differences in phosphate and iodate regeneration and utilization rates. If the major portion of the re-mineralization process occurs within a depth of few tens of meters, iodate concentrations higher than those observed in deep water will be found.

The high iodate concentration observed in this

Table III-1-1 Properties at the iodate concentration maxima\*

	Station	Latitude	$\text{IO}_3^-$ ( $\mu\text{M}$ )	Salinity (%)	Depth (m)	Current (cm/sec)	$\text{O}_2$ (ml/l)
		<u>33°W</u>					
I.**	2089	01°32.1'N	0.530	35.564	97	40-50W	2.59
II.	2086	00°02.0'N	0.560	36.232	77	90-100E	4.13
	2085	00°19.0'S	0.563	36.381	75	60-70E	4.13
		<u>28°W</u>					
I.	2073	02°07.7'N	0.663	35.559	63	60-70W	3.94
	2074	01°22.4'N	0.607	35.854	57	20-30W	3.78
II.	2075	00°43.6'N	0.495	36.100	56	20-30E	4.28
	2076	00°02.2'S	0.462	36.283	78	80-90E	4.19
III.	2078	00°41.5'S	0.550	36.106	67	30-40E	3.93
	2079	00°58.9'S	0.523	35.900	67	10-20E	3.53
	2080	01°00.2'S	0.537	35.753	67	0-10 E	2.99
		<u>22°W</u>					
II.	2067	00°31.3'N	0.514	36.033	55	20-30E	4.18
	2068	00°00.0'N	0.534	36.190	59	70-80E	4.31
	2069	00°28.9'S	0.694	36.196	69	70-80E	4.18
III.	2070	01°00.3'S	0.577	35.855	68	30-40E	3.47
	2071	01°29.9'S	0.550	35.709	59	0-10E	3.49
		<u>16°W</u>					
I.	2056	02°03.4'N	0.580	35.683	59	20-30W	3.45
II.	2059	00°00.2'N	0.514	36.032	50	90-100E	5.16
III.	2064	02°01.2'S	0.500	35.661	40	0-10E	3.22
		<u>10°W</u>					
I.	2044	01°58.6'N	0.588	35.678	78	0-10E	3.20
II.	2046	00°37.1'N	0.513	35.990	59	40-50E	3.35
III.	2051	01°21.0'S	0.664	35.800	39	10-20E	3.35

\* Oxygen, salinity and current data from Bruce and Katz (1975).

\*\* I - Northern core. II - Equatorial core.  
III - Southern core.

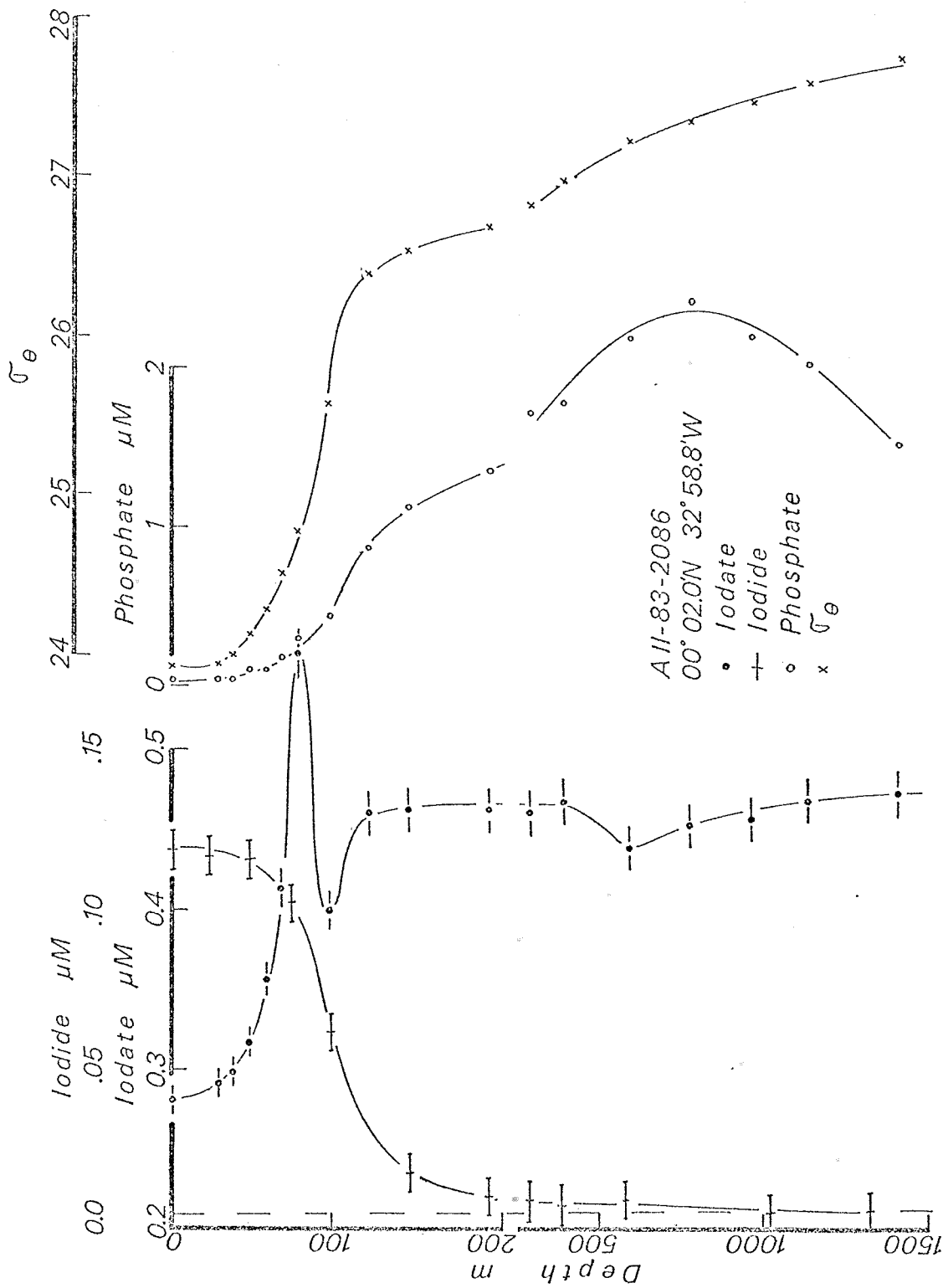


Fig. III-1-25 Iodate, iodide, phosphate and  $\sigma_\theta$  profiles of station AII-83-2086 (00° 02'N, 32° 59'W). Broken line denotes the iodide blank.



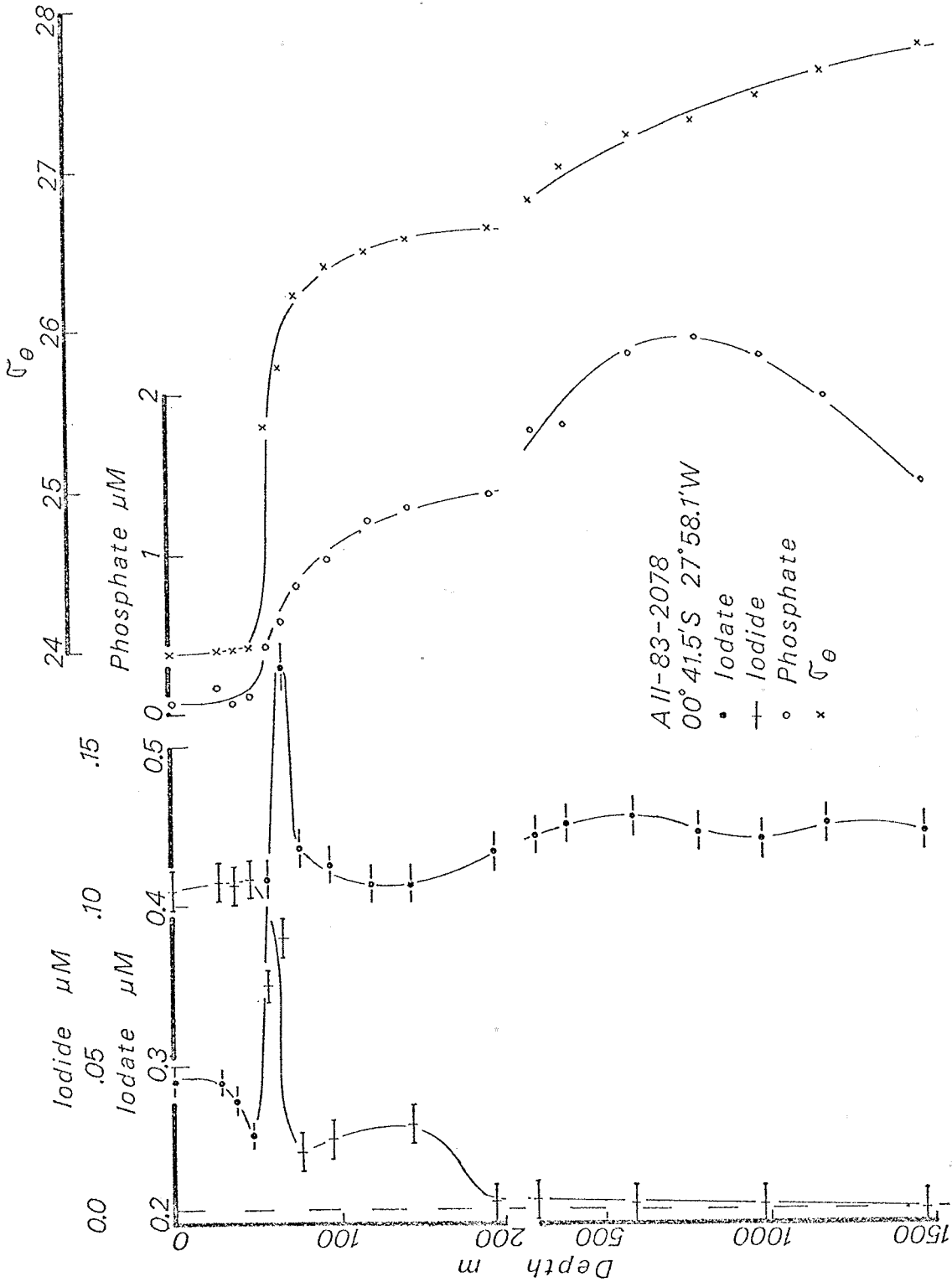


Fig. III-1-26 Iodate, iodide, phosphate and  $\sigma_\theta$  profiles of station AII-83-2078 (00° 42'S, 27° 58'W). Broken line denotes the iodide blank.

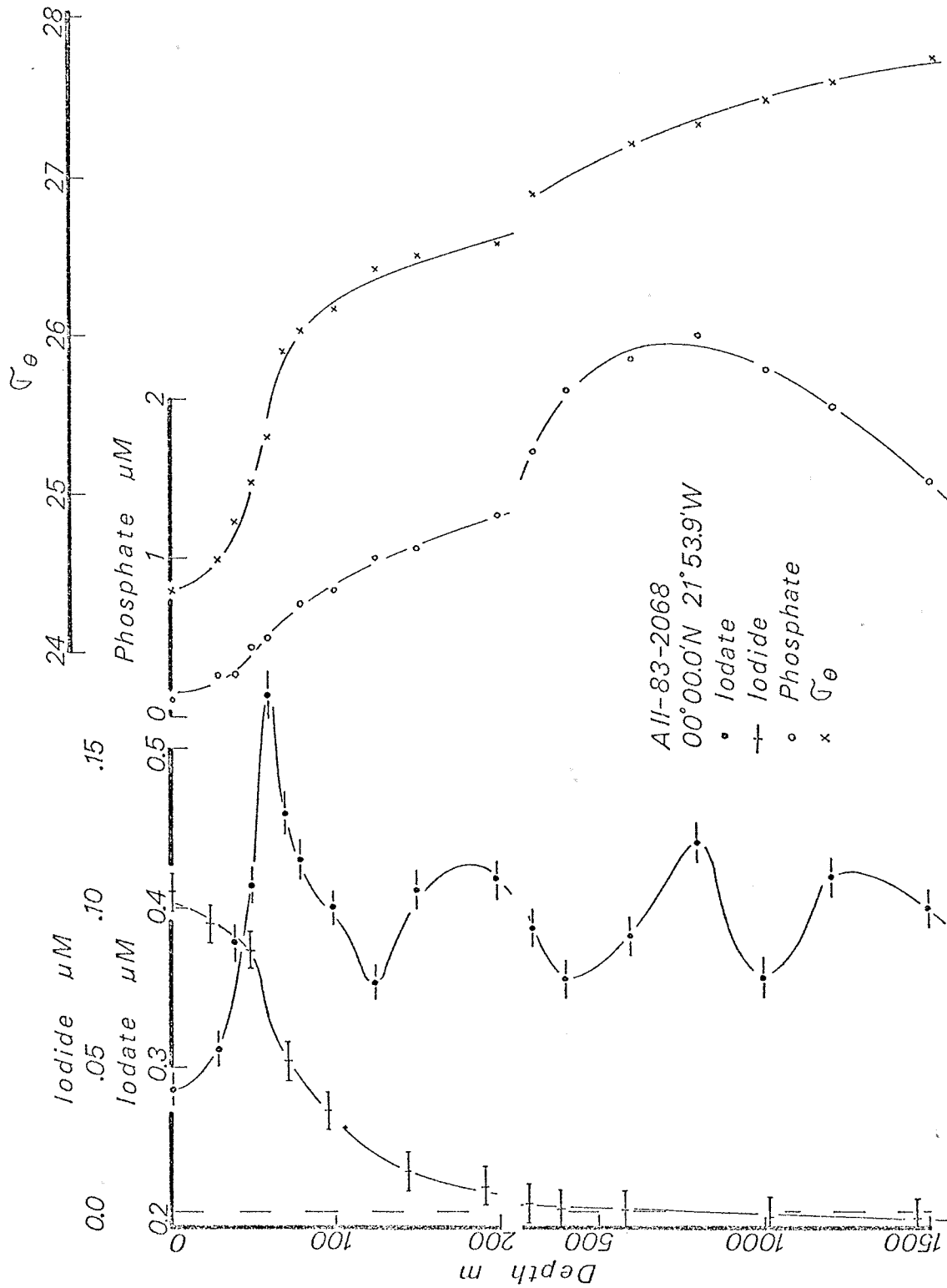


Fig. III-1-27 Iodate, iodide, phosphate and  $\sigma_{\theta}$  profiles of station AII-83-2068 (00° 00'N, 21° 54'W). Broken line denotes the iodide blank.

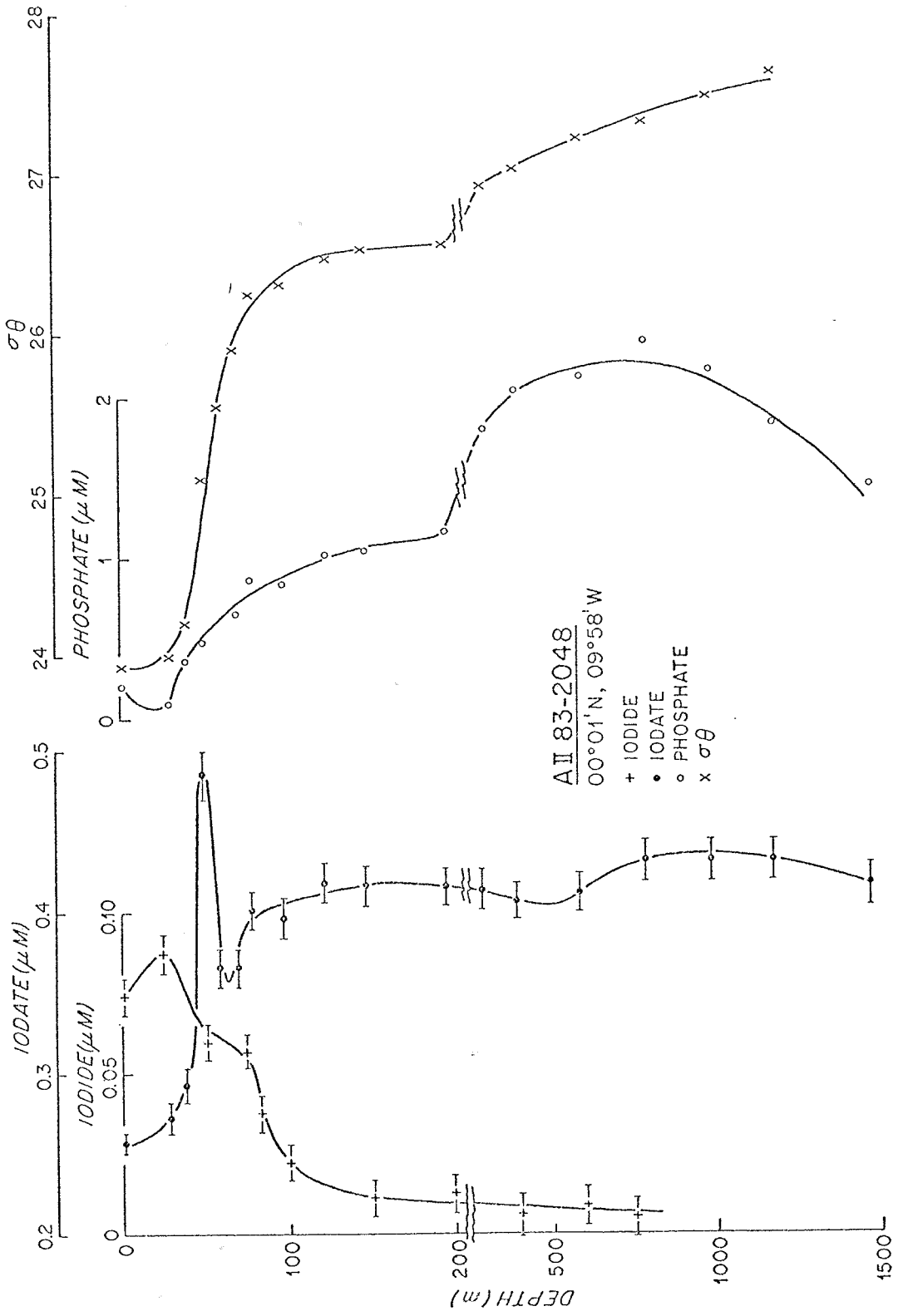


Fig. III-1-28 Iodate, iodide, phosphate and  $\sigma_\theta$  profiles of station AII-83-2048 (00° 01' N, 09° 58' W).

study may be caused either by advection or in-situ production. Based on the present data, in-situ production seems less likely. First, the profiles of iodide (figures III-1-25 to III-1-28) do not show any extraordinary features at the iodate maximum. If iodide is the intermediate in the formation of iodate by re-mineralization, one would expect to see a corresponding maximum close to that depth. Secondly, there is no systematic east to west variation in the iodate concentrations although it is known that productivity increases towards the African coast (Corcoran and Mahnken, 1969); however, alternatively, this may be explained by the inability to sample at exactly the depth with the highest iodate concentration at every station.

Advection can qualitatively describe these observations. Productivity is known to be high along the northwestern and western coastal regions of African due to upwelling (Ryther, 1963; Corcoran and Mahnken, 1969). Waters with high iodate concentration may be formed here. These waters are swept towards the equator by the North and South Equatorial Currents. Metcalf and Stalcup (1967) (produced in graphic form by Philander, 1973) showed that the Undercurrent is sandwiched between two branches of the South Equatorial Current. The edges of these Currents may form the northern and southern cores of high iodate waters. High productivity has also been observed along the north eastern Brazilian coast around the mouth of the Amazon (Zeitschel,

1969) and thus high iodate water may also be found there. The Equatorial Undercurrent is an extension of the Northern Brazilian Current (Metcalf and Stalcup, 1967). Some of the water from the South Equatorial Current may be entrained too. Consequently, it can also have high iodate concentrations. There are regions with no iodate maxima in between the cores. These may be waters untouched by these currents and subsequently show the normal distribution of iodate in the water column. Part of the high variability of iodate concentrations in the Undercurrent may also be contributed to the meandering of the Undercurrent. The core of the Undercurrent oscillates in both the vertical and horizontal planes (Rinkel, 1969; reviewed in Philander, 1973) with a periodicity of weeks (Duing et al., 1975). Consequently, in a longitudinal section, one may be sampling the Undercurrent at different phases repeatedly. However, present evidence suggests that the meandering of the Undercurrent is confined between  $1^{\circ}\text{N}$  and  $1^{\circ}\text{S}$  (Duing et al., 1975). Thus, the cores observed at  $2^{\circ}\text{N}$  and  $2^{\circ}\text{S}$  cannot be part of this system.

These observations raise some questions concerning the marine geochemistry of iodine. First, these surface water masses are relatively young. If iodate is generated by the re-mineralization of organisms, the rate of oxidation of iodide will have to be high if iodine occurs in organisms as iodide (Shaw, 1962). I have not been able to demonstrate

the oxidation of iodide chemically in sea water in the laboratory at any measurable rate (see chapter IV for details). A biologically catalyzed oxidation of iodide is one of the possibilities. Sugawara and Terada (1967) have suggested such a mechanism based on their laboratory experiments with algae. Furthermore, the exact source of the water masses with high iodate cannot be established until a better understanding of the circulation in the Equatorial Atlantic can be obtained and a study of the distribution of iodine in the highly productive areas is made.

## III.2 The marine chemistry of iodine in anoxic basins

### III.2.1 Introduction

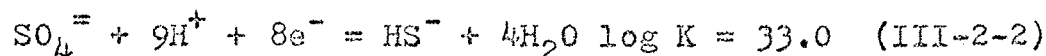
Anoxic conditions in natural waters are generated when vertical mixing and advective transport, usually in restricted basins, are insufficient to replenish the oxygen consumed by organisms. All the anoxic basins have strong pycnoclines which hamper vertical mixing and shallow sills which effectively minimize the renewal of the anoxic deep waters by advection. The strong pycnocline may be maintained either by a sharp temperature gradient or a sharp salinity gradient. As a result of inhibited mixing, the residence time of the anoxic water is long and, consequently, the changes caused by biological-chemical interactions are large. Thus, although anoxic basins, by volume, constitute an insignificant portion of the world oceans, they have attracted much attention from chemical and biological oceanographers (Richards, 1965; Spencer and Brewer, 1971; Tuttle and Jannasch, 1973; Brewer and Murray, 1973; Jannasch et al., 1974) and they open up new routes to an understanding of basic biological-chemical interactions in the sea.

Biochemical processes often involve electron transfers (Lehninger, 1965). The terminal electron acceptor under oxic conditions is oxygen and the end product is water. As oxygen is depleted, some organisms may use nitrate, sulfate and eventually carbon dioxide in succession as alternate terminal electron acceptors (Richards, 1965). Consequently,

reduced forms of nitrogen, sulfur and carbon such as nitrite, molecular nitrogen, ammonia, thiosulfate, sulfide and methane may be formed. Since the pE of the open oceans is presumably poised by the oxygen-water couple at 12.5 (Sillen, 1961) according to the equation



the removal of oxygen causes a drastic drop in pE. Thorsen (1970) and Brewer and Murray (1973) estimated that in anoxic basins, the sulfate-sulfide couple has the largest redox buffer capacity. Thus, the pE will be poised at -4 by this couple in the absence of oxygen according to the equation



This large, biologically induced change in redox potential brings about accompanying changes in the speciation and distribution of multi-oxidation-state elements such as iron and manganese (Spencer and Brewer, 1971). The presence of sulfide also causes a re-partition of many trace elements (for example, zinc and copper) between the dissolved and particulate phases as most sulfides are highly insoluble (Spencer et al., 1972).

Anoxic basins are also well known nutrient traps (Fanning and Pilson, 1972; Brewer and Murray, 1973). Nutrients are transported into the deep anoxic layer by biogenic particles and re-mineralization may occur within the water column or in the sediments. Physical removal of the re-gen-



erated dissolved nutrients is prevented by the weak mixing processes. However, some microbes live close to the oxic-anoxic interface. They derive their energy by chemosynthesis (Sorokin, 1964; Tuttle, private communication). Consequently, they may remove some of the nutrients at such depths (Brewer and Murray, 1973).

In this section, I shall report the distribution of dissolved iodine in two anoxic basins, the Black Sea and the Cariaco Trench, and in the oxic Venezuela Basin which serves as a comparison for normal oceanic conditions. The distribution of iodine in anoxic basins is heretofore unknown. However, since iodine is bioactive and since the iodate-iodide transition occurs at a pE between the oxygen-water and the sulfate-sulfide couples, iodine may exhibit a combination of the behaviors described above. Moreover, if iodide is indeed diffusing into the bottom waters from the sediments as suggested by Tsunogai (1971b), this process should be most conspicuous in the anoxic basins where the residence time of the deep water is long and the sediments are rich in organic material and strongly reducing.

## The Black Sea

The Black Sea is the world's largest anoxic basin. It is connected only to the Mediterranean Sea via the Bosphorus, the Sea of Marmara and the Dardanelles. The maximum sill depth in the Bosphorus is 34 m (Gunnerson and Ozturgut, 1974). A number of rivers including the Danube and the Dnepr, which have average flows of 6200 and 1700 m<sup>3</sup>/sec (Leopold, 1960), flow into the Black Sea and create a light, less saline surface layer on a subsurface outflow. The deep inflow of saline Mediterranean water is sporadic (Bogdanova, 1961) with estimates of the annual flow ranging from 328 km<sup>3</sup>/yr (Merz and Moller, 1928) to negligible (Ulloyot and Ilgaz, 1946). The average flow is often quoted as about 190 km<sup>3</sup>/yr (Spencer and Brewer, 1971; Brewer and Murray, 1973; Ostlund, 1974). Thus, whereas the surface salinity of the Black Sea may vary from 17.2 ‰ to 18.3 ‰ depending on the proximity to terrestrial runoffs, in the deep water the salinity is relatively constant at 22.4 ‰ (Brewer, 1971). The potential temperature is also quite variable at the surface and in winter the surface waters are cooler than the deep waters, though vertical mixing is inhibited by the strong salinity gradient. The strong vertical stratification is thus maintained solely by the salinity difference between the surface and the deep waters. The absolute level of the salinity of the Black Sea is much lower than that of the open oceans, consequently, it should

not be classified as a typical marine basin. Profiles of the salinity and potential temperature of the Black Sea are shown in figure III-2-1.

The maximum depth of the Black Sea is about 2200 m (Ross et al., 1974) and the oxygen-sulfide boundary occurs at about 150 to 250 m (Brewer, 1971). The anoxic zone can be further subdivided according to the radiocarbon ages. The formal C-14 age of the water between 300 and 1700 m is about 1000 years, whereas, below 1700 m, the age may well exceed 2000 years old and the water is probably renewed only by eddy diffusion (Ostlund, 1974). The deep inflow of Mediterranean water may occur at various depths, although, based on the formal radiocarbon ages and the temperature-salinity relationship, it has to occur above 1700 m (Ostlund, 1974; Brewer and Murray, 1973). The vertical advective velocity and eddy diffusion coefficient in the mixing zone between about 100 m and 300 m have been estimated to be 0.5 m/yr and  $0.014 \text{ cm}^2/\text{sec}$  respectively (Spencer and Brewer, 1971).

#### The Cariaco Trench

The Cariaco Trench, the second largest known anoxic basin of the world, is a depression situated on the northern Venezuelan continental margin at roughly  $10^{\circ}30'N$  and  $65^{\circ}31'W$ . It is approximately 100 miles long and 40 miles wide and has a maximum depth of about 1400 m. It is separ-

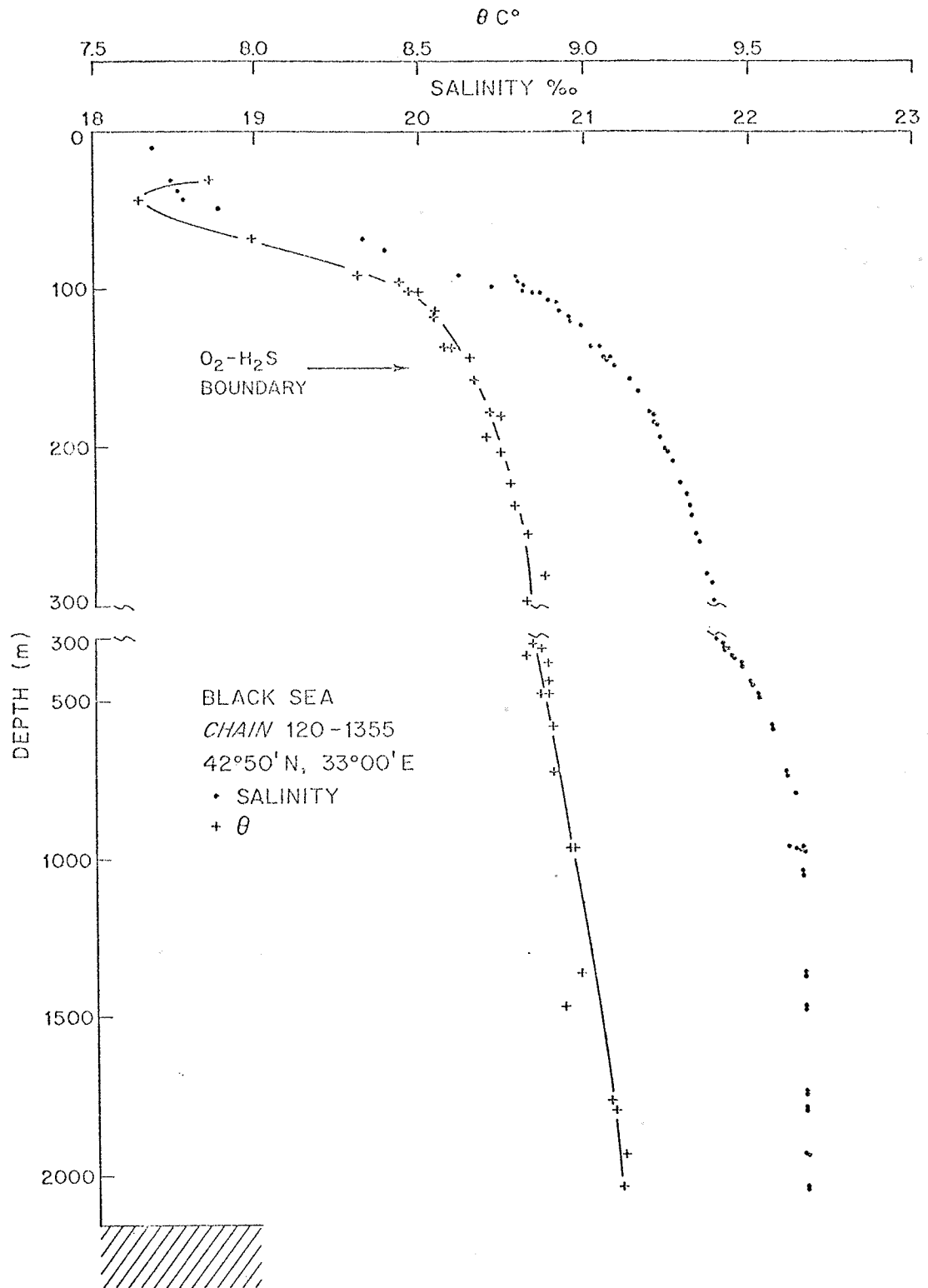


Fig. III-2-1 Salinity and  $\theta$  profiles in the Black Sea at station CHAIN-120-1355 (42°50'N, 33°00'E). • represents salinity. + represents  $\theta$ .

ated from the Caribbean Sea by a sill at a depth of about 150 m. Above this sill depth, the waters of the Cariaco Trench mix freely with the surface waters of the open sea. The Trench is subdivided into two deep basins (eastern and western) with a saddle at about 900 m below sea level in between (Maloney, 1966). The salinity decreases from about 36.8 ‰ at the surface to 36.185 ‰ in the deep water and the potential temperature decreases from about 26°C to 16.75°C. Thus, unlike the Black Sea, the Cariaco Trench is a true marine basin and its vertical stratification is maintained solely by the strong thermal gradient instead of by a salinity gradient. Profiles of salinity and potential temperature are shown in figure III-2-2.

The deep water of the Cariaco Trench is renewed by slow flushing. Estimates of the residence time of the anoxic water vary widely. Fanning and Pilson (1972) subdivided the anoxic zone into two layers and suggested that advective renewal only occurs from 300 m to 1000 m. Below 1000 m, eddy diffusion is the only means for mixing. They suggested the residence time of the water in the upper layer to be 800 years on the basis of a silicate balance. Richards and Vaccaro (1956) and Richards (1975) reported a residence time of 70 years by using phosphate as the tracer. Deuser (1973) estimated a range of 22 years to 570 years with a geometric mean of 112 years based upon estimates of the rate of oxidation of organic matter; Presley (1974) sug-

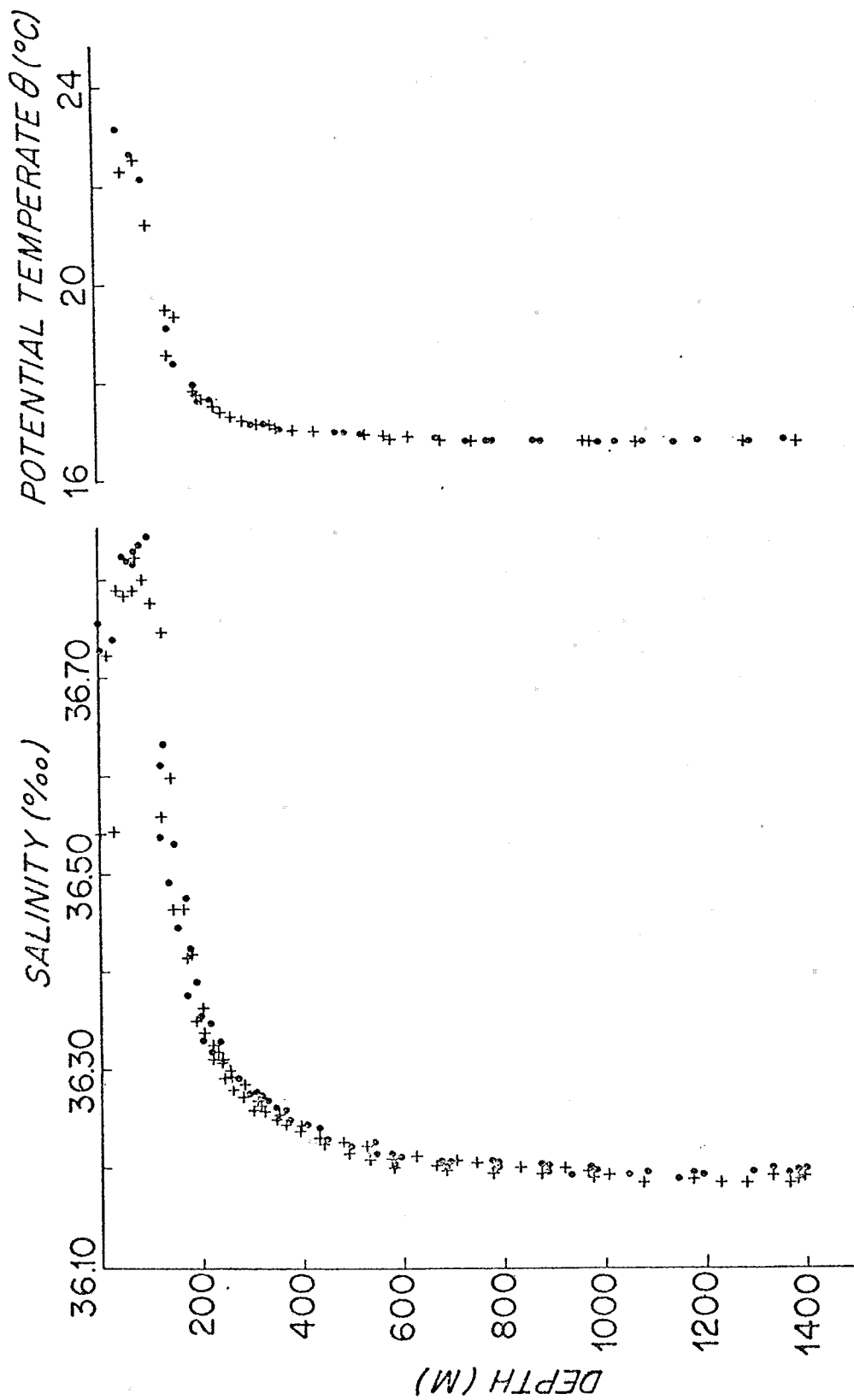


Fig. III-2-2 Profiles of salinity and  $\theta$  in the Cariaco Trench. + Western Basin; • Eastern Basin.

gested a range of 50 to 100 years from the sulfur accumulation rate in the sediments. Radiocarbon dating gives a residence time of about 100 years (Ostlund, private communication).

The shorter residence time of the anoxic waters in the Cariaco Trench, relative to the Black Sea, suggests that it may be a less stable system. The potential density ( $\sigma_\theta$ ) of the deep water is about 26.50. At the oxygen-sulfide boundary at about 300 m,  $\sigma_\theta$  is 26.46 and at the sill depth at 150 m,  $\sigma_\theta$  is 26.35. Thus, the overall density gradient of the Cariaco Trench is only 0.15 in  $\sigma_\theta$  whereas in the Black Sea it is about 1.0 in  $\sigma_\theta$ .

### III.2.2 Sampling and analytical methods

Samples were obtained from one station in each of the two basins of the Cariaco Trench, one station in the Venezuela Basin and one station in the Black Sea during cruises AII-79 and CHAIN-120. The locations of the stations are shown in figure III-2-3. Samples were either analyzed on board for iodate or frozen at  $-5^{\circ}\text{C}$  in polyethylene bottles immediately after collection and transferred back to Woods Hole for analysis. This method for the storage of samples has been shown to be reliable (Wong, 1973). All samples were analyzed for iodate by photometric micro-titration with a precision of better than 1% (Wong and Brewer, 1974). Iodide profiles were obtained from the eastern basin of the Cariaco Trench, the Venezuela Basin and the Black Sea. The samples were analyzed by neutron activation analysis as described in section II.4 with a precision of  $\pm 5\%$  and a reagent blank of about  $0.005 \mu\text{M}$ . The data from these cruises are compiled in Appendices B and C.



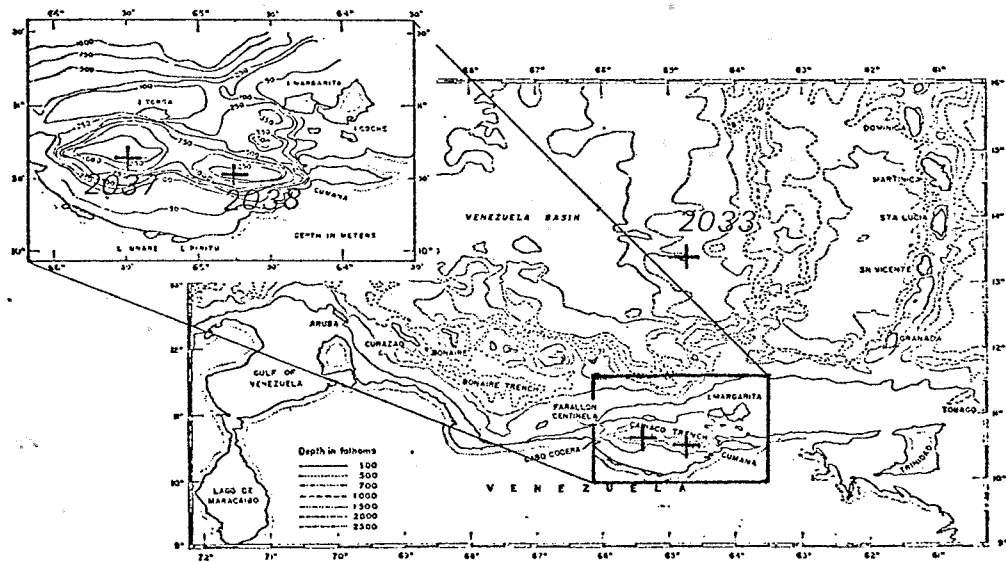
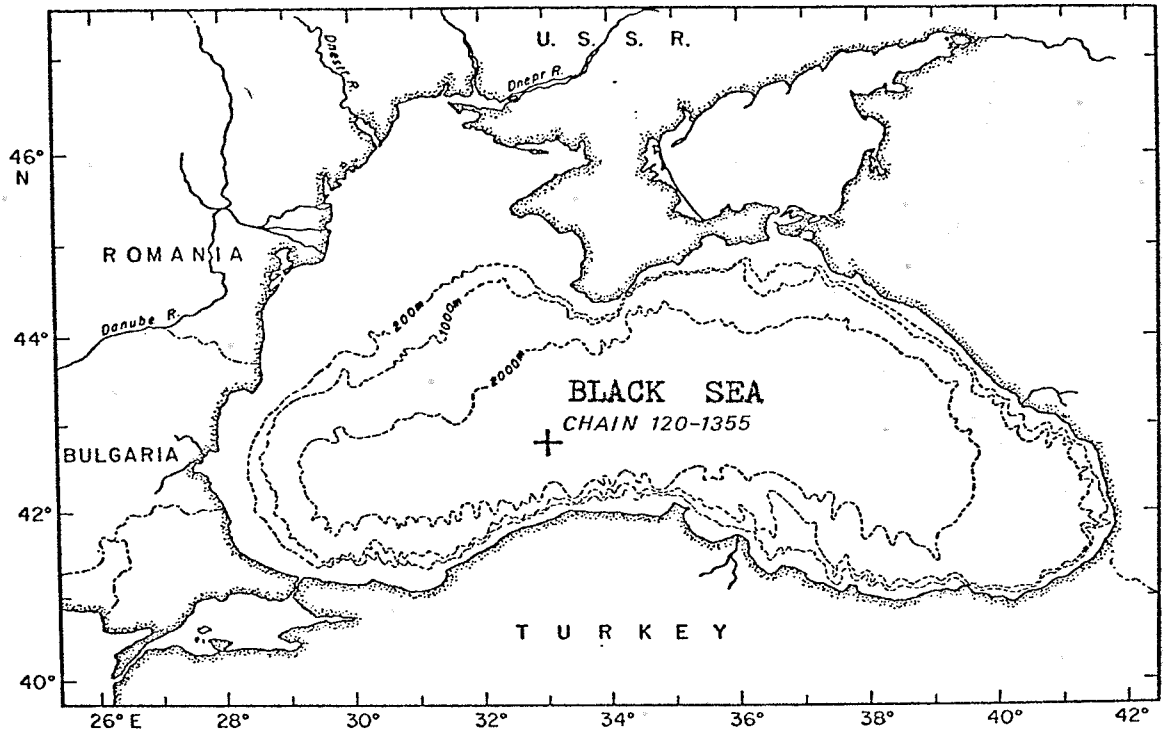


Fig. III-2-3 The positions of the stations in the Black Sea, the Cariaco Trench and the Venezuela Basin.

### III.2.3 Results and discussion

#### Iodine in oxic and anoxic basins

The distributions of iodate and iodide in the oxic Venezuela Basin (figure III-2-4) are similar to previous observations from other parts of the open oceans (Tsunogai, 1971b; Tsunogai and Henmi, 1971; Wong and Brewer, 1974). The iodate concentration is lowest at the surface (0.3  $\mu\text{M}$ ) and it increases with depth to about 0.5  $\mu\text{M}$ . A mid-depth maximum is also observed. It corresponds with a phosphate maximum and a oxygen minimum and may be the result of the re-mineralization of organisms (Wong and Brewer, 1974). In contrast, the iodide concentration is highest in the surface waters and decreases rapidly with depth to below the detection limit (0.005  $\mu\text{M}$ ) below the euphotic zone. A thin sub-surface iodide maximum is observed at 100 m with a concentration of about 0.38  $\mu\text{M}$ , corresponding with a sub-surface salinity maximum. A sub-surface iodide maximum of such magnitude has not been documented before and the present data are insufficient for a detailed discussion of its origin.

In the anoxic basins, as a result of the drastic drop in pE, iodine exhibits markedly different behavior below the oxic zone. The profiles are shown in figures III-2-5 to III-2-7. The oxygen-sulfide boundaries occur at 150 m in the Black Sea and 265 m in the Cariaco Trench. In the

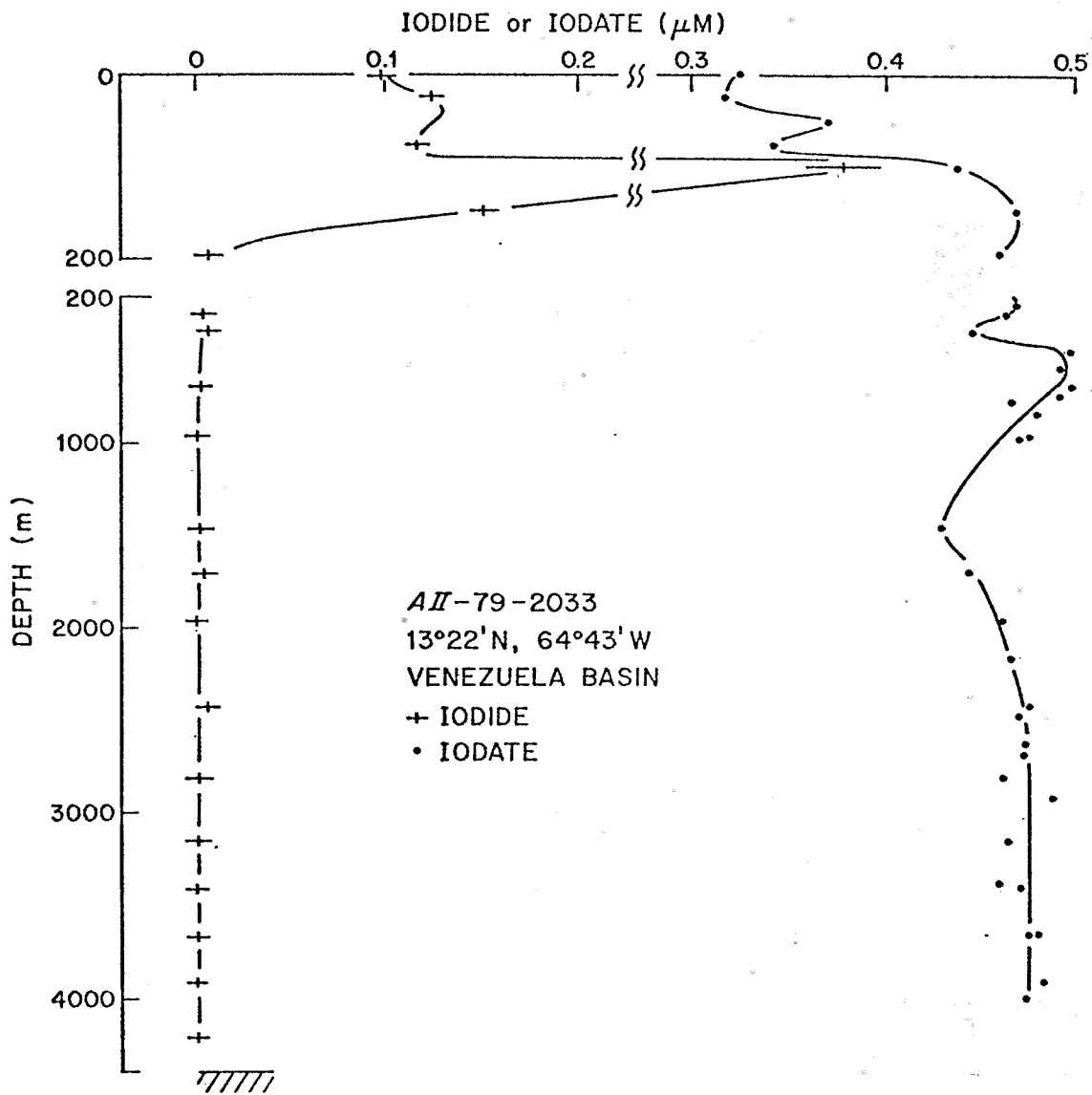
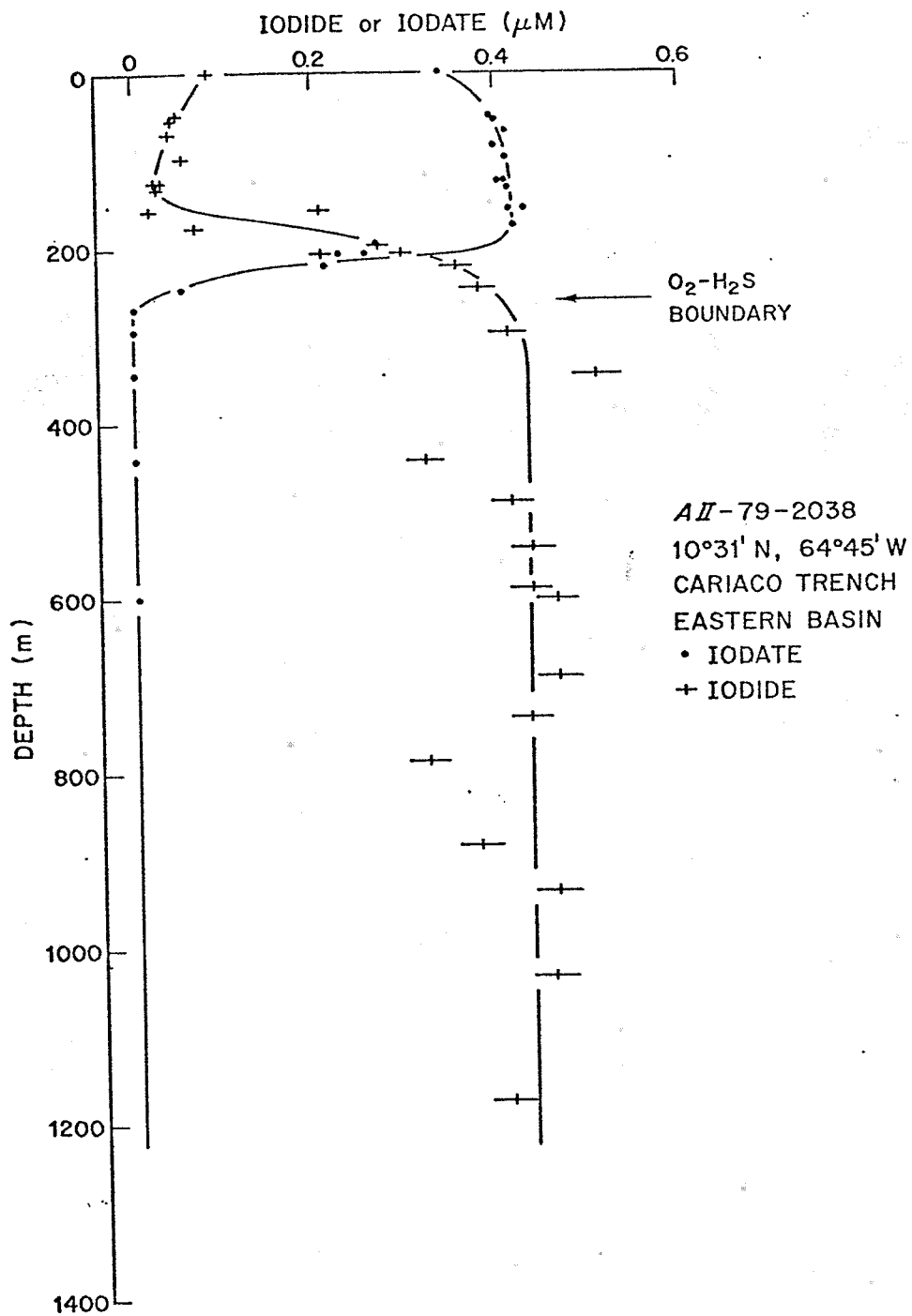


Fig. III-2-4 Profiles of iodate and iodide in the Venezuela Basin at station AII-79-2033 (13°22'N, 64°43'W).

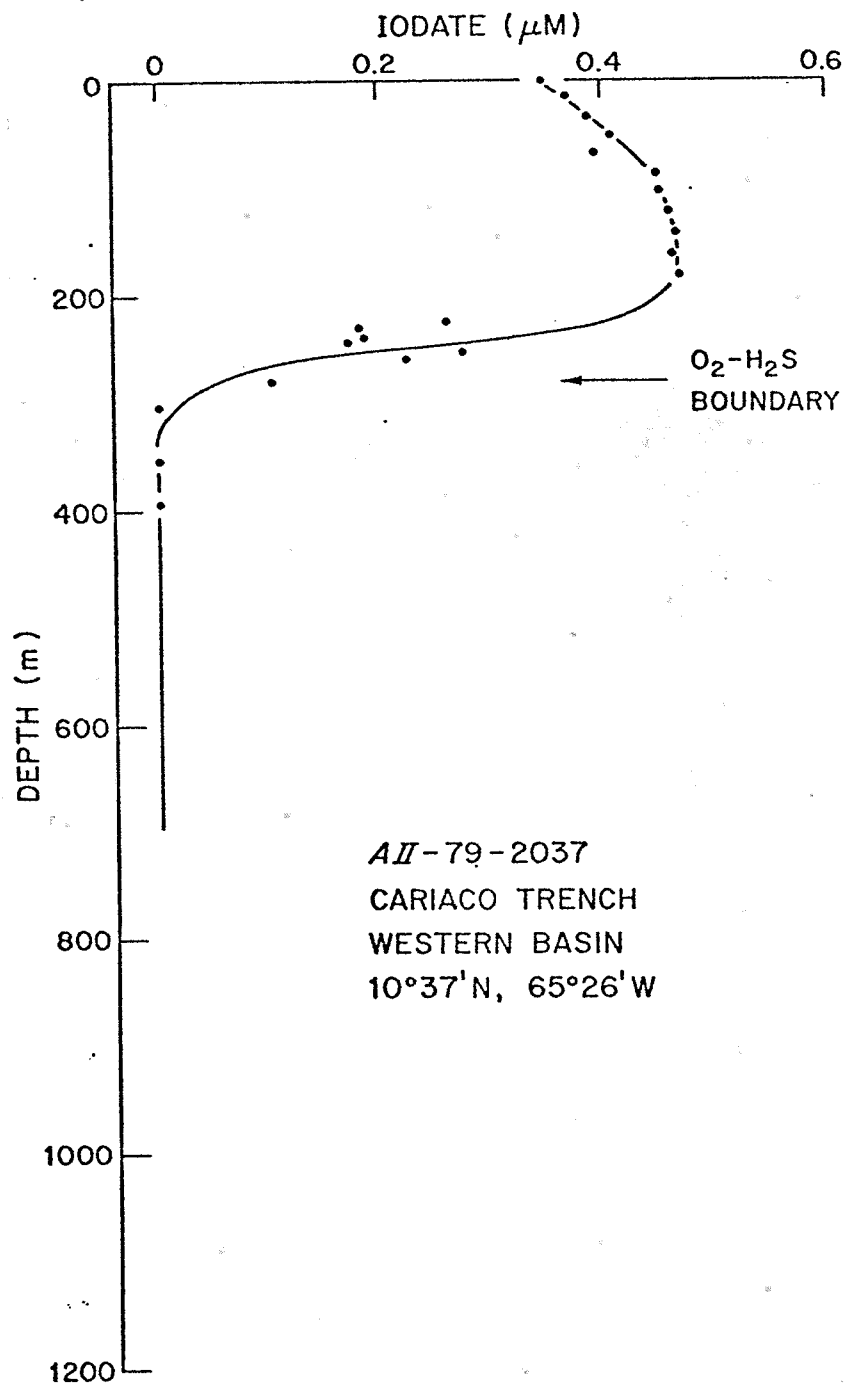
• represents iodate. + represents iodide with a 5% or 0.006  $\mu\text{M}$  error bar whichever is larger.



///////

Fig. III-2-5 Profiles of iodate and iodide in the Cariaco Trench at station AII-79-2038 (10°31'N, 64°45'W).

• represents iodate. + represents iodide. Error bar of iodide is 5% of the concentration.



///////

Fig. III-2-6 Profile of iodate in the Cariaco Trench at station AII-79-2037 (10°37'N, 65°26'W).

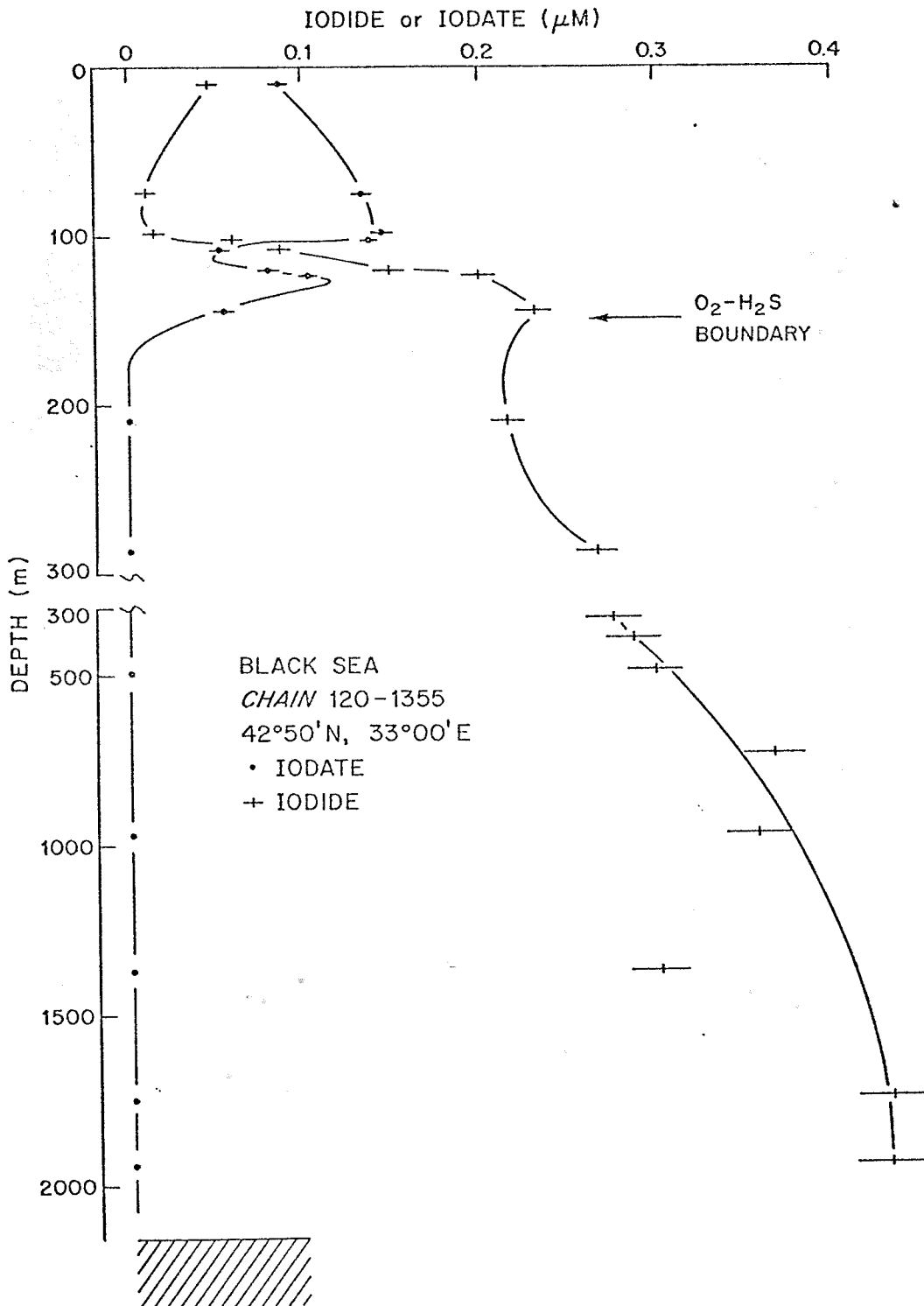
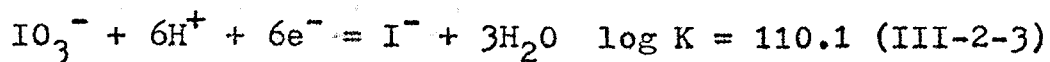


Fig. III-2-7 Profiles of iodate and iodide in the Black Sea at station CHAIN-120-1355 (42°50'N, 33°00'E). • represents iodate. + represents iodide.

oxic zone, an iodate minimum (0.88  $\mu\text{M}$  in the Black Sea; 0.340 and 0.369  $\mu\text{M}$  in the eastern and western basins of the Cariaco Trench) is again present at the surface, and the concentration increases with depth to 0.146  $\mu\text{M}$  in the Black Sea, and 0.431  $\mu\text{M}$  and 0.469  $\mu\text{M}$  in the two basins of the Cariaco Trench. However, at about 100 m in the Black Sea and 180 m in the Cariaco Trench, the concentration starts to drop sharply and reaches zero at approximately the oxygen-sulfide boundary. In contrast, the concentrations of iodide are high at the surface (0.047  $\mu\text{M}$  in the Black Sea; 0.086  $\mu\text{M}$  in the Cariaco Trench) and they decrease to minimum concentrations at 75 m (0.011  $\mu\text{M}$ ) and 160 m (0.019  $\mu\text{M}$ ) in the Black Sea and the Cariaco Trench respectively. Below these depths, the concentrations increase rapidly. Below the oxygen-sulfide boundary, the iodide concentration remains approximately constant at about 0.44  $\mu\text{M}$  in the Cariaco Trench. In the Black Sea, there is a clear general increasing trend towards the bottom from 0.22  $\mu\text{M}$  to 0.43  $\mu\text{M}$ .

The interconversion of iodide and iodate is represented by the equation



The change in the speciation of iodine in the anoxic zone can be predicted from the thermodynamic properties of this reaction. A concentration diagram of the iodine system at

a pH of 8.1 and a total iodine concentration of 0.5  $\mu\text{M}$  is shown in figure III-2-8. In the oxic layer where the pE is 12.5 (Sillen, 1961) iodate will be the dominant form. By contrast, the pE in the anoxic zone is -4 (Spencer and Brewer, 1971) and iodide will be the predominating species.

The conversion of iodate to iodide occurs between 100 m and 150 m in the Black Sea and 160 m and 265 m in the Cariaco Trench. Between these depths, oxygen and sulfide co-exist at low concentrations and their combined redox buffer capacity at most depths is between +1 meq/kg and -1 meq/kg as shown in table III-2-1. In comparison with the redox buffer capacities in truly oxic or anoxic waters, this is remarkably low (<20%) and suggests a chemical instability in this zone where the redox potential may fluctuate with the degree of mixing between oxic and anoxic waters. The pE of a body of natural water is calculated from the couple having the highest redox buffer capacity to poise the system. In this mixing zone, the picture seems unclear. If iodide and iodate are at chemical equilibrium so that they may be used as indicators, the pE will be between 10.0 and 10.7 and suggest that neither the oxygen-water couple nor the sulfate-sulfide couple is poisoning the pE.

The profiles of specific total iodine, which is defined as the ratio of total iodine to salinity, of the three basins are shown in figure III-2-9. In all cases, there is a slight depletion in the surface waters with



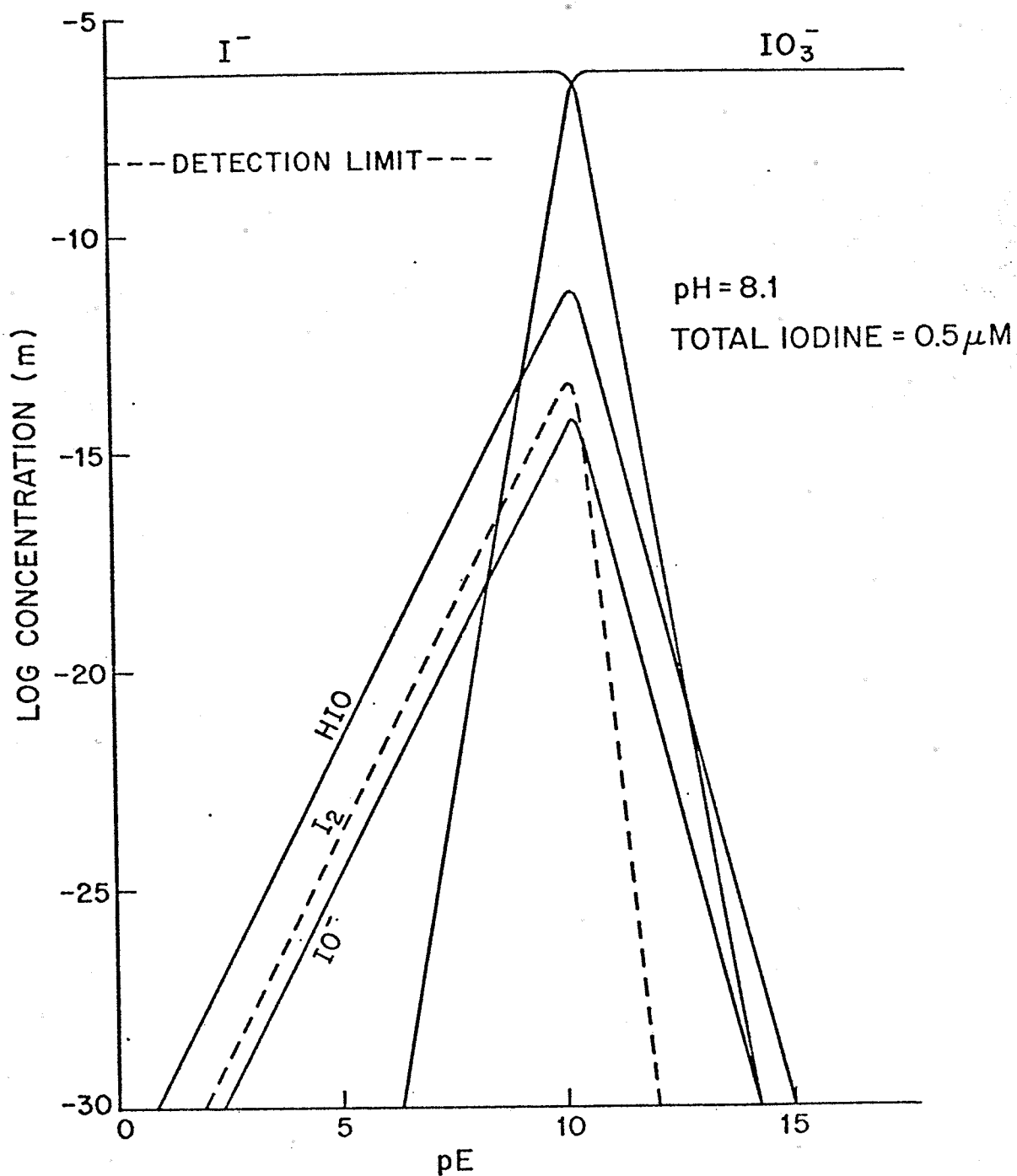


Fig. III-2-8 A concentration diagram of the iodine system in an aqueous solution at pH of 8.1 and total iodine concentration of  $5 \times 10^{-7} M$ .

Table III-2-1 The redox buffer capacity of oxygen and sulfide in the mixing zone and the oxic and anoxic layers.\*\*

Depth (m)	Oxygen (ml/l)	$(\beta_E)_{O_2}^1$ (meq/kg)	$HS^-$ ( $\mu M$ )	$(\beta_E)_{HS^-}^2$ (meq/kg)	$\Sigma \beta^3$ (meq/kg)	
The Cariaco Trench: Western Basin, Station AII-79-2030, 10°37'N, 65°26'W						
0	4.567	-7.51	0	0	-7.51	oxic layer
172	1.217	-2.00	0	0	-2.00	
196	0.441	-0.73	0	0	-0.73	
206	0.323	-0.53	0.50	0.07	-0.46	
226	0.394	-0.65	0.18	0.03	-0.62	
243	0.074	-0.12	0	0	-0.12	
263	0.072	-0.12	0	0	-0.12	
1391	0	0	35.18	5.18	+5.18	anoxic layer
The Cariaco Trench: Eastern Basin, Station AII-79-2031, 10°32'N, 64°46'W						
0	4.56	-7.50	0	0	-7.50	oxic layer
168	1.82	-2.99	0	0	-2.99	
192	0.67	-1.10	0	0	-1.10	
214	0.16	-0.26	0	0	-0.26	
233	0	0	0	0	0	
246	0	0	0	0	0	
263	0.07	-0.12	0.08	0.01	-0.11	
1391	0	0	37.02	5.45	+5.45	anoxic layer

Table III-2-1 (continued)

The Black Sea: Station CHAIN-120-1355, 42°50'N, 33°00'E

	7.49*	-12.31	0	0	-12.31	oxic layer
95	0.41	-0.67	0	0	-0.67	
105	0.34	-0.56	3.28	0.48	-0.08	
115	0.34	-0.56	0.50	0.07	-0.49	
125	0.27	-0.44	28.03	4.13	+3.69	
135	0	0	0.39	0.06	+0.06	
145	0	0	33.20	4.89	+4.89	
1947	0	0	522.8	76.96	+76.96	anoxic layer

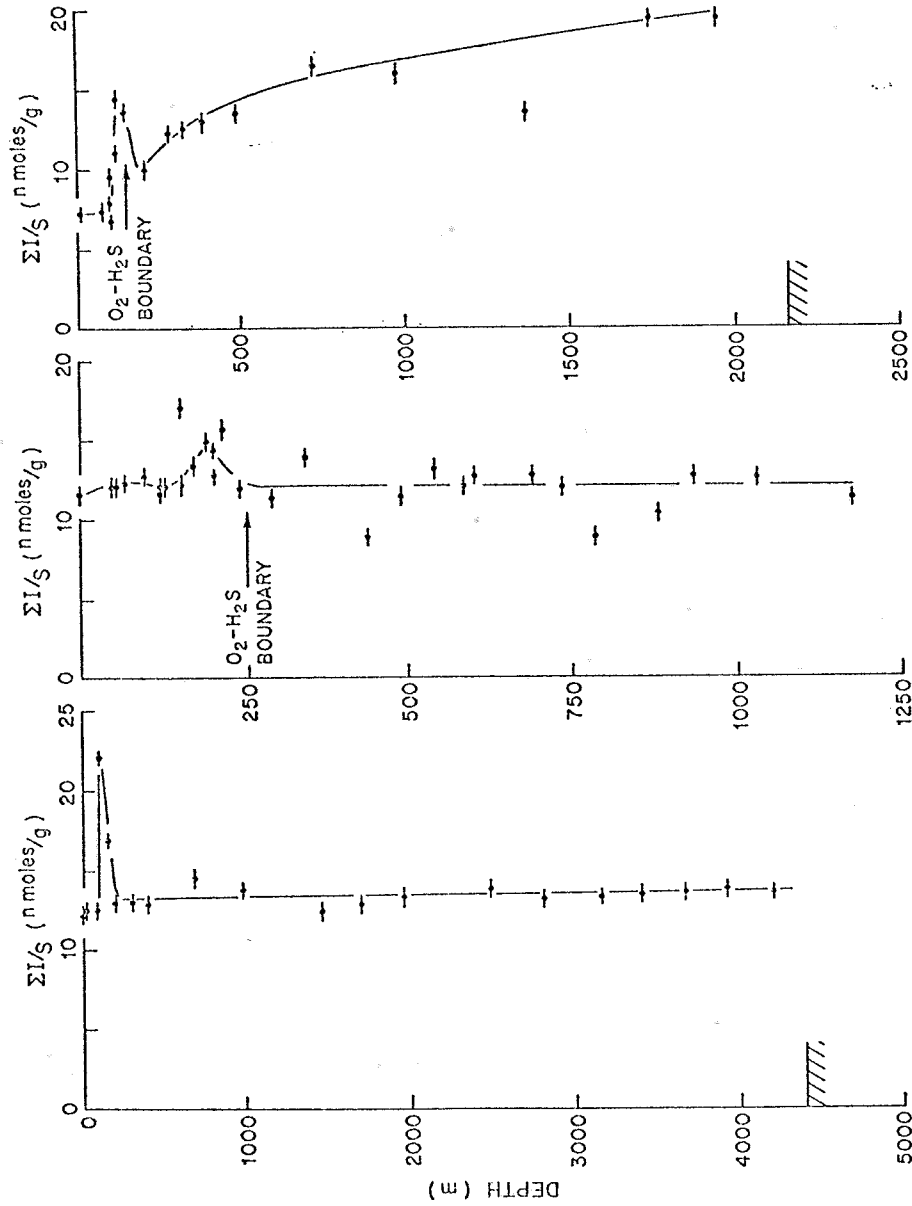
1  $(\beta_E)_{O_2} = (\partial M_{O_2} / \partial pE) = -1.64 (O_2)$  in meq/kg.  $(O_2)$  in ml/l.

2  $(\beta_E)_{HS^-} = (\partial M_{HS^-} / \partial pE) = 0.147 M_{HS^-}$ ;  $(\beta_E)_{HS^-}$  in meq/kg,  $M_{HS^-}$  in  $\mu M$ .

3  $\Sigma \beta = (\beta_E)_{O_2} + (\beta_E)_{HS^-}$ .

\* Value from the nearby station AII-57-1462 at 43°01'N, 33°03'E (Brewer, 1971).

\*\* For a more detailed discussion of the calculation of redox buffer capacities, see Thorstenson (1970) and Brewer and Murray (1973).



AI-79-2033  
 VENEZUELA BASIN  
 13°22'N, 64°43'W

AI-79-2038  
 CARIACO TRENCH  
 EASTERN BASIN  
 10°31'N, 64°45'W  
 TOTAL DEPTH: 1450 m

CHAIN 120-1355  
 BLACK SEA  
 42°50'N, 33°00'E

Fig. III-2-9 Profiles of specific total iodine in the Venezuela Basin, the Cariaco Trench and the Black Sea.

value of 7.3 nmoles/g and 11.6 nmoles/g in the Black Sea and the Cariaco Trench respectively. This depletion may be caused by the uptake of iodine by organisms.

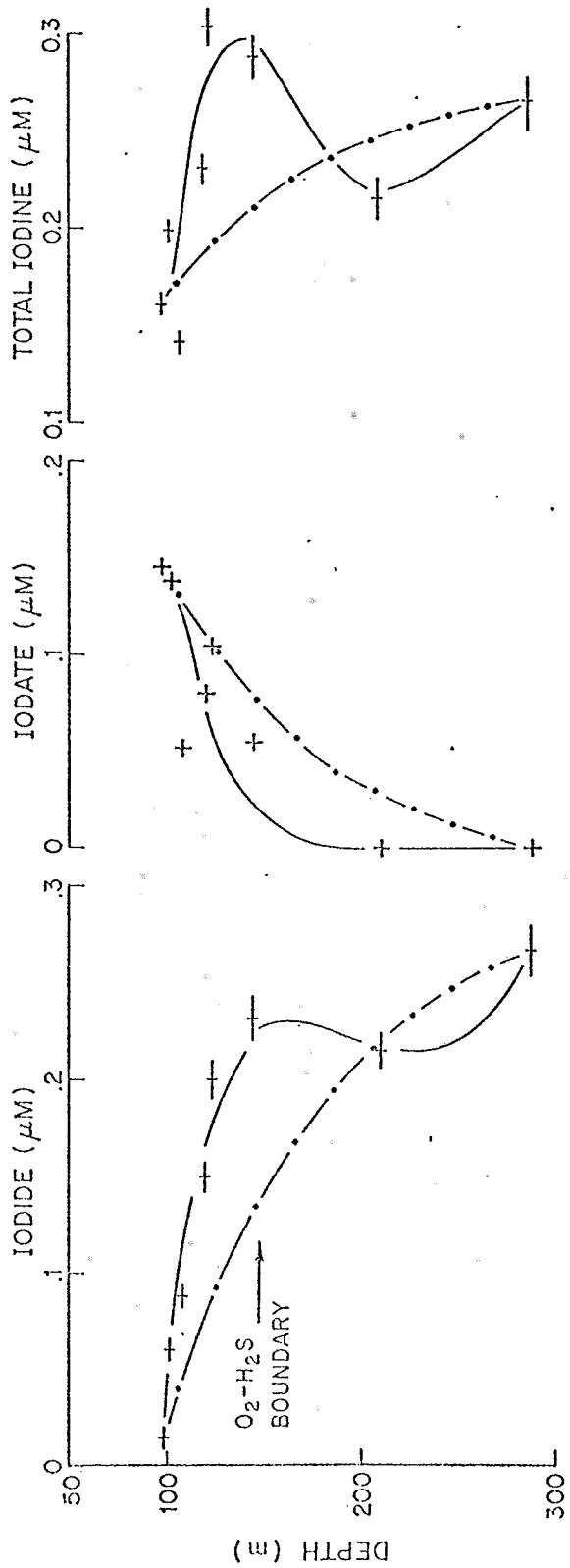
In the anoxic zone of the Cariaco Trench, within the noise of the data, specific total iodine may be considered constant at 12.3 nmoles/g. However, in the Black Sea there is an increasing trend with depth from 10.0 to 19.4 nmoles/g. This may be caused either by the advection of water of high iodine content into the Black Sea, or a diffusion of iodine into the bottom water from the underlying sediments. The specific total iodine in the deep Venezuela Basin is only about 14 nmoles/g. and there is no a priori reason to suppose that the inflowing Mediterranean water should be much different from other oceans. Thus, an advective source for this increased iodine seems unlikely although it cannot yet be completely ruled out. There is however ample evidence suggesting a flux of iodide out of the sediments. In addition to Tsunogai's observation (1971) of excess iodide in the deep Pacific, Price and co-workers (Price et al., 1970; Price and Calvert, 1973) have reported an enrichment of iodine in surface sediments. The concentrations correlated linearly with the organic carbon content and decreased exponentially with depth. Iodine is also enriched in interstitial waters and concentrations up to 150  $\mu\text{M}$  have been reported (Bojanowski and Paslawska, 1970). Pavlova and Shiskina (1973) further showed that the concen-

tration increases with depth. These observations suggest a possible post-depositional diagenetic remobilization of iodine from organic-rich sediments in reducing environments. Thus, diffusion of iodine into the bottom water appears to be a plausible explanation for the high specific total iodine in the Black Sea. The difference between the Cariaco Trench and the Black Sea in this respect may be due to the longer residence time of the water in the latter. Other factors, such as the iodine concentration gradient in the interstitial waters and the composition of the sediments will certainly affect the distribution too, however, there are no available data at the present time for a more detailed assessment.

The distributions of iodide, iodate and total iodine in the mixing zones of the Black Sea and the Cariaco Trench are shown in figures III-2-10 and III-2-11. These data are compared with the profiles expected from simple mixing between two boundary conditions by vertical advection and diffusion as described in Spencer and Brewer (1971). This steady state one dimensional model is formulated as

$$\frac{dc}{dt} = K \frac{d^2c}{dz^2} - w \frac{dc}{dz} = 0 \quad (\text{III-2-4})$$

where K is the vertical eddy diffusivity and w is the vertical advective velocity. The solution of this equation is



$C_m = 0.0151 \mu\text{M}$  at 98 m  
 $C_0 = 0.2669 \mu\text{M}$  at 286 m

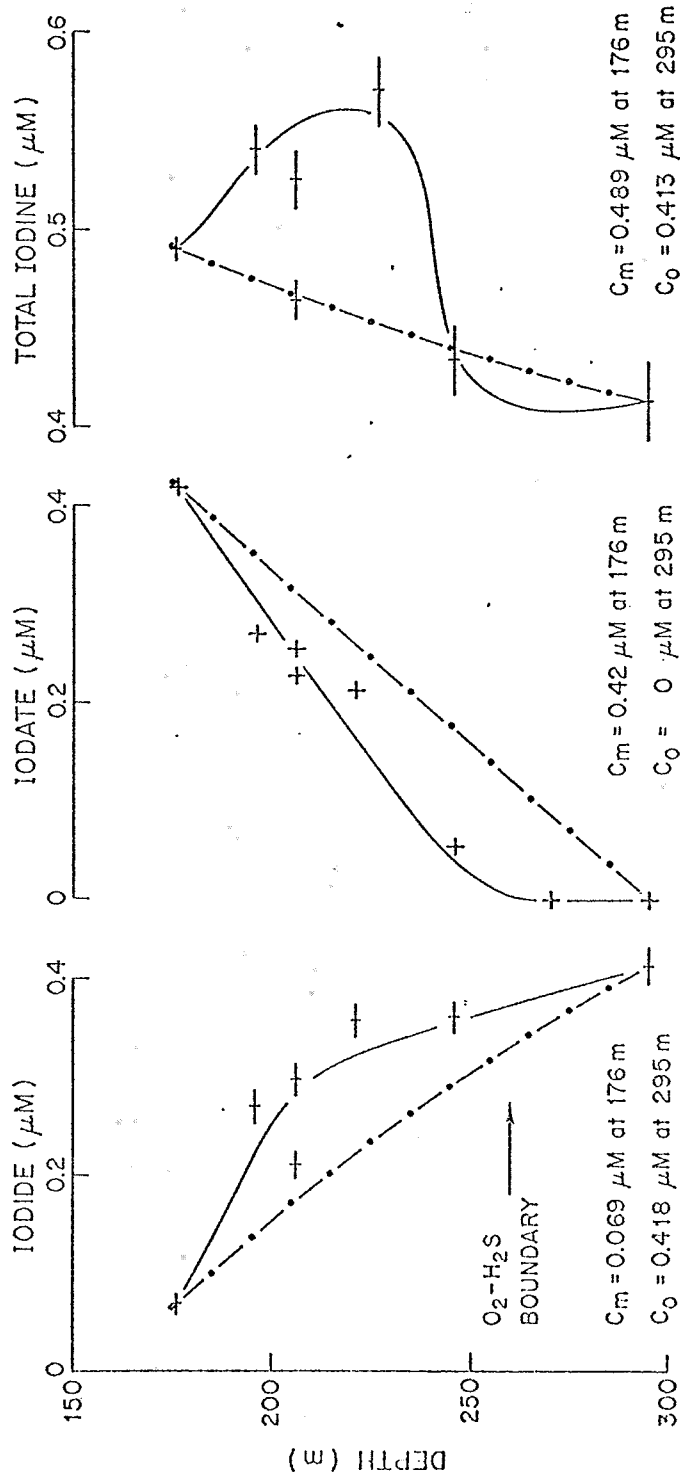
$C_m = 0.146 \mu\text{M}$  at 98 m  
 $C_0 = 0.000 \mu\text{M}$  at 286 m

$C_m = 0.161 \mu\text{M}$  at 98 m  
 $C_0 = 0.267 \mu\text{M}$  at 286 m

CHAIN 120-1355 42°51'N 33°00'E  
 BLACK SEA

• MODEL FIT FOR A STABLE CONSERVATIVE TRACER  
 + OBSERVED DATA  
 $z^* = 0.09 \text{ km}$

Fig. III-2-10 The distribution of iodide, iodate and total iodine in the mixing zone of the Black Sea.



AZ-79-2038 10°31' N, 64°45' W

CARIACO TRENCH EASTERN BASIN

• MODEL FIT FOR A STABLE CONSERVATIVE TRACER

+ OBSERVED DATA

$z^* = 0.23 \text{ km}$

Fig. III-2-11 The distribution of iodide, iodate and total iodine in the mixing zone of the Cariaco Trench.



$$(C - C_0) = (C_m - C_0) \frac{(e^{z/z^*} - 1)}{(e^{z_m/z^*} - 1)} \quad (\text{III-2-5})$$

where  $C_0$  is the concentration at the lower boundary  $z_0$ ,  $C_m$  is the concentration at the upper boundary  $z_m$ , and  $z^*$  is the ratio of  $K/w$  (Craig, 1969). The model is applicable only over linear regions of the  $\theta$ - $S$  diagram where horizontal velocities and concentration gradients may be neglected. The assumption of a true steady state in the Cariaco Trench is questionable. It may however closely approach a steady state in short time intervals.  $z^*$  can be estimated from the profiles of salinity or potential temperature. The values used here are 0.23 km and 0.09 km for the Cariaco Trench and the Black Sea respectively. Iodate appears to be consumed over the entire depth interval of the mixing zone in both basins, reflecting the chemical reduction of iodate to iodide. Iodide is produced in the same intervals, which may be the result of the combined effects of the reduction of iodate and the re-mineralization of particles. In the Black Sea, there is some consumption below 200 m which may possibly be attributed to biological activity (Brewer and Murray, 1973). For total iodine, there is production above the interface and slight consumption below it. Spencer and co-workers (Spencer and Brewer, 1971; Spencer et al., 1972) have observed similar features in dissolved manganese and iron. They suggested the localized dissolution of the mineral oxides in a strong pycnocline

as an explanation. A similar mechanism may also be operating in the iodine system, whereby iodine-rich biogenic particles may preferentially re-mineralize in the pycnocline. In the lower mixed layer, the consumption may again be explained by chemosynthesis. The interconversion of iodine between iodate and iodide will not affect the distribution of total iodine. A more rigorous model is inappropriate at the present time because it calls for a priori knowledge of the functionality of the production and consumption term with depth as in Spencer and Brewer (1971). Since the distribution of iodine in the mixed layer is controlled by a host of processes as described earlier, quantification of such a term will be difficult. Moreover, the growing complexity of this term may prohibit an analytical solution of the advection-diffusion equation with the limited known boundary conditions.

In general, the profiles of iodate, iodide and total iodine in the mixed layer of the Cariaco Trench show features similar to the Black Sea, however, they are usually more subdued. This may reflect the fact that the Black Sea is a more stable system with longer residence time and a stronger pycnocline.

The redox potential of the oceans

The common oxidation states of iodine are: (1) -1 as hydroiodic acid and iodides; (2) 0 as elemental iodine; (3) +1 as hypoiodous acid and hypoiodites; and (4) +5 as iodic acid and iodates. The distribution of iodine among these species as a function of pE at a pH of 8.1 and a total iodine concentration of 0.5  $\mu\text{M}$  is shown in figure III-2-8. A more detailed discussion on the thermodynamics of the iodine system is given in section IV.2.

In oxic waters, if the pE is poised by the  $\text{O}_2/\text{H}_2\text{O}$  couple, its value will be 12.5 (Sillen, 1961) and iodate will be the only measurable species. Brewer and Murray (1973) suggested that the pE is poised by the  $\text{SO}_4^{=}/\text{HS}^-$  couple in anoxic waters so that the pE will be -4. At such a pE, iodide will be the only detectable iodine species. The present analytical capability has a detection limit for iodate or iodide of about 0.005  $\mu\text{M}$ . My observations from the anoxic and oxic basins confirm these predictions except in the surface waters where the disequilibrium is attributed to biological perturbation (Tsunogai and Sase, 1969).

Breck (1974) has recently suggested that the pE of the oceans is poised by the  $\text{O}_2/\text{H}_2\text{O}_2$  couple. He calculated the lower limit of the pE of the ocean to be 8.5 and proceeded to use this value for the prediction of chemical speciations in the oceans. However, this pE value is inconsistent with the observed distribution of the iodine

species. Figure III-2-8 shows that at a pE of 8.5, the concentrations of iodate and iodide will be  $10^{-17}$  M and  $10^{-6.3}$  M respectively. This implies that iodate should not be detectable with the presently available analytical methods and this is contrary to the fact that iodate is ubiquitous in the open oceans and it is the predominant species. In oxic deep waters where biological perturbations of chemical equilibria may be minimal, the iodide concentration is indistinguishable from the blank of 0.005  $\mu$ M and iodate constitutes all the measurable iodine (figure III-2-4). This observation is more consistent with a pE of 12.5 as calculated from the  $O_2/H_2O$  couple. If one takes the upper limit of the iodide concentration in the deep waters as 0.005  $\mu$ M, one can calculate the lower limit of the pE of the oceans to be 10.7.

Liss et al. (1973) suggested that the iodate-iodide couple may act as a sensor for the effective pE level in the oceans. The interconversion between iodide and iodate involves the transfer of six electrons. Consequently, the concentration ratio of these two species will be extremely sensitive to pE changes. Given the detection limits of iodate and iodide to be both at about 0.005  $\mu$ M ( $10^{-8.3}$  M), one can calculate the usable range of this sensor to be 10.0 to 10.7 as shown in figure III-2-8. Thus, it is apparent that at least at the present time, the iodate-iodide couple is not a desirable tool for measuring

pE in the oceans which may have a range of 12.5 to -4.

### III.3 The distribution of iodine in a coastal basin, the Gulf of Maine

#### III.3.1 Introduction

If the distribution of the dissolved iodine species in the surface waters of the oceans is controlled by biological activity (Tsunogai and Sase, 1969; Tsunogai and Henmi, 1971; Tsunogai, 1971b; Wong and Brewer, 1974), seasonal effects may indirectly induce changes in this distribution. These seasonal effects are probably more prominent in the coastal waters of the temperate zone where seasonal changes in productivity are more pronounced. In this section, I shall present data on the distribution of iodine in the winter of 1974-1975 in a coastal basin, the Gulf of Maine.

### III.3.2 Sampling and analytical methods

I have occupied three stations in the Gulf of Maine, two in the Wilkinson Basin (AII-86-2122 and AII-86-2138) and one in the Murray Basin (AII-86-2151) during cruise AII-86 within the period of January 4 - 11, 1975. The locations of the stations are shown in figure III-3-1. Samples were frozen immediately after collection and were shipped back to Woods Hole for analysis. Samples from station 2122 were analyzed for both iodate and iodide while samples from stations 2138 and 2151 were analyzed for iodate only. Iodate was analyzed by photometric micro-titration with a precision of better than  $\pm 1\%$  (Wong and Brewer, 1974) while iodide was analyzed by instrumental neutron activation analysis with a precision of  $\pm 5\%$  (Wong and Brewer, 1976). The reagent blank of the activation analysis is about 0.005  $\mu\text{M}$  and the data reported here have not been blank corrected. The complete data set is shown in Appendix D.

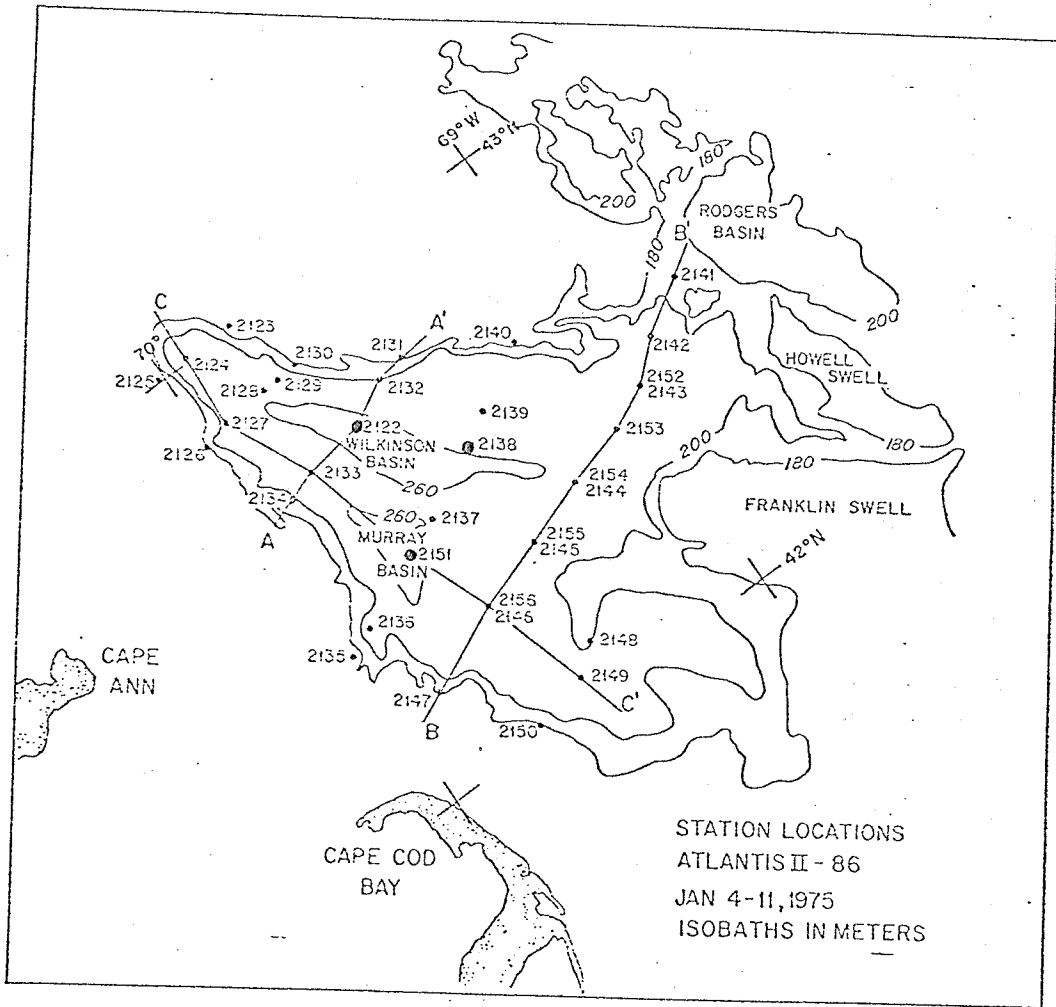


Fig. III-3-1 The cruise track and station locations of cruise AII-86.



### III.3.3 The Gulf of Maine and the Murray-Wilkinson Basin

The Gulf of Maine is a semi-enclosed basin bounded by Maine to the north, Massachusetts to the west, Georges Bank to the south, and Browns Bank and Nova Scotia to the east. The Murray-Wilkinson Basin is one of the depressions in the Gulf and it is situated between  $42^{\circ}\text{N}$  and  $43^{\circ}\text{N}$ , and  $69^{\circ}\text{W}$  and  $70^{\circ}\text{W}$ . It is elongated (NNW-SSE) and is about 80 miles long. It has a maximum depth of about 285 meters and is surrounded by a sill at about 150 meters depth. It is connected to the Rogers Basin to the east, the Franklin Basin to the southeast and the Platts Basin to the north by passages at depths of about 185 m, 185 m and 170 m respectively. The deep part of the Murray-Wilkinson Basin is subdivided by the Wilkinson Divide at about 250 m into the Wilkinson Basin and the Murray Basin.

The surface layers of the Gulf mix freely with coastal waters and their properties are probably significantly influenced by local events. Among all the basins in the Gulf, the Murray-Wilkinson Basin has the most stable deep water and it is renewed by slope and coastal waters of Labrador origin (Colton, 1968). A more detailed description of the hydrography of the Basin has been prepared by Spencer and Brewer (1975).

### III.3.4 Results and discussion

Although the winter of 1974 to 1975 was not a particularly severe one, the effect of overturn in the water column is clearly evident. There is only a weak thermocline between 140 m and 200 m where the potential temperature drops about 1°C and the  $\sigma_\theta$  of the bottom water is only about 0.8  $\sigma_\theta$  units higher than that of the surface water. The sill is also situated at about 150 m. Above 140 m, the water is well mixed and none of the properties (salinity, potential temperature,  $\sigma_\theta$ , oxygen, silicate and phosphate) measured show any significant gradient (figure III-3-3 to III-3-8) although sometimes there are differences in the absolute values between one station and another. The stations were occupied in the order of 2122, 2138 and 2151. Between stations 2122 and 2138, there was a severe winter storm with snow and freezing rain and its effects on the properties of the surface waters are difficult to assess quantitatively. However, most of the properties (salinity,  $\theta$ ,  $\sigma_\theta$ , and oxygen) in the top 70 m of station 2138 do exhibit noticeable deviations from the other stations.

Productivity at this time of the year is probably low. Although no C-14 uptake measurements were made, the nutrient values in the surface waters seem to be consistent with this interpretation. Phosphate and silicate in the surface waters are about 0.9  $\mu\text{M}$  and 9  $\mu\text{M}$  respectively. Such values are exceedingly high. In typical open ocean surface

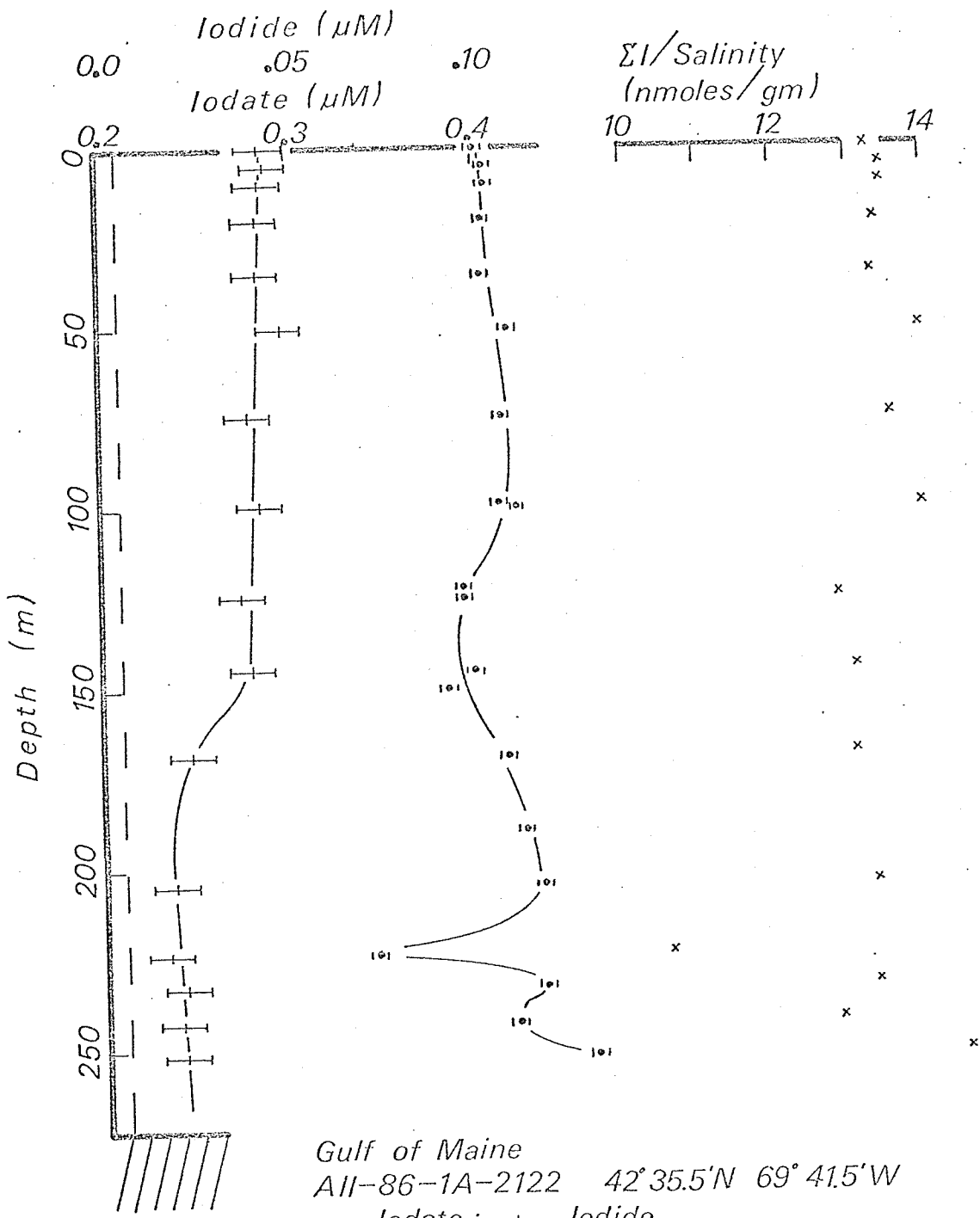


Fig. III-3-2 Profiles of iodate, iodide and specific total iodine at station AII-86-2122, 42° 35.5'N, 69° 41.5'W, the Gulf of Maine.

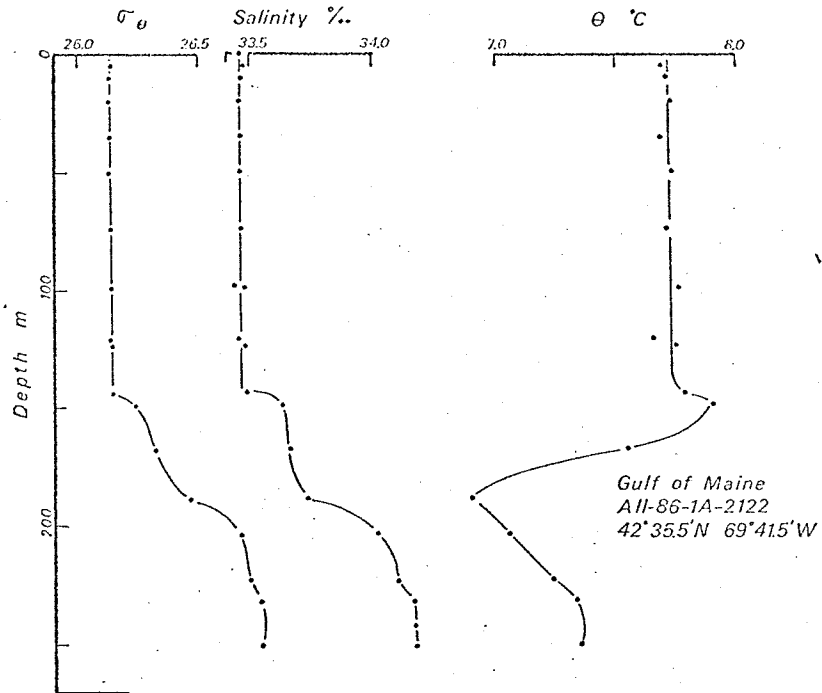


Fig. III-3-3 Profiles of  $\sigma_{\theta}$ , salinity and potential temperature at station AII-86-2122, 42° 35.5'N, 69° 41.5'W, the Gulf of Maine.

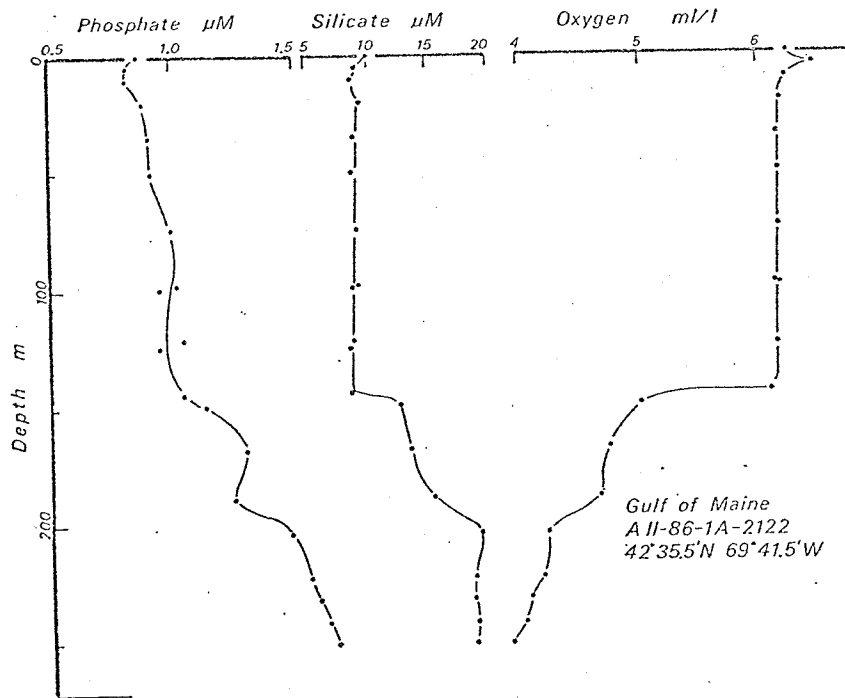


Fig. III-3-4 Profiles of phosphate, silicate and oxygen at station AII-86-2122, 42° 35.5'N, 69° 41.5'W, the Gulf of Maine.

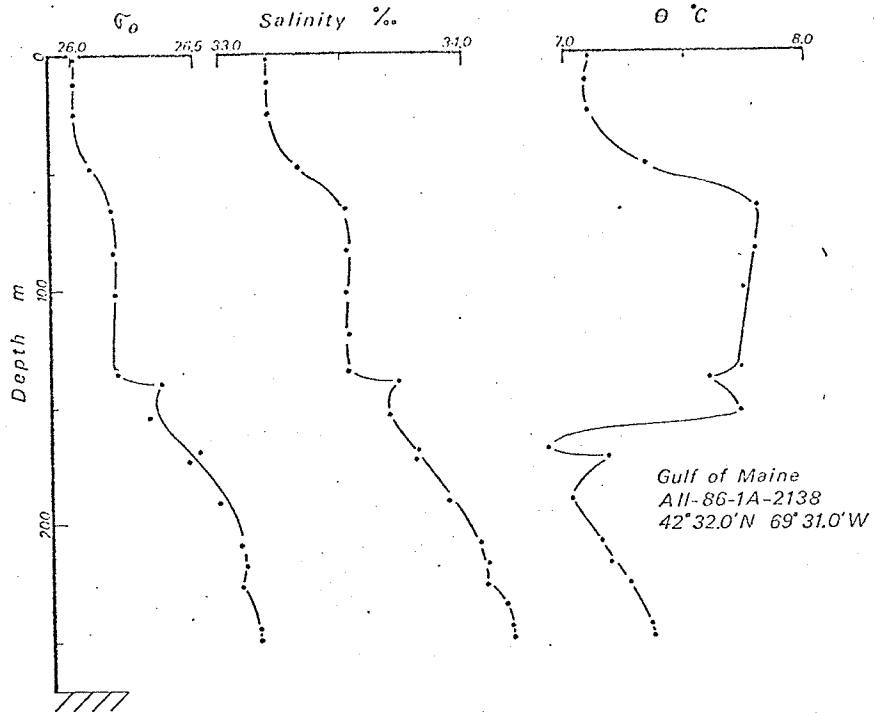


Fig. III-3-5 Profiles of  $\sigma_t$ , salinity and potential temperature ( $\theta$ ) at station AII-86-2138, 42° 32'N, 69° 31'W, the Gulf of Maine.

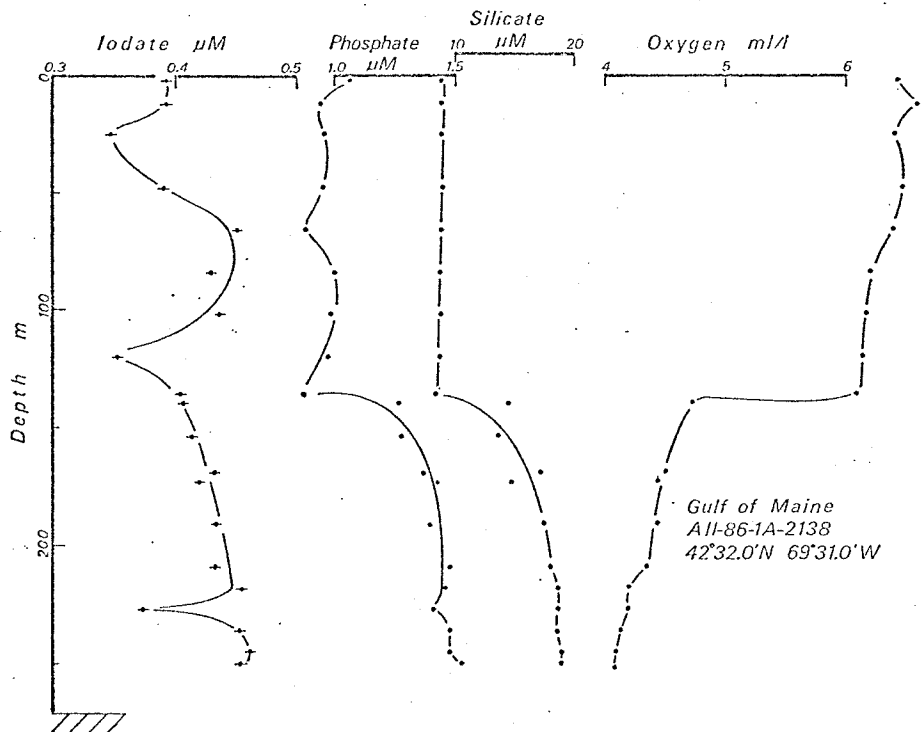


Fig. III-3-6 Profiles of iodate, phosphate, silicate and oxygen at station AII-86-2138, 42° 32'N, 69° 31'W, the Gulf of Maine.

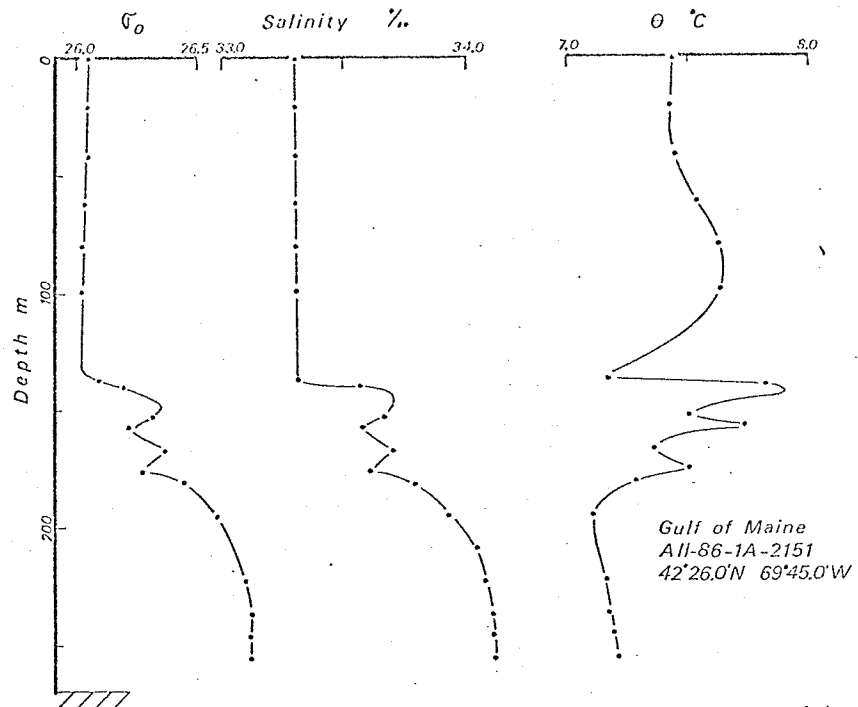


Fig. III-3-7 Profiles of  $\sigma_t$ , salinity and potential temperature ( $\theta$ ) at station AII-86-2151,  $42^\circ 26'N$ ,  $69^\circ 45'W$ , the Gulf of Maine.

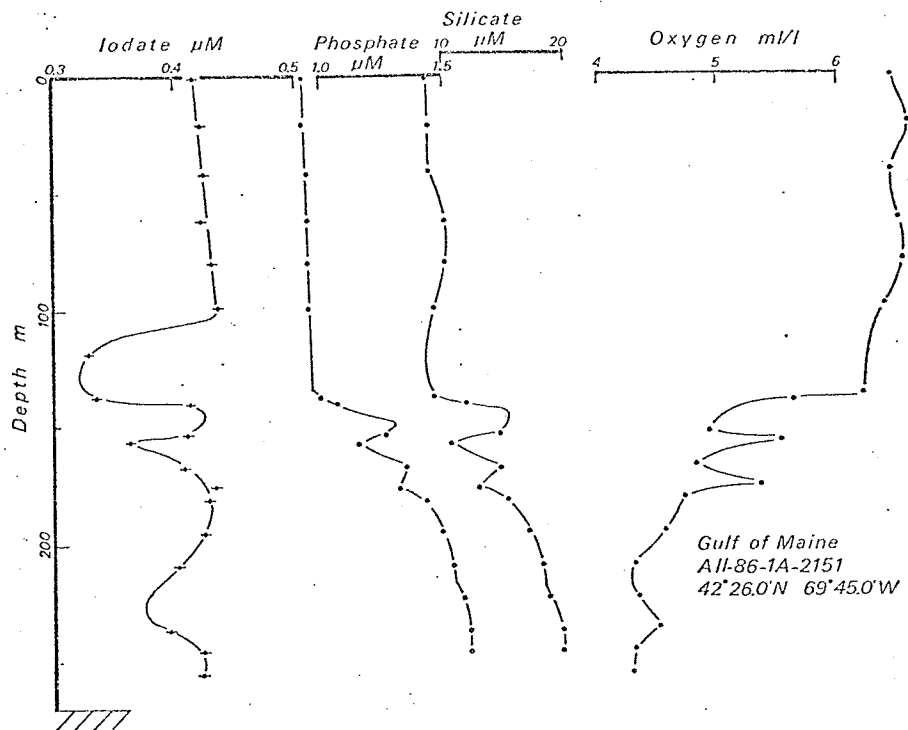


Fig. III-3-8 Profiles of iodate, phosphate, silicate and oxygen at station AII-86-2151,  $42^\circ 26'N$ ,  $69^\circ 45'W$ , the Gulf of Maine.

waters with a moderate productivity, phosphate and silicate are usually only about 0.1  $\mu\text{M}$  in both cases (GEOSECS preliminary reports). The high nutrient levels observed here imply low surface productivity.

The profiles of iodate and iodide are shown in figures III-3-2, III-3-6 and III-3-8 for stations 2122, 2138 and 2151 respectively. The iodate concentrations in the top 100 m of stations 2122 and 2151 are rather uniform with minor variations between 0.40 and 0.44  $\mu\text{M}$ . This uniformity is common to all properties and reflects vigorous winter mixing. Station 2138 seems to be anomalous and considerably larger variations in the concentrations of iodate in the surface layers can be observed. A much lower concentration is found in the top 50 m with a minimum concentration of 0.35  $\mu\text{M}$  at 25 m. Between 50 m and 100 m, the concentration is similar to the other stations. Salinity,  $\theta$  and phosphate also exhibit deviations from uniformity in the top 50 m of the same station. Actually, the salinity and  $\theta$  of the surface waters of this station are the lowest and give rise to a distinct surface minimum. This anomaly may be caused by dilution of the surface waters by rain and snow during the storm.

Below 100 m, considerable variation can be observed in all properties within each station and from station to station. A sharp break can be observed in the profiles of all properties between 120 m and 150 m where

the sill situates. This break in the iodate profiles seems to occur at slightly shallower depths than the other properties. Iodate increases smoothly with depth from about 150 to 200 m at stations 2122 and 2138. At station 2151, the profile exhibits complex fine structures between 130 and 200 m. Similar features are found in profiles of phosphate, silicate, oxygen, salinity and  $\theta$ , and may represent mixing between different water types.

Below 200 m, all the other properties show only subtle variations. However, a distinct iodate minimum is observed at all three stations at about 225 m. In the profiles of the other properties, there is no or occasionally a weak suggestion of an inflexion at this depth. The present data are insufficient for making a more detailed assessment of the cause of this minimum.

The most striking, although not unexpected, observation is the absence of the marked depletion of iodate (up to 50%) in the surface waters which has frequently been reported (Tsunogai and Henmi, 1971; Tsunogai, 1971b; Wong and Brewer, 1974). In this winter, in the Gulf of Maine, any depletion of iodate (if one is present at all) is hidden within the variations, real or experimental, of the profiles. This behavior of iodate seems to support the proposal that iodate is removed by its reduction to iodide through biological agents (Tsunogai and Sase, 1969). Consequently, during winters, when productivity is low, the depletion of



iodate will be least pronounced.

The profile of iodide from station 2122 (figure III-1-2) is consistent with this interpretation of the distribution of iodate. Iodide is also rather uniform in the top 150 m as a result of vigorous vertical mixing. However, its absolute concentration of 0.04  $\mu\text{M}$  is only about 40% of the nearby Woods Hole surface water (0.123  $\mu\text{M}$ , Wong and Brewer, 1975) and <50% of the moderately productive Equatorial Atlantic waters (0.10  $\mu\text{M}$ , Wong, 1976; see also section III.1) probably as a result of a lower biological activity in the winter time.

The iodide concentration decreases noticeably below 150 m to a minimum of about 0.02  $\mu\text{M}$ . However, its concentration even below the thermocline is always significantly above the blank of 0.005  $\mu\text{M}$ . There are three possible sources for this iodide which is thermodynamically unstable and is probably produced only in surface waters or reducing environments: (1) the sinking and subsequent advection of iodide rich surface waters along isopycnals; (2) the downward diffusion of iodide from the surface waters through the thermocline; and (3) the diffusion of iodide from the underlying sediments. All three mechanisms seem to be possible here. The first mechanism implies that the deep water is young so that the iodide has not been completely removed by oxidation. The deep water of this Basin is probably young as it originates from the nearby Labrador slope water (Colton, 1968). The

thermocline is also weak as a result of winter mixing with a  $\sigma_\theta$  difference between the surface and deep water of only 0.6 to 0.7  $\sigma_\theta$  unit. Thus, diffusion through the thermocline cannot be ruled out. Moreover, below 200 m, there is also a general trend of increasing iodide concentration towards the bottom. Although this increase in concentration is small and is within the analytical uncertainty, it points to the possibility of a flux of iodide from the sediments as suggested by Tsunogai (1971b).

### III.4 The distribution of iodine in marine suspended matter

#### III.4.1 Introduction

The present status of our knowledge on the geochemistry of the marine iodine system has been briefly reviewed in section I.2. This evidence suggests that particulate iodine is likely to be important in the cycling of iodine in the ocean. In this section, I shall report measurements of particulate iodine in samples obtained from the Atlantic during the GEOSECS (Geochemical Ocean Sections Study) expedition.

### III.4.2 Sampling and analytical method

Samples were obtained from 13 stations of the GEOSECS (Geochemical Ocean Sections Study) expedition. The cruise track and the positions of the stations are shown in figure III-4-1. Stations where particulate iodine data are available are marked as solid triangles. The analytical method has been described in detail in section II.5. Briefly, for each sample, about 10 l of sea water is pressure filtered through a 0.6  $\mu$  (37 mm in diameter) Nuclepore filter. The sea salts are carefully washed away. The filter is dried and then pressed into a pellet (4 mm x 1 mm). The pellets are analyzed by neutron activation analysis using the facilities at the Rhode Island Nuclear Science Center at Narragansett, Rhode Island. A listing of the data is shown in Appendix E.

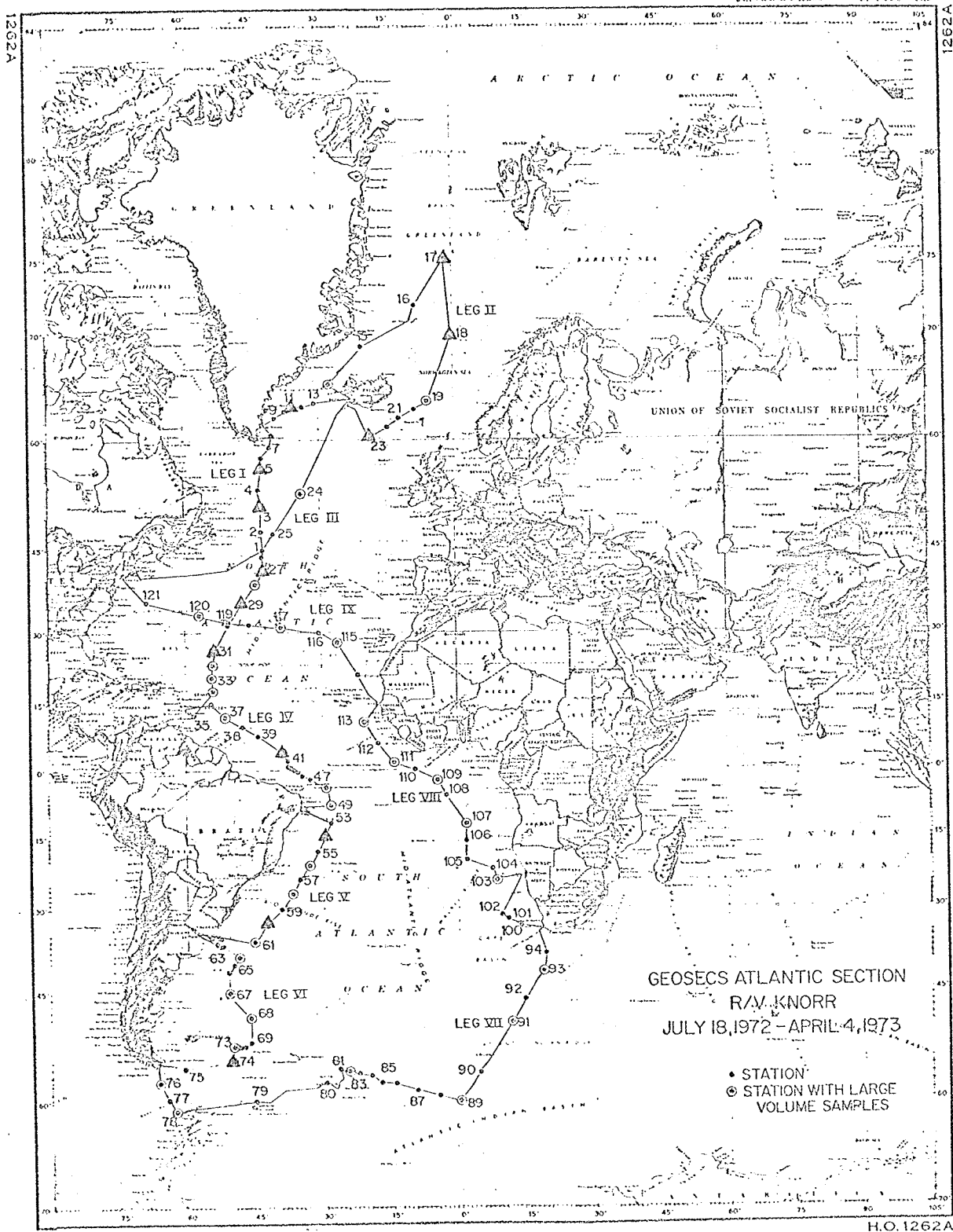


Fig. III-4-1 The cruise track and station positions of the GEOSECS Atlantic section. Stations where particulate iodine data are available are marked as solid triangles.

N0-66

### III.4.3 Results and discussion

Most of the particles in the surface waters are likely to be biogenic. Consequently, the particulate composition may be close to that of marine organisms. On the other hand, particles close to the bottom of the ocean may have a composition similar to surface sediments. Iodine concentrations usually range between 100 and 300 ppm in marine organisms (Bowen, 1966) and between 60 and 800 ppm in surface sediments (Price et al., 1971; Price and Calvert, 1973). Table III-4-1 shows the iodine content of suspended matter collected closest to the surface and the bottom of the Atlantic at thirteen stations. The concentrations are normalized to the dry weight of the total suspended matter. The ranges of concentrations of iodine in the particulate matter from the surface and the bottom waters are 32 to 1256 ppm and 19 to 225 ppm with mean concentrations of 271 ppm and 112 ppm respectively. These thirteen stations cover a large geographical area ( $75^{\circ}\text{N}$  to  $55^{\circ}\text{S}$ ). The wide ranges of the concentrations of particulate iodine in the surface and bottom waters probably reflect real geographical variations. However, the means of these values are within the range of iodine content in marine organisms and surface sediments. Thus, although no previous data are available for a direct comparison, the values reported here seem to be reasonable.

Table III-4-1 Iodine content of particulate matter collected  
 closest to the surface and the bottom of the Atlantic  
 during the GEOSECS expedition

Station Number	Distance from Bottom (m)	Iodine Content* (ppm)	Distance from Surface (m)	Iodine Content* (ppm)
3	62	54	19	150
5	228	87	7	81
11	156	71	7	259
17	179	80	40	73
18	74	194	18	1256
23	2	138	1	117
27	100	118	7	186
29	75	106	150	571
31	679	19	29	176
40	662	116	1	125
54	208	225	8	242
60	10	179	2	257
74	31	71	8	32
Mean		112		271

\* Relative to the dry weight of total suspended matter.

Figure III-4-2 shows typical profiles of particulate iodine and total particulate matter. The most prominent feature in particulate iodine is the sharp maximum in the surface waters. The highest concentration observed is 127 ng/kg (relative to the weight of sea water filtered) at 18 m in station 18. The maximum may occur at the surface or at a few tens of meters below the surface. In all cases, the maximum occurs within the euphotic zone. Below this zone, the concentration drops sharply to about 1 to 2 ng/kg and it remains approximately constant with depth until the nepheloid layer, where an increase in concentration towards the bottom is frequently observed. Total particulate matter shows similar features although the increase in concentration in the nepheloid layer is more marked.

The sharp maximum in the euphotic zone is probably caused by a high rate of fixation of iodine by biological activity. The sharp drop of concentration at about the thermocline implies a rapid cycling of iodine between its dissolved and particulate phases within the euphotic zone as a large portion of the biogenic particles is re-mineralized. The concentration of total suspended matter also decreases sharply in the same depth interval and this seems to indicate a dissolution of particulate material. This distribution of particulate iodine in the surface layers is similar to particulate organic carbon, phosphorus and nitrogen (Menzel and Ryther, 1964; Holm-



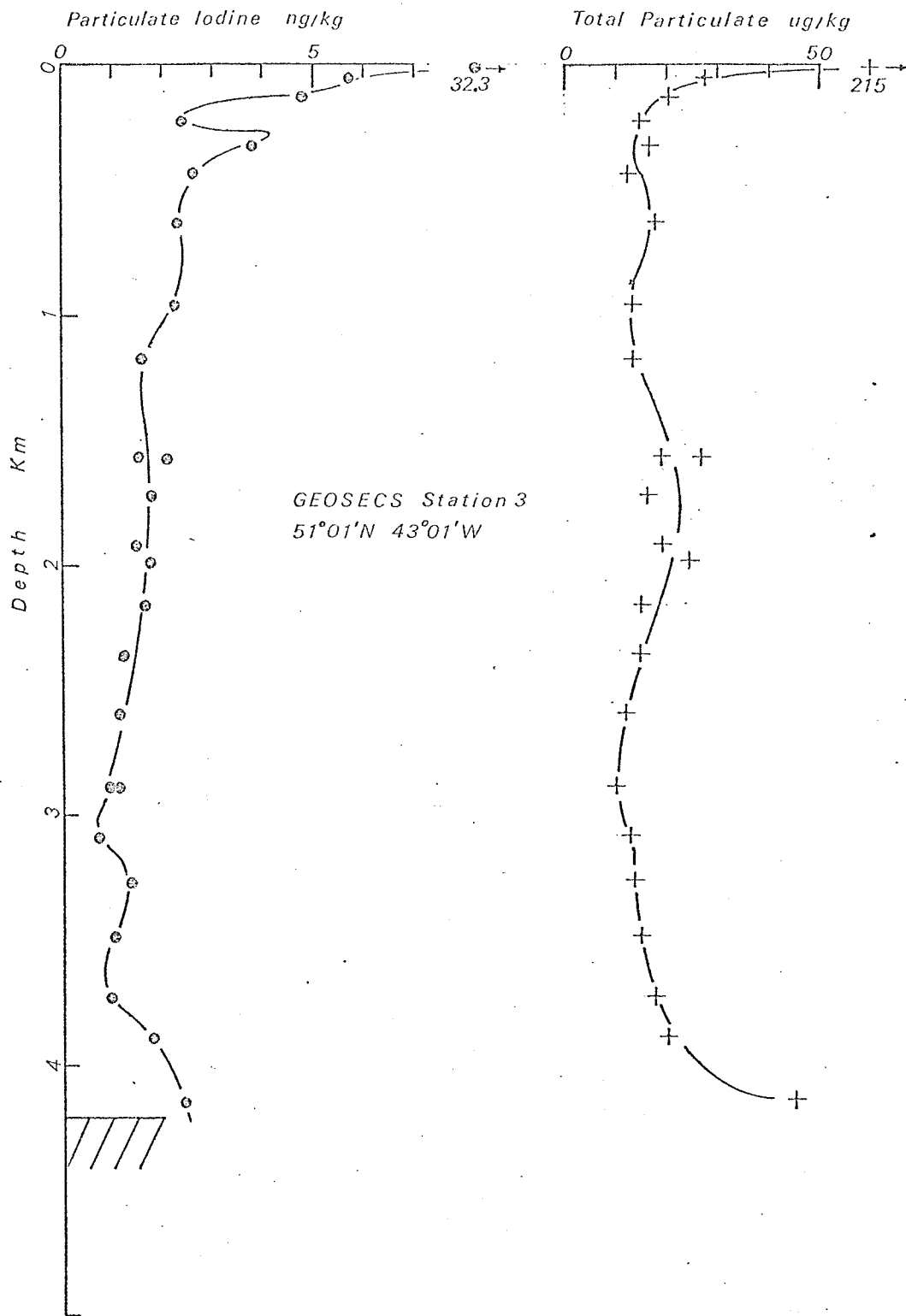


Fig. III-4-2 Typical profiles of particulate iodine and total particulate matter.

Hansen et al., 1966; Hobson and Menzel, 1969; Holm-Hansen, 1972) and it suggests that they may be controlled by similar processes. Rapid cycling of biological material within the euphotic zone is well known. Williams et al. (1969) estimated that only 0.5% of the photosynthetically fixed carbon enters the deep sea. In the bottom water, the increase in particulate iodine concentration is possibly caused by the re-suspension of surface sediments as the total particulate concentration also increases markedly.

Inorganic detrital contribution to particulate iodine is probably insignificant. In marine suspended matter, the iodine content is always a few tens of ppm or higher throughout the entire water column. This is about two orders of magnitude higher than the concentration in rocks. Profiles of particulate iodine in units normalized to the dry weight of total particulate matter are much noisier than those normalized to a unit weight of sea water. This is probably due to the larger uncertainty in the determination of total particulate weight. However, there is still a tendency of higher particulate iodine content in surface waters with an average of about 200 ppm. Below the euphotic zone, the concentration is approximately constant at around 100 ppm even in the nepheloid layer. Table III-4-1 seems to bear out this relationship although considerable variations may occur from station to station. Since clay detrital particles are usually resistant to dissolution, this cannot be

used to explain these variations in concentration with depth.

A profile of the ratio of particulate iodine to particulate scandium (I/Sc) is shown in figure III-4-3. Particulate scandium has a detrital origin and is likely to be related to the clay fraction. The profile shows high I/Sc in the surface waters. It decreases rapidly with depth to a background level which remains low even in the nepheloid layer. In the surface waters, the particles are mostly biogenic. Consequently, iodine concentration is high and the scandium concentration is low and thus I/Sc is high. In deep waters, the degradable biogenic particles have already been decomposed leaving only a residual amount of iodine behind. As a result, I/Sc is low. In the bottom waters, only particles most resistant to degradation remain. A significant or even major portion of them may have a detrital origin. The increase in particulate iodine probably reflects only the increase in total suspended matter. Thus, the accompanying increase in particulate scandium concentration is sufficient to compensate for this effect and the I/Sc therefore remains low.

Figure III-4-4 shows a section of particulate iodine in the Western Atlantic from 75°N to 55°S. The surface waters seem to be characterized by concentrations above 5 ng/kg. The higher concentrations (above 10 ng/kg) are confined to the higher latitudes where biological

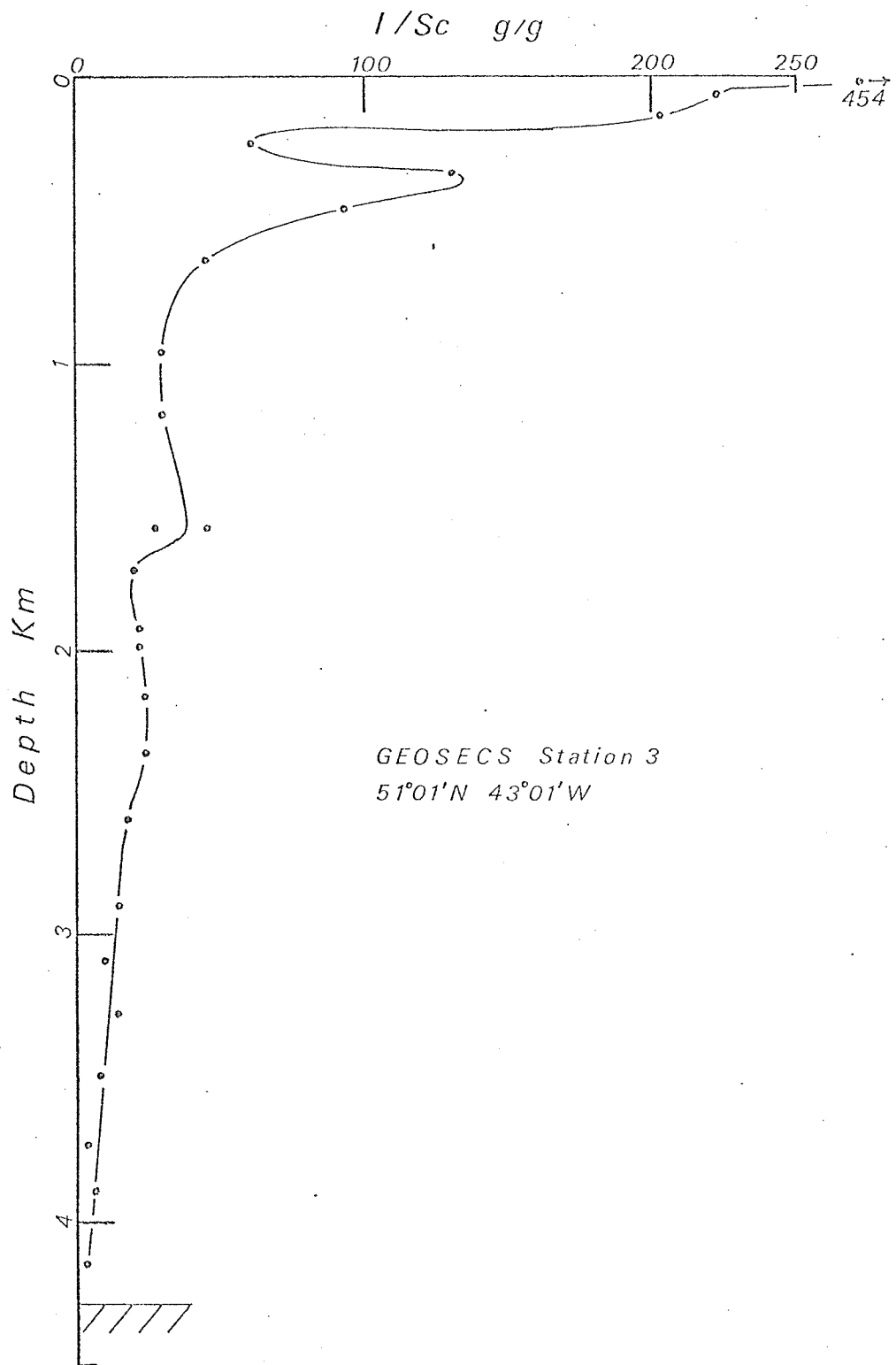


Fig. III-4-3 A profile of the ratio of particulate iodine to particulate scandium (I/Sc).

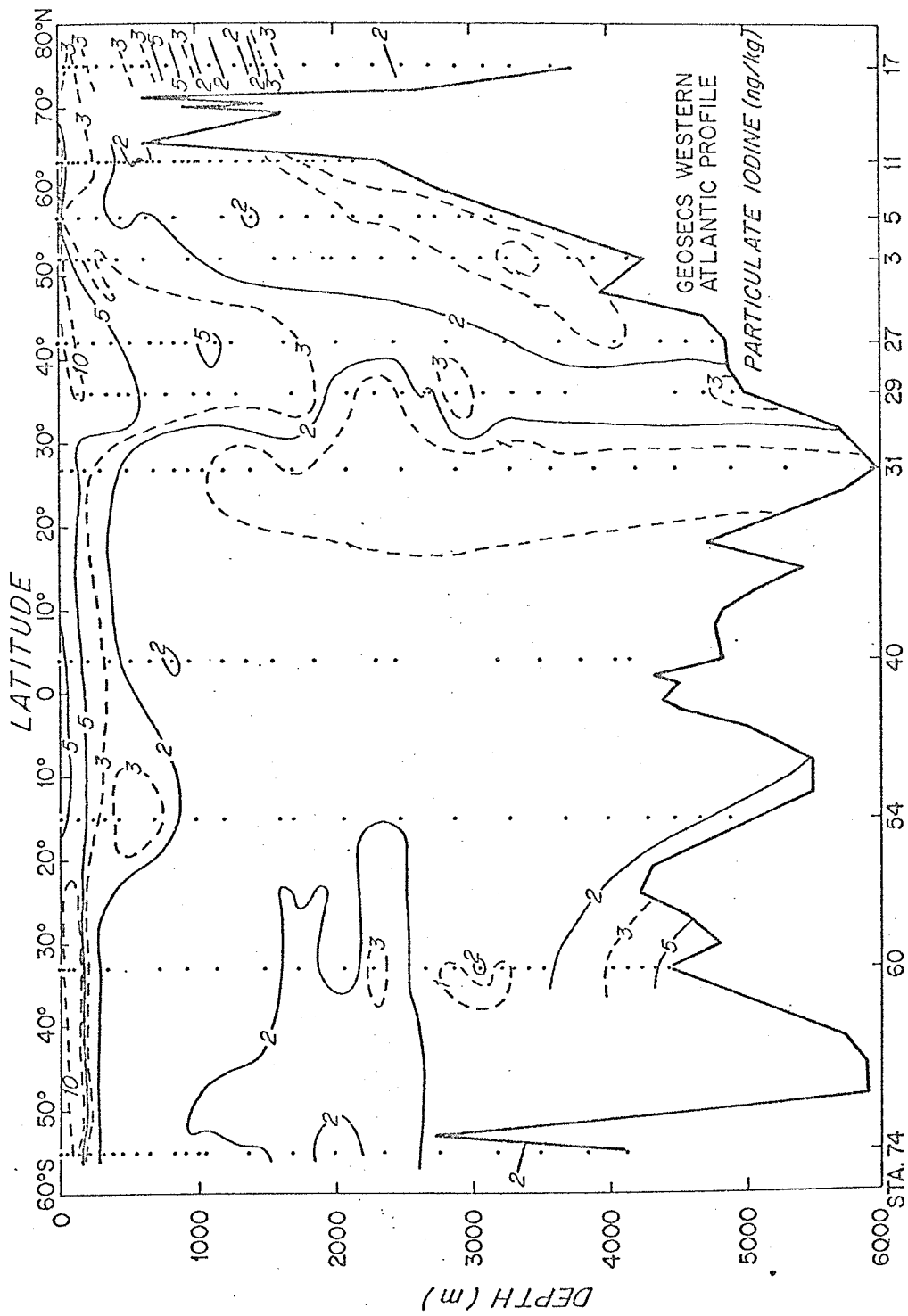


Fig. III-4-4 A section of particulate iodine in the Western Atlantic from 75°N to 55°S.

activity is highest. In the deep waters, the concentrations are generally below 2 ng/kg.

There is evidence suggesting the transport of particles with the water masses along isopycnals. At station 17, at 75°N, the thermocline is weak. The  $\sigma_\theta$  surfaces are almost vertical. As a result, particulate iodine is uniformly high down to about 2300 m. This distribution suggests downward mixing. There is also a tongue of water with high particulate iodine concentration that extends down to about 2000 m between 30°N and 50°N and this may represent the sinking of the Labrador Sea Water. The  $\sigma_\theta$  surfaces also show an accompanying sharp dip in this region. Station 31 at 27°N is in the middle of the North Atlantic gyre. The productivity of this region is low (Koblentz-Mishke et al., 1970) and this is reflected in the low particulate iodine concentrations throughout the entire water column. In this station, below 900 m, the concentration never exceeds 1 ng/kg, the lowest level observed in the entire Atlantic. Higher particulate iodine concentrations are observed in the nepheloid layer at stations 3, 29, 54, 60 and 74.

The standing crop of particulate iodine in the top 200 m of the water column of each station has been estimated and tabulated in table III-4-2. The map of the distribution of primary productivity compiled by Koblentz-Mishke et al. (1970) is shown in figure III-4-5 and the approximate positions of the stations are marked on the map. Al-

Table III-4-2 Standing crops of particulate iodine in  
the top 200 m of the Atlantic

Station Number	Latitude	Longitude	Standing Crop (mg-I/ sq. m)
3	51°50'N	43°07'W	2.1
5	56°56'N	42°34'W	0.8
11	63°32'N	35°14'W	2.8
17	74°55'N	01°11'W	0.6
18	69°59'N	00°07'W	6.4
23	60°24'N	18°40'W	1.7
27	41°57'N	41°59'W	2.3
29	36°00'N	47°00'W	1.0
31	27°00'N	53°31'W	1.3
40	03°55'N	38°32'W	1.0
54	15°02'S	29°32'W	1.5
60	32°58'S	42°30'W	3.3
74	55°00'S	50°07'W	1.7

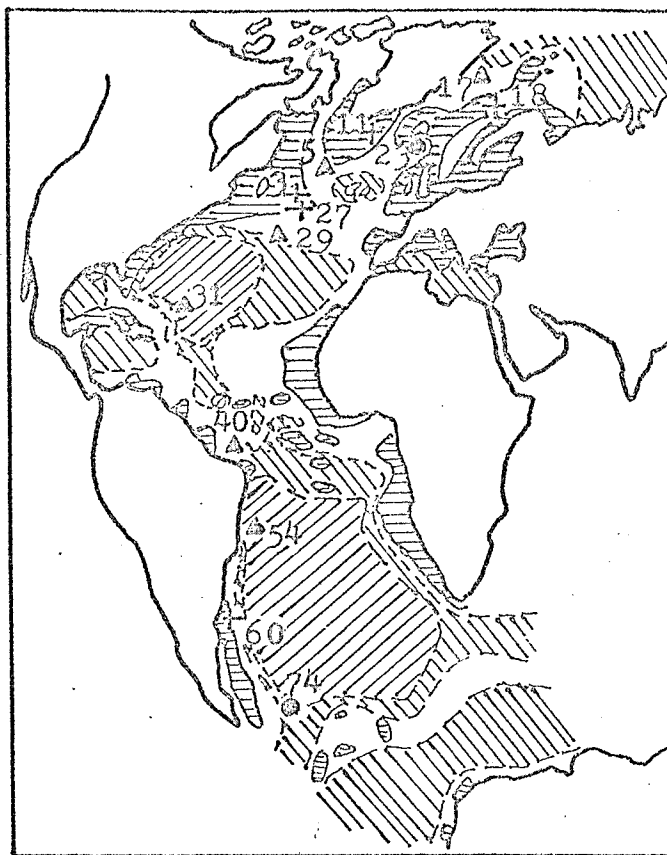

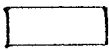

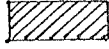


Fig. III-4-5 The distribution of primary productivity in the Atlantic Ocean (Koblentz-Mishke et al., 1970).

 >250 mg C/m <sup>2</sup> /yr	 150-250 mg C/m <sup>2</sup> /yr
 100-150 mg C/m <sup>2</sup> /yr	 <100 mg C/m <sup>2</sup> /yr

+ - Station with standing crop of >2.0 mg I/m<sup>2</sup>.  
 o - Station with standing crop of 1.5 to 2.0 mg I/m<sup>2</sup>.  
 Δ - Station with standing crop of <1.5 mg I/m<sup>2</sup>.



though this map of productivity is rather crude, a qualitative correlation between the standing crops of particulate iodine and productivity is still apparent. Standing crops above  $2 \text{ mg-I/m}^2$  in stations 3, 11, 18, 27 and 60 are all associated with high productivity whereas in the middle of the gyre, stations 29, 31 and 54, the standing crops are below  $1.5 \text{ mg-I/m}^2$ . Finer details can be observed with the help of more refined maps of productivity. The marked difference in the standing crops between stations 17 and 18 probably reflects the large difference in productivity between the Norwegian Sea and the Greenland Sea as shown by the more detailed map by Berge (1958). Zones of high productivity also hug the coasts of the southern tip of Greenland and the north-eastern coasts of Canada, whereas, in between these zones in the Labrador Sea, the productivity is lower (Steeman Nielsen, 1958). The distribution of the standing crop of particulate iodine in this area is consistent with this pattern with higher concentrations at station 11, 3 and 27 and lower concentration at station 5.

CHAPTER IV. THE INTERCONVERSION OF THE DISSOLVED IODINE  
SPECIES IN THE OCEAN

#### IV.1 Introduction

In this section, our present understanding on the effects of thermodynamics, chemical kinetics and biological activity on the interconversion of dissolved iodine species will be reviewed. Based on this information and data from further laboratory studies, the relative stability and the fate of the various species of dissolved iodine will be assessed. The plausibility of invoking these species as agents in geochemical processes will be examined.

#### IV.2 The thermodynamic properties of the aqueous iodine system

Iodine shows five principal oxidation states:

(1) -1 as hydroiodic acid and iodides; (2) 0 as elemental iodine; (3) +1 as hypoiodous acid and hypoiodites; (4) +5 as iodic acid and iodates; and (5) +7 as periodic acid and periodates. Other oxidation states (+4 and +3) have been reported but they are treated merely as chemical curiosities (Latimer, 1952). Some thermodynamic properties of the iodine system are summarized in tables IV-2-1 and IV-2-2.

The relative abundances of the various species at equilibrium, at a total iodine concentration of  $5 \times 10^{-7}M$ , as a function of pE and the detection limits of our present analytical capability are shown in figure IV-2-1. Above a pE of 10.7, iodate is the dominant form, while, below a pE of 10.0, iodide will be dominant. Iodate and iodide co-exist in measurable quantities only within the pE range of 10.0 to 10.7. All the other species are presently undetectable. The concentration diagram does not show the relative stabilities of all the species. It only presents the composition of the mixture at equilibrium. The relative stabilities of the different species of a single element may be better shown by an oxidation state diagram (Johnson, 1968) which has not yet been used by oceanographers. It is a plot of the electrode potential for the conversion

Table IV-2-1 The thermodynamic properties of some iodine species

Formula	State	$H_f^{\circ}$ Kcal	$S^{\circ}$ cal/deg	$F_f^{\circ}$ Kcal	Source
$I^{-}$	aq	13.37	26.14	-12.35	1
$I_3^{-}$	aq	-12.4	41.5	-12.31	1
$I_5^{-}$	aq			-6.9	3
$I_2$	g	14.876	62.280	4.63	1
$I_2$	c	0	27.9	0	1
$I_2$	aq	5.0		3.926	2
$IO_3^{-}$	aq	-55.0	27.7	-32.4	1
$H_2IO_4^{+}$	aq			-25.4	1,3
HIO	aq	-38(?)		-23.5	2
$IO^{-}$	aq	-34(?)		-8.5	2
$HIO_4$	aq			-15.02	3
$IO_4^{-}$	aq			-12.7	3
$H_4IO_6^{-}$	aq			-123.88	3
$HIO_5^{-}$	aq			-58.11	3
$IO_5^{-}$	aq			-43.11	3
ICl	c	-8.03	24.5	-3.24	2
$ICl_3$	c	-21.1	41.1	-5.36	1
$HIO_3$	aq			-33.34	3
ICl	aq			-4.0	2

\* Garrels and Christ (1965)

1 Rossini, Wagman, Evans, Levine and Jaffe (1952)

2 Latimer (1952)

3 Anonymous (1960)

aq - aqueous; g - gaseous; c - crystalline

Table IV-2-2 Thermodynamic properties for the interconversion of iodine species\*

Reaction	log K		$\Delta G^\circ/n$ (a)		$\Delta G^\circ/n$ (b)	
			Kcal/mole	eV/mole	Kcal/mole	eV/mole
$\text{IO}_3^- + 6\text{H}^+ + 6\text{e}^- = \text{I}^- + 3\text{H}_2\text{O}$	110.1		25.04	1.086	3.27	0.143
$\text{IO}_3^- + 6\text{H}^+ + 5\text{e}^- = \frac{1}{2}\text{I}_2(\text{aq}) + 3\text{H}_2\text{O}$	99.2		27.07	1.174	1.24	0.055
$\text{IO}_3^- + 4\text{H}^+ + 4\text{e}^- = \text{IO}^- + 2\text{H}_2\text{O}$	65.6		22.37	0.970	5.94	0.259
$\text{IO}_3^- + 3\text{H}_2\text{O} + 6\text{e}^- = \text{I}^- + 6\text{OH}^-$	26.0		5.91	0.256	22.40	0.973
$\text{IO}_3^- + 3\text{H}_2\text{O} + 5\text{e}^- = \frac{1}{2}\text{I}_2(\text{aq}) + 6\text{OH}^-$	15.5		4.23	0.186	24.08	1.046
$\text{IO}_3^- + 2\text{H}_2\text{O} + 4\text{e}^- = \text{IO}^- + 4\text{OH}^-$	9.6		3.28	0.142	25.03	1.087
$\text{IO}^- + 2\text{H}^+ + 2\text{e}^- = \text{I}^- + \text{H}_2\text{O}$	44.4		30.27	1.313	-1.96	-0.084
$\text{HIO} + \text{H}^+ + \text{e}^- = \frac{1}{2}\text{I}_2(\text{aq}) + \text{H}_2\text{O}$	22.9		31.24	1.354	-2.93	-0.125
$\text{IO}^- + \text{H}_2\text{O} + 2\text{e}^- = \text{I}^- + 2\text{OH}^-$	16.4		11.18	0.485	17.13	0.744
$\text{IO}^- + \text{H}_2\text{O} + \text{e}^- = \frac{1}{2}\text{I}_2(\text{aq}) + 2\text{OH}^-$	5.9		8.04	0.349	20.27	0.880
$\frac{1}{2}\text{I}_2(\text{aq}) + \text{e}^- = \text{I}^-$	10.5		14.35	0.622	13.96	0.607
$\text{I}_3^- = \text{I}_2 + \text{I}^-$	-2.86	(c)				
$\text{I}_2(\text{aq}) + \text{H}_2\text{O} = \text{HIO} + \text{I}^- + \text{H}^+$	-12.3	(d)				

\* All data from Sillen and Martell (1964), Garrels and Christ (1965) and Stumm and Morgan (1970) except where noted.

- (a) Relative to the  $\text{H}_2\text{-H}^+$  couple. (b) Relative to the  $\text{H}_2\text{O-O}_2$  couple.  
 (c) From Burger and Liebafsky (1973) and (d) From Burger and Liebafsky (1973) and  
 Katzin and Gebert (1955). Allen and Kefer (1955).

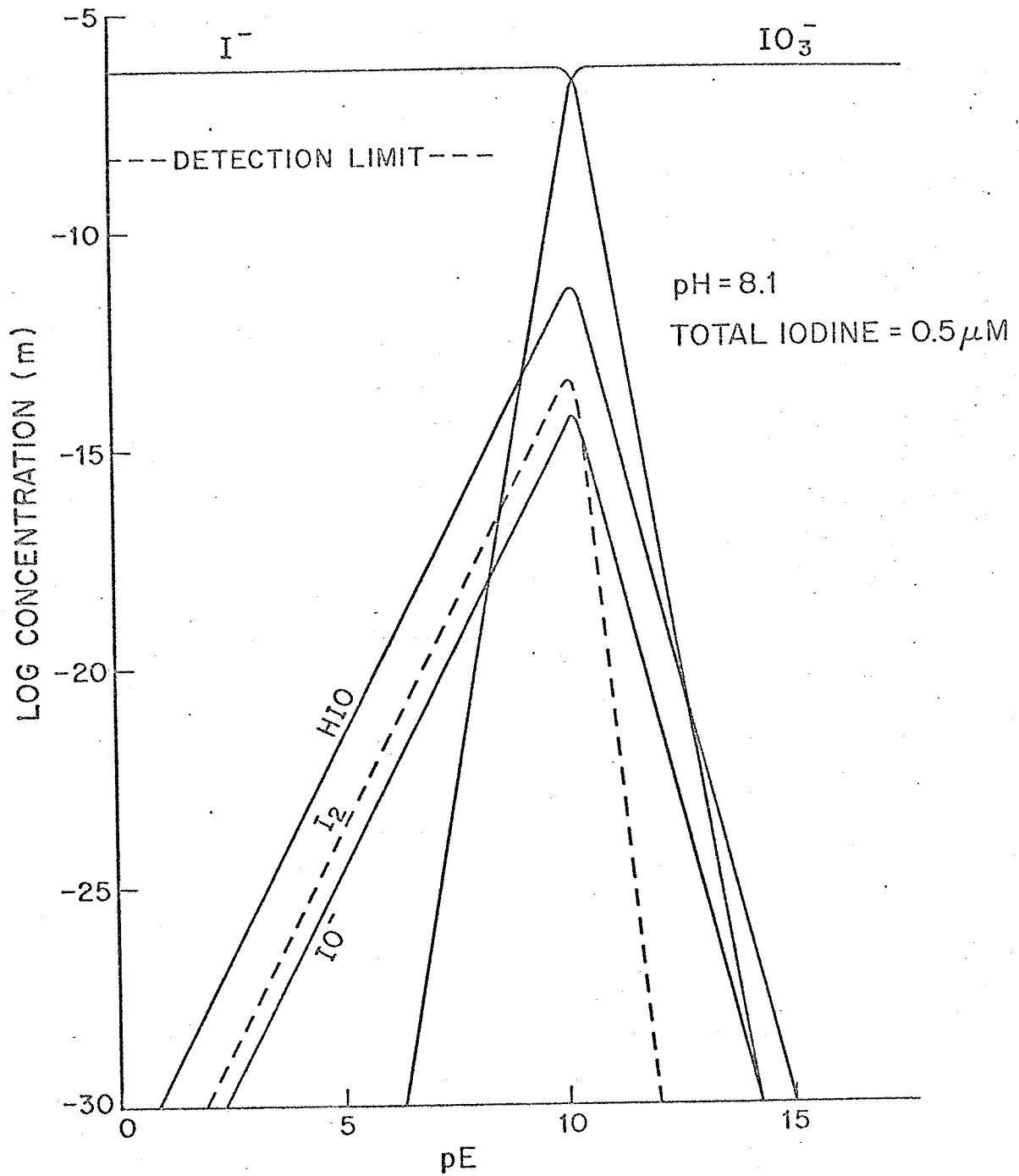


Fig. IV-2-1 A concentration diagram of the iodine system in an aqueous solution at pH of 8.1 and total iodine concentration of  $5 \times 10^{-7} M$ .

of an element from a certain oxidation state to its standard state against the oxidation state. It shows the stability of a certain oxidation state towards oxidation, reduction and disproportionation. It also points out the possibility of the existence of metastable species. Oxidation potentials are usually given in two sets in standard textbooks, with one set determined in 1 N acid and the other in 1 N base (Douglas and McDaniel, 1965). The reference state used by chemists is the hydrogen-hydronium ion couple. In natural waters, hydrogen does not occur in significant quantities. The oxygen-water or the oxygen-hydroxide ion couple seems to be the more appropriate reference state. Thus, in acid, the reference couple will be



and, in base, the reference couple will be



The oxidation state diagram of the iodine system is shown in figure IV-2-2 and the thermodynamic parameters used in the construction of the diagram are shown in table IV-2-3.

In an acidic solution, iodate is the most stable form. Iodide will be oxidized to elemental iodine which is metastable. Hypiodite will disproportionate to form iodate and elemental iodine whereas periodate will be reduced to iodate. Although elemental iodine is less stable than iodate, it is a metastable form and it will not be oxidized



The Oxidation State Diagram  
of the Aqueous Iodine System

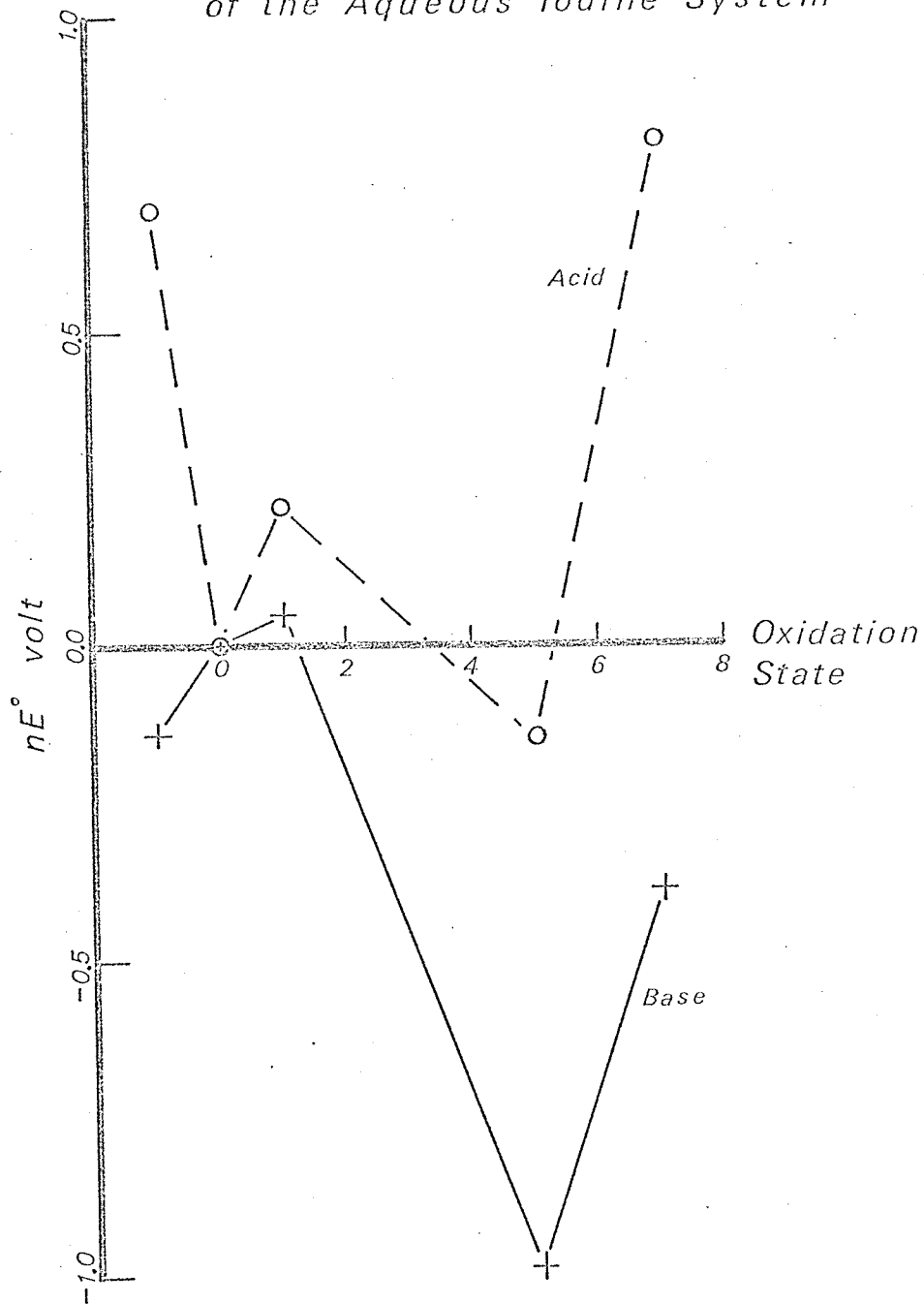


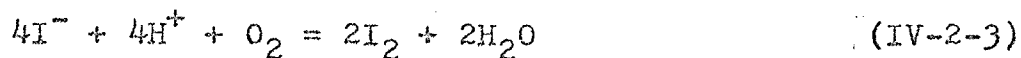
Fig. IV-2-2 The oxidation state diagram of the iodine system in an aqueous solution. In acid, the  $O_2-H_2O$  couple is used as a reference. In base, the  $O_2-OH^-$  couple is used as the reference.



to iodate unless it is first oxidized to hypoiodite and this step is thermodynamically unfavorable. Thus, a solution of iodide in an acidic medium will be oxidized to elemental iodine which will persist in such an oxidation state.

In a basic solution, iodate is still the most stable form. However, iodide is now the metastable species. Both elemental iodine and hypoiodite are subject to disproportionation giving iodide and iodate as the final products. Periodate will again be reduced to iodate. Thus, iodide will persist in a basic solution and its oxidation to iodate may be initiated only if it is first oxidized to elemental iodine. Although the ocean is neither 1 N in acid nor 1 N in base, one may expect iodine to exhibit behaviors more similar to those in a basic solution since sea water has a pH of 8.1 (Sillen, 1961).

The stability of the iodine system relative to the other more common redox couples in the ocean is shown in the electron free energy level diagram in figure IV-2-3. The data are compiled in tables IV-2-1 and IV-2-4. In this diagram, the oxidized species of a couple lower down in the energy scale will oxidize the reduced member of a couple higher up when all species are in their standard states. Thus, in an acidic solution, oxygen will oxidize iodide to iodine according to the equation



whereas, in a basic solution, the corresponding reaction

# Electron Free Energy Levels

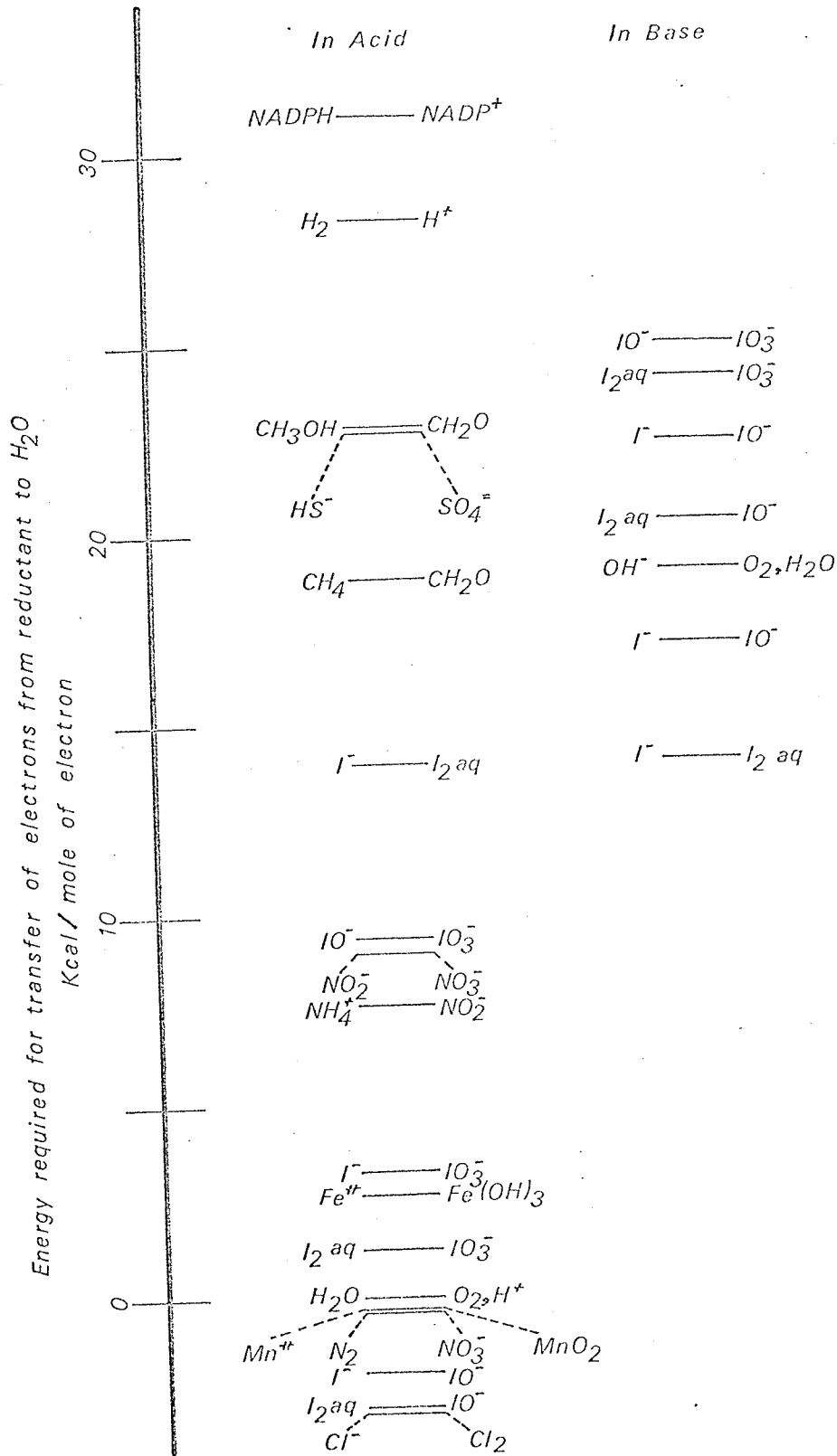


Fig. IV-2-3 The electron free energy level diagram of the iodine system and some relevant couples.

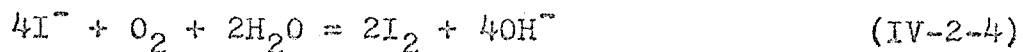
Table IV-2-4 The thermodynamic properties of some common redox couples in natural waters\*

Reaction	log K		$\Delta G^\circ/n$ (a)		$\Delta G^\circ/n$ (b)	
			$\frac{\text{Kcal}}{\text{mole}}$	$\frac{\text{eV}}{\text{mole}}$	$\frac{\text{Kcal}}{\text{mole}}$	$\frac{\text{eV}}{\text{mole}}$
$2\text{NO}_3^- + 12\text{H}^+ + 10\text{e}^- = \text{N}_2(\text{g}) + 6\text{H}_2\text{O}$	210.5	28.72	1.25	21.05	-0.41	-0.021
$\text{NO}_3^- + 2\text{H}^+ + 2\text{e}^- = \text{NO}_2^- + \text{H}_2\text{O}$	28.3	19.31	0.837	14.15	9.00	0.392
$\text{NO}_2^- + 8\text{H}^+ + 6\text{e}^- = \text{NH}_4^+ + 2\text{H}_2\text{O}$	90.8	20.65	0.896	15.14	7.66	0.333
$\text{CH}_2\text{O} + 4\text{H}^+ + 4\text{e}^- = \text{CH}_4(\text{g}) + \text{H}_2\text{O}$	27.8	9.47	0.411	6.94	18.84	0.818
$\text{CH}_2\text{O} + 2\text{H}^+ + 2\text{e}^- = \text{CH}_3\text{OH}$	8.0	5.44	0.236	3.99	22.87	0.993
$\text{SO}_4^{2-} + 9\text{H}^+ + 8\text{e}^- = \text{HS}^- + 4\text{H}_2\text{O}$	33.0	5.63	0.244	4.13	22.68	0.985
$\text{NADP}^+ + \text{H}^+ + 2\text{e}^- = \text{NADPH}$	-4.0	-2.73	-0.118	-2.0	31.04	1.347
$\text{MnO}_2(\text{s}) + 4\text{H}^+ + 2\text{e}^- = \text{Mn}^{2+} + 2\text{H}_2\text{O}$	42.0	28.65	1.243	21.0	-0.34	-0.014
$\text{Fe}(\text{OH})_3(\text{s}) + 3\text{H}^+ + \text{e}^- = \text{Fe}^{2+} + 3\text{H}_2\text{O}$	18.8	25.65	1.112	18.8	2.66	0.117
$\text{Cl}_2(\text{g}) + 2\text{e}^- = 2\text{Cl}^-$	46.0	31.38	1.361	23.0	-3.07	-0.132

\* Data from Sillen and Martell (1964), Garrels and Christ (1965) and Stumm and Morgan (1970).

(a) Relative to the  $\text{H}_2\text{-H}^+$  couple.

(b) Relative to the  $\text{H}_2\text{O-O}_2$  couple.



will not occur.

The other redox couples presented in the figure are frequently involved in biochemical reactions. Reduced species such as sulfide, nitrite, ammonia, methane and methanol, which may be produced as metabolic byproducts, all have the potential of changing the oxidation state of iodine. A particularly interesting redox couple is the NADPH (reduced nicotinamide-adenine-dinucleotide phosphate) and the  $\text{NADP}^+$  couple. The interconversion between these two species is a well known route for electron transfer in biochemical processes (Lehninger, 1965). The electron free energy level of this couple is high and it implies that biological processes involving the interconversion between NADPH and  $\text{NADP}^+$  may induce the interconversion between iodide and iodate if these two reactions can be coupled together.

### IV.3 The complexation of iodide in sea water

Since sea water is a complex mixture of ions, the association of ions to form complexes and ion-pairs such as  $\text{MgSO}_4^0$  (Garrels and Thompson, 1962) is well recognized. The formation of complexes will change the chemical behavior of an element. Thus, in considering the physical chemistry of iodide, the possibility of complexation must be examined.

I have studied the complexation of iodide by potentiometric titrations of solutions with standard iodide solutions using an iodide specific electrode as a detector. The electrode potential is given by the Nernstian equation

$$E = E^0 - 59.16 \log C_I \quad (\text{IV-3-1})$$

at 25°C where E is the observed electrode potential in mV,  $E^0$  is a characteristic empirical constant and  $C_I$  is the activity of the iodide ions. If  $C_T$  is the total concentration of iodide and  $C_c$  is the concentration that has undergone complexation, then

$$C_I = C_T - C_c \quad (\text{IV-3-2})$$

$$\text{and } E = E^0 - 59.16 \log (C_T - C_c). \quad (\text{IV-3-3})$$

If no complexation occurs,  $C_c = 0$  and  $\log C_T$  will be a linear function of E. On the other hand, in the presence of complexing agents, a plot of E against  $\log C_T$  will no longer be linear unless  $C_c$  is a linear function of  $C_T$  so that  $C_c = k C_T$  where k is a constant. However, as such a titration proceeds, the complexing capacity of the solution is reduced and may finally be exhausted. Consequently,  $C_c$  will probably

be more dependent on the complexing capacity than on the amount of iodide added to the solution.

Figure IV-3-1 shows the potentiometric titration of 2 l of a 0.01 M  $\text{Na}_2\text{B}_4\text{O}_7 \cdot 10\text{H}_2\text{O}$  and 0.5 M NaCl solution with standard iodide solutions at 25°C. The borate acts as a pH buffer, poisoning the pH of the solution at about 9. The sodium chloride sets the ionic strength of the solution which will be about 0.53 molal. The iodide concentration in the solution after each addition of the standard iodide solution is calculated from the concentration and the volume of the titrant added. The electrode potential is linearly related to the log of the concentrations above  $10^{-5}\text{M}$  with a slope of -54 mV per concentration decade. Figure IV-3-1 also shows the results of a similar titration of 2 l of Woods Hole surface water (salinity ~34 to 35‰) which has a comparable ionic strength of 0.67 molal (Kester and Pytkowicz, 1969). The electrode potential is again linearly related to the log of the concentrations above  $10^{-5}\text{M}$  with a slope of -52 mV per concentration decade.

The linear relationships and similar slopes suggest that iodide behaves identically in sea water and in sodium chloride solution. Rechnitz et al. (1966) reported a range of the slope of -53 to -59 mV per concentration decade for the calibration of an iodide electrode in carefully prepared standard iodide solutions using sodium nitrate as the ionic strength adjuster and under meticu-



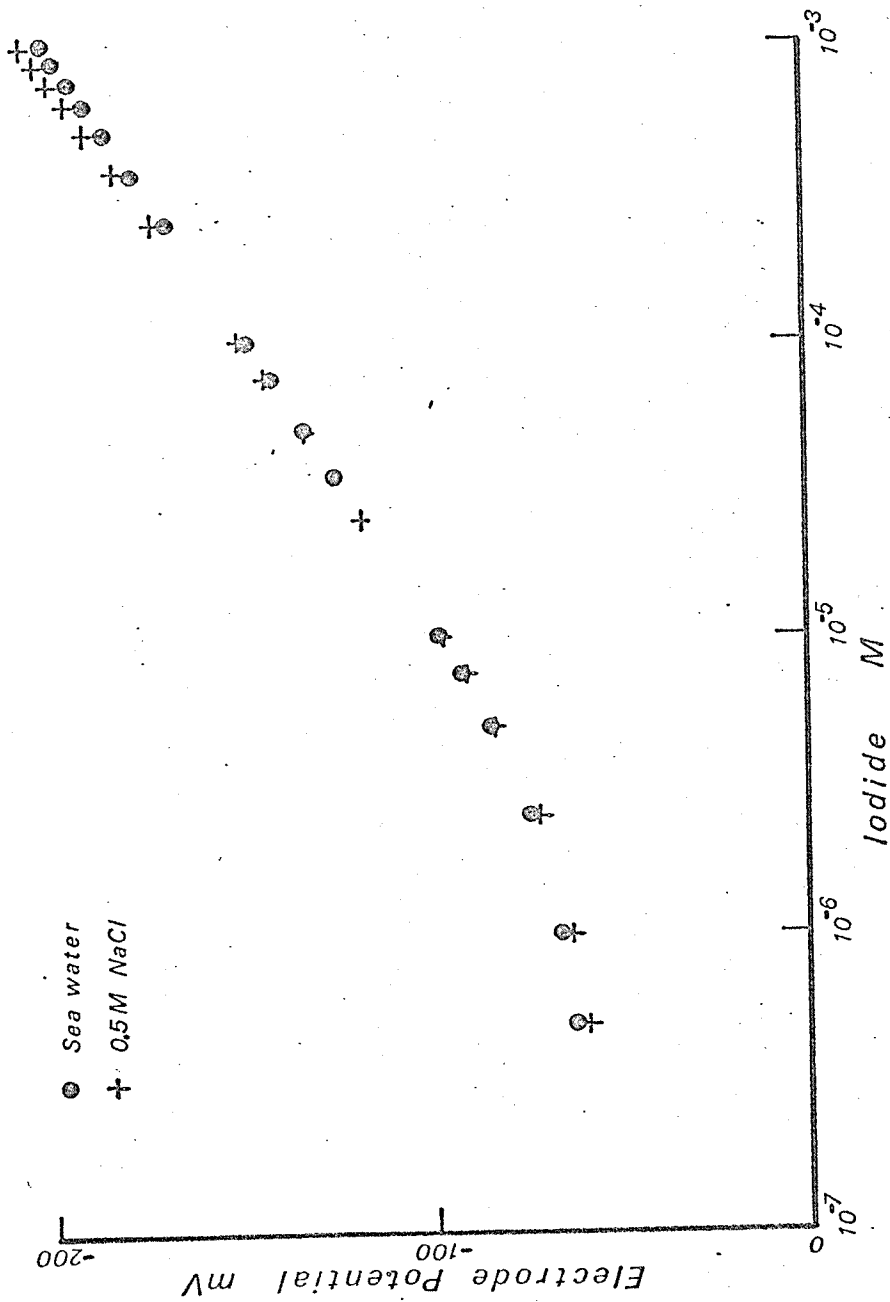
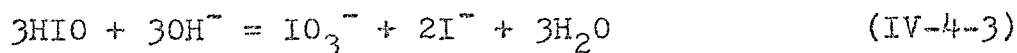
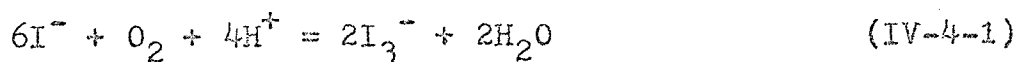


Fig. IV-3-1 Potentiometric titrations of sea water and a 0.5 M sodium chloride solution with standard iodide solutions.

lously controlled experimental conditions. The agreement between the reported slopes and those determined in this study also suggests that the complexation of iodide in sea water is unlikely. This interpretation also agrees with the calculation in table I-2-4 which shows that the percent of contact ion-pairs of iodide estimated from partial molal volumes is negligible within the uncertainty of the calculation.

#### IV.4 Chemical kinetics in the interconversion of aqueous iodine species

The oxidation of iodide to iodate has not been studied previously. A study of the literature showed that experiments were designed mainly to observe the oxidation to adjacent oxidation states. Past efforts were focused on three reactions:



Studies on reaction (IV-4-1) were always done in strongly acidic medium. The results of earlier investigators (Plotnikov, 1907, 1908; Winther, 1924, 1926; Berthoud and Nicolet, 1927, 1928) contradict each other. More recently, careful investigations from two different groups (Abel, 1952, 1954, 1958a, 1958b; Sigalla and Herbo, 1957, 1958) finally yielded consistent results. They suggested the rate law

$$d(\text{I}_3^-)/dt = k (\text{O}_2) (\text{I}^-) (\text{H}^+) \quad (\text{IV-4-4})$$

Sigalla and Herbo (1957) reported  $k$  at 25°C to be  $8 \times 10^{-3} \text{ M}^{-2} \text{ min}^{-1}$  and Abel also reported  $k$  of similar magnitude (1952, 1958a). A summary of the available data is shown in table IV-4-1. However, while Abel favored a mechanism involving a series of reactions with one electron transfers, the formation of free radicals and chain reactions, Sigalla and Herbo proposed a series of reactions with two electron

Table IV-4-1 The dark auto-oxidation of iodide

Rate Law	Rate Constant	Reference
$d(I_3^-)/dt = k(O_2)(I^-)^{3/2}(H^+)^{4/3}$	---	Plotnikov (1907)
$d(I_3^-)/dt = k(O_2)(I^-)^{2/3}(H^+)^{2/3}$	---	Plotnikov (1908)
$d(I_3^-)/dt = k \cdot 10^2 (O_2)^{3/2} (I^-)^2 (H^+)$ $a = -1.51(I^-)^{1/3}$	---	Winther (1924, 1926)
$\frac{1}{2} \frac{d(I_3^-)}{dt} = k(O_2)(H^+)^{\frac{1}{2}}(I^-)^x$ $0.55 \leq x \leq 1.55$	---	Berthoud and Nicolet (1927, 1928)
$d(I_3^-)/dt = k(O_2)(I^-)(H^+)$	25°C: $8.0 \times 10^{-3} M^{-2} min^{-1}$	Sigalla and Herbo (1951)
$d(I_3^-)/dt = k(O_2)(I^-)(H^+)$ $= k' P_{O_2} (I^-)(H^+)$	25°C: $7.8 \times 10^{-3} M^{-2} min^{-1}$ $9.6 \times 10^{-6} atm^{-1} M^{-1} min^{-1}$ 40°C: $1.3 \times 10^{-2} M^{-2} min^{-1}$ $1.3 \times 10^{-5} atm^{-1} M^{-1} min^{-1}$	Abel (1958a)
$d(I_3^-)/dt = k(O_2)(I^-)(H^+)$	---	Alridge (1966)

transfers and without the production of free radicals or the initiation of a chain reaction. Alridge (1966) studied the reaction again and arrived at the same rate law but he failed to further clarify the mechanisms. However, all the proposed mechanisms involve intermediates such as  $\text{IO}^-$ ,  $\text{HIO}$  or atomic iodine although their stability in aqueous solutions has not been thoroughly investigated.

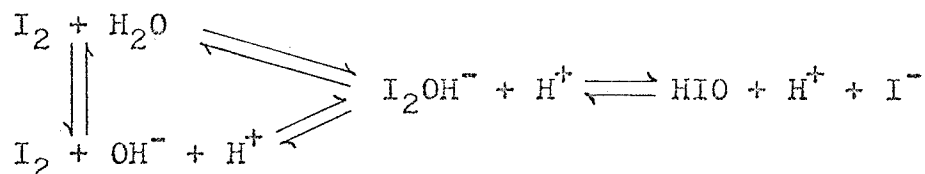
Appropriate precautions should be taken in extrapolating these observations to natural conditions as these experiments were all performed in artificial medium with an acid concentration of no less than 0.1 N, iodide concentration of no lower than 0.06 M and plentiful supply of oxygen. Catalysis by trace constituents has been carefully and intentionally removed. In the ocean, the pH is 8, the iodide concentration is less than 0.5  $\mu\text{M}$  and the oxygen concentration is usually less than 225  $\mu\text{M}$ . Moreover, sea water contains numerous trace constituents and some of them may catalyze the reaction. Some of the known catalysts are cupric ion (Sigalla and Herbo, 1958) and iron (Alridge, 1966). If indeed the rate law can be extrapolated to the ocean, the rate of formation of elemental iodine from iodide at 25°C will be  $9 \times 10^{-21} \text{ M min}^{-1}$  or  $1.3 \times 10^{-11} \text{ } \mu\text{M day}^{-1}$ , an undetectable rate indeed.

The hydrolysis of elemental iodine in basic solution is extremely fast. Earlier chemists "assumed that the speed with which equilibrium is established precludes

any adequate investigation" (Morgan, 1954). Most of the reactions involved in the hydrolysis of the halogens, with the exception of chlorine, occur in about  $10^{-3}$  second or less. Eigen and Kustin (1962) were able to study these reactions by using a T-jump relaxation technique. For the overall reaction (IV-4-2), they determined the rate constant  $k$  to be  $3 \text{ sec}^{-1}$  with  $(\text{H}^+)$  of  $10^{-5}\text{M}$ ,  $(\text{I}_2)$  of  $10^{-3}\text{M}$  and an ionic strength ( $\mu$ ) of 0.1 molal. Thus, the rate law is

$$d(\text{HIO})/dt = (3 \text{ sec}^{-1}) (\text{I}_2) \quad (\text{IV-4-5})$$

and the half life of elemental iodine will be less than 0.5 second. Again, the experimental conditions are appreciably different from the oceanic conditions. However, if their study can be used as an indication of what is happening in nature, it implies that the life time of elemental iodine in the ocean will be extremely short. This seems to corroborate the field observations since elemental iodine has never been detected although its formation has been proposed (Shaw, 1959; Miyake and Tsunogai, 1963). The mechanism for the hydrolysis of elemental iodine is complicated and Eigen and Kustin suggested the following scheme



However, this mechanism has not yet been verified by other investigators.

The disproportionation of hypoiodite to form

iodate in a basic solution has been studied by a number of chemists since the turn of the century. Forster (1903) proposed the first rate law and Skrabal and coworkers (1907, 1908, 1911, 1914, 1916, 1934) followed with a series of reports. The historical development has been reviewed by Morgan (1954) and the proposed rate laws are summarized in table IV-4-2. The most recent report by Li and White (1943) gave the rate law as

$$-d(\text{IO}^-)/dt = k_1(\text{IO}^-)^2 + k_2(\text{IO}^-)^2(\text{I}^-)/(\text{OH}^-) \quad (\text{IV-4-6})$$

where  $k_1 = 2.9 \text{ M}^{-1} \text{ min}^{-1}$  and  $k_2 = 104 \text{ M}^{-1} \text{ min}^{-1}$ . This rate law was obtained from strongly alkaline solution. The hydroxide ion concentration varied from 0.923 M to 0.177 M and the iodide concentration varied from 0.085 M to 0.015 M. In the ocean,  $(\text{OH}^-)$  is about  $10^{-6} \text{ M}$  and  $(\text{I}^-)$  is less than 0.1  $\mu\text{M}$ .  $(\text{IO}^-)$  must be less than the total iodine concentration of 0.5  $\mu\text{M}$ . If this rate law is assumed to be applicable to sea water, then, as an upper limit,  $-d(\text{IO}^-)/dt$  is  $3.3 \times 10^{-12} \text{ M min}^{-1}$  or  $5 \times 10^{-9} \text{ M day}^{-1}$ . This rate is slow and may not be measurable in the laboratory easily.

Table IV-4-2 The disproportionation of hypoiodite

Rate Law	Rate Constant	Reference
$-d(\text{IO}^-)/dt = k(\text{I}^-)(\text{IO}^-)(\text{HIO})$	---	Forster (1903)
$-d(\text{IO}^-)/dt = k(\text{I}^-)(\text{HIO})^2(\text{H}^+)$	---	Skrabal (1907)
$-d(\text{IO}^-)/dt = k(\text{IO}^-)(\text{HIO})$	---	Clareus (1913) Skrabal and Hohlbaum (1916)
$-d(\text{IO}^-)/dt = k(\text{IO}^-)^2$	---	Liebhafsky and Makower (1933)
$-d(\text{IO}^-)/dt = k_1(\text{IO}^-)^2 + k_2(\text{IO}^-)^2(\text{I}^-)/(\text{OH}^-)$	25°C: $k_1 = 2.9 \text{ M}^{-1}\text{min}^{-1}$ $k_2 = 109 \text{ M}^{-1}\text{min}^{-1}$	Li and White (1943)



#### IV.5 Biologically mediated interconversion of the iodine species

That iodine is concentrated in some marine organisms has been known for a long time. Bowen (1966) gave concentration factors of 1200 and 6200 for mixed plankton and brown algae respectively. Enrichment factors as high as  $10^4$  have been reported for some brown algae (Mauchline and Templeton, 1964). A summary of the existing data is shown in section I.2.4. Early studies (Bailey and Kelly, 1955; Tong and Chaikoff, 1955; Klemperer, 1957) focused on the mechanism for attaining and sustaining such high concentration gradients between the cell and its surrounding medium. A common conclusion of these studies is that only iodide is removed from sea water into the cell. Inside the cell, iodine occurs mainly as iodide, although a fraction of it may occur in organic forms. However, upon hydrolysis, only a trace of the organic iodine is left. The major portion of it is converted into inorganic iodide. Shaw (1959, 1960) investigated the possibility of accompanying changes in the speciation of iodine during iodide accumulation by the brown sea weed *Laminaria digitata*. He reported that, in agreement with some earlier studies (Dangeard, 1928a, 1928b, 1930; Kylin, 1930; Roche et al., 1949), iodide can be oxidized to iodine by marine algae and the oxidation can proceed in the dark. The elemental iodine then quickly undergoes hydrolysis to form hypiodous acid, which, being a neutral mole-

cule at the pH of sea water, can easily diffuse into the tissues. Inside the tissues, hypiodous acid may either be reduced back to iodide or be converted into organic iodine. Since the tissues have a lower permeability to ions than to neutral molecules, iodide is retained inside the tissues. He presented a scheme as shown in figure IV-5-1 (Shaw, 1959, 1962). More recently, Gozlan (1968) also reported the occurrence of iodine-producing bacteria.

Sugawara and Terada (1967) studied the assimilation of iodine by a species of the marine alga, *Navicula*. They reported that the alga preferentially assimilated iodide ions. Little or no uptake of iodate ions occurred. In fact, excessive amounts of iodate can hamper the growth of the algae. There is evidence indicating the conversion of iodide to iodate and vice versa during the growth of the algae.

The reduction of iodate to iodide by bacteria has been reported by Tsunogai and Sase (1969). They concluded that bacteria that are capable of reducing nitrate to nitrite, using nitrate reductase as the enzyme, can also reduce iodate to iodide. They also claimed the detection of the formation of elemental iodine in the process.

These studies indicate that biological activity is important in the interconversion of the iodine species. Both the oxidation of iodide and the reduction of iodate can be induced by such processes. However, since these studies

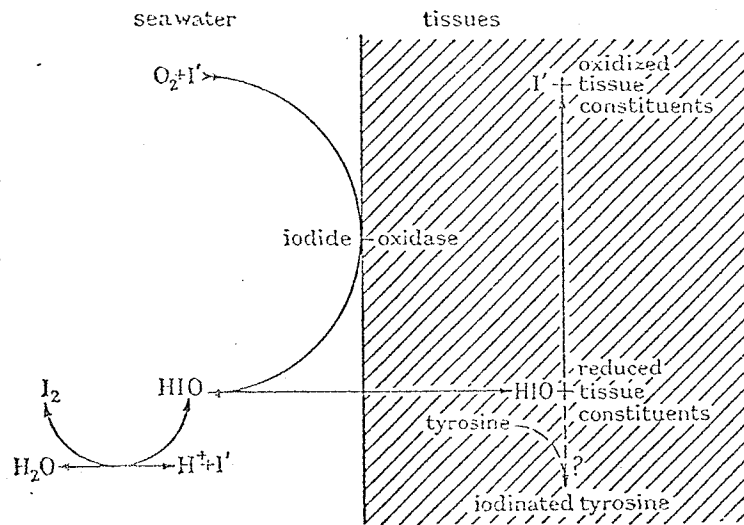
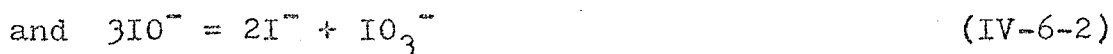


Fig. IV-5-1 A possible mechanism of iodide absorption by brown algae proposed by Shaw (1959).

are limited to a few species of algae and bacteria, it is as yet unclear whether these processes are quantitatively important in affecting the oceanic distributions.

#### IV.6 Previous laboratory studies

Sugawara and Terada (1958) were the earliest investigators to study the stability of various species of iodine in sea water. They added in excess of 50 mg of elemental iodine to a liter of sea water and observed a gradual decrease in the elemental iodine concentration and a corresponding increase in the iodate concentration. Less than 40% of the elemental iodine added was left after 25 days. This rate is substantially slower than those determined in artificial media (see section IV.4). Nonetheless, this experiment shows that elemental iodine is unstable in sea water and Sugawara and Terada favored the hydrolysis of elemental iodine to hypoiodite and its subsequent disproportionation to iodate and iodide as an explanation for their observations according to the reactions



They also suggested that the direct oxidation of iodide to a higher oxidation state, such as hypoiodite, is difficult.

Recently, Truesdale (1974) has re-examined this problem. He suggested that elemental iodine in sea water may behave differently at trace concentrations. He limited the addition of elemental iodine to less than 1400 ug  $I_2$ -l/l. He also observed a rapid disappearance of elemental iodine in sea water. Less than 15% of the added elemental iodine is left after 24 hours. In low iodine concentration (260

ug  $I_2$ -I/l), all the elemental iodine disappears after 30 minutes. The rate of the reaction decreases with time. However, in the first half an hour, the rate is always about 240  $\mu M$ /day. He suggested that the elemental iodine initially reacts with organic compounds either by reduction to form iodide or by iodination to form iodinated derivatives. At low elemental iodine concentrations, the organic compounds in sea water may be able to consume all the elemental iodine. At higher elemental iodine concentrations, after these organic compounds are exhausted, the slower reactions, the hydrolysis and subsequent disproportionation of elemental iodine to form iodate, may then proceed. Thus, according to Truesdale (1974), the fate of elemental iodine in sea water will mainly be



where R is an unknown organic compound. There are some doubts about the reliability of these results. Truesdale purged all the oxygen from his reaction mixture with nitrogen before initiating his experiments because oxygen is an interferent in his analytical method. The effect of the absence of oxygen on the reaction pathways is not known. An inert nitrogen atmosphere instead of the natural oxidizing atmosphere may suppress oxidation and thus favor the reduction of iodine. Consequently, his conclusions should be treated with caution.

## IV.7 Laboratory studies

### IV.7.1 The oxidation of iodide in an aqueous solution

#### IV.7.1.1 Experimental

Potassium iodide is added to solutions with known pH and ionic strengths so that the final concentration is about 1 mM in iodide. The medium may be filtered Woods Hole surface water or an artificial solution. Two liters of the solution are quickly transferred into a reaction vessel in a constant temperature water bath. Air or oxygen is bubbled through the solution. The pH, temperature and iodide concentration inside the reaction vessel are monitored by a combination pH electrode, a thermometer and an iodide ion specific electrode. The temperature bath is covered with styrofoam sheets to minimize heat loss and direct light. A sketch of the apparatus is shown in figure IV-7-1.

#### IV.7.1.2 Results and discussion

Figures IV-7-2 and IV-7-3 show the results from five experiments in various solutions at different pH values. In the first three experiments (figure IV-7-2), a medium which is 0.1 M in potassium nitrate and 1 mM in potassium iodide was used. The pH was buffered at 9, 12 and 6.7 respectively and the temperature was maintained at 49°C. A decrease in electrode potential will indicate an increase in the iodide concentration. Thus, as the oxidation of iodide proceeds, the electrode potential should increase in

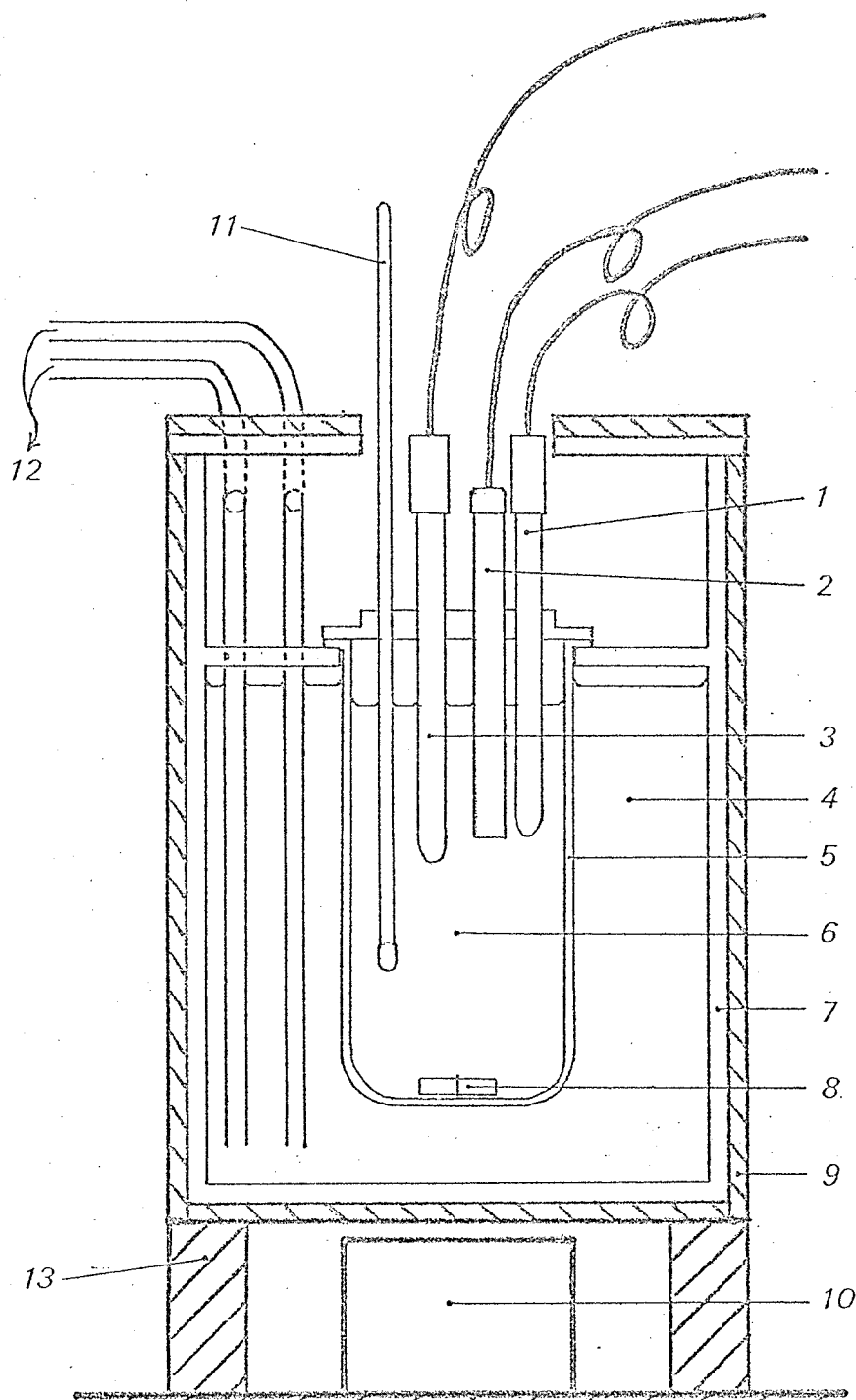


Fig. IV-7-1 An apparatus for studying the interconversion of iodine species. 1 reference electrode; 2 iodide electrode; 3 pH electrode; 4 constant temperature bath; 5 reaction vessel; 6 reaction mixture; 7 plexiglass water bath; 8 stirring bar; 9 styrofoam sheet; 10 magnetic stirrer; 11 thermometer; 12 to temperature regulator; 13 wooden block.



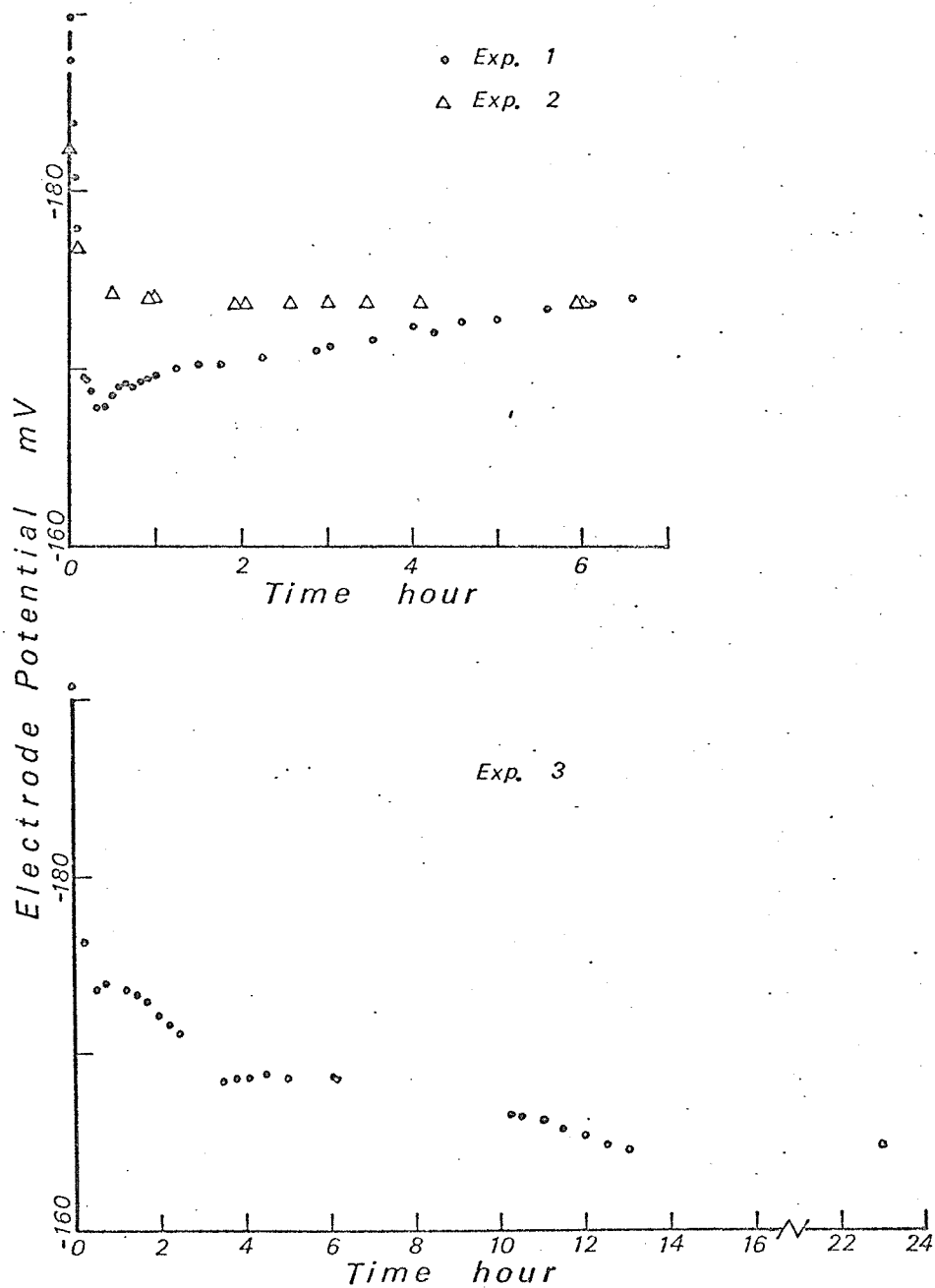


Fig. IV-7-2 Dark auto-oxidation of iodide. Exp. 1: pH 9.1; 49°C; 0.01M  $\text{Na}_2\text{B}_4\text{O}_7 \cdot 10\text{H}_2\text{O}$ . Exp. 2: pH 12.0; 49°C; saturated with  $\text{Ca}(\text{OH})_2$ . Exp. 3: pH 6.7; 49°C; 0.025M  $\text{Na}_2\text{HPO}_4 \cdot 7\text{H}_2\text{O}$  and 0.025M  $\text{KH}_2\text{PO}_4$ .

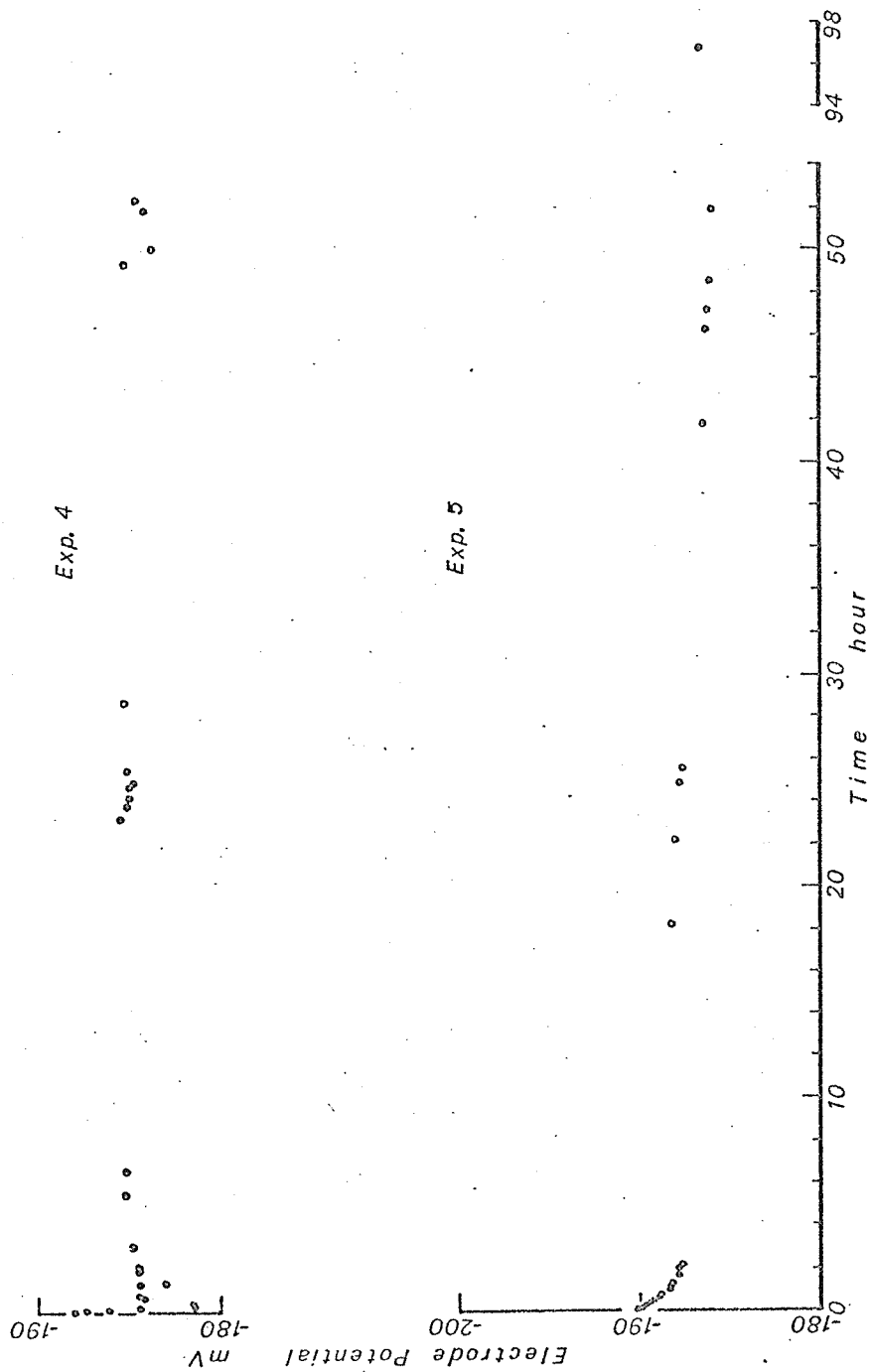


Fig. IV-7-3 Dark auto-oxidation of iodide. Exp. 4: pH 1; 25°C; 0.1M HCl. Exp. 5: pH 0.9; 25°C.

the positive direction. No consistent trend was observed. At pH 9, there was in fact a decrease in electrode potential of 6 mV in  $6\frac{1}{2}$  hours. No electrode potential changes could be detected at pH 12 in 6 hours, while at pH 6.7, it increased in a haphazard manner for about 9 mV in 23 hours. (The sharp change in electrode potential in the initial 30 to 60 minutes was caused by the temperature equilibration between the reaction mixture and the temperature bath.)

In the fourth experiment (figure IV-7-3), a 0.5 M sodium chloride and 0.1 M hydrochloric acid solution was used. The iodide concentration was 0.5 mM and the pH was 1. The bath temperature was maintained at 25°C. The variations in electrode potential were only about 1 to 2 mV in 53 hours and should be considered constant within the experimental uncertainties. No change could be observed even when oxygen instead of air was bubbled through the solution. A similar experiment was done using sea water which had been titrated to a pH of 0.9 with hydrochloric acid (figure IV-7-3). The electrode potential dropped 2.5 mV in the first 3 hours. It then drifted downwards slowly for the next 95 hours. The total drop in electrode potential in the entire experiment of 98 hours was only 4 mV.

These experiments did not provide any conclusive information. In retrospect, the use of an electrode as a sensor for the disappearance of iodide in this study is actually a poor choice. The change in electrode potential

( $\Delta E$ ) is a logarithmic function of the change in iodide concentration since

$$\Delta E = 59.16 \log (a_{I_t}/a_{I_0}) \quad (\text{IV-7-1})$$

where  $a_{I_t}$  is the activity of iodide at time  $t$ ,  $a_{I_0}$  is the initial iodide activity and  $\Delta E$  is in mV. Thus, with slow reactions which do not go to completion, observations will be made in a region where the electrode response is least sensitive to concentration changes. In this series of experiments, the maximum change in electrode potential was an increase of 9 mV in 13 hours in experiment 3. This  $\Delta E$  corresponds to a 30% decrease in the initial concentration. In the other experiments,  $\Delta E$  was less than 2 mV but it may still represent a 9% decrease in concentration. However, over such a long time span for the experiments (7 to 97 hours), other factors, such as electrode drift, may be sufficient to account for these changes in electrode potentials too. Moreover, there is no systematic change in the rate of disappearance of iodide with varying pH. Even within an experiment at constant pH, the change in electrode potential with time is often haphazard. In one of the experiments, the change in electrode potential would actually suggest an increase in the iodide concentration. This is physically impossible. The only generalization that may be derived from these data is perhaps that iodide is not easily oxidized in aqueous solutions. The rate of the reaction is too slow to be observed with the techniques used here.

IV.7.2 The change in iodate concentration in sea water  
with time

IV.7.2.1 Experimental

Woods Hole surface water is collected and filtered through Whatman 40 filter papers. The filtered sea water is divided into sub-samples which are stored in 250 ml polyethylene bottles at room temperature (about 25°C). A sample is transferred to the freezer after each preset time interval. All the samples are analyzed for iodate at the end of the experiment by the colorimetric method as described in section II.3. The initial sea water frozen immediately after collection is used for the construction of a calibration curve.

IV.7.2.2 Results and discussion

Figure IV-7-4 shows the results from an experiment for a duration of 52 days. The sea water has been analyzed before the experiment was started and it was found to contain 22.3 ug/l of iodate-iodine and 15.7 ug/l of iodide-iodine. Within the error bar ( $\pm 5\%$ ), no change in iodate concentration could be observed after 52 days of storage at room temperature. The best fit by the linear least square method gives

$$(\text{IO}_3^-) = 0.002 t + 22.34 \quad (\text{IV-7-2})$$

where  $t$  is time in days. The correlation coefficient is 0.05 and the standard deviation of the slope is  $\pm 0.547$ .

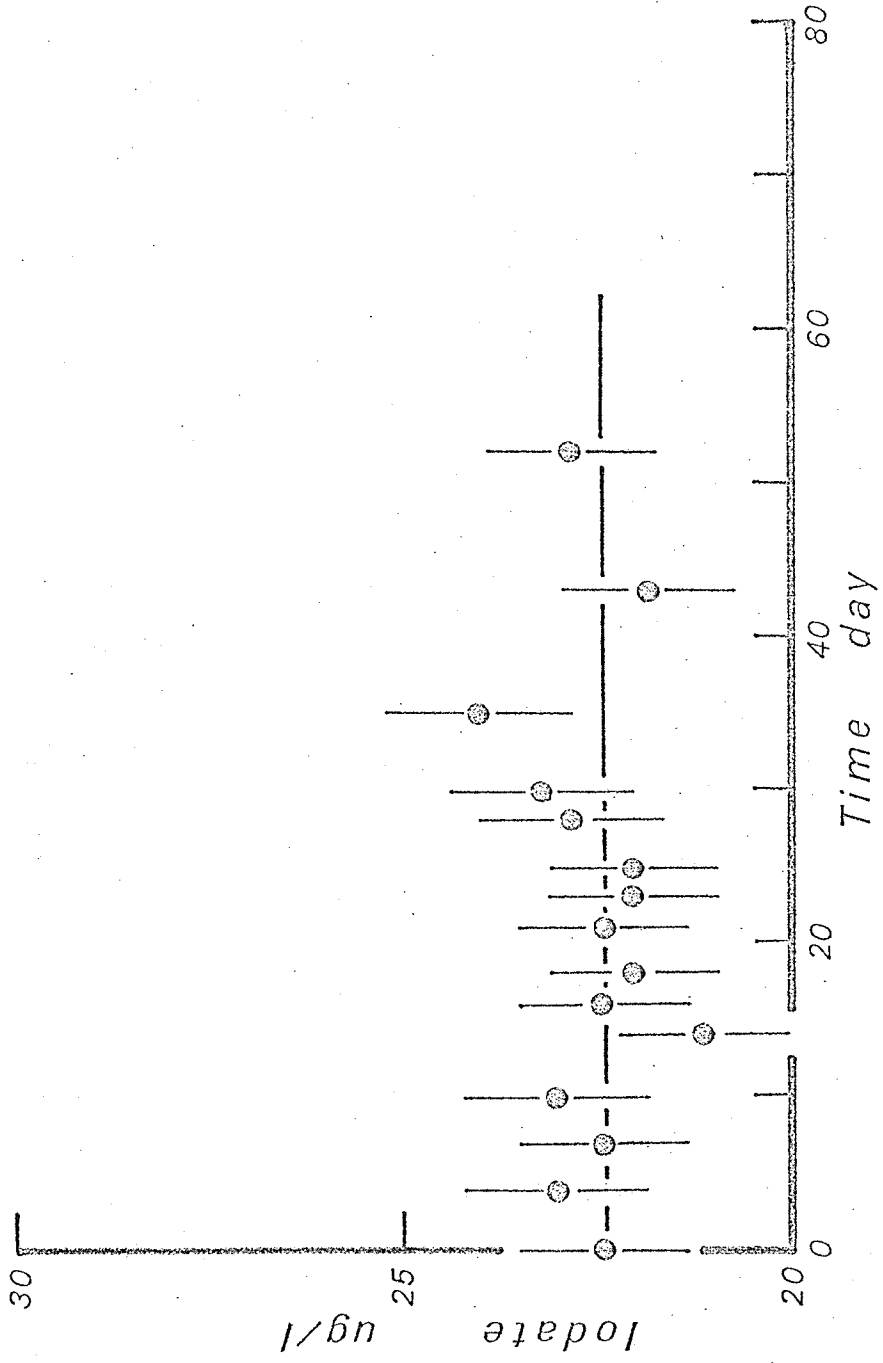


Fig. IV-7-4 Rate of production of iodate in sea water at 25°C.

Thus, if indeed iodate has been produced by the oxidation of iodide within the period of 52 days, it is undetectable with this method and the change is less than the experimental uncertainty of  $\pm 1$  ug-I/l.

### IV.7.3 The stability of elemental iodine in an aqueous solution

#### IV.7.3.1 Experimental

Standard iodine solution (3% w/v in potassium iodide)

10 g of distilled water and 7.5 g of potassium iodide are transferred into a stoppered weighing bottle. 0.0317 g of elemental iodine ( $\frac{1}{2}$  mmole  $I_2-I$ ) is added to the solution. The mixture is gently swirled until the elemental iodine is completely dissolved. The solution is transferred into a 250 ml volumetric flask. The weighing bottle is washed three times with small amounts of distilled water and the washings are also added to the volumetric flask. The solution is then diluted to volume. The concentration of iodine is determined by titrating 25 ml of this iodine solution with a standard sodium thiosulfate solution (4.0356 mM) using the starch-iodine color for the detection of the end-point. The amount of iodate present in the iodine solution as an impurity is determined from the difference in the amount of thiosulfate consumed between an unacidified and an acidified sample of the iodine solution. The concentrations of iodine and iodate in the standard iodine solution are 0.9243 mM  $I_2-I$  and 0.02588 mM  $IO_3^-I$  from the average of two determinations.



## Procedure

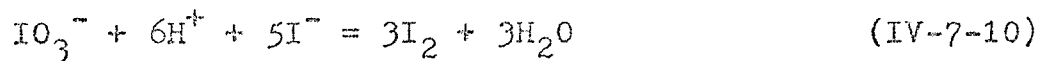
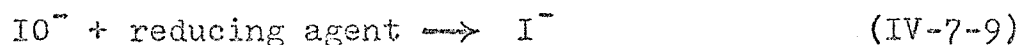
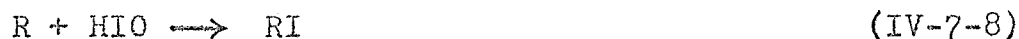
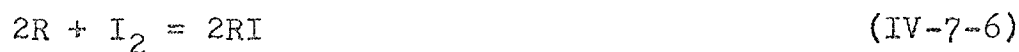
Two liters of an artificial solution or sea water are transferred into a reaction vessel in a constant temperature bath. The solution is stirred at a constant rate. The pH of the solution is monitored with a combination pH electrode. After the reaction mixture has thermally equilibrated with the water bath, 5 ml of the standard iodine solution is added. Forty ml of this mixture is pipetted into each of two 50 ml volumetric flasks at fixed time intervals. In one flask, the solution is diluted to volume and its absorbance is measured as quickly as possible in a 10 cm cell at 353 nm. To the other flask, which contains 1 ml of 0.1 M sulfuric acid before the addition of the sample, 2 ml of a 5% (w/v) potassium iodide solution is added and the mixture is diluted to volume. After allowing the mixture to stand for 5 minutes with occasional shaking, its absorbance at 353 nm is measured.

In the first two experiments, the medium was Woods Hole surface water filtered through a Whatman 40 filter paper. The third one was distilled water titrated to a pH of 8.2 with a 0.1 M sodium hydroxide solution. The fourth one was a 0.5 M sodium chloride and 2.25 mM sodium bicarbonate solution. The pH was adjusted to 8.2 by titrating the solution with a 0.1 M sodium hydroxide solution.

#### IV.7.3.2 Results and discussion

The inorganic iodine species added to the medium gave the following concentrations: 292.5 ug I<sub>2</sub>-I/l, 8.2 ug IO<sub>3</sub><sup>-</sup>-I/l and 57 mg I<sup>-</sup>-I/l. The amount of elemental iodine added is at the lower end of the concentration range used by Truesdale (1975) and should not mask his proposed reactions with the organic compounds. The amount of elemental iodine in the solution was monitored by measuring the absorbance of the solution at 353 nm in a 10 cm cell. At this wavelength, both elemental iodine and the tri-iodide ion absorb strongly (Awtrey and Connick, 1951) while the other iodine species do not absorb significantly.

Some of the reactions that may be involved in the experiments are



R represents some unknown organic compounds.

Figure IV-7-5 shows the results from four experiments in various media. If elemental iodine is stable in an aqueous solution at a pH of around 8, only reaction IV-7-3

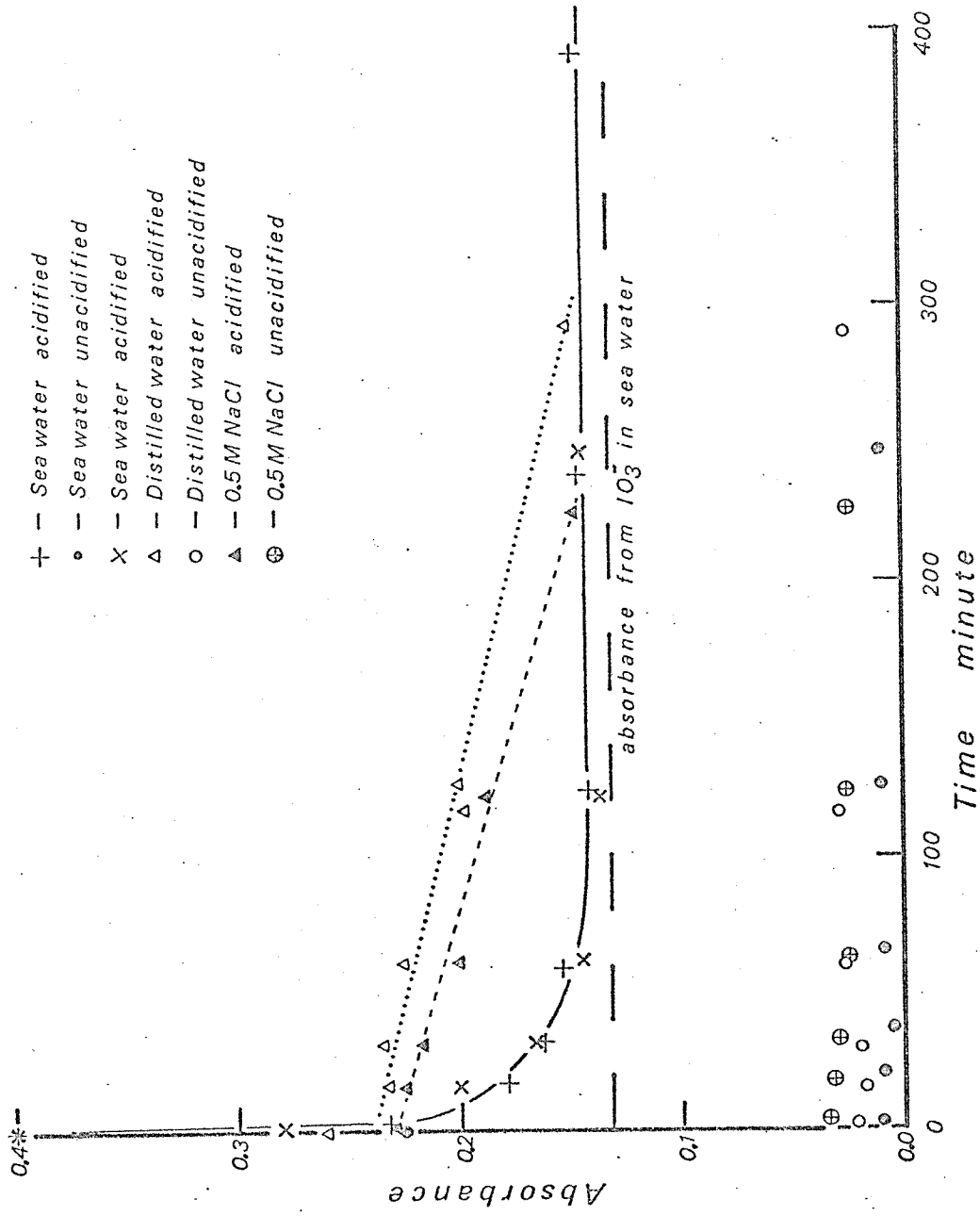


Fig. IV-7-5 The stability of elemental iodine in various media.

will occur and it will yield a constant absorbance with time in both the acidified and the unacidified samples. In reality, in the unacidified samples, the absorbance is only about 0.01 to 0.03. Although it is rather constant with time, it is much lower than the expected value of 0.22. (This value is estimated from the amount of elemental iodine present and a calibration curve obtained by generating known amounts of elemental iodine through the reaction of iodate with excess iodide in an acidic solution.) This consumption of elemental iodine occurs within a minute or two - the shortest time within which an absorbance reading can be made - and supports the previous reports that iodine is unstable in sea water (Sugawara and Terada, 1958; Truesdale, 1974). Since the reaction occurs in both sea water and distilled water, the reaction seems to be only pH dependent and is likely to be the hydrolysis of elemental iodine.

Upon acidification, the absorbance increases sharply. In sea water, part of this absorbance is due to the iodate present as shown by reaction IV-7-10. This background absorbance is denoted as a broken line in figure IV-7-6. The restoration of the absorbance by acidification implies that the reaction that consumes elemental iodine is a reversible one. Thus, reactions such as reaction IV-7-6, which is favored by Truesdale (1974), are not likely to occur since such reactions are usually irreversible.

The absorbance of the acidified samples decreases

slowly long after the initial elemental iodine has been consumed, as suggested by the constant and low absorbances of the unacidified samples. This implies the presence of an intermediate which can be converted back to elemental iodine upon acidification as discussed previously. Moreover, this intermediate has to be reactive and it is this intermediate rather than elemental iodine that is irreversibly consumed with time.

The most likely candidate for this intermediate is hypiodous acid since earlier studies have shown that the hydrolysis of iodine to form hypiodous acid is rapid in an alkaline solution and this reaction (reaction IV-7-4) is reversible (see sections IV.2 and IV.4 for a more detailed discussion). It is also a very reactive species and it can undergo reactions such as IV-7-7, IV-7-8 and IV-7-9. The disproportionation of hypiodite to form iodate (reaction IV-7-7) cannot account for the observed decrease in absorbance with time in the acidified samples since one mole of HIO will produce two moles of  $I_2-I$  either through reaction IV-7-4 or through the combination of reactions IV-7-7 and IV-7-10. Since iodate is stable in an aqueous solution, if reaction IV-7-7 is the only reaction occurred, there will be no change in absorbance with time. The other routes for the removal of hypiodite will be its reduction to iodide by an organic or an inorganic reducing agent (reaction IV-7-9) or the iodination of organic species (reaction IV-7-8).

Neither route can be ruled out at the present time.

In sea water, the absorbance of the acidified samples drops to the background level within 2 hours. This level is slightly higher than the absorbance from the iodate initially present in the sea water and this excess (0.015 absorbance unit) is probably caused by the trace of iodate in the standard iodine solution. For practical purposes, one may probably assume that all the hypiodite is consumed within 2 hours. Thus, the reaction that consumes hypiodite seems to occur much faster than the disproportionation of hypiodite to form iodate (reaction IV-7-7). In the artificial media prepared with distilled water, less than 40% of the initial absorbance is lost in 2 hours and this implies that hypiodite is consumed at a much slower rate in these solutions. The presence of sodium chloride or changes in ionic strength cannot be the cause since the reaction occurs equally slowly in the 0.5 M sodium chloride solution (figure IV-7-6). A major difference between distilled water and the coastal surface sea water is in their organic contents. It is possible that the much lower concentration of organic compounds in distilled water is limiting reactions IV-7-8 and IV-7-9 which are suggested earlier as the routes for the removal of hypiodite. Alternatively, one may attribute the difference in reaction rate to the possible absence of catalysts in trace quantities in the artificial media.

The loss of iodine from the solution by volatili-

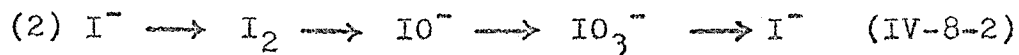
zation is unimportant in this study. Truesdale (1974) has examined this possibility and found that the volatilization of iodine does not occur at the pH of sea water. I have also avoided the bubbling of gases through the reaction mixture, kept the reaction temperature low (25°C) and finished each experiment within 3 hours in order to further minimize this problem. Thus, no elemental iodine should have been lost during the experiments from the reaction mixture. Loss by volatilization may also occur in the acidified samples in the volumetric flasks. However, I have checked the stability of the absorbance of the tri-iodide ion in acidified samples with time and found that there is no observable change in absorbance in over an hour. In my experiments, the absorbance of each acidified sample was measured within half an hour after the generation of the tri-iodide ions. Thus, the decrease in absorbance with time cannot be explained by this mechanism.

In summary, my experiments have shown that elemental iodine is unstable in sea water. Its major decomposition route is probably not by its direct reaction with organic compounds. Iodine probably undergoes hydrolysis to form hypoiodous acid which further reacts with either reducing agents to form iodide or organic molecules to form iodinated compounds. These reactions seem to occur much faster than the disproportionation of hypoiodite to form iodate.

#### IV.8 A possible oceanic iodine cycle

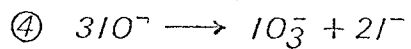
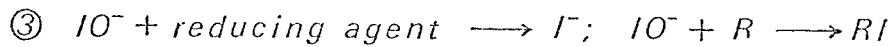
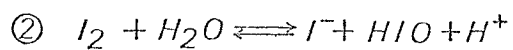
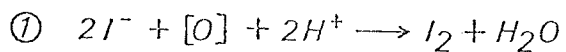
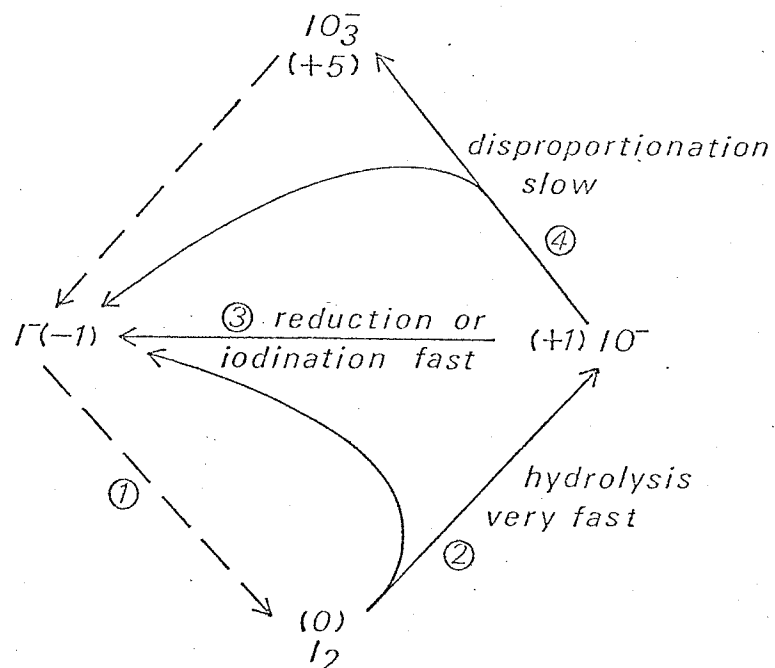
A tentative cycle of iodine in the ocean is shown in figure IV-8-1. Only elemental iodine and hypoiodite are included as possible intermediates between iodide and iodate because they are the only remaining iodine species that show significant stability in aqueous solutions. The oxidation of iodide to iodate does not necessarily have to go through these species. However, since my experiments suggest that this reaction occurs with difficulty if it occurs at all, this implies the presence of intermediate species which act as energy barriers. Elemental iodine and hypoiodite are two possibilities.

The oxidation of iodide to elemental iodine is thermodynamically unfavorable in a basic solution (sections IV.2 and IV.4), but there is evidence suggesting that organisms can use enzymes, such as iodide oxidase, to catalyze the reaction (Shaw, 1959; section IV.5). If elemental iodine is formed, it may be transformed to iodate chemically via hypoiodite by hydrolysis and disproportionation. However, other molecules may compete for hypoiodite and reduce it to the -1 oxidation state. Thus, two cycles may be involved



Apparently, cycle (1) proceeds much faster than cycle (2). However, once iodate is formed through cycle (2), it will remain stable in sea water. The only known way to remove





— — — thermodynamically unfavorable reactions

Fig. IV-8-1 A possible oceanic iodine cycle.

iodate in the open ocean is by bacterial reduction to form iodide (Tsunogai and Sase, 1969). This reduction of iodate is thermodynamically unfavorable and a biological mediation must be invoked.

CHAPTER V. CONCLUDING REMARKS

Reliable analytical methods have been developed for the determination of iodate, iodide and particulate iodine in sea water. These techniques are straightforward and their precisions are sufficient for studying the variations in the marine environments.

In addition to physical processes such as advection and diffusion, the distribution and speciation of dissolved iodine in the ocean seem to be controlled by redox potential changes and biological activity also. The drastic shift in redox potential from oxygenated to sulfide-bearing water in anoxic basins brings about accompanying reduction of iodate to iodide as predicted from thermodynamic considerations. In the open oceans, the occurrence of iodide is confined to the euphotic zone and the iodate concentrations at corresponding depths are low. This distribution is consistent with the suggestion that iodide is produced by the enzymatic reduction of iodate by organisms (Tsunogai and Sase, 1969). In coastal waters, the speciation and distribution of iodine may also be affected by the seasonal changes in productivity. Particulate iodine also plays an important role in the cycling of iodine in the ocean. Relative to rocks and minerals, marine suspended matter has much higher iodine content. The iodine-containing particles seem to be biogenic. The concentration of particulate iodine is highest in the euphotic zone and it drops sharply with depth to a background level. This dis-

tribution is similar to the distributions of bioactive elements such as phosphorus and nitrogen in marine suspended matter. The standing crops of particulate iodine in the top 200 m also seem to correlate with surface productivity. The preferential dissolution of particles in strong pycnocline also affects the distribution of dissolved iodine in the water column. The thermodynamically favorable autoxidation of iodide to iodate in sea water may also be mediated by biological activity. Iodide seems to be quite stable in sea water. I was not able to show the oxidation of iodide to iodate at a measurable rate. On the other hand, elemental iodine is extremely unstable with a life time of seconds to minutes in sea water. Thus, elemental iodine must be produced at a very fast rate if it is the vehicle for the transfer of iodine from the oceans to the atmosphere as suggested by Miyake and Tsunogai (1963). The diffusion of iodine from the sediments into the water column probably occurs in the Black Sea. However, in the open ocean, this process is not clearly evident from the distribution of iodide in the bottom water.

There are still discrepancies in our understanding of the marine geochemistry of iodine. Some of the major gaps in our knowledge are: (1) the form and physiological functions of iodine in marine organisms; (2) the rate and products of the re-mineralization of iodine in organisms; (3) the possible diagenesis of iodine in the sediments and

subsequent diffusion of iodine into the bottom water; (4) the agent for the transfer of iodine from the ocean into the atmosphere; and (5) the interconversion among the oxidized and reduced species of iodine via biological and chemical processes. This study has defined the importance of, pointed out the possible answers to and provided some of the necessary tools for future investigations of these questions.

## REFERENCES

- Abel, E. (1952). Mechanismus und Kinetik der Oxydation von Jodion durch Sauerstoff. *Monatsh. Chem.*, 83, 818-828.
- Abel, E. (1954). Über die vermutliche Struktur des Autoxydation-svorganges in unbelichtetem wässrigem System. Bemerkungen zum Mechanismus der Autoxydation von Jodion und von Sulfit. *Monatsh. Chem.*, 85, 722-729.
- Abel, E. (1958a). Jodatomb-Katalyse der Autoxydation of Jodion. *Z. Elektrochem.*, 62, 1160-1162.
- Abel, E. (1958b). Zur Autoxydation von Jodion im Dunkeln. *Monatsh. Chem.*, 89, 313-316.
- Adams, F. and R. Dams (1969). A compilation of precisely determined gamma-transition energies of radionuclides produced by reactor irradiation. *J. Radioanalyt. Chem.*, 3, 99-125.
- Aldridge, F. T. (1966). The dark autoxidation of iodide ion in aqueous acid solution. Ph. D. Thesis. UCLA.
- Allen, T. L. and R. M. Keefer (1955). The formation of hypoiodous acid and hydrated iodine cation by the hydrolysis of iodine. *J. Amer. Chem. Soc.*, 77, 2957-2960.
- Anonymous (1951). Iodine. Its properties and technical applications. Chilean Iodine Educational Bureau, Inc. New York.
- Anonymous (1960). Technical Report 684. Enthalpies libre de formation standards, a 25°C. Centre Belge d'Etude de la Corrosion, Brussels.
- Atteberry, R. W. and G. E. Boyd (1950). Separation of seventh group anions by ion-exchange chromatography. *J. Amer. Chem. Soc.*, 72, 4805-4806.
- Awtrey, A. D. and R. E. Connick (1951). The absorption spectra of  $I_2$ ,  $I_3^-$ ,  $I^-$ ,  $IO_3^-$ ,  $S_4O_6^{2-}$  and  $S_2O_3^{2-}$ . Heat of the reaction  $I_3^- = I_2 + I^-$ . *J. Amer. Chem. Soc.*, 73, 1842-1843.
- Baily, B. A. and S. Kelly (1955). Iodine exchange in *Asco-phyllum*. *Biol. Bull.*, 109, 13-21.
- Ballaux, B., R. Dams and J. Hoste (1969). Neutron activation analysis of high-purity selenium. Part IV. Simultaneous determination of chlorine, bromine and iodine. *Anal.*

- Chim. Acta, 45, 337-340.
- Barkley, R. A. and T. G. Thompson (1960a). Determination of chemically combined iodine in sea water by amperometric and catalytic methods. Anal. Chem., 32, 154-158.
- Barkley, R. A. and T. G. Thompson (1960b). The total iodine and iodate-iodine content of sea-water. Deep-Sea Res., 7, 24-34.
- Berge, G. (1958). The primary production in the Norwegian Sea in June 1954 measured by an adapted  $^{14}\text{C}$  technique. Rapp. P-V Reun. Cons. Perm. Int. Explor. Mer., 144, 85-91.
- Berthoud, A. and G. Nicolet (1927). Cinetique de l'oxydation de l'acide iodhydrique par l'oxygene libre dans l'obscurite et sous l'action de la lumiere. Helv. Chim. Acta, 10, 475-486.
- Berthoud, A. and G. Nicolet (1928). Cinetique de l'oxydation de l'acide iodhydrique par l'oxygene libre dans l'obscurite et sans l'action de la lumiere. J. Chim. Phys., 25, 163-181.
- Bogdanova, A. K. (1961). The distribution of Mediterranean waters in the Black Sea. Okeanologiya, 1, 983-993 (English Translation).
- Bojanowski, R. and S. Paslawska (1970). On the occurrence of iodine in bottom sediments and interstitial waters of the Southern Baltic Sea. Acta Geophys. Polonica, 18, 277-285.
- Bolin, B. (1959). Note on the exchange of iodine between the atmosphere, land and sea. Int. J. Air Pollution, 2, 127-131.
- Bowen, H. J. M. (1959). The determination of chlorine, bromine and iodine in biological material by activation analysis. Biochem. J., 73, 381-384.
- Bowen, H. J. M. (1966). Trace Elements in Biochemistry. Academic Press, New York.
- Breck, W. G. (1974). Redox levels in the sea. In: The Sea, E. D. Goldberg, editor, 5, 153-179. Wiley and Sons, New York.
- Brewer, P. (1971). Hydrographic and chemical data from the Black Sea. Woods Hole Oceanographic Institution, Refer-



ence No. 71-65.

- Brewer, P. G. and J. W. Murray (1973). Carbon, nitrogen and phosphorus in the Black Sea. *Deep-Sea Res.*, 20, 803-818.
- Brewer, P. G. (1975). Minor elements in sea water. In: *Chemical Oceanography*, J. P. Riley and G. Skirrow editors, 2nd edition, 1, 415-496, Wiley, New York.
- Bruce, J. G. and J. E. Katz (1976). Observations in the Equatorial Atlantic during GATE, June and July, 1974 from Atlantis II. Technical Report, Woods Hole Oceanographic Institution, in press.
- Burger, J. D. and H. A. Liebhafsky (1973). Thermodynamic data for aqueous iodine solutions at various temperatures. *Anal. Chem.*, 45, 600-603.
- Clarens, M. J. (1913). Sur la transformation spontanee des hypochlorites en chlorates et des hypobromites en bromates. *Compt. rend.*, 157, 216-219.
- Cohen, S. and C. G. Ruchhoft (1941). Sulfamic acid modification of the Winkler method for dissolved oxygen. *Ind. Eng. Chem. Anal. Ed.*, 13, 622-625.
- Colton, J. B. (1968). Recent trends in subsurface temperatures in the Gulf of Maine and contiguous waters. *J. Fish. Res. Bd. Can.*, 25, 2427-2437.
- Corcoran, E. F. and C. V. W. Mahnken (1969). Productivity of the tropical Atlantic Ocean. In: *Symposium of the Oceanography and Fisheries Resources of the Tropical Atlantic*, Abidjan (Ivory Coast) 1966, UNESCO, pp. 57-67.
- Cosgrove, J. F., R. T. Bastian and G. H. Morrison (1958). Determination of traces of mixed halides by activation analysis. *Anal. Chem.*, 30, 1872-1874.
- Courtois, B. (1813). Decouverte d'une substance nouvelle (iode) das vareck. *Ann. Chim. (Phys.)* 1, 88, 304-310.
- Craig, H. (1969). Abyssal carbon and radiocarbon in the Pacific. *J. Geophys. Res.*, 74, 5491-5506.
- Dangeard, P. (1928a). Sur le degagement d'iode libre chez les algues marines. *Compt. Rend.*, 186, 892-894.

- Dangeard, P. (1928b). Action favorisante de l'iodure de potassium sur l'iodovolatilisation. Compt. Rend., 187, 1156-1158.
- Dangeard, P. (1930). Sur l'influence de l'oxygene dans l'iodovolatilisation. Compt. Rend., 190, 131-133.
- Dean, G. A. (1963). The iodine content of some New Zealand drinking waters with a note on the contribution from sea spray to the iodine in rain. New Zealand J. Sci., 6, 208-214.
- DeGeiso, R. C., W. Rieman III and S. Lindenbaum (1954). Analysis of halide mixture by ion-exchange chromatography. Anal. Chem., 2, 1840-1841.
- Deuser, W. G. (1973). Cariaco Trench: Oxidation of organic matter and residence time of anoxic water. Nature, 242, 601-603.
- Douglas, B. E. and D. H. McDaniel (1965). Concepts and Models of Inorganic Chemistry. Ginn, Waltham.
- Dubravic, M. (1955). Determination of iodine in natural waters. Analyst, 80, 295-300.
- Duce, R. A., J. T. Wasson, J. W. Winchester and F. Burns (1963). Atmospheric iodine, bromine and chlorine. J. Geophys. Res., 68, 3943-3947.
- Duce, R. A., J. W. Winchester and T. W. Van Nahl (1965). Iodine, bromine and chlorine in the Hawaiian marine atmosphere. J. Geophys. Res., 70, 1775-1799.
- Duing, W., P. Hiscard, E. Katz, J. Meinke, L. Miller, K. V. Moroshkin, G. Philander, A. A. Ribnikov, K. Voigt and R. Weisberg (1975). Meanders and long waves in the Equatorial Atlantic. Nature, 257, 280-284.
- Eigen, M. and K. Kustin (1962). The kinetics of halogen hydrolysis. J. Amer. Chem. Soc., 84, 1355-1361.
- Fanning, K. A. and M. E. Q. Pilson (1972). A model for the anoxic zone of the Cariaco Trench. Deep-Sea Res., 19, 847-863.
- Fiadeiro, M. and J. D. H. Strickland (1968). Nitrate reduction and the occurrence of a deep nitrite maximum in the ocean off the west coast of South America. J. Mar. Res., 26, 187-201.

- Forster, E. C. L. (1903). The rate of formation of iodates in alkaline solutions of iodine. *J. Phys. Chem.*, 7, 640-651.
- Fuge, R. (1974). Iodine. In: *Handbook of Geochemistry*, K. H. Wedepohl editor, Vol. II-4, Sections B-M and O, Springer Verlag, New York.
- Garrels, R. M. and C. L. Christ (1965). *Solutions, Minerals, and Equilibria*. Harper and Row, New York.
- Garrels, R. M. and M. E. Thompson (1962). A chemical model for sea water at 25°C and one atmosphere total pressure. *Amer. J. Sci.*, 263, 57-66.
- Goldberg, E. D. (1963). The ocean as a chemical system. In: *The Sea*, M. N. Hill editor, 2, 3-25, Interscience, New York.
- Goldberg, E. D., W. S. Broecker, M. G. Gross and K. K. Turekian (1971). Marine chemistry. In: *Radioactivity in the Marine Environment*, National Academy of Science, pp. 137-146.
- Goldschmidt, V. M. (1954). *Geochemistry*. Clarendon, Oxford.
- Gozlan, R. S. (1968). Isolation of iodine-producing bacteria from aquaria. *Antonie Leeu.*, 34, 226.
- Gross, J. (1962). Iodine and bromine. In: *Mineral Metabolism, An Advance Treatise*, C. Comar and F. Bronner editors, Academic Press, New York. pp. 221-285.
- Gunnerson, C. G. and E. Ozturgut (1974). The Bosphorus. In: *The Black Sea - Geology, Geochemistry and Biology*, E. T. Degens and D. A. Ross editors, The American Association of Petroleum Geologists, pp. 99-114.
- Hanson, W. C. (1963). Iodine in the environment. In: *Radioecology*, J. Schultz and W. Klement editors, Rheinhold, New York. pp. 581-601.
- Herring, J. R. and P. S. Liss (1973). A new method for the determination of iodine species in sea water. *Deep-Sea Res.*, 21, 777-783.
- Heurtebise, M. (1971). Semi-automated determination of iodine in biological fluids by activation analysis. *J. Radioanalyt. Chem.*, 7, 227-233.

- Hills, G. J. (1956). Iodine. In: Mellor's Comprehensive Treatise on Inorganic and Theoretical Chemistry, Supplement II, Part I, F, Cl, Br, I, At. Longmans, New York.
- Hiyama, Y. and J. M. Khan (1964). On the concentration factors of radioactive I, Co, Fe and Ru in marine organisms. *Rec. Oceanogr. Wks. Jap.*, 7, 79-106.
- Hobson, L. A. and D. W. Menzel (1969). The distribution and chemical composition of organic particulate matter in the sea and sediments off the east coast of South America. *Limn. Oceanogr.*, 14, 159-163.
- Holland, H. D. (1965). The history of ocean water and its effect on the chemistry of the atmosphere. *Proc. Nat. Acad. Sci.*, 53, 1173-1183.
- Holm-Hansen, O. (1972). The distribution and chemical composition of particulate material in marine and fresh waters. *Mem. Ist. Ital. Idrobiol.*, 29 Seppl., 37-51.
- Holm-Hansen, O., J. D. H. Strickland and P. M. Williams (1966). A detailed analysis of biologically important substances in a profile off Southern California. *Limn. Oceanogr.*, 11, 548-561.
- Jannasch, H. W., H. G. Truper and J. H. Tuttle (1974). Microbial sulfur cycle in the Black Sea. In: *The Black Sea - Geology, Geochemistry and Biology*. E. T. Degens and D. A. Ross editors. The American Association of Petroleum Geologists. pp. 419-425.
- Johannesson, J. K. (1958). Oxidized iodine in seawater. *Nature*, 182, 251.
- Johnson, D. A. (1968). *Some Thermodynamic Aspects of Inorganic Chemistry*. Cambridge University Press.
- Johnson, D. L. (1972). Bacterial reduction of arsenate in sea water. *Nature*, 240, 44-45.
- Johnson, D. L. and M. E. Q. Pilson (1972). Arsenate in the Western North Atlantic and adjacent regions. *J. Mar. Res.*, 30, 140-149.
- Kappanna, A. N., G. T. Gadre, H. M. Bhavnagary and J. M. Joshi (1962). Minor constituents of Indian sea-water. *Curr. Sci.*, 31, 273-274.

- Katzin, L. I. and E. Gebert (1955). The iodide-iodine-tri-iodide equilibrium and ion activity coefficient ratios. *J. Amer. Chem. Soc.*, 77, 5814-5819.
- Kester, D. R. and R. M. Pytkowicz (1969). Sodium, magnesium and calcium sulfate ion-pairs in seawater at 25°C. *Limn. Oceanogr.*, 14, 686-692.
- Klemperer, H. G. (1957). The accumulation of iodide by *Fucus ceranoides*. *Biol. J.*, 67, 381-390.
- Koblentz-Mishke, O. J., V. V. Volkovinsky and J. G. Kabanova (1970). Plankton primary production of the world ocean. In: *Scientific Exploration of the South Pacific*. W. S. Wooster editor. National Academy of Sciences. pp. 183-193.
- Kolehmainen, S., S. Takatolo and J. K. Miettinen (1969). A tracer experiment with I-131 in an oligotrophic lake. In: *Symposium in Radioecology*. D. Nelson and F. Evan editors. USAEC, Oak Ridge. pp. 462-473.
- Kolthoff, I. M. and R. Belcher (1957). *Volumetric Analysis. Vol. III. Titration Methods: Oxidation-Reduction Reactions*. Interscience.
- Kramer, J. R. (1965). History of sea water. Constant temperature-pressure equilibrium models compared to liquid inclusion analyses. *Geochim. Cosmochim. Acta*, 29, 921-945.
- Kuenzler, E. J. (1969). Elimination of iodine, cobalt, iron and zinc by marine zooplankton. In: *Symposium in Radioecology*. D. Nelson and F. Evan editors. USAEC, Oak Ridge. pp. 278-284.
- Kylin, H. (1930). Uber die jodidspaltende Fahigkeit der Phaophyceen. *Z. physio. Chem., Hoppe-Seyler's*, 191, 200-210.
- Latimer, W. M. (1952). *Oxidation Potentials*. 2nd edition. Prentice-Hall, New York.
- Laurens, G. (1835). De l'eau de la partie de la Mediterranee qui baigne les cotes de Marseille. *J. Pharm. Sci. Access.*, 21, 90-94.
- Lehninger, A. L. (1965). *Bioenergetics*. Benjamin, New York.
- Leopold, L. B. (1960). Rivers. *Amer. Scientist*, 50, 511-537.

- Li, C. H. and C. F. White (1943). Kinetics of hypoiodite decomposition. *J. Amer. Chem. Soc.*, 65, 335-339.
- Liebhafsky, H. A. and B. Makower (1933). The rate of bromate formation in aqueous solutions containing hypobromous acid and its anion. *J. Phys. Chem.*, 37, 1037-1046.
- Liss, P. S., J. R. Herring and E. D. Goldberg (1973). The iodide/iodate system in seawater as a possible measure of redox potential. *Nature*, 242, 108-109.
- Lovelock, J. E., R. J. Maggs and R. J. Wade (1973). Halogenated hydrocarbon in and over the Atlantic. *Nature*, 241, 194-196.
- Low, E. M. (1949). Iodine and bromine in sponges. *J. Mar. Res.*, 8, 97-105.
- Macadam, S. (1852). *Chem. Gaz.*, 10, 281.
- Maloney, N. J. (1966). Geomorphology of continental margin of Venezuela. Part I. Cariaco Basin. *Bol. Inst. Ocean. U. Oriente*, 5, 38-53.
- Malvano, R., G. Buzzigoli, M. Scarlattini, G. Cenderelli, C. Gandolfi and P. Grosso (1972). The determination of iodine in materials of biological interest. A comparative evaluation of neutron-activation and automated colorimetric methods. *Anal. Chim. Acta*, 61, 201-220.
- Marchand, E. (1855). *Mem. Acad. Med. Paris*, 19, 121.
- Matthews, A. D. and J. P. Riley (1970). A study of Sugawara's method for determination of iodine in seawater. *Anal. Chim Acta*, 51, 295-301.
- Mauchline, J. and W. L. Templeton (1964). Artificial and natural radioisotopes in the marine environment. *Oceanogr. Mar. Biol. Ann. Rev.*, 2, 229-279.
- Menzel, D. W. and J. H. Ryther (1964). The composition of organic matter in the Western North Atlantic. *Limn. Oceanogr.*, 9, 179-186.
- Merz, A. and L. Moller (1928). Hydrographische Untersuchungen in Bosporus und Dardanellen. *Veroff. Inst. Meeresforsch. Berl. Neue Folge*, 18, 284 pp.
- Metcalf, W. G. and M. C. Stalcup (1967). The origin of the Atlantic Equatorial Undercurrent. *J. Geophys. Res.*, 72, 4959-4975.

- Metcalf, W. G., A. D. Voorhis and M. C. Stalcup (1962). The Atlantic Equatorial Undercurrent. *J. Geophys. Res.*, 67, 2499-2508.
- Millero, F. J. (1969). The partial molal volumes of ions in sea water. *Limn. Oceanogr.*, 14, 376-385.
- Miyake, Y. and S. Tsunogai (1963). Evaporation of iodine from the ocean. *J. Geophys. Res.*, 68, 3989-3993.
- Morgan, K. J. (1954). Some reactions of inorganic iodine compounds. *Quarterly Rev.*, 8, 123-146.
- Moyers, J. L. and R. A. Duce (1974). The collection and determination of atmospheric gaseous bromine and iodine. *Anal. Chim. Acta*, 69, 117-127.
- Neuman, G. (1969). The Equatorial Undercurrent in the Atlantic. In: *Symposium of the Oceanography and Fisheries Resources of the Tropical Atlantic, Abidjan (Ivory Coast) 1966*. UNESCO. pp. 33-44.
- Nielsen, S. (1958). A survey of recent Danish measurements of the organic productivity in the sea. *Rapp. P-v Reun. Cons. Perm. Int. Explor. Mer.*, 144, 92-95.
- Ohno, S. (1971). Determination of iodine and bromine in biological materials by neutron-activation analysis. *Analyst*, 96, 423-426.
- Okuda, T., J. Benitez and E. Fernandez A. (1969). Vertical distribution of inorganic and organic nitrogen in the Cariaco Trench. *Bol. Inst. Ocean. Oriente.*, 8, 28-34.
- Ostlund, H. G. (1974). Expedition "Odysseus 65": Radiocarbon age of Black Sea deep water. In: *The Black Sea - Geology, Geochemistry and Biology*. E. T. Degens and D. A. Ross editors. The American Association of Petroleum Geologists. pp. 127-132.
- Owens, M. S. and J. A. Warburton (1973). Analysis of iodine in Antarctic snow. *Antarctica J.*, 8, 343-344.
- Pavlova, G. A. and O. V. Shishkina (1973). Accumulation of iodine in interstitial water during metamorphism in relation to the iodine distribution in Pacific sediments. *Geochem. International*, 10, 804-813.
- Petek, M. and M. Branica (1968). Hydrographical and biotical conditions in North Adriatic - III. Distribution of zinc and iodate. *Thalassia Jugosl.*, 5, 257-261.

- Petek, M. and M. Branica (1969). Determination of zinc and iodate in sea water by pulse polarography. Rapp. proc. verb. reunions. Comm. intern. l'explor. sci. Mer. Med., 19, 767.
- Pfaff, C. (1825). Jb. Chem. Phys., 15, 378.
- Philander, S. G. H. (1973). Equatorial Undercurrent: measurements and theories. Rev. Geophys. Space Phys., 11, 513-570.
- Pillai, V. K. (1956). Chemical studies on Indian seaweeds. I. Mineral constituents. Proc. Indian Acad. Sci., 44B, 3-29.
- Plotnikov, J. (1907). Die photochemische Oxydation von Jodwasserstoff durch Sauerstoff. Z. Phys. Chem., 58, 214-244.
- Plotnikov, J. (1908). Die photochemische Oxydation des Jodwasserstoff durch Sauerstoff. II. Z. Phys. Chem., 64, 215-228.
- Presley, B. J. (1974). Rates of sulfate reduction and organic carbon oxidation in the Cariaco Trench (Abstract). Trans. Amer. Geophys. Union, 55, 319-320.
- Price, N. B. and S. E. Calvert (1973). The geochemistry of iodine in oxidised and reduced recent marine sediments. Geochim. Cosmochim. Acta, 37, 2149-2158.
- Price, N. B., S. E. Calvert and P. G. Jones (1970). The distribution of iodine and bromine in the sediments of the Southwestern Barents Sea. J. Mar. Res., 28, 22-34.
- Rankama, K. and T. G. Sahama (1950). Geochemistry. U. of Chicago Press.
- Rechnitz, G. A., M. R. Kresz and S. B. Zamochnick (1966). Analytical study of an iodide-sensitive membrane electrode. Anal. Chem., 38, 973-976.
- Reith, J. F. (1930). Der Jodgehalt von Meerwasser. Rec. Trav. Chim. Pays.-Bas., 49, 142-150.
- Richards, F. A. (1965). Anoxic basins and fjords. In: Chemical Oceanography. J. P. Riley and G. Skirrow editors. 1, 611-646. Academic Press, New York.
- Richards, F. A. (1975). The Cariaco Basin (Trench). Oceanogr. Mar. Biol. Ann. Rev., in press.



- Richards, F. A. and R. F. Vaccaro (1956). The Cariaco Trench, an anaerobic basin in the Caribbean Sea. *Deep-Sea Res.*, 3, 214-228.
- Riley, J. P. (1965a). Historical introduction. In: *Chemical Oceanography*. J. P. Riley and G. Skirrow editors. 1, 1-41. Academic Press, New York.
- Riley, J. P. (1965b). Analytical chemistry of sea water. In: *Chemical Oceanography*. J. P. Riley and G. Skirrow editors. 2, 295-424. Academic Press, New York.
- Riley, J. P. and R. Chester (1971). *Introduction to Marine Chemistry*. Academic Press, New York.
- Rinkel, M. O. (1969). Some features of relationships between the Atlantic Equatorial Undercurrent and its associated salinity core. In: *Proceedings of the Symposium on Oceanography and Fisheries Resources of the Tropical Atlantic, Abidjan (Ivory Coast) 1966*. UNESCO. pp. 193-212.
- Roche, J., N-v. Thoai and M. Lafon (1949). Sur le mecanisme enzymatique de la formation d'iode aux depens des iodures par les laminaires. *Compt. rend. soc. biol.*, 143, 1327-1329.
- Ross, D. A., E. Uchupi, K. E. Prada and J. C. MacIlvaine (1974). Bathymetry and microtopography of Black Sea. In: *The Black Sea - Geology, Geochemistry and Biology*. E. T. Degens and D. A. Ross editors. The American Association of Petroleum Geologists. pp. 1-10.
- Rossini, F. D., D. D. Wagman, W. H. Evans, S. Levine and I. Jaffe (1952). Selected value of chemical thermodynamic properties. *Natl. Bur. Stand. Circ. 500*. U. S. Dept. Commerce.
- Ryther, J. H. (1963). Geographic variations in productivity. In: *The Sea*. M. N. Hill editor. 2, 347-380. Interscience, New York.
- Sagi, T. (1969). The ammonia content in sea water in the Western North Pacific Ocean. *Oceanogr. Mag.*, 21, 113-119.
- Schnepfe, M. N. (1972). Determination of total iodine and iodate in sea water and in various evaporites. *Anal. Chim. Acta*, 58, 83-89.

- Seto, F. Y. B. and R. A. Duce (1972). A laboratory study of iodine enrichment on atmospheric sea-salt particles produced by bubbles. *J. Geophys. Res.*, 77, 5339-5349.
- Shaw, T. I. (1959). The mechanism of iodide accumulation by the brown sea weed *Laminaria digitata*. The uptake of I<sup>131</sup>. *Proc. Roy Soc. Lon., Ser. B*, 150, 356-371.
- Shaw, T. I. (1960). The mechanism of iodide accumulation by the brown sea weed *Laminaria digitata*. II. Respiration and iodide uptake. *Proc. Roy. Soc. Lon., Ser. B*, 152, 109-117.
- Shaw, T. I. (1962). Halogens. In: *Physiology and Biochemistry of Algae*. R. A. Lewin editor. Academic Press, New York. pp. 247-253.
- Shaw, T. I. and L. H. N. Cooper (1957). The state of iodine in seawater. *Nature*, 180, 250.
- Shaw, T. I. and L. H. N. Cooper (1958). Oxidized iodine in seawater. *Nature*, 182, 251-252.
- Shishkina, O. V. and G. A. Pavlova (1965). Iodine distribution in marine and oceanic bottom muds and in their pore fluids. *Geochem. International*, 2, 559-565.
- Sigalla, J. and C. Herbo (1957). Cinetique et mecanisme de l'oxydation de l'iodure par l'oxygene dissour. *J. Chim. Phys.*, 54, 733-738.
- Sigalla, J. and C. Herbo (1958). Cinetique et mecanisme de l'oxydation de l'iodure par l'oxygene dissous en presence de sels de cuivre. *J. Chim. Phys.*, 55, 407-412.
- Sillen, L. G. (1961). The physical chemistry of seawater. In: *Oceanography*. M. Sears editor. American Association for the Advancement of Science. pp. 549-581.
- Sillen, L. G. (1963). How has sea water got its present composition? *Svensk. Kem. Tids.*, 75, 161-177.
- Sillen, L. G. and A. E. Martell (1964). Stability Constants of Metal-Ion Complexes. Spec. Publ. No. 17. The Chemical Society, London.
- Skopintsev, B. A. and L. A. Michailovskaya (1933). Iodine content of White Sea Water. *Trud. Inst. Oceanogr. Moscow*, 3, 79.

- Skrabal, A. (1907). Zur Kenntnis der unterhalogenigen Säuren und der Hypohalogenite I. Die Kinetik der Hypojodite und Hypobromite in starkalkalischer Lösung. Sitz. Akad. Wiss. Wien, 116, 215-278.
- Skrabal, A. (1908). Zur Kenntnis der unterhalogenigen Säuren und der Hypohalogenite II. Die Kinetik der Hypobromite in schwach alkalischer Lösung. Sitz. Akad. Wiss. Wien, 117, 827-852.
- Skrabal, A. (1911). Zur Kenntnis der unterhalogenigen Säuren und der Hypohalogenite III. Die Einfluss der Elektrolyte die Geschwindigkeit der Hypojoditreaktion. Sitz. Akad. Wiss. Wien, 120, 27-44.
- Skrabal, A. (1934). Die Halogenbleichlaugen - Reaktionen. Z. Elektrochem., 40, 232-246.
- Skrabal, A. and Hohlbaum (1916). Sitz. Akad. Wiss. Wien, 125, 3.
- Skrabal, A. and S. R. Weberitsch (1914). Zur Kenntnis der Halogensauerstoffverbindungen. X. Die Kinetik der Bromatbildung aus Brom. Sitz. Akad. Wiss. Wien, 123, 1205-1224.
- Sneed, M. C., J. L. Maynard and R. C. Brasted (1954). Comprehensive Inorganic Chemistry. Vol. 3. The halogens. Van Nostrand, New York.
- Sorokin, J. I. (1964). On the primary production and bacterial activities in the Black Sea. J. Cons. perm. int. Explor. Mer., 29, 41-60.
- Spencer, D. W. and P. G. Brewer (1971). Vertical advection diffusion and redox potentials as controls on the distribution of manganese and other trace metals dissolved in waters of the Black Sea. J. Geophys. Res., 76, 5877-5892.
- Spencer, D. W. and P. G. Brewer (1975). The distribution of some chemical elements between dissolved and particulate phases in sea water. USAEC report COO-3566-11.
- Stumm, W. and J. J. Morgan (1970). Aquatic Chemistry. Wiley-Interscience, New York.
- Sugawara, K. (1957). The distribution of some minor bio-elements in Western Pacific waters. In: Proc. Regional Symp. Phys. Oceanogr. Tokyo, 1955. UNESCO. pp. 169-174.

- Sugawara, K., T. Koyama and K. Terada (1955). A new method of spectrophotometric determination of iodine in natural water. *Bull. Chem. Soc. Jap.*, 28, 494-497.
- Sugawara, K. and K. Terada (1957). Iodine distribution in the Western Pacific Ocean. *J. Earth Sci.*, 5, 81-90.
- Sugawara, K. and K. Terada (1958). Oxidized iodine in seawater. *Nature*, 182, 250-251.
- Sugawara, K. and K. Terada (1967). Iodine assimilation by a marine *Navicula* sp. and the production of iodate accompanied by the growth of the algae. *Inform. Bull. Planktology Japan, Commemoration Number of Dr. Y. Matsue*, 213-218.
- Sugawara, K., K. Terada, S. Kanamori, N. Kanamori and S. Okabe (1962). On different distribution of calcium, strontium, arsenic and molybdenum in the northwestern Pacific, Indian and Antarctic Oceans. *J. Earth Sci.*, 10, 34-50.
- Thorstenson, D. C. (1970). Equilibrium distribution of small organic molecules in natural waters. *Geochim. Cosmochim. Acta*, 34, 745-770.
- Tong, W. and I. L. Chaikoff (1955). Metabolism of  $I^{131}$  by the marine algae, *Nereocystis luetkeana*. *J. Biol. Chem.*, 215, 473-484.
- Truesdale, V. W. (1974). The chemical reduction of molecular iodine in seawater. *Deep-Sea Res.*, 21, 761-766.
- Truesdale, V. W. (1975). 'Reactive' and 'unreactive' iodine in seawater -- a possible indication of an organically bound iodine fraction. *Mar. Chem.*, 3, 111-119.
- Truesdale, V. W. and C. P. Spencer (1974). Studies on the determination of inorganic iodine in seawater. *Mar. Chem.*, 2, 33-47.
- Tsunogai, S. (1971a). Determination of iodine in seawater by an improved Sugawara method. *Anal. Chim. Acta*, 55, 444-447.
- Tsunogai, S. (1971b). Iodine in the deep water of the ocean. *Deep-Sea Res.*, 18, 913-919.
- Tsunogai, S. and T. Henmi (1971). Iodine in the surface water of the ocean. *J. Oceanogr. Soc. Jap.*, 27, 67-72.

- Tsunogai, S. and T. Sase (1969). Formation of iodide-iodine in the ocean. *Deep-Sea Res.*, 16, 489-496.
- Turekian, K. K. (1971). Rivers, tributaries and estuaries. In: *Impingement of Man on the Ocean*. D. W. Hood editor. Wiley and Sons, New York. pp. 9-73.
- Tuttle, J. H. and H. W. Jannasch (1973). Sulfide and thio-sulfate-oxidizing bacteria in anoxic marine basins. *Mar. Biol.*, 20, 64-70.
- Ullyot, P. and O. Ilgaz (1946). The hydrography of the Bosphorus: an introduction. *Geogra. Rev.*, 36, 44-66.
- U. S. Dept. Interior, Fish and Wildlife Serv., Bur. of Comm. Fish. (1966). Annual report of the Bureau of Commercial Fisheries Radiobiological Laboratory Beaufort, N. C., 1965. Circ. 244. Wash. D. C.
- Vinogradov, A. D. (1953). *The Elementary Composition of Marine Organisms*. Sears Foundation for Marine Research. Yale University, New Haven.
- Vogel, A. I. (1953). *A Text-book of Quantitative Inorganic Analysis*. Longmans, New York.
- Voipio, A. (1961). The iodine content of Barents Sea Water. *Rapp. Cons. Explor. Mer.*, 149, 38.
- Wada, E. and A. Hattori (1972). Nitrite distribution and nitrate reduction in deep sea waters. *Deep-Sea Res.*, 19, 123-132.
- Wheaton, R. M. and W. C. Bauman (1951). Properties of strongly basic anion exchange resin. *Ind. Eng. Chem.*, 43, 1088-1093.
- Williams, P. M., H. Oeschger and P. Kinney (1969). Natural radiocarbon activity of the dissolved organic carbon in the North-east Pacific Ocean. *Nature*, 224, 256-258.
- Wilson, B. J. (1966) *The Radiochemical Manual*. 2nd edition. The Radiochemical Centre, Amersham.
- Winkler, L. H. (1916). De Jodid- und Jodate- iongehalt des Meereswassers. *Z. Angew. Chem.*, 29, 205-207.
- Winkler, L. W. (1918). Gravimetric analysis. V. Chlorides, bromides, and iodides. *Z. Angew. Chem.*, 31, 101-103.

- Winther, C. (1924a). Die Oxydation des Jodwasserstoffs im Dunkeln und im Lichte. *Z. Phys. Chem.*, 108, 236-274.
- Winther, C. (1924b). Die Oxydation des Jodwasserstoffs. II. *Z. Phys. Chem.*, 113, 275-278.
- Wong, G. T. F. (1973). The marine chemistry of iodate. M. S. Thesis. M. I. T.
- Wong, G. T. F. (1976). The distribution of iodine in the upper layers of the Equatorial Atlantic. *Deep-Sea Res.*, in press.
- Wong, G. T. F. and P. G. Brewer (1974). The determination and distribution of iodate in South Atlantic waters. *J. Mar. Res.*, 32, 25-36.
- Wong, G. T. F. and P. G. Brewer (1976). The determination of iodide in seawater by neutron activation analysis. *Anal. Chim. Acta*, 81, 81-90.
- Young, E. G. and W. M. Langille (1958). The occurrence of inorganic elements in marine algae of the Atlantic provinces of Canada. *Can. J. Bot.*, 36, 301-310.
- Zafirioiu, O. C. (1975). Reaction of methyl halides with seawater and marine aerosols. *J. Mar. Res.*, 33, 75-81.
- Zalevskaya, T. L. and G. I. Starobinets (1969). Chromatographic (ion-exchange) separation of mixtures of halide ions. *J. Anal. Chem. USSR*, 24, 564-567.
- Zeitschel, B. (1969). Productivity and microbiomass in the tropical Atlantic in relation to the hydrographic conditions (with emphasis on the eastern area). In: *Symposium of the Oceanography and Fisheries Resources of the Tropical Atlantic, Abidjan (Ivory Coast) 1966*. UNESCO. pp. 69-84.
- Zirino, A. and S. Yamamoto (1972). A pH- dependent model for the chemical speciation of copper, zinc, cadmium and lead in seawater. *Limn. Oceanogr.*, 17, 661-671.

APPENDIX A . DISSOLVED IODINE MEASUREMENTS IN THE EQUATORIAL  
ATLANTIC DURING CRUISE AII-83 (JUNE, JULY, 1974)

Station 2044 1°58.6'N 10°00.7'W		Station 2045 1°21.6'N 10°02.2'W		Station 2046 0°37.1'N 10°00.5'W		Station 2048 0°01.3'N 9°58.2'W	
Depth (m)	Iodate (uM)	Depth (m)	Iodate (uM)	Depth (m)	Iodate (uM)	Depth (m)	Iodate (uM)
1	0.249	1	0.244	1	0.242	1	0.257
29	0.235	30	0.249	30	0.273	29	0.273
39	0.231	40	0.266	40	0.302	39	0.293
49	0.226	50	0.264	50	0.373	49	0.486
59	0.302	59	---	59	0.513	59	0.366
69	0.457	69	0.422	69	0.495	69	0.366
78	0.588	79	0.453	79	0.431	78	0.402
98	0.437	99	0.422	99	0.422	98	0.397
123	0.575	124	0.470	124	0.425	123	0.419
147	0.470	149	0.417	149	0.439	147	0.417
196	0.435	198	0.448	198	0.451	196	0.417
294	0.448	297	0.439	297	0.448	294	0.415
392	0.446	396	0.431	396	0.393	392	0.408
588	0.435	594	0.437	594	0.451	588	0.413
784	0.433	792	0.444	792	0.455	784	0.433
980	0.437	990	0.444	990	0.453	980	0.433
1170	0.437	1176	0.444	1188	0.457	1176	0.433
1455	0.431	1455	0.437	1485	0.451	1470	0.419

Station 2050 0°40.2'S 10°04.2'W		Station 2051 1°21.0'S 10°01.8'W		Station 2052 2°00.2'S 10°00.0'W		Station 2056 2°03.4'N 16°04.4'W	
Depth (m)	Iodate (uM)	Depth (m)	Iodate (uM)	Depth (m)	Iodate (uM)	Depth (m)	Iodate (uM)
1	0.282	1	0.277	1	0.262	1	0.220
23	0.304	30	0.306	30	0.300	29	0.176
30	0.342	39	0.664	40	0.435	39	0.214
38	0.386	49	0.557	50	0.484	49	0.236
53	0.371	69	0.446	59	0.477	59	0.580
61	0.393	78	0.419	69	0.433	69	0.469
76	0.426	98	0.410	79	0.446	78	0.443
96	0.437	123	0.399	99	0.415	98	0.409
117	0.444	196	0.435	124	0.415	123	0.423
160	0.431	294	0.448	149	0.413	144	0.411
252	0.446	392	0.437	198	0.408	180	0.425
340	0.435	588	0.428	298	0.433	280	0.398
522	0.433	784	0.419	595	0.446	366	0.425
696	0.444	980	0.451	794	0.446	528	0.427
870	0.444	1080	0.453	992	0.423	700	0.427
1044	0.453	1170	0.448	1190	0.408	864	0.342
1305	0.439			1488	0.431	1095	0.423



Station 2057 1°26.3'N 16°04.9'W		Station 2058 0°40.3'N 16°01.2'W		Station 2059 0°00.2'N 16°02.0'W		Station 2060 0°19.9'S 16°01.9'W	
Depth	Iodate	Depth	Iodate	Depth	Iodate	Depth	Iodate
1	0.171	1	0.249	1	0.222	1	0.262
29	0.185	30	0.358	30	0.274	30	0.338
38	0.218	40	0.320	36	0.383	39	0.494
48	0.211	50	0.409	42	0.411	49	0.451
58	0.211	60	0.309	50	0.514	59	0.429
67	0.403	70	0.383	55	0.438	69	0.429
77	0.376	80	0.396	61	0.400	79	0.414
96	0.314	100	0.369	69	0.409	99	0.414
120	0.391	125	0.360	79	0.380	123	0.385
144	0.387	149	0.405	99	0.405	148	0.407
192	0.398	199	0.398	124	0.418	197	0.365
288	0.398	299	0.427	149	0.403	296	0.416
384	0.418	398	0.425	198	0.414	394	0.407
576	0.398	598	0.409	297	0.423	493	0.383
768	0.367	797	0.427	396	0.436		
960	0.327	996	0.358	594	0.431		
1152	0.418	1195	0.400	792	0.425		
1440	0.403	1494	0.378	990	0.423		
				1188	0.438		
				1485	0.431		

Station 2061* 0°38.2'S 16°00.7'W		Station 2062 0°57.0'S 16°05.1'W		Station 2063 1°19.6'S 16°03.4'W		Station 2064 2°10.2'S 15°59.9'W	
Depth (m)	Iodate (uM)	Depth (m)	Iodate (uM)	Depth (m)	Iodate (uM)	Depth (m)	Iodate (uM)
1	0.207	1	0.298	1	0.280	1	0.314
25	0.274	29	0.307	30	0.294	30	0.300
33	0.311	39	0.320	39	0.311	40	0.500
42	0.256	49	0.385	49	0.409	50	0.460
50	0.262	58	0.434	59	0.394	60	0.451
58	0.256	68	0.431	69	0.416	69	0.449
66	0.342	78	0.445	79	0.425	79	0.434
83	0.365	98	0.443	99	0.429	99	0.423
104	0.398	122	0.443	124	0.429	124	0.445
125	0.398	147	0.443	148	0.431	149	0.445
166	0.400	196	0.447	198	0.429	198	0.458
252	0.403	295	0.445	298	0.436	298	0.447
340	0.403	395	0.443	398	0.434	397	0.443
528	0.407	495	0.445	599	0.436	595	0.465
712	0.414			799	0.436	794	0.465
890	0.391			999	0.431	992	0.476
1068	0.409			1198	0.431	1190	0.447
1335	0.409			1497	0.420	1488	0.463

\* Post-tripped  
Data discarded.

Station 2066 1°00.4'N 21°59.5'W		Station 2067 0°31.3'N 21°56.5'W		Station 2068 0°00.0'S 21°53.9'W		Station 2069 0°28.9'S 21°58.5'W	
Depth (m)	Iodate (uM)	Depth (m)	Iodate (uM)	Depth (m)	Iodate (uM)	Depth (m)	Iodate (uM)
1	0.307	1	0.293	1	0.286	1	0.257
29	0.286	28	0.293	29	0.311	30	0.277
39	0.318	37	0.302	39	0.379	40	0.322
49	0.487	46	0.394	49	0.415	50	0.449
59	0.469	55	0.514	59	0.534	59	0.687
69	0.428	64	0.471	69	0.460	69	0.694
79	0.437	74	0.440	78	0.431	79	0.595
99	0.433	92	0.394	98	0.401	99	0.385
123	0.433	115	0.401	123	0.354	124	0.397
148	0.433	139	0.381	148	0.412	149	0.392
198	0.426	186	0.379	197	0.419	198	0.399
297	0.437	280	0.417	296	0.388	297	0.403
396	0.397	376	0.410	394	0.356	397	0.412
595	0.367	473	0.424	592	0.383	498	0.412
793	0.397			791	0.442		
991	0.392			990	0.357		
1189	0.433			1188	0.421		
1487	0.338			1485	0.401		

Station 2070 1°00.4'S 22°01.4'W		Station 2071 1°29.9'S 22°02.9'W		Station 2073 2°07.8'N 28°09.0'W		Station 2074 1°22.4'N 28°00.4'W	
Depth (m)	Iodate (uM)	Depth (m)	Iodate (uM)	Depth (m)	Iodate (uM)	Depth (m)	Iodate (uM)
1	0.266	1	0.279	1	0.286	1	0.295
29	0.275	30	0.277	27	0.303	29	0.298
39	0.347	40	0.289	36	0.303	38	0.333
49	0.336	49	0.329	45	0.300	48	0.577
59	0.482	59	0.550	54	0.331	57	0.607
68	0.577	69	0.431	63	0.663	67	0.455
78	0.449	79	0.412	72	0.523	76	0.413
98	0.426	99	0.442	90	0.440	95	0.448
123	0.421	124	0.442	113	0.464	119	0.455
147	0.424	148	0.442	135	0.464	143	0.460
196	0.424	198	0.446	180	0.474	191	0.335
296	0.426	297	0.419	270	0.464	288	0.382
396	0.426	396	0.455	360	0.420	386	0.385
596	0.437	495	0.455	540	0.464	583	0.342
797	0.401			720	0.471	771	0.375
996	0.412			900	0.424	957	0.415
1195	0.440			1092	0.478	1145	0.488
1494	0.440			1380	0.464		

Station 2075 0°43.6'N 28°04.3'W		Station 2076 0°02.2'S 28°00.5'W		Station 2077 0°16.5'S 28°01.9'W		Station 2078 0°41.5'S 27°58.1'W	
Depth (m)	Iodate (uM)	Depth (m)	Iodate (uM)	Depth (m)	Iodate (uM)	Depth (m)	Iodate (uM)
1	0.291	1	0.170	1	0.254	1	0.290
28	0.286	29	0.163	27	0.254	29	0.290
38	0.288	39	0.265	36	0.254	38	0.278
47	0.298	49	0.317	45	0.263	48	0.256
56	0.495	58	0.455	53	0.326	58	0.417
66	0.340	68	0.462	62	0.333	67	0.550
75	0.371	78	0.446	71	0.419	77	0.437
94	0.422	97	0.398	90	0.401	96	0.426
118	0.436	121	0.426	113	0.398	120	0.414
141	0.399	146	0.414	136	0.401	144	0.414
189	0.422	195	0.417	182	0.401	194	0.435
285	0.441	591	0.417	276	0.407	294	0.444
380	0.446	786	0.439	371	0.423	392	0.451
570	0.429	979	0.373	469	0.414	588	0.455
760	0.410	1470	0.403			784	0.446
950	0.389					980	0.441
1142	0.460					1176	0.451
1433	0.453					1470	0.446

Station 2079 0°58.8'S 28°02.8'W		Station 2080 1°20.2'S 28°01.7'W		Station 2081 2°00.7'S 28°01.0'W		Station 2083 1°27.5'S 33°02.2'W	
Depth (m)	Iodate (uM)	Depth (m)	Iodate (uM)	Depth (m)	Iodate (uM)	Depth (m)	Iodate (uM)
1	0.057	1	0.204	1	0.213	1	0.286
29	0.125	29	0.211	29	0.229	29	0.291
38	0.158	38	0.229	38	0.240	38	0.295
58	0.197	48	0.272	48	0.265	48	0.288
67	0.523	58	0.426	57	0.469	58	0.288
77	0.453	67	0.537	67	0.401	67	0.291
96	0.328	77	0.362	76	0.428	77	0.303
120	0.335	96	0.367	95	0.437	96	0.460
144	0.337	120	0.369	119	0.410	120	0.467
194	0.344	144	0.374	143	0.428	144	0.467
291	0.360	193	0.365	192	0.435	193	0.481
493	0.353	292	0.376	293	0.435	292	0.476
		390	0.383	392	0.482	390	0.476
		587	0.403	590	0.435	587	0.495
		784	0.401	783	0.444	781	0.497
		980	0.392	978	0.444	974	0.488
		1176	0.378	1169	0.426	1169	0.497
		1470	0.394	1464	0.455	1461	0.495

Station 2084 0°40.6'S 32°59.1'W		Station 2085 0°19.0'S 33°00.8'W		Station 2086 0°02.0'N 32°58.8'W		Station 2087 0°26.4'N 32°57.3'W	
Depth (m)	Iodate (uM)	Depth (m)	Iodate (uM)	Depth (m)	Iodate (uM)	Depth (m)	Iodate (uM)
1	0.279	1	0.284	1	0.281	1	0.293
29	0.277	28	0.295	29	0.291	29	0.293
39	0.281	38	0.312	38	0.298	38	0.298
49	0.277	47	0.310	48	0.317	48	0.307
59	0.295	66	0.434	58	0.356	58	0.324
69	0.443	75	0.563	67	0.413	67	0.450
78	0.464	94	0.434	77	0.560	77	0.448
98	0.410	118	0.462	96	0.399	96	0.422
123	0.424	141	0.464	120	0.460	120	0.485
147	0.431	191	0.470	144	0.462	144	0.467
196	0.460	290	0.462	193	0.462	193	0.464
294	0.460	388	0.467	291	0.460	292	0.459
392	0.455	488	0.464	389	0.467	391	0.474
588	0.467			587	0.439	492	0.399
784	0.448			774	0.453		
980	0.464			958	0.457		
1176	0.460			1124	0.469		
1470	0.457			1395	0.474		

Station 2088 0°46.0'N 32°58.0'W		Station 2089 1°32.1'N 33°02.9'W	
Depth (m)	Iodate (uM)	Depth (m)	Iodate (uM)
1	0.225	1	0.267
28	0.265	29	0.324
38	0.274	39	0.295
47	0.274	49	0.298
56	0.272	58	0.366
66	0.293	68	0.361
75	0.307	78	0.394
94	0.356	97	0.530
118	0.394	121	0.460
141	0.469	146	0.478
190	0.469	193	0.467
287	0.453	289	0.481
386	0.450	582	0.502
590	0.453	774	0.502
974	0.485	1160	0.504
1170	0.464	1449	0.490
1464	0.488		

Station 2048 0°01.3'N 9°58.2'W		Station 2068 0°00.0'S 21°53.9'W		Station 2078 0°41.5'S 27°58.1'W		Station 2086 0°01.1'N 32°59.8'W	
Depth (m)	Iodide* (uM)	Depth (m)	Iodide* (uM)	Depth (m)	Iodide* (uM)	Depth (m)	Iodide* (uM)
1	0.070	1	0.101	1	0.100	1	0.114
25	0.083	24	0.091	29	0.110	24	0.112
50	0.055	48	0.083	38	0.108	48	0.111
74	0.052	71	0.048	48	0.112	73	0.098
83	0.033	95	0.032	58	0.071	97	0.057
99	0.018	143	0.013	67	0.086	145	0.013
149	0.007	190	0.008	77	0.018	193	0.006
198	0.008	285	0.003	96	0.022	290	0.005
396	0.002	380	0.001	144	0.027	387	0.002
594	0.004	575	0.001	194	0.003	580	0.005
743	0.001	1013	-0.001	294	0.003	1021	0.001
1040	-0.001	1452	-0.002	588	0.002	1315	0.001
1337	-0.002			980	0.002		
				1470	0.000		

\* The data tabulated here have been corrected for the reagent blank which is 0.0046 uM ± 0.00145 uM.

APPENDIX B. DISSOLVED IODINE MEASUREMENTS AND HYDROGRAPHIC  
DATA FROM THE VENEZUELA BASIN AND THE CARIACO TRENCH  
DURING CRUISE AII-79

Station AII-79-2033 Venezuela Basin. 13°22'N 64°43'W. Total Depth: 4400 m.									
Depth (m)	Sal. (‰)	θ (°C)	O <sub>2</sub> (ml/l)	PO <sub>4</sub> <sup>-3</sup> (μM)	SiO <sub>2</sub> (μM)	I <sup>-*</sup> (μM)	IO <sub>3</sub> <sup>-</sup> (μM)	ΣI (μM)	ΣI/Sal (nmole/g)
0	34.828	26.401	4.54	0	0	0.098	0.325	0.423	12.1
25	35.658	---	4.55	0	0	0.124	0.318	0.442	12.4
51	36.341	25.768	3.93	0.035	0	---	0.370	---	---
76	36.678	---	4.11	0.039	0	0.116	0.342	0.458	12.5
100	36.906	---	3.88	0.170	0	0.377	0.438	0.815	22.1
148	36.685	---	3.45	0.228	0	0.151	0.469	0.620	16.9
196	36.322	17.309	3.34	0.276	1.30	0.007	0.460	0.467	12.9
		17.299							
246	36.080	15.857	3.46	0.424	3.35	---	0.469	---	---
		15.844							
296	35.865	---	3.37	0.491	3.35	0.004	0.464	0.468	13.0
394	35.334	11.127	2.94	0.475	7.73	0.007	0.446	0.453	12.8
		11.101							
492	34.930	---	2.77	1.04	12.57	---	0.497	---	---
589	34.760	6.898	2.87	1.16	14.53	---	0.492	---	---
		6.888							
688	34.751	---	3.09	1.18	17.23	0.003	0.498	0.501	14.4
737	34.754	5.809	3.18	1.17	17.88	---	0.492	---	---
		5.795							
780	34.774	5.565	3.46	1.15	18.81	---	0.467	---	---
		5.557							
838	34.816	---	3.65	1.10	18.90	---	0.480	---	---
878	34.876	---	3.75	1.04	17.23	---	0.471	---	---
948	---	4.901	---	---	---	---	---	---	---
976	34.918	5.169	4.17	0.966	17.60	0.001	0.476	0.477	13.7
1460	34.956	4.099	5.07	0.873	18.62	0.002	0.430	0.432	12.4
		4.114							
1706	34.964	---	5.13	0.851	19.09	0.004	0.444	0.448	12.8
1955	34.991	3.919	5.20	0.825	20.30	0.000	0.462	0.462	13.2
		3.915							

Station AII-79-2033 (continued)

2167	34.974	3.890	5.22	0.815	20.11	---	0.466	---	---
		3.871							
2425	34.975	---	5.24	0.819	18.72	0.006	0.476	0.482	13.8
2478	34.979	---	5.00	0.812	17.88	---	0.471	---	---
2663	34.977	3.848	4.94	0.799	20.02	---	0.474	---	---
		3.873							
2692	34.976	3.832	5.41	0.812	19.65	---	0.473	---	---
		3.842							
2810	34.979	3.867	5.00	0.860	19.83	0.001	0.462	0.463	13.2
		3.855							
2925	34.977	---	5.32	0.819	19.93	---	0.488	---	---
3156	34.976	3.823	5.33	0.831	19.09	0.001	0.465	0.466	13.3
		3.837							
3383	34.981	---	5.01	0.812	21.69	---	0.460	---	---
3409	34.978	---	5.14	0.825	19.65	-0.000	0.471	0.471	13.5
3666	34.978	3.843	5.14	0.815	21.23	---	0.481	---	---
		3.827							
3670	34.980	3.824	5.03	0.819	19.27	0.000	0.476	0.476	13.6
		3.821							
3915	34.981	---	5.09	0.803	20.39	-0.000	0.484	0.484	13.8
4209	34.979	3.844	4.90	0.812	21.32	0.000	0.475	0.475	13.6
		3.824							

\* Iodide concentrations have been corrected for the reagent blank which is 0.0046 μM.

Station AII-79-2038 Cariaco Trench Eastern Basin.						10°31'N 64°45'W.		
Depth (m)	Sal. (‰)	$\theta$ (°C)	$PO_4^{-3}$ ( $\mu M$ )	$NH_4^+$ ( $\mu M$ )	$I^{-*}$ ( $\mu M$ )	$IO_3^-$ ( $\mu M$ )	$\Sigma I$ ( $\mu M$ )	$\Sigma I/Sal$ (nmole/g)
0	36.758	---	---	---	0.086	0.340	0.426	11.6
49	36.822	23.180	0.098	---	0.051	0.395	0.446	12.1
54	36.817	---	0.108	---	0.045	0.400	0.445	12.1
69	36.818	---	0.131	---	0.042	0.411	0.453	12.3
83	36.833	---	0.151	---	---	0.401	---	---
98	36.843	22.173	0.141	---	0.056	0.412	0.468	12.7
123	36.632	---	0.341	---	0.033	0.410	0.443	12.1
123	36.537	---	0.479	---	0.024	0.404	0.428	11.7
133	36.492	---	0.532	---	0.027	0.414	0.441	12.1
157	36.445	18.399	0.630	---	0.019	0.431	0.450	12.3
	36.423	---	0.669	---	0.208	0.415	0.623	17.1
176	36.375	---	0.840	---	0.069	0.420	0.489	13.4
196	36.355	17.689	0.925	---	0.271	0.270	0.541	14.9
206	36.331	---	0.991	0.178	0.209	0.255	0.464	12.8
	36.333	---	1.001	---	0.297	0.228	0.525	14.4
221	36.320	---	0.948	0.167	0.357	0.213	0.570	15.7
246	36.301	17.370	1.332	---	0.380	0.054	0.434	12.0
		17.375						
270	36.292	---	1.371	0.237	---	0.000	---	---
295	36.277	---	1.414	0.587	0.413	0.000	0.413	11.4
345	36.262	17.086	1.483	0.999	0.509	0.000	0.509	14.0
418	36.209	---	1.608	1.810	---	---	---	---
442	36.233	---	1.604	2.003	0.321	0.000	0.321	8.9
491	36.223	16.900	1.637	2.385	0.416	---	0.416	11.5
541	36.227	---	1.667	2.797	0.478	---	0.478	13.2
587	36.211	16.841	1.680	3.734	0.437	---	0.437	12.1
		16.833						
600	36.191	---	1.667	3.346	0.463	0.000	0.463	12.8
688	36.202	---	1.657	3.612	0.465	---	0.465	12.8
737	36.252	16.799	1.572	2.991	0.434	---	0.434	12.0

Station AII-79-2038 (continued)

786	36.199	---	1.782	4.656	0.322	---	0.322	8.9
796	36.202	---	1.693	3.997	---	---	---	---
882	36.196	16.795	1.791	5.096	0.376	---	0.376	10.4
		16.800						
934	36.195	---	1.791	5.263	0.461	---	0.461	12.7
1031	36.193	16.772	1.745	4.330	0.456	---	0.456	12.6
1081	36.196	16.770	1.798	5.092	---	---	---	---
1173	36.197	16.756	1.824	5.775	0.409	---	0.409	11.3
		16.758						

\* Iodide concentrations have been corrected for the reagent blank which is 0.0046  $\mu M$ .



Lat. 10-32N Long. 64-46W

AII 79 Sta. 2031

Eastern Basin

Corr. Depth	S ‰	Pot. Temp. $\theta_{\circ C}$	O <sub>2</sub> ml/l	Sulf. ( $\mu M$ )	SiO <sub>2</sub>
0	36.725	25.153	4.56		-
24	.738		4.52		-
72	.826	22.639	3.52		-
120	.611		2.52		4.84
144	.531	19.112	2.16		6.33
168	.474		1.82		9.68
192	.391	18.001	.67		18.72
214	.348	17.679	.16		24.77
233	.328		-		27.93
246	.310	17.397	-		32.50
263	.300	17.368	.07	.08	33.43
281	.294		-	1.04	35.94
304	.277	17.199	-	3.24	37.52
313	.274		-	3.08	39.57
323	.272	17.179		3.49	40.03
342	.263			8.86	44.13
361	.258	17.096		9.61	44.88
356	.256			9.21	44.79
374	.251			10.88	45.72
405	.247			12.96	46.93
433	.238	16.990		16.43	49.63
482	.227	16.930		11.47	
492	.224	16.922		14.53	53.17
530	.219	16.888		14.67	
541	.219			18.96	53.17
580	.215	16.859		16.75	
590	.215	16.832		22.82	56.98
679	.208	16.816		21.03	
689	.208			26.50	57.73
777	.207	16.789		23.69	
785	.206	16.799		28.35	58.94
876	.203	16.784		27.26	
885	.205			31.78	61.64
976	.201	16.772		31.95	
981	.200	16.793		44.93	62.38
1147	.190	16.761		35.39	64.43
1196	.194			35.39, 35.39	64.43
1296	.195	16.756		35.84	65.18
1330	.197			37.09, 37.22	65.46
1364	.195	16.766		37.50	65.64
1383	.196			37.38, 37.34	65.36
1391	.196	16.772		37.02	66.01

Station AII-79-2037 Cariaco Trench Western Basin.

10°37'N 65°26'W

Lat. 10-37N Long. 65-26W

AII 79 Sta. 2030

Western Basin

Depth (m)	Sal. (‰)	(°C)	PO <sub>4</sub> <sup>-3</sup> (µM)	NH <sub>4</sub> <sup>+</sup> (µM)	IO <sub>3</sub> <sup>-</sup> (µM)	Corr. Depth	S o/oo	°C	O <sub>2</sub> m <sup>3</sup> /l	Sulfide (µM)	SiO <sub>2</sub> (µM)
18	36.724	---	0.013	0.115	0.369	0	36.542	26.57	4.567		0
35	36.791	---	0.026	0.085	0.369	25	.543		4.568		0.65
52	36.783	22.346	0.125	0.070	0.407	74	.822	22.55	3.554		0.74
70	36.785	---	0.210	---	0.394	123	.509	18.65	2.530		5.49
88	36.799	---	0.188	0.214	0.448	147	.466		1.835		8.85
104	36.776	21.226	0.220	0.141	0.450	172	.415	17.78	1.217		12.94
122	36.746	---	0.269	0.096	0.460	196	.349	17.69	0.441		22.25
142	---	19.490	---	---	---	206	.338	17.51	0.323	.50	24.38
158	36.598	19.341	0.394	0.134	0.463	226	.313	17.41	0.074	.18	29.33
182	36.463	---	0.594	0.173	0.469	243	.295	17.32	0.072		32.21
182	36.470	---	0.692	0.041	---	263	.273	17.25	0.012		38.64
205	36.384	17.729	0.876	0.041	0.230	282	.261		0.012		33.71
224	36.326	---	0.935	---	0.182	302	.264	17.19	0		36.87
231	36.319	---	0.906	---	0.186	314	.263	17.18	0		38.64
235	36.306	---	0.974	---	0.171	327	.251	17.11	0		37.52
245	36.309	17.372	0.874	0.096	0.276	341	.251	17.11	0		39.94
253	36.301	---	1.066	---	0.276	371	.238		0		41.25
260	36.294	17.370	1.109	---	0.223	371	.238		0		43.30
261	36.288	17.368	1.024	0.167	0.102	371	.238		0		49.53
304	36.269	---	1.603	0.354	0.000	368	.247	17.05	0		52.51
352	36.255	17.448	1.822	0.895	0.000	392	.241		0		54.38
392	36.243	17.075	1.509	1.322	0.000	441	.225		0		55.02
431	36.232	17.049	1.532	1.669	---	450	.217	16.88	0		58.38
480	36.229	17.070	1.568	2.240	---	535	.209	16.86	0		59.78
526	36.224	16.893	1.575	3.425	---	584	.205	16.80	0		61.55
574	36.212	---	1.742	3.275	---	683	.201		0		62.10
623	36.214	16.859	1.709	3.030	---	780	.195	16.77	0		62.94
664	36.206	---	1.719	3.224	---	878	.190	16.77	0		62.85
706	36.209	---	1.636	3.331	---	1075	.189		0		64.25
747	36.207	16.807	1.693	3.672	---	1178	.187	16.76	0		64.62
825	36.201	---	1.677	3.341	---	1230	.187		0		63.22
813	36.198	16.786	1.700	4.167	---	1331	.185		0		63.59
866	36.198	16.771	1.793	4.620	---	1369	.188		0		64.34
1008	36.196	16.771	1.775	4.387	---	1390	.193	16.76	0		

APPENDIX C. DISSOLVED IODINE MEASUREMENTS AND HYDROGRAPHIC  
DATA FROM THE BLACK SEA DURING CRUISE CHAIN-120

Station CHAIN-120-1355 Black Sea. 42°50'N 33°00'E. Total Depth: 2160 m.								
Depth (m)	Sal. (‰)	$\theta$ (°C)	$O_2$ (ml/l)	$H_2S$ ( $\mu M$ )	$I^{-*}$ ( $\mu M$ )	$IO_3^-$ ( $\mu M$ )	$\Sigma I$ ( $\mu M$ )	$\Sigma I/Sal$ (nmole/g)
10	18.371				0.047	0.088	0.135	7.3
10	18.374							
10	18.376							
31	18.483	7.858						
38	18.526							
43	18.562	7.642						
49	18.777							
68	19.654	7.992						
75	19.785		2.29		0.011	0.135	0.146	7.4
91	20.240	8.310						
95	20.599	8.438						
97	20.627							
98	20.431		0.41		0.015	0.146	0.161	7.9
101	20.633	8.467						
102	20.690		0.34	3.28	0.060	0.139	0.199	9.6
102	20.732	8.495						
107	20.782							
108	20.829		0.34	0.50	0.088	0.053	0.141	6.8
114	20.850	8.546						
117	20.907	8.545						
120	20.913		0.27	28.03	0.150	0.081	0.231	11.1
123	20.975			0.39	0.200	0.104	0.304	14.5
136	21.036	8.553						
137	21.092	8.597						
143	21.114							
143	21.156	8.652						
144	21.140				0.232	0.055	0.287	13.6
149	21.191			12.57				
157	21.281	8.665						

Station CHAIN-120-1355 (continued)

165	21.325			28.03				
178	21.392	8.711						
180	21.415	8.744						
184	21.416							
186	21.440							
194	21.460	8.704						
201	21.488							
203	21.506	8.745						
209	21.533			7.90	0.216	0.000	0.216	10.0
223	21.583	8.775						
230	21.620							
237	21.638	8.789						
243	21.653							
255	21.675	8.825						
260	21.703							
281	21.742	8.881						
286	21.773			151.3	0.267	0.000	0.267	12.3
297	21.784							
304	21.802							
323	21.836	8.843						
328	21.843			215.2	0.276		0.276	12.6
335	21.864	8.867						
343	21.850							
395	21.894	8.822						
366	21.903							
382	21.948	8.870						
388	21.950			292.0	0.287		0.287	13.1
444	22.004	8.873						
450	22.010							
482	22.053	8.886						
483	22.054	8.865						
490	22.058			359.3	0.300	0.000	0.300	13.6
490	22.225							

Station CHAIN-120-1355 (continued)

580	22.131	8.900					
588	22.137						
726	22.216	8.895					
735	22.222		496.2	0.366		0.366	16.5
971	22.300	8.948					
980	22.334						
967	22.228	8.963					
973	22.295		525.0	0.357	0.000	0.357	16.0
1365	22.335	8.981					
1371	22.328		510.6	0.303	0.000	0.303	13.6
1472	22.335	8.934					
1478	22.336						
1740	22.342	9.069					
1746	22.338		545.0	0.433	0.000	0.433	19.4
1794	22.341	9.085					
1800	22.343						
1937	22.336	9.116					
1943	22.347		522.8	0.432	0.000	0.432	19.3
2042	22.340	9.105					
2048	22.343						

\* Iodide concentrations have been corrected for the reagent blank which is 0.0046 uM.

APPENDIX D. DISSOLVED IODINE MEASUREMENTS AND HYDROGRAPHIC  
DATA FROM THE GULF OF MAINE DURING CRUISE AII-86.

Station AII-86-2122 42°35.5'N 69°41.5'W

Depth m	Pres. db	Temp. °C	Sal. ‰	O <sub>2</sub> ml/l	Sil. µM/l	Theta °C	Sigth	PO <sub>4</sub> µM/l	Dynht m	IO <sub>3</sub> <sup>-</sup> µM	I <sup>-</sup> µM
0			33.464	6.25	10.20			.87		0.402	0.038
5	5	7.690	33.476	6.47	9.13	7.690	26.144	.82	.009	0.407	0.040
10	10	7.710	33.468	6.24	8.84	7.709	26.135	.82	.019	0.408	0.039
20	20	7.730	33.463	6.19	9.52	7.728	26.129	.89	.038	0.406	0.038
35	35	7.690	33.465	6.16	8.93	7.687	26.136	.91	.066	0.405	0.037
50	50	7.740	33.465	6.18	8.84	7.735	26.129	.92	.095	0.419	0.044
74	74	7.720	33.471	6.17	9.13	7.713	26.137	1.0	.141	0.415	0.035
98			33.441	6.14	9.22			1.02		0.413	---
99	100	7.770	33.484	6.18	8.84	7.760	26.141	.95	.189	0.422	0.040
121	122	7.670	33.460		8.84	7.658	26.136	1.05	.231	0.393	---
124	125	7.760	33.486	6.15	8.54	7.748	26.144	.95	.236	0.393	0.032
144	145	7.800	33.495	6.10	8.54	7.786	26.145	3.05	.275	0.398	0.035
149	150	7.920	33.637	5.02	12.53	7.905	26.239	1.14	.284	0.383	---
168	169	7.570	33.671	4.76	13.40	7.554	26.317	1.3	.318	0.416	0.019
189	190	6.920	33.746	4.68	15.34	6.903	26.466	1.25	.354	0.425	---
204	205	7.080	34.026	4.24	19.23	7.061	26.665	1.48	.376	0.434	0.014
223	224	7.260	34.112	4.19	18.64	7.239	26.708	1.56	.403	0.344	0.012
232	234	7.350	34.178	4.09	18.55	7.338	26.746	1.59	.416	0.434	0.016
242			34.184	4.04	18.74			1.63		0.419	0.015
251	253	7.380	34.188	3.94	18.64	7.356	26.751	1.67	.441	0.461	0.016

\* Iodide concentrations have been corrected for reagent blank which is 0.0046 µM.

Station AII-86-2138 42°32.0'N 69°31.0'W

Depth m	Pres. db	Temp. °C	Sal. ‰	O <sub>2</sub> ml/l	Sil. µM/l	Theta °C	Sigth	PO <sub>4</sub> µM/l	Dynht m	IO <sub>3</sub> <sup>-</sup> µM
2	2	7.104	33.200	6.42	8.84	7.104	26.010	1.06	.000	0.393
12	12	7.090	33.200	6.59	8.84	7.089	26.012	.94	.020	0.393
25	25	7.100	33.201	6.40	8.84	7.098	26.012	.96	.046	0.347
48	48	7.340	33.321	6.46	8.84	7.336	26.073	.95	.092	0.391
66	66	7.800	33.510	6.38	8.74	7.794	26.156	.88	.127	0.451
84	85	7.790	33.515	6.19	8.64	7.782	26.162	1.00	.161	0.430
102	103	7.740	33.512	6.16	8.64	7.730	26.167	.98	.195	0.437
120			33.523	6.13	8.64			.97		0.353
136	137	7.730	33.517	6.08	8.16	7.717	26.173	.87	.259	0.404
140	141	7.600	33.726	4.72	14.27	7.586	26.355	1.26	.266	0.407
154	155	7.730	33.687	4.96	13.50	7.715	26.306	1.28	.291	0.416
169	170	6.930	33.803	4.50	16.99	6.915	26.510	1.36	.316	0.433
173	174	7.180	33.793	4.43	14.57	7.164	26.468	1.42	.322	0.421
191	192	7.030	33.924	4.43	17.19	7.012	26.591	1.39	.350	0.434
209	210	7.150	34.049	4.34	17.77	7.130	26.673	1.47	.376	0.433
218	219	7.190	34.083	4.19	18.35	7.169	26.695	1.45	.389	0.455
227	229	7.270	34.077	4.18	18.35	7.248	26.679	1.40	.402	0.374
236			34.160	4.12	18.35			1.47		0.454
245	247	7.360	34.182	4.08	18.64	7.336	26.749	1.47	.427	0.462
250	252	7.370	34.187	4.07	18.64	7.346	26.751	1.52	.434	0.454

Station AII-86-2151 42°26.0'N 69°45.0'W

Depth m	Pres db	Temp. °C	Sal. o/oo	O <sub>2</sub> ml/l	SiI μM/l	Theta °C	Sigth	PO <sub>4</sub> μM/l	Dynth m	IO <sub>3</sub> μM/l
1	1	7.440	33.304	6.44	8.64	7.440	26.045	.93	.000	0.416
21	21	7.430	33.304	6.58	8.84	7.428	26.047	.93	.040	0.422
42	42	7.450	33.305	6.43	8.84	7.446	26.045	.95	.081	0.425
62	62	7.540	33.305	6.49	10.10	7.534	26.033	.95	.121	0.422
80	80	7.630	33.306	6.52	10.10	7.622	26.021	.95	.158	0.431
99	100	7.640	33.307	6.37	9.13	7.631	26.020	.95	.196	0.435
118										0.329
137	138	7.170	33.307	6.20	9.22	7.157	26.087	1.00	.272	0.335
140	141	7.830	33.559	5.65	11.75	7.816	26.191	1.07	.278	0.412
153	154	7.510	33.653	4.93	14.57	7.495	26.311	1.26	.301	0.410
157	158	7.740	33.567	5.52	10.49	7.725	26.211	1.15	.309	0.362
167	168	7.370	33.691	4.82	14.66	7.354	26.361	1.34	.327	0.407
176	177	7.510	33.598	5.35	12.72	7.493	26.268	1.31	.342	0.432
181	182	7.290	33.780	4.72	15.15	7.273	26.442	1.42	.351	0.427
195	196	7.110	33.917	4.56	16.90	7.092	26.575	1.49	.373	0.423
209			34.031	4.30	18.06			1.53		0.401
223	224	7.170	34.069	4.33	18.45	7.149	26.686	1.57	.414	---
237	239	7.180	34.098	4.51	19.52	7.158	26.708	1.60	.434	0.394
246	248	7.200	34.102	4.30	19.52	7.177	26.709	1.60	.446	0.422
256	258	7.220	34.109	4.28		7.196	26.711	--	.460	0.421

1268



APPENDIX E. IODINE CONTENT OF SUSPENDED PARTICULATE MATTER  
COLLECTED DURING THE GEOSecs ATLANTIC EXPEDITION

Station 3			Station 5			Station 11			Station 17		
Depth (m)	Particulate I (ng/kg)	51°00.5'N 43°06.9'W	Depth (m)	Particulate I (ng/kg)	56°56.1'N 42°33.7'W	Depth (m)	Particulate I (ng/kg)	63°31.9'N 35°13.8'W	Depth (m)	Particulate I (ng/kg)	74°54.6'N 1°11.2'W
19	32.25		7	10.31		7	85.39		40	2.08	
59	3.71		31	2.14		31	17.14		101	3.40	
136	4.79		83	2.33		83	3.84		152	2.70	
322	2.43		118	2.11		118	3.83		202	2.90	
441	2.43		168	1.83		168	3.75		303	4.40	
635	2.84		209	2.46		209	3.22		395	4.50	
832	2.32		308	1.60		308	2.38		549	2.68	
1177	2.35		409	1.98		409	2.37		622	2.87	
1572	1.54		459	1.47		459	2.01		787	7.16	
1725	2.10		568	2.06		568	1.85		1100	1.54	
1908	1.77		668	1.41		668	1.92		1297	2.20	
2150	1.45		729	1.39		729	2.10		1404	1.63	
2395	1.65		861	1.38		861	1.73		1503	3.03	
2639	1.22		986	0.93		986	2.09		1601	2.23	
2883	1.12		1005	0.69		1005	1.83		1798	2.85	
3014	0.93		1011	0.93		1011	1.77		2041	2.12	
3233	1.33		1105	0.55		1105	1.55		2293	2.38	
3433	1.01		1207	0.90		1207	1.67		2502	1.83	
3630	1.22		1406	1.47		1406	1.61		2712	1.55	
3836	1.22		1612	0.71		1612	1.60		2906	1.28	
4130	2.42		1757	1.01		1757	1.79		3102	1.28	
			1807	1.15		1807	1.60		3295	1.35	
			1863	1.42		1863	1.85		3585	1.38	
			1953	1.37		1953	1.65				
			2051	1.37		2051	1.79				
			2152	1.37		2152	1.65				
			2210	1.36		2210	1.79				

Station 18			Station 23			Station 27			Station 29		
69°59.4'N 0°6.9'W			60°24.4'N 18°39.5'W			41°57.0'N 41°59.0'W			36°00.0'N 47°00.0'W		
Depth (m)	Particulate I (ng/kg)	Particulate I (ng/kg)	Depth (m)	Particulate I (ng/kg)	Particulate I (ng/kg)	Depth (m)	Particulate I (ng/kg)	Particulate I (ng/kg)	Depth (m)	Particulate I (ng/kg)	Particulate I (ng/kg)
18	127.09	15.40	1	9.19	6.50	7	17.50	16.11	150	7.58	7.85
44	21.38	9.19	27	11.49	17.50	72	9.28	7.81	239	7.12	4.07
95	12.91	70	70	6.43	141	141	7.62	3.70	360	4.24	3.70
116	11.76	101	101	4.92	252	252	5.94	4.02	430	4.07	3.70
168	11.75	149	149	4.12	390	390	4.50	4.27	441	3.70	3.70
193	11.82	220	220	5.00	550	550	3.44	4.31	502	3.65	3.65
243	12.72	270	270	2.56	672	672	2.15	4.91	639	1.46	1.46
441	6.50	322	322	2.24	770	770	2.40	4.27	794	0.88	0.88
551	4.76	401	401	1.91	831	831	2.11	4.31	980	2.35	2.35
751	3.49	473	473	2.98	932	932	2.59	4.31	1090	1.28	1.28
850	3.70	546	546	2.36	1150	1150	2.08	5.18	1302	4.38	4.38
950	3.74	623	623	2.43	1268	1268	1.30	3.78	1702	2.65	2.65
1033	3.17	674	674	2.01	1640	1640	0.97	2.15	2104	2.30	2.30
1134	4.44	727	727	2.03	2029	2029	1.16	2.40	2506	2.24	2.24
1324	3.65	777	777	1.99	2435	2435	1.16	2.11	2897	2.35	2.35
1514	1.73	827	827	4.05	2836	2836	1.30	2.08	2702	4.38	4.38
1733	3.55	888	888	3.84	3229	3229	1.14	2.08	2906	2.65	2.65
1928	3.55	966	966	3.23	3633	3633	1.16	2.08	3105	2.30	2.30
2093	3.35	1036	1036	2.67	4036	4036	1.16	2.08	3504	2.24	2.24
2433	4.81	1487	1487	2.90	4383	4383	1.16	2.08	3702	2.53	2.53
2538	3.24	1120	1120	2.09	4577	4577	1.62	2.08	3900	2.11	2.11
2737	3.86	1144	1144	2.90	4767	4767	1.62	2.08	4296	3.77	3.77
2833	3.27	1375	1375	2.65					4497		
3012	6.53	1422	1422	1.96					4916		
3163		1546	1546	3.24							
		1505	1505	2.94							
		1564	1564	2.91							
		1584	1584	2.06							
		1656	1656	2.74							
		1728	1728	2.63							
		1843	1843	2.79							
		1939	1939	2.60							
		2017	2017	3.21							
		2084	2084	3.40							
		2172	2172	2.84							
		2245	2245	2.82							
		2310	2310	3.19							
		2411	2411	1.85							
		2482	2482	6.56							
		2521	2521	16.33							

Station 31			Station 40			Station 54			Station 60		
Depth (m)	Particulate I (ng/kg)	27°00.0'N 53°30.5'W	Depth (m)	Particulate I (ng/kg)	3°55.3'N 38°31.6'W	Depth (m)	Particulate I (ng/kg)	15°02.0'S 29°31.5'W	Depth (m)	Particulate I (ng/kg)	32°58.0'S 42°30.0'W
29	7.14		1	3.95		8	4.57		2	9.93	
100	6.48		80	5.56		138	9.22		22	11.99	
202	4.61		216	4.10		238	3.93		65	15.82	
301	2.85		378	2.80		324	2.84		95	20.56	
502	1.84		524	1.32		459	3.07		244		
703	1.50		675	1.55		689	4.16		281		
854	1.35		821	2.17		998	1.42		353	1.84	
951	1.11		949	1.62		1197	1.25		433		
1052	1.19		1067	1.55		1595	1.61		533		
1222	0.87		1185	1.55		1694	1.42		628		
1402	0.80		1294	1.25		2077	1.79		729	1.77	
1700	1.13		1555	1.55		2478	1.90		828		
2100	0.72		1562	1.70		2880	1.35		928	1.54	
2500	0.76		1859	1.44		3280	1.35		1036		
2900	0.86		2299	1.44		3680	1.36		1146	1.59	
3300	0.61		2448	1.28		3987	1.84		1261		
3600	0.55		2749	1.74		4287	1.58		1374	1.39	
3900	0.45		3209	1.22		4486	1.49		1483		
4200	0.62		3510	1.61		4678	1.41		1576	2.64	
4500	0.50		3811	1.33					1723		
4900	0.58		4062	1.33					1873	1.07	
5300	0.57		4162	1.36					2071	3.33	

-272-

Station 74		
Depth (m)	Particulate I (ng/kg)	54°59.5'S 50°06.8'W
8	5.60	
57	9.16	
126	11.96	
208	2.19	
308	1.66	
383	1.07	
461	1.50	
556	1.46	
603		
654	1.30	
831	1.26	
919	1.98	
988	1.16	
1060	1.80	
1321	1.97	
1676	2.07	
1960	1.39	
2268	2.15	
2705	1.87	
3185	1.89	
3496	2.54	
3843	2.68	
4112	2.43	